REFERENCE ONLY

UNIVERSITY OF LONDON THESIS

Degree PhD Year 2005 Name of Author NEEN J K.

The Mantoux test: a model for tracking T cell differentiation in the skin during secondary immune challenge

Submitted by

John Richard Reed

In December 2004

For the Degree of Doctor of Philosophy

Department of Immunology & Molecular Pathology,

Royal Free and University College Medical School,

University of London.

ProQuest LLC
789 East Eisenhower Parkway
P.O. Box 1346
Ann Arbor, MI 48106-1346

Abstract

In this study, we hypothesized that T cells differentiate in the skin as a consequence of localised proliferation at the site of secondary immune challenge in humans. One consequence of cellular proliferation is telomere shortening, which can be counteracted by telomerase. It is recognised that telomerase is up-regulated in activated T cells that are resident in lymphoid tissues or the blood. We have used the Mantoux Test (MT), a secondary immune response, to determine the degree of cellular differentiation in the skin and its consequences during an episode of cutaneous inflammation. We have established a skin suction blister technique to isolate lymphocytes from MTs up to 19 days after induction for flow cytometric analysis, heteroduplex analysis, cell culture and measurement of telomerase activity (TRAP assay). Skin biopsies were also collected for immunohistochemical staining. Marked antigen-specific $CD4^+$ T cell expansion with preserved clonality was observed in the skin during the MT. In contrast to recent murine studies, we found that this expansion was mediated in part by the extensive proliferation of $CD4^+$ T cells in the skin. This was associated with substantial telomeric shortening in the antigen-specific $CD4^+$ T cells in the skin, indicating accelerated cellular differentiation. Despite the development of a highly differentiated population of $CD4^+$ T cells during the MT, there appeared to be no increase in the proportion of anergic / suppressive $CD4^+CD25^+$ T cells, which might mediate the down-regulation of inflammation during resolution. The erosion of telomeres appeared to be mediated by the reversible inhibition of telomerase by type 1 interferons *in vivo*. This reversible inhibition was distinct from the irreversible down-regulation of telomerase that was observed when MT skin T cells were repeatedly activated *in vitro* culminating in cell senescence. The inhibition of telomerase activity in T cells during secondary immune responses in the skin represents a possible control checkpoint that may limit uncontrolled T cell expansion in non-lymphoid tissues *in vivo*.

Table of contents

List of figures

List of tables

Publications, presentations and prize list

Papers

Reed JR, Vukmanovic-Stejic M, Fletcher JM, Soares MVD, Cook JE, Orteu CH, Jackson SE, Birch KE, Foster GR, Salmon M, Beverley PCL, Rustin MHA, Akbar AN. Telomere erosion in memory T cells induced by telomerase inhibition at the site of antigenic challenge *in vivo*. ***J Exp Med*** 2004; **199:** 1433-1443. (Reed and Vukmanovic-Stejic joint first authors)

Comment in: **Science** 2004; **304:** 1415.

Abstracts

Reed JR, Buckley CD, Bofill M, Poulter L, Salmon M, Rustin MHA, Akbar AN. The role of CXCR4 and CCR7 Expression in the Resolution of T Cell Mediated Cutaneous Inflammation. ***J Invest Dermatol*** 2001; **117:** 806 & ***Immunology*** 2001; **104** (Suppl. 1)**:** 25.

Vukmanovic-Stejic M, Taams LS, Reed JR, Smith JS, Dunne PJ, Salmon M, Rustin MHA, Akbar AN. Suppression of PPD Induced Responses by $CD4^{+}CD25^{+}$ Regulatory T Cells. ***J Invest Dermatol*** 2002; **119:** 310.

Reed JR, Vukmanovic-Stejic M, Orteu CH, Salmon M, Rustin MHA, Akbar AN. Identification of Antigen-Specific Lymphocytes, CCR7 Expression and the Role of Apoptosis During Resolving Cutaneous Inflammation. ***J Invest Dermatol*** 2002; **119:** 299.

Reed JR, Vukmanovic-Stejic M, Buckley CD, Lowdell M, Rustin MHA, Salmon M, Akbar AN. $CD4^+CD25^+$ regulatory T cells and the resolution of antigen-specific inflammation in humans *in vivo.* ***Immunology*** 2002; **107** (Suppl 1): 6, ***Br J Dermatol*** 2003: **148:** 863 & ***J Invest Dermatol*** 2003; **121:** x (148).

Vukmanovic-Stejic M, Reed JR, Soares M, Cook J, Foster GR, Beverley P, Salmon, Rustin MHA, Akbar AN. Telomere shortening and downregulated telomerase activity during resolving cutaneous inflammation in humans *in vivo.* ***J Invest Dermatol*** 2003; **121:** x (148).

Reed JR, Vukmanovic-Stejic M, Cook J, Fletcher J, Orteu CH, Salmon M, Beverley P, Rustin MHA, Akbar AN. Accelerated telomere erosion during cutaneous T cell mediated inflammation. ***Br J Dermatol*** 2004; **150:** 805 & ***Br J Dermatol*** 2004; **151** (Suppl.): 11.

Oral presentations

Reed JR, Buckley CD, Bofill M, Poulter L, Salmon M, Rustin MHA, Akbar AN. The role of CXCR4 and CCR7 expression in the resolution of T cell mediated cutaneous inflammation. *European Society of Dermatological Research, Annual Meeting, Stockholm, September 2001.*

Reed JR, Vukmanovic-Stejic M, Orteu CH, Bofill M, Poulter L, Buckley CD, Salmon M, Rustin MHA, Akbar AN. CCR7 expression and the importance of apoptosis in the resolution of cutaneous antigen-specific inflammation. *British Society of Investigative Dermatology, Annual Meeting, Norwich, March 2002.*

Reed JR, Vukmanovic-Stejic M, Soares M, Fletcher J, Rustin MHA, Akbar AN. Accelerated telomere erosion during cutaneous T cell mediated inflammation. *British Society of Investigative Dermatology, Annual Meeting, Sheffield, April; 2004 & British Association of Dermatologists, Annual Meeting, Belfast, July 2004.*

Poster presentations

Reed JR, Buckley CD, Bofill M, Poulter L, Salmon M, Rustin MHA, Akbar AN. The role of CXCR4 and CCR7 expression in the resolution of T cell mediated cutaneous inflammation. *European Society of Dermatological Research, Stockholm, September 2001 & British Society for Immunology, Harrogate, December 2001.*

Reed JR, Vukmanovic-Stejic M, Orteu CH, Bofill M, Poulter L, Buckley CD, Salmon M, Rustin MHA, Akbar AN. CCR7 expression and the role of apoptosis in the resolution of antigen-specific cutaneous inflammation. *Keystone Symposium, Steamboat Springs, Colorado, USA, April 2002.*

Reed JR, Vukmanovic-Stejic M, Orteu CH, Bofill M, Poulter L, Buckley CD, Salmon M, Rustin MHA, Akbar AN. Identification of Antigen-Specific Lymphocytes, CCR7 Expression and the Role of Apoptosis During Resolving Cutaneous Inflammation. *Society of Investigative Dermatology, Los Angeles, May 2002.*

Vukmanovic-Stejic M, Taams LS, Reed JR, Smith JS, Dunne PJ, Salmon M, Rustin MHA, Akbar AN. Suppression of PPD induced responses by $CD4^{+}CD25^{+}$ regulatory T cells. *Society of Investigative Dermatology, Los Angeles, May 2002.*

Reed JR, Vukmanovic-Stejic M, Buckley CD, Lowdell M, Rustin MHA, Salmon M, Akbar AN. $CD4^+CD25^+$ regulatory T cells and the resolution of antigen-specific inflammation in humans *in vivo. British Society for Immunology, Harrogate, December 2002, British Society of Investigative Dermatology, Southampton, April 2003 & International Investigative Dermatology, Miami, April 2003*

Vukmanovic-Stejic M, Reed JR, Soares M, Cook J, Foster GR, Beverley P, Salmon, Rustin MHA, Akbar AN. Telomere shortening and downregulated telomerase activity during resolving cutaneous inflammation in humans *in vivo. International Investigative Dermatology, Miami, April 2003.*

Prizes

BSID Best Registrar Oral Presentation – British Society of Investigative Dermatology Annual Meeting 2004.

BAD Best Registrar Oral Presentation – British Association of Dermatologists Annual Meeting 2004.

Acknowledgements

The work presented in this thesis involved many members of the research group as well as the collaboration of people from other institutions, all of whom I would like to thank.

This PhD was carried under the supervision of Dr Malcolm Rustin and Professor Arne Akbar. Malcolm provided tremendous support and encouragement throughout the project. His advice was also invaluable in dealing with the clinical and ethical hurdles that were encountered during the project. Arne has been a constant source of ideas, encouragement and enthusiasm. This has made immunology fun and exciting. He has certainly taught me that there is always a positive side to a negative result!

Dr Milica Vukmanovic-Stejic has also acted as a supervisor and we have worked very closely together throughout this project. She has been instrumental in not only teaching me the cell culture and flow cytometry techniques used, but has also kept me focused and showed me what is important.

A number of individuals were of critical importance in performing some of the additional techniques that were used in this project. Dr Maria Soares and Sarah Jackson were responsible for carrying out the TRAP assays and Dr Joanne Cook and Professor Peter Beverley (Edward Jenner Institute for Vaccine Research, Compton, UK) performed the heteroduplex analysis. Professor Graham Foster and his team (Royal London Hospital, London, UK) undertook the type 1 interferon anti-viral assay and Dr John Curnow and Professor Mike Salmon (MRC Centre for Immune Regulation, Birmingham, UK) kindly performed the multiplex bead assay. The anergy induction experiments were performed by Dr Padraic Dunne.

I received a great amount of help and advice from Dr Jean Fletcher, particularly with regards to mastering the flow-FISH technique. Dr Cate Orteu was influential in encouraging me to join the group and continue on the research with the model that she was instrumental in developing. Some of her immunohistochemical data has been re-presented in this thesis. I am also grateful to Aida Condez who helped with the immunohistochemistry performed. I would also like to thank Margarita Bofill for her help and scientific advice.

My thanks also go to Jose Akbar for all of the numerous occasions when her kitchen was turned into a make-shift 'laboratory' and used for late night experimental work!

I am also grateful to all of the consultants at the Churchill Hospital, Oxford, who have been extremely patient and supportive whilst I have completed the writing of this thesis.

I must also thank all of the volunteers, without whom this project would not have been possible.

Finally, I would like to acknowledge Dermatrust, who funded my PhD and supported many of the conferences, which I had the opportunity to attend.

A personal note

It is true to say that I can't remember many days during this project that I didn't enjoy, even on the bad result days! I'm sure people will try to remind me of them, but those days don't stand out! Certainly, I never had the 'oh no it's work tomorrow' Sunday night feeling during my research time! The focus and progress of the project will have been partly responsible for that, but a significant factor is the people, who I have been working with! Without Arne, Malcolm, Milica, Jean, Maria, Fiona, Padraic and Arthur as well as Jo, Katie, Lavina, and Sarah as friends and colleagues the work would not have been the same or as much fun. Thank you for all of your help and friendship. In particular, Milica and Arne have been enormously supportive and encouraging as supervisors and bosses, and again it would not have been half as much fun without them.

Of course, none of this would have been possible without the backing of Debbie, who has stomached numerous late evenings and weekend absences during the laboratory and writing-up stages. She has been a hundred times more encouraging and tolerant than I ever was when she was writing-up. Without her support and help, the past four years would not have been as enjoyable as they have been. Thank you and sorry! All of this has taken place as our family has expanded from 1 to 3 children. Lara, Ella and Jack have learnt a lot about skin biology and blisters, but have also ensured that I did not become too science obsessed.

Finally, to all of you in the lab, I'm sure I did fill my share of tip-boxes, but if I didn't, sorry!

Abbreviations

APC	Antigen presenting cell
APC	Allophycocyanin
ACAD	Activated T cell autonomous death
ACID	Activation-induced cell death
BCG	Bacillus of Calmette and Guérin
BDCA	Blood dendritic cell antigen
BSA	Bovine serum albumin
bp	Base pairs
CCL	CC chemokine ligand
CCR	CC chemokine receptor
CD	Cluster of differentiation
CLA	Cutaneous lymphocyte antigen
CM	Complete medium
Cpm	Counts per minute
CTACK	Cutaneous T cell-attracting chemokine
CTLA-4	Cytotoxic T lymphocyte antigen 4
Cy3 / 5	Cyanin 3 or 5
DC	Dendritic cell
DISC	Death-inducing signalling complex
DMEM	Dulbecco's modification of Eagle's medium
DNA	Deoxyribonucleic acid
dNTP	Deoxynucleotide triphosphates
ds	Double strand
EI	Erythema-index
ERK	Extracellular signal-regulated kinase
FACS	Fluorescence activated cell sorter
FADD	Fas-associated death domain protein
FCS	Foetal calf serum
FISH	Fluorescence in situ hybridisation
FITC	Fluoroscein isothiocyanate

FLICE	FADD-like interleukin 1β converting enzyme
FLIP	FLICE inhibitory protein
FucT-VII	α(1,3)-fucosyltransferase VII
FSC	Forward scatter
GM-CSF	Granulocyte monocytes-colony stimulating factor
HDA	Heteroduplex analysis
IBD	Inflammatory bowel disease
ICAM	Intercellular adhesion molecule
ICOS	Inducible co-stimulator
IDO	Indoleamine 2,3-dioxygenase
IFN	Interferon
IFNAR	IFN-α/β receptor
IL	Interleukin
JAK	Janus kinase
KC	Keratinocyte
KLRG1	Killer cell lectin-like receptor G1
LC	Langerhans cell
LCMV	Lymphocytic choriomeningitis virus
LFA	Leucocyte function-associated antigen
LPS	Lipopolysaccharide
MACS	Magnetic cell sorting
MCP	Monocyte chemotactic peptide
MDC	Macrophage-derived chemokine
MFI	Median fluorescent intensity
MHC	Major histocompatibility complex
MIP	Macrophage-inflammatory protein
MT	Mantoux test
mRNA	Messenger ribonucleic acid
PAGE	Polyacrylamide gel electrophoresis
PB	Peripheral blood
PBMC	Peripheral blood mononuclear cells
PBS	Phosphate buffered saline

PBSA	Phosphate buffered saline with bovine serum albumin and sodium azide
PCR	Polymerase chain reaction
PD	Population doubling
PE	Phycoerythrin
PECy5.5	Phycoerythrin-cyanin 5.5
PerCP	Peridinin chlorophyll protein
Pfu	*Pyrococcus furiosus*
PKC	Protein kinase C
PNA	Peptide nucleic acid
PPD	Tuberculin purified protein derivative
PTP	Protein tyrosine phosphatase
RBC	Red blood cell
RFUCMS	Royal Free & University College Medical School
RPE-Cy5	R-phycoerythrin-cyanin 5
RPMI	Roselyn Park Medical Institute
RT	Room temperature
SB	Skin suction blister
SD	Standard deviation
SEM	Standard error of the mean
SSC	Side scatter
SCID	Severe combined immune deficiency
SLC	Secondary lymphoid-tissue chemokine
STAT	Signal tranducers and activators of transcription
T_{CM}	Central memory T cell
T_{EM}	Effector memory T cell
T_H	T helper cell
Taq	*Thermus aquaticus*
TARC	Thymus- and activation regulated chemokine
TB	Tuberculosis
TCR	T cell receptor
TER	Telomerase RNA

TERT	Telomerase reverse transcriptase
TGF	Transforming growth factor
TLR	Toll-like receptor
TNF	Tumour necrosis factor
TRADD	TNF-receptor-associated death domain protein
TRAP	Telomeric repeat amplification protocol
TRF	Telomeric repeat-binding factor
T_{reg}	$CD4^+CD25^+$ regulatory T cells
VEGF	Vascular endothelial cell growth factor
TRITC	Tetramethylrhodamine isothiocyanate
WBC	White blood cell

1 Introduction

1.1 Overview and hypothesis

Unravelling the mechanisms that regulate immune responses remains one of the principal aims of immunological research. In doing so, more focused manipulation of the human immune system should be achievable. This would allow conditions characterised by insufficient immune regulation such as autoimmune diseases and chronic inflammatory dermatoses to be more effectively treated. On the other hand, it would also permit the boosting of immunity to enhance vaccination or tumour immunity.

In the battle against infectious pathogens, non-lymphoid tissues such as the skin and mucosa commonly represent the front-line. Their defence crucially depends on the close co-operation of the innate and adaptive arms of the immune system[1;2]. The innate immune system can only recognise a restricted number of microbial products, whereas the adaptive immune system has evolved to mount specific responses against the vast array of pathogenic antigens to which humans are constantly exposed. The number of specific precursors within the naive lymphocyte pool that can respond to a particular antigen are consequently very limited. Adaptive immune responses are, therefore, critically dependent on the proliferation and clonal expansion of antigen-specific cells for their efficacy. Equally, it is vital that constraints are applied to prevent over-expansion, which might then result in immunopathology (Figure 1.1). Indeed, the elimination of antigenic material renders the expanded clonal population of effector lymphocytes largely redundant and this leads to the vast majority of cells being cleared by apoptosis[3]. A minority, however, do survive to form long-lived memory cells and this results in a state of immunological memory whereby secondary responses are more rapid and intense than primary responses[4-6]. Apoptosis, therefore, plays a critical role in regulating adaptive immune responses and ensuring that

homeostasis is achieved once the infection has been neutralised. Other possible constraints on T cells during an immune response *in vivo* include:

1. The limitation of their proliferative capacity and
2. Active suppression of their expansion / function.

It is unclear what role these constraints play in regulating immunity *in vivo*.

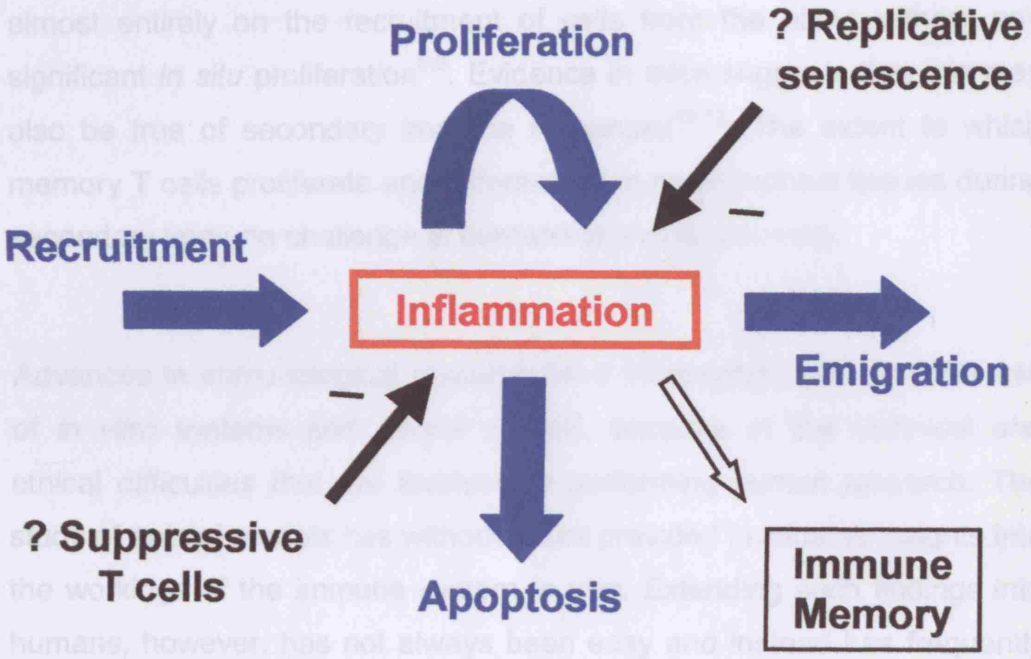

Figure 1.1 The dynamic balance of T cell infiltration into a tissue during an immune response.

Tissue homeostasis following an immune response is dependent on a dynamic balance of T cell recruitment, proliferation, death and emigration, which results in the resolution of inflammation and development of immune memory. Immune responses may also be constrained by the suppressive effects of regulatory T cells and limitations on the proliferative capacity of antigen-specific T cells.

The adaptive immune system comprises of T and B cells within the lymphocyte pool. T cells consist of $CD4^+$ (helper) and $CD8^+$ (cytotoxic) subsets. During a primary adaptive immune response, it is generally accepted that the clonal expansion of antigen-specific T cells takes place almost exclusively in the draining lymph nodes to which activated and

mature dendritic cells have migrated following the uptake of antigen in peripheral non-lymphoid tissues. T cells that recognise processed antigen in the context of peptide-MHC complexes then become activated, proliferate and undergo a process of differentiation whereby they gain modified functional and migratory properties[6;7]. This allows the activated antigen-specific T cells to migrate into the inflamed non-lymphoid tissue and mediate the clearance of antigen[4-6]. T cell infiltration within inflamed non-lymphoid tissue during primary immune challenge appears to depend almost entirely on the recruitment of cells from the blood without any significant *in situ* proliferation[8;9]. Evidence in mice suggests that this may also be true of secondary immune responses[10-12]. The extent to which memory T cells proliferate and differentiate in non-lymphoid tissues during secondary immune challenge in humans *in vivo* is unknown.

Advances in immunological research have increasingly relied on the use of *in vitro* systems and animal models, because of the technical and ethical difficulties that are involved in performing human research. The study of animal models has without doubt provided invaluable insights into the workings of the immune system *in vivo*. Extending such findings into humans, however, has not always been easy and instead has frequently led to the identification of inter-species differences in the workings of the immune system[13-18]. In view of this, the publication of immunological research performed on human subjects has recently been actively encouraged by a high profile journal[19]. Research into the biology of memory $CD4^+$ T cells in humans and mice has also been limited in comparison to the $CD8^+$ subset. This reflects the lack of suitable major histocompatibility complex (MHC) class matched/peptide tetrameric complexes, which have revolutionised the study of antigen-specific $CD8^+$ T cells.

Human skin is ideal for undertaking research into the dynamics of an on-going immune response in a non-lymphoid tissue in view of its

accessibility. The Mantoux test represents a cutaneous memory $CD4^+$ T cell mediated immune response that is induced by the intradermal injection of tuberculin purified protein derivative (PPD). This has previously been used as a model to investigate cutaneous immunity in humans[20-26]. In contrast to mice, using this model, we have previously noted extensive T cell proliferation in the skin[25]. We hypothesized that as a consequence of this localised cutaneous proliferation, T cells undergo differentiation in the skin during the Mantoux test, resulting in functional and regulatory sequelae. The main objectives of this project, therefore, were to use the Mantoux test model to:

1. Determine the extent of T cell differentiation in the skin during an episode of antigenic challenge, and subsequently
2. Examine the mechanisms influencing differentiation and
3. Investigate the immunoregulatory consequences.

1.2 T cell mediated immune responses

The generation of immunological memory is a key feature of adaptive immune responses. This refers to the state of heightened immunological responsiveness that follows re-exposure to the same antigen[5]. T cell responses are characterised by 3 main phases: 1) activation and expansion, 2) death and contraction, and 3) memory cell formation and maintenance[4].

1.2.1 T cell activation and expansion

Primary T cell responses are mediated by naive T cells, which circulate between the blood and secondary lymphoid organs i.e. the lymph nodes, Peyer's patches and spleen[27;28]. Primary immune responses are initiated in the secondary lymphoid organs and depend on naive T cells recognising processed peptide antigen complexed to MHC molecules on the surface of antigen-presenting cells (APC)[29;30]. This results in triggering of the T cell receptor (TCR)/CD3 complex as well as the CD4 or CD8 co-

receptors and leads to the formation of an immunological synapse between the T cell and APC. Optimal T cell triggering, however, depends on the ligation of a number of co-stimulatory, accessory and adhesion molecules e.g. CD28, LFA-1 (leucocyte function-associated antigen-1), CD40 ligand (CD40L), ICOS (inducible co-stimulator), OX40 (CD134), CD2, CD27 and 4-1BB (CD137)[31-33]. These molecules either provide additional signals to augment T cell activation and expansion or enhance TCR signalling by stabilising the immunological synapse and by promoting the recruitment of intracellular signalling molecules. In particular, ligation of CD28 by CD80 and CD86, which are expressed on the surface of activated mature APCs, induces enhanced interleukin-2 (IL-2) secretion and prevents apoptosis or the induction of anergy[34]. $CD4^+$ T cells appear to have more stringent activation requirements than $CD8^+$ T cells in terms of co-stimulation and duration of antigenic stimulation. This may reflect the more limited expression of MHC class II molecules compared to MHC class I molecules[33].

Optimal T cell signalling induces stimulated naive T cells to proliferate and undergo a process of differentiation to become effector T cells. Evidence suggests that T cell activation commits cells to undergo a pre-determined number of cell divisions, although the actual extent of proliferation may be partly influenced by the amount of antigen that is available *in vivo*[35-38]. This programmed proliferation may ensure that significant clonal expansion of rare antigen-specific T cells is attained even when antigen is limiting. The size of this clonal burst influences memory cell formation and appears to be intrinsically more profound in activated $CD8^+$ T cells than $CD4^+$ T cells[39-43]. The relative activation and expansion of either subset, however, will be affected by the nature of the antigen that is driving the immune response.

The number and proportion of antigen-specific T cells present during an immune response is dependent on the antigen, site and phase of the

immune response being studied. Quantification of antigen-specific T cells is also influenced by the sensitivity of the technique used to identify the cells[44]. The advent of class I MHC tetramers and intracellular cytokine staining have dramatically increased the sensitivity of such estimates compared to limiting dilution analysis[45]. Indeed, it is now recognised that during acute Epstein-Barr virus infection in humans, up to 44% of $CD8^+$ T cells may be specific for a particular viral epitope[46]. Similarly, in mice, at the peak of the immune response to lymphocytic choriomeningitis virus (LCMV) infection, up to 50-70% of $CD8^+$ T cells are antigen-specific[47].

T cell activation also launches a program of cellular differentiation, which is linked to proliferation[48;49], and at least in $CD4^+$ T cells probably requires continued exposure to antigen and cytokine signals[50]. This results in epigenetic changes that are mediated by histone acetylation, methylation and phosphorylation, which lead to alterations in the chromatin structure and result in the increased access of transcription factors to nucleosomal binding sites[48;51-53]. The outcome of this differentiation process is the generation of effector T cells, which can secrete a wider range of cytokines and directly or indirectly mediate the killing of the target pathogen. $CD4^+$ effector T cells provide help either to enhance $CD8^+$ T cell differentiation or to activate macrophages and B cells. $CD8^+$ effector T cells on the other hand demonstrate direct cytotoxic activity through the secretion of perforins, granzymes and cytokines such as interferon-γ (IFN-γ) and tumour necrosis factor (TNF). Effector $CD4^+$ T cells show increasingly polarised patterns of cytokine production as they become more differentiated. IL-12 and IFN-α promote the development of T_H1 polarised cells, which secrete IFN-γ and TNF-β, whereas IL-4 promotes the generation of T_H2 polarised T cells, which secrete IL-4, IL-5, IL-10 and IL-13[6;54]. Some $CD4^+$ T cells can produce both types of effector cytokines and are termed T_H0. In addition, there is a subset of $CD4^+$ T cells that only secrete IL-2 despite demonstrating primed characteristics and these appear to represent a less differentiated population of cells that are referred to as non-polarised T cells (T_{np})[55-57]. Generally, T_H1 responses

are protective against intracellular organisms, whereas T_H2 responses promote resistance to extracellular infections. T cell activation, therefore, results in dramatic clonal expansion and cellular differentiation, the extent of which is dependent on proliferation[48;49]. This leads to the development of effector T cells, which generally mediate the rapid elimination of pathogens.

Expansion of the antigen-specific population during a primary immune response appears to be dependent on proliferation in secondary lymphoid organs. The increase in cell numbers in inflamed non-lymphoid tissues, therefore, depends almost entirely on the recruitment and retention of cells that have undergone clonal expansion within the lymph node rather than as a result of *in situ* proliferation[8;9]. Interestingly, lymphotoxin-α deficient mice, which lack secondary lymphoid tissue, are still capable of mounting protective immunity, but the immune response is delayed and the mice are more susceptible to lower doses of antigen[58]. Secondary lymphoid tissue, therefore, appears not to be absolutely required to initiate immunity, but facilitates and accelerates the induction of an immune response thereby resulting in a protective advantage[58].

T cell activation also leads to the up-regulation of cytotoxic T lymphocyte antigen 4 (CTLA-4) (CD152), which interacts with CD80 and CD86 on APCs with greater affinity than CD28. Ligation of CTLA-4 acts to limit the T cell response by inhibiting IL-2 production and delaying cell cycle progression[59]. The importance of CTLA-4 in regulating immune function is highlighted in CTLA-4 knockout mice, which develop autoimmunity and fatal lymphoproliferative disease[60;61]. Signalling through CTLA-4, therefore, plays a critical role in the down-regulation of T cell function[59].

1.2.2 Death and contraction

Effector T cells become redundant following the removal of antigen and the vast majority (~90-95%) of these cells rapidly die during the resolution

of the immune response[9;40;43;46;47;62]. This helps to minimise the risk of effector T cells inducing immunopathology in the host and prevents the immune system from becoming over-burdened and congested with redundant cells[6;54;63]. The death of unwanted T cells is a complex process that appears to involve multiple pathways that result predominantly in apoptosis[64;65], although recent evidence suggests that necrotic cell death may also play a role[66]. Two main mechanisms regulate the fate of activated antigen-specific T cells: 1) activation-induced cell death (AICD) and 2) cytokine deprivation[63], which has more recently been referred to as activated T cell autonomous death (ACAD)[65].

AICD is mediated by signalling initiated through the ligation of CD95 (Fas) and TNF-α receptors[64;65]. Activation of these receptors leads to oligomerisation and the assembly of a death-inducing signalling complex (DISC), which results in the activation of caspases that initiate the apoptotic program[64;65]. T cell activation leads to the up-regulation of CD95 and CD95 ligand[67]. Furthermore, IL-2[68;69] and IFN-γ[70;71] render activated T cells more susceptible to apoptosis. T cells, therefore, become increasingly sensitive to AICD following activation as well as being more capable of inducing AICD in other cells.

ACAD results from the cytokine deprivation of lymphocytes as antigen becomes limited and inflammation is being down-regulated. T cell activation and differentiation is associated with the down-regulated expression of the anti-apoptotic molecules Bcl-2 and Bcl-x_L, which renders these cells susceptible to apoptosis[72-74]. This can be prevented by the pro-survival functions of IL-2, and the related cytokines IL-4, IL-7, IL-15 and IL-21[72;75-77]. These cytokines all signal through receptors, which share the common γ-chain of the IL-2 receptor (CD132), and promote Bcl-2 and Bcl-x_L expression as well as inducing proliferation. Type 1 interferons (IFN-α and β) can also rescue activated T cells from apoptosis by promoting Bcl-x_L expression without resulting in up-regulated Bcl-2 expression or the

induction of cell cycling[78-81]. Therefore as antigen is cleared and levels of pro-survival cytokines become limiting, activated T cells become increasingly susceptible to apoptosis. Indeed, studies using the Mantoux test model support the *in vivo* role of ACAD in mediating apoptosis during the resolution of the immune response, whereas AICD mediated via the CD95 pathway appeared to limit expansion during the peak of the response[25].

1.2.3 Memory cell formation and maintenance

Despite the dramatic contraction of cell numbers that occurs during the resolution of the primary immune response, an enlarged pool of antigen-specific T cells survives to form the memory population, which then persists over a long period of time[4-6]. The size of this pool, at least for $CD8^+$ T cells, is influenced by the clonal burst size[47;82]. The cellular precursors of memory cells and the exact pathway by which the memory population is formed are still unclear[33]. Increasing evidence, however, supports a linear model of differentiation whereby a subset of effector cells escapes apoptosis and reverts to a relatively quiescent population of memory cells[83-87]. The transition process may be more complex for $CD4^+$ T cells in light of recent data that showed that activated $CD4^+$ T cells were less able to form memory cells if they were capable of IFN-γ production[88]. This observation is in line with an alternative progressive model of differentiation, which proposes that memory T cells can develop without becoming functional effector cells[89-91]. In this model, T cell differentiation and survival depends on the signal strength that the T cell encounters. This results in the generation of two different memory subsets: 1) a lymph node homing subset that lacks immediate effector function (central memory T cells (T_{CM})) and 2) a non-lymphoid tissue homing subset that display immediate effector function (effector memory T cells (T_{EM}))[89]. The central memory population of T cells exist at an intermediate stage of differentiation and on antigenic re-challenge can differentiate to T_{EM} cells. Recent evidence, however, suggests that during memory cell formation following viral clearance in mice $CD8^+$ T_{EM} convert to T_{CM} and that

antigenic re-challenge is required for T_{CM} to revert to effector T cells[85]. This implies that T_{CM} and T_{EM} cells are not distinct subsets, but actually represent part of a linear differentiation pathway. Lineage relationships between memory T cell subsets in humans have been proposed, but these studies have so far focused either on non-activated polyclonal T cell populations[89] or antigen-specific T cells in persistent viral infections, which may influence T cell differentiation[92-94]. Further research in humans and mice is required to clarify the pathways that lead to memory cell formation and determine whether different mechanisms govern this in $CD4^+$ and $CD8^+$ T cell subsets.

Unlike naive cells, $CD4^+$ and $CD8^+$ T memory cells do not require exposure to antigen and/or MHC molecules for their survival, but may be dependent on a low level of proliferation[6;77;95;96]. IL-7 and IL-15 play an important role in mediating memory $CD8^+$ T cell survival and proliferation respectively[6;77]. Interestingly, a recent study showed that the IL-7 receptor is selectively expressed on approximately 5-15% of effector $CD8^+$ T cells and identifies the precursors of the surviving memory cell population[97]. The mechanisms that regulate $CD4^+$ T cells are less well defined[6;77], but IL-7 may also act as an important survival factor[98]. Stromal factors such as type 1 IFNs are recognised to rescue T cells from apoptosis[78-81], and may mediate memory T cell survival via the production of IL-15[99]. In the absence of further infection, antigen-specific memory $CD8^+$ T cells appear to be more stably maintained in comparison to memory $CD4^+$ T cells[43]. Heterologous viral infection, however, can substantially reduce the frequency of pre-existing memory $CD8^+$ T cells, whereas the frequency of memory $CD4^+$ T cells appears to be relatively unaffected[100]. These differences suggest that the $CD4^+$ and $CD8^+$ T cell pools are differentially regulated.

Interestingly, recent evidence in mice points to the localisation and persistence of memory cells in non-lymphoid tissues as well as secondary

lymphoid organs[11;101-104]. These cells appear to play an important role in protective immunity[102;104], although their function seems to be independent of proliferation since some studies have suggested that memory T cells resident within non-lymphoid tissues do not expand when they are re-activated[10-12]. This is probably a result of the non-lymphoid microenvironment rather than an intrinsic property of the cells, because antigen-specific memory T cells isolated from non-lymphoid tissue have been shown to proliferate *in vitro*[10]. Evidence in mice, therefore, suggests that antigen-specific T cells do not proliferate within non-lymphoid tissues during primary[8;9] and secondary immune responses[10-12].

1.2.4 Characteristics of memory cells

Memory or recall immune responses occur more rapidly and are more pronounced than primary responses[4-6]. The increase in frequency of antigen-specific cells within the memory T cell pool plays a significant role in mediating this heightened responsiveness[43;46;85;105]. Memory T cells, however, also exhibit qualitative differences that play a vital role in enhancing reactivity[106-108]. Indeed, some evidence suggests that these qualitative changes may be more important than an increased precursor frequency[108;109]. Qualitative changes appear to result in less stringent memory T cell activation requirements compared to naive cells[106]. Studies have shown that memory T cells can respond to lower concentrations of antigen, a shorter duration of antigenic stimulation and less costimulatory signals than naive T cells[106]. Furthermore, entry into cell cycle following TCR stimulation occurs more quickly[108]. In murine $CD8^+$ T cells, this can be explained by the high expression of cyclin-dependent kinase 6 in a preactivated state, which favours rapid cell division after re-challenge with antigen[110]. Effector function also develops more rapidly in activated memory T cells, as a result of increased expression of effector cytokine mRNA[108] and associated epigenetic changes that are incurred following the naive to memory transition process[48;51-53]. Memory T cells also express different patterns of adhesion molecules and chemotactic receptors, which

enhances their ability to interact with APCs and allows their migration into inflamed non-lymphoid tissues[6;106].

Unlike the B cell receptor, the TCR on T cells does not appear to undergo somatic hypermutation. Affinity maturation within the T cell pool may, however, be mediated by the selection of clones that express TCRs with higher antigenic affinity. In support of this concept in humans, it is recognised that effector and memory cells exhibit a more limited TCR repertoire in comparison to naive cells[111]. Furthermore, clonal expansions in the $CD8^+$ T cell subset are detected with increasing frequency with age[112] and are known to persist following acute viral infection[42]. In contrast, clonal expansions in the $CD4^+$ T cell subset are rarely detected in the peripheral blood with increasing age[112] and are not detected during acute viral infection[42]. Studies in mice suggest that antigenic challenge leads to the selective expansion of high affinity clones and this results in decreasing TCR diversity[106;113-117]. Most of this work focused on $CD8^+$ T cells, but decreased TCR diversity in $CD4^+$ T cells following antigenic challenge suggests that affinity maturation can also occur in this subset. High affinity clones appear to be better at interacting with APCs and consequently prevent the expansion of low affinity clones[118]. Indeed, recent evidence suggests that they may strip antigen from the surface of APCs and therefore prevent antigenic peptide being exposed to low affinity clones[119].

1.2.5 Markers of memory and effector T cells

CD45 isoforms

Tracking the differentiation of T cells during an immune response relies on the use of various markers to identify the naive, effector and memory subsets. The Leucocyte Common Antigen (CD45) exists as a number of different isoforms, which for over a decade have been used to differentiate naive from effector and memory T cells[120]. CD45 is a receptor-like protein

tyrosine phosphatase (PTP), which is expressed on nucleated haematopoietic cells including all leucocytes and comprises up to 10% of their cell surface[121]. The precise function of CD45 has yet to be elucidated, but it appears to play a critical role in T cell signal transduction[121-123] and deficiency in humans and mice results in severe combined immune deficiency (SCID)[124]. A ligand for CD45 has yet to be identified, but structural similarities with other receptor tyrosine kinases with defined ligands supports the presumption that a specific ligand does exist[121;122]. Different isoforms are formed by the alternative splicing of exons 4-6, which have been designated A-C respectively. CD45RA antibody detects the isoform that results from the expression of exon 4, whilst CD45RB and CD45RC antibodies detect isoforms formed by the expression of exons 5 and 6 respectively. Absent expression of these exons results in the smallest isoform, which is detected by the CD45RO antibody.

The relative expression of the various CD45 isoforms depends on the state of T cell differentiation (Figure 1.2). The CD45RA isoform is expressed on all naive T cells, whereas following T cell activation expression of CD45RO is rapidly up-regulated and CD45RA is lost over the course of a few days[7]. All $CD45RA^+$ naive $CD4^+$ T cells also express high levels of CD45RB, whereas primed $CD45RO^+CD4^+$ T cells can be subdivided into high and low CD45RB expressing subsets[73]. $CD45RO^+CD45RB^{high}CD4^+$ T cells have been relatively recently primed, whereas $CD45RO^+CD45RB^{low}CD4^+$ T cells have undergone numerous rounds of division and are more highly differentiated[73]. Interestingly, evidence in humans has recently shown that a large proportion of memory $CD8^+$ T cells can re-express CD45RA and lose CD45RO expression in a process that has been referred to as reversion[46;92;112;125-127]. Unlike naïve $CD8^+$ T cells, revertant memory cells express high levels of LFA-1 (leucocyte function-associated antigen-1) and low levels of L-selectin (CD62L) and the chemokine receptor CCR7. Memory $CD8^+$ T cells are, therefore, comprised of $CD45RA^-CD45RO^+$ and $CD45RA^+CD45RO^-$ subsets[125]. The exact role of $CD45RA^+$ revertant memory cells has yet to be clarified[92;126], but they may form a more stable, non-cycling memory

population[126]. CD45RA and CD45RO can be used more reliably to differentiate naive and effector / memory populations in the $CD4^+$ T cell subset, although limited evidence suggests that a small minority of $CD4^+$ memory T cells can also revert from the $CD45RO^+$ to the $CD45RA^+$ phenotype[112;128;129]. Other markers are, therefore, often used to identify memory T cell populations.

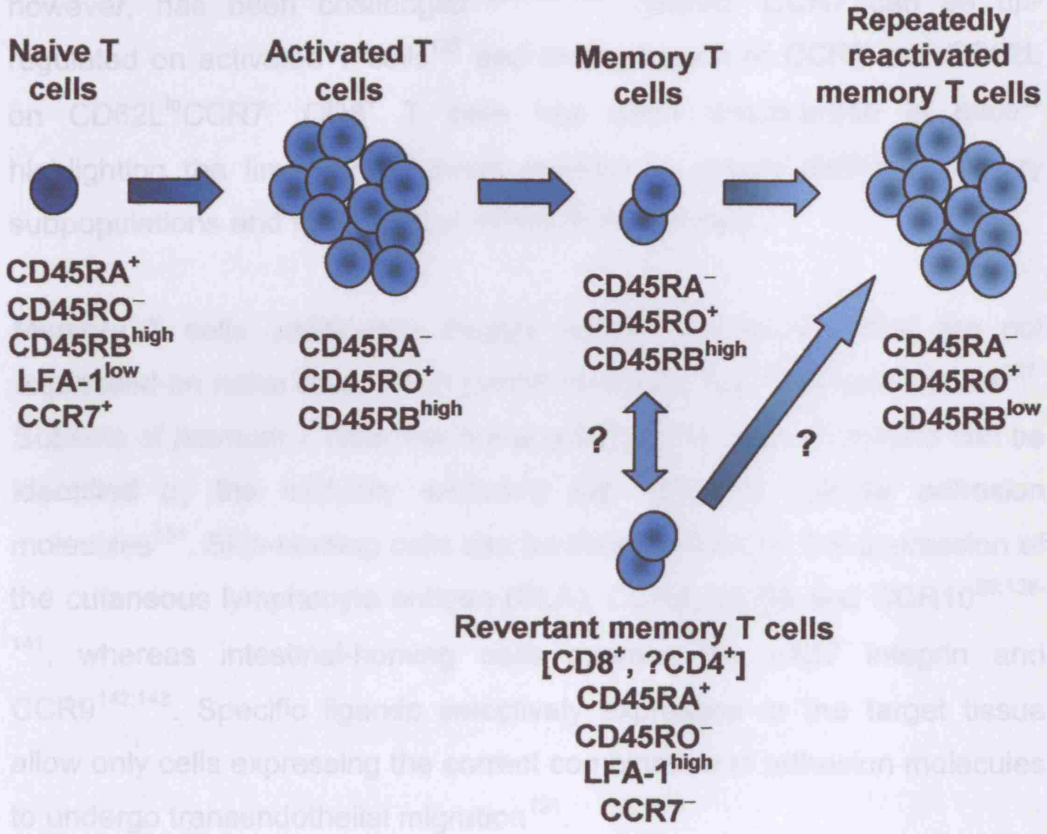

Figure 1.2 The identification of T cell subsets using CD45 isoforms

CD45RA, CD45RO and CD45RB can be used to identify $CD4^+$ T cell subsets. The use of these markers is less specific in $CD8^+$ T cells, since memory $CD8^+$ T cells can re-express CD45RA and lose CD45RO expression i.e. revertant memory T cells.

Other markers

In mice, high expression of CD44 is often used to identify memory cells[6], but this is not apparent in humans. L-selectin (CD62L) and the chemokine

receptor CCR7 mediate the entry of T cells into secondary lymphoid tissues[130;131] and their relative expression has been used to identify subsets of memory T cells[89]. CD45RA$^-$ memory T cells can, therefore, be subdivided into CD62L^{hi}CCR7$^+$ and CD62L^{lo}CCR7$^-$ subpopulations, which equates with the putative T_{CM} and T_{EM} subsets respectively[89;132]. Indirect evidence in mice also supports the concept of T_{CM} and T_{EM} subsets[101;102]. The use of CCR7 and CD62L to distinguish two functional subsets, however, has been challenged[85;92;133-136]. Indeed, CCR7 can be up-regulated on activated T cells[137] and re-expression of CCR7 and CD62L on CD62L^{lo}CCR7$^-$ CD8$^+$ T cells has been documented in mice[85] highlighting the limitation of these markers in clearly defining memory subpopulations and their cellular differentiation status.

Memory T cells additionally display adhesion molecules that are not expressed on naive cells, which permit homing to non-lymphoid tissues[131]. Subsets of memory T cells that home either to the skin or intestine can be identified by the mutually exclusive expression of specific adhesion molecules[131]. Skin-homing cells can be distinguished by the expression of the cutaneous lymphocyte antigen (CLA), CCR4, CCR8 and CCR10[20;138-141], whereas intestinal-homing cells express the $\alpha4\beta7$ integrin and CCR9[142;143]. Specific ligands selectively expressed in the target tissue allow only cells expressing the correct combination of adhesion molecules to undergo transendothelial migration[131].

T cell activation results in the up-regulation of CD25 and CD69, which are frequently referred to as activation markers. CD25 is the high affinity α-chain of the IL-2 receptor (IL-2R), which is up-regulated, although only transiently, on recently activated CD4$^+$ T cells[144;145]. It has, however, recently been recognised that CD25 identifies a subpopulation of resting memory CD4$^+$ T cells that when activated demonstrated suppressive activity[146-148]. CD69 is a phosphorylated type II transmembrane glycoprotein belonging to the C-type lectin family, activation of which may enhance T cell function[149]. It is undetectable in resting T cells, but is

rapidly expressed early after triggering of CD2 or the TCR/CD3 complex[150-152]. CD69 is transiently expressed in activated T cells *in vitro*[153;154], but recent *in vivo* data in mice has shown that the majority of memory T cells isolated from non-lymphoid tissues continue to express CD69 long after antigenic clearance[103;155;156]. The consequences of maintaining this activated phenotype are unknown.

The loss of expression of the co-stimulatory molecules CD27 and CD28 on memory T cells can also be used to identify cells with a more highly differentiated phenotype[93;157-159].

A specific and stable marker for effector and memory T cells, therefore, remains to be elucidated. Class I tetramers are used to detect expanded populations of antigen-specific $CD8^+$ T cells, which in the absence of adoptive transfer strategies can be regarded as being virtually all of memory phenotype. The application of tetramer technology to $CD4^+$ T cells has yet to be established. The expression of the $CD45RA^-CD45RO^+$ phenotype, therefore, currently represents the best method of identifying memory $CD4^+$ T cells in humans.

1.3 Potential constraints on T cell responses

The induction of T cell apoptosis mediated by AICD and ACAD represents the best-characterised constraint on cellular expansion during an immune response. Other potential mechanisms that may limit the magnitude of an immune response include T cell replicative senescence, anergy and active immune suppression mediated by regulatory T cells. The exact immunoregulatory role that these factors play *in vivo* has yet to be elucidated.

1.3.1 Telomeres, telomerase and replicative senescence

Replicative senescence

Normal somatic cells have a limited capacity for division, and when this limit is reached the cells enter a state known as replicative senescence[160;161]. This is sometimes referred to as the 'Hayflick limit' in recognition of the seminal experiments performed by Leonard Hayflick, who demonstrated that normal human fibroblasts are restricted in the extent to which they can divide *in vitro*[162]. Replicative senescence is characterised by a state of irreversible growth arrest, which can result in selected changes in cell function and for some cell types resistance to apoptosis[160;161;163]. Molecular changes include the expression of senescence-associated β-galactosidase activity and presence of unusual heterochromatic foci[163]. This obviously has critical implications for T and B cells that are dependent on massive clonal expansion in order to mount an effective immune response to combat each episode of antigenic challenge. Senescence can be induced by a number of different stimuli that result in physiological stress. These include oxidative damage of DNA, expression of certain oncogenes, supraphysiological mitogenic signals and induction of chromatin decondensation[161;164;165]. However, it is thought that the leading mechanism, which results in the replicative senescence of somatic cells, is telomere shortening[13;166;167]. This is considered to be a strategy for preventing malignant cellular expansion. Indeed, the ability to by-pass telomere-induced senescence is thought to be critical in the development of malignancy[168].

Telomeres

The ends of linear chromosomes are made up of complexes of repetitive DNA and proteins known as telomeres, which protect chromosomes from end-to-end fusion and prevent the degradation of coding non-telomeric DNA[169;170]. Telomeres 'cap' the ends of chromosomes, preventing them from being recognised as double-strand (ds) DNA breaks that can lead to the activation of DNA repair mechanisms and growth arrest[171;172]. The protective effect of telomeres is complemented by the interaction of

telomerase, which is a ribonucleoprotein reverse transcriptase that can elongate telomeres[169;173]. In mammalian cells, telomeric DNA consists of hexanucleotide repeats of TTAGGG, which form a tract of duplex repeats that ends in a much shorter single-stranded G rich 3' overhang[169;170] (Figure 1.3). It is thought that telomeres form a T-loop that results from the insertion of the G-rich 3' overhang into a D-loop formed far back in the ds-DNA telomere tract[174;175] (Figure 1.4). Recent evidence has demonstrated that the 3' overhang sequence can trigger cell senescence, suggesting that a stable telomere T-loop structure acts to conceal the 3' overhang from the internal cellular milieu[176-178]. The capping process involves the binding of a number of different telomeric DNA-binding proteins that stabilise the T-loop and also play a role in regulating telomere length[169-171] (Figure 1.4).

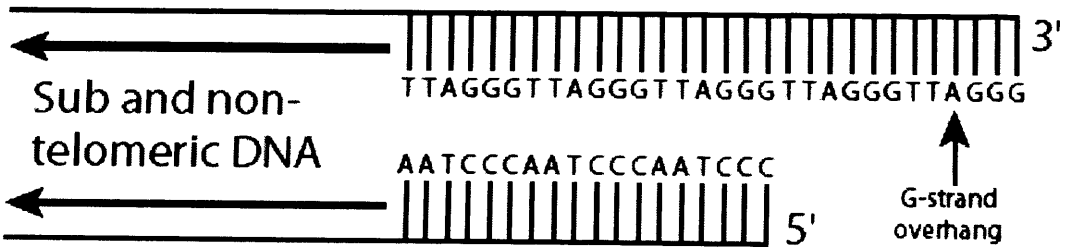

Figure 1.3 Structure of telomeric DNA

Telomeric DNA consists of hexanucleotide repeats of TTAGGG, which form a tract of duplex repeats that ends in a much shorter single-stranded G rich 3' overhang.

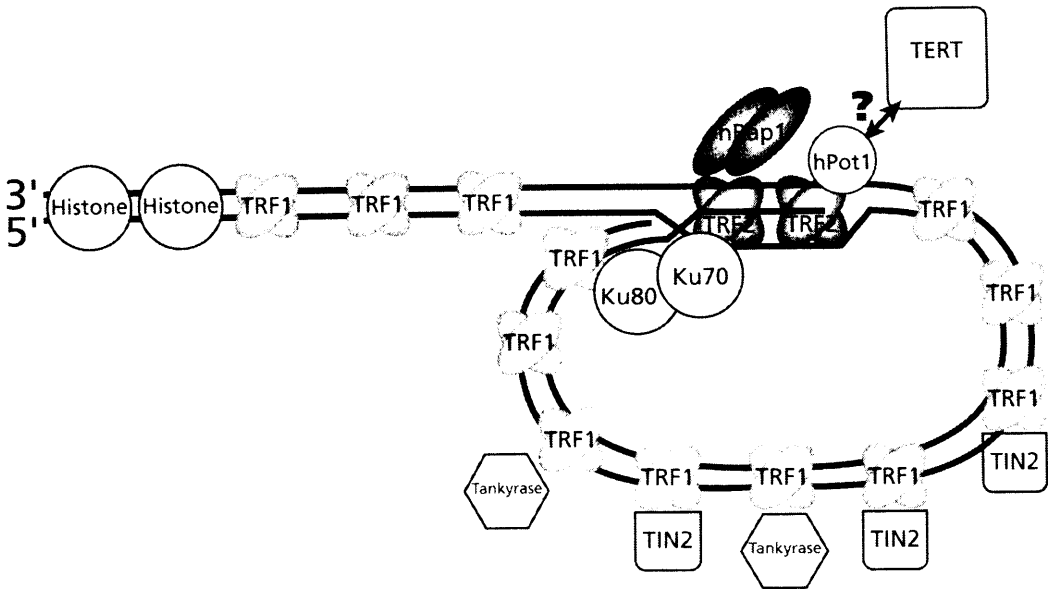

Figure 1.4 Human telomere T-loop structure and associated proteins

Telomeres form a T-loop that results from the insertion of the G-rich 3' overhang into a D-loop formed far back in the ds-DNA telomere tract. DNA-binding proteins stabilise the T-loop and also play a role in regulating telomere length. Telomeric repeat-binding factor 1 (TRF1) and TRF2 form homodimers that bind directly to duplex telomeric DNA via a single Myb-like motif in each C-terminal region[179]. TRF2 is preferentially located at the 3' overhang D-loop insertion site and appears to be critically involved in T loop formation[174]. TRF2 as well as TRF1 may act as negative regulators of telomere length since over-expression leads to telomere shortening[180]. Tankyrase may regulate the access of telomerase to the telomeric complex, since over-expression displaces TRF1 and results in telomere elongation[181]. TIN2 on the other hand probably acts as a negative regulator of telomere length through TRF1[182]. The Ku70/Ku80 heterodimer (Ku) can interact with TRF1 or TRF2 and is essential for chromosome stability. Ku can also associate with telomerase and may therefore represent another control that regulates access of telomerase to the telomeric DNA[183]. Human Rap1 localises to telomeres in a TRF2-dependent manner and over-expression leads to telomere elongation[184]. Pot1 (protection of telomeres 1) binds directly only to single-stranded telomeric DNA, but co-localises with TRF2 and Rap1. Recent evidence suggests it may facilitate telomere elongation by telomerase[185]. It is essential for chromosome stability and is believed to act as an additional mechanism by which the single-stranded mechanism 3' overhang is concealed[186;187].

The critical importance of telomeres lies in the fact that DNA is not fully replicated during cell division. A labile RNA primer is required to initiate unidirectional replication by DNA polymerase, and this occurs at multiple

origins in eukaryotic chromosomes creating numerous replicons[188]. DNA replication is characterised by a Y-shaped replication fork composed of parental duplex DNA and two daughter duplex strands consisting of one parental and one newly synthesized daughter strand (Figure 1.5). DNA polymerase, however, can only replicate DNA in a 5' to 3' direction and is unable to fully replicate the 5' end of the lagging daughter strand, creating the so-called 'end-replication problem[189]. The presence of telomeres at the ends of the chromosomes means that the coding portion of the genome is fully replicated and only non-coding telomeric DNA is lost. Interestingly, 3' overhangs are present on both telomeres and this is thought to result from additional end processing by nucleases[190;191].

In the absence of compensatory mechanisms, 50-200 base pairs (bp) of telomeric DNA are lost with each cell division[189;192;193]. Repeated cell division, therefore, results in progressive telomere shortening until a critical length is reached when cell cycle arrest and replicative senescence are triggered[194]. In humans, telomeres measure from 5 to 15 kilobases (kb) in length. Senescence has been reported to be triggered in human fibroblasts cultured *in vitro*, when the mean telomere length measures between 6.3 and 8.3 kb[195]. Telomere length can, therefore, be used to give an indication of a cell's residual replicative capacity. To be more precise, it is the length of the shortest telomere rather than the average telomere length that probably determines the residual replicative capacity and when telomere dysfunction is triggered[196].

In comparison to humans, most laboratory mice (e.g. *Mus musculus domesticus)* have considerably longer telomeres that range from 20 to 150 kb in length[171;180;197]. It is also noteworthy that the average human lifespan is substantially longer than in mice. This has led some investigators to question the validity of extending the results of studies on telomeres in mice to humans[13-15]. A related mouse species (*Mus spretus*) does have

telomeres similar in length to those in humans, but this has not yet been used to study lymphocyte telomere biology.

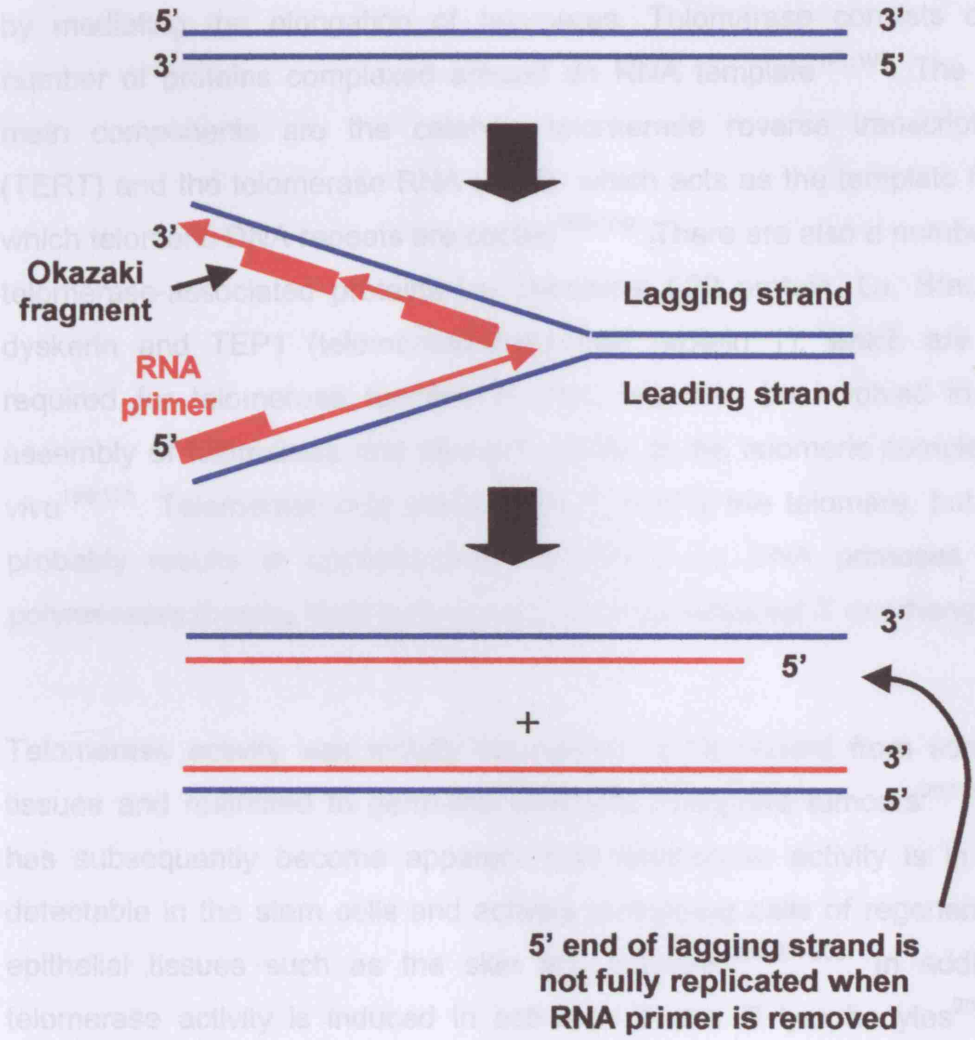

Figure 1.5 The DNA end-replication problem

DNA polymerase can only replicate DNA in a 5' to 3' direction. The leading strand is synthesized as a continuous strand in the 5' to 3' direction and generates a blunt end. The daughter strand that grows in the 3' to 5' direction is synthesized discontinuously as a series of short fragments known as Okazaki fragments and is referred to as the lagging strand. The synthesis of an Okazaki fragment terminates just before the RNA primer of the preceding fragment. A gap is left when this primer is removed, and this is then filled by an exonuclease and DNA ligase[188;191]. The gap left by the RNA primer that initiated the synthesis of the final Okazaki fragment is, however, not filled leaving an un-replicated portion of DNA and a 3' overhang. Longer overhangs can be generated if the final RNA primer is laid down internal to the DNA terminus. The overall effect is one of telomere shortening.

Telomerase

The relationship between telomere length and replicative capacity is in fact more complex, because telomerase can compensate for telomere erosion by mediating the elongation of telomeres. Telomerase consists of a number of proteins complexed around an RNA template[171;198]. The two main components are the catalytic telomerase reverse transcriptase (TERT) and the telomerase RNA (TER), which acts as the template from which telomeric DNA repeats are copied[198-200]. There are also a number of telomerase-associated proteins i.e. ribosomal L22 protein, La, Staufen, dyskerin and TEP1 (telomerase-associated protein 1), which are not required for telomerase function *in vitro*, but may be involved in the assembly of telomerase and mediate activity at the telomeric complex *in vivo*[169;171]. Telomerase only extends the 3' end of the telomere, but this probably results in opposite-strand synthesis by DNA primases and polymerases thereby limiting the length of single-stranded 3' overhang[201].

Telomerase activity was initially considered to be absent from somatic tissues and restricted to germ-line cells and malignant tumours[202;203]. It has subsequently become apparent that telomerase activity is in fact detectable in the stem cells and actively multiplying cells of regenerative epithelial tissues such as the skin and intestine[198;204-206]. In addition, telomerase activity is induced in activated T and B lymphocytes[207-211]. Similarly, low levels of telomerase expression have recently been demonstrated in normal human fibroblasts as they pass through the S phase of cell cycle[212]. Indeed, telomerase activity appears to be closely associated with entry into cell cycle and proliferation[213-216].

The importance of telomerase *in vivo* has been documented by studying telomerase-deficient mice generated by the inactivation of the TER genes[217-219]. First generation mice are normal, but successive generations of intercrossed TER knockout mice demonstrate progressive telomere shortening. By the sixth generation, mice are infertile and exhibit

premature greying, alopecia, intestinal villous atrophy, delayed wound healing and impaired bone marrow regeneration following haemopoietic ablation. Furthermore, T and B cells from these mice showed reduced proliferative responses to mitogens *in vitro*. These mice had shorter lifespans compared to wild-type and earlier generation knockout mice, but they did not exhibit an increase in other age-related changes such as osteoporosis, cataracts or atherosclerosis[217-219]. This points to a critical role for telomerase in the maintenance of proliferative tissues. Interestingly, there was a higher frequency of spontaneous malignant tumours, although subsequent studies have shown that these mice are resistant to skin carcinogenesis[220]. This indicates the importance of telomeres in promoting chromosomal stability, but also highlights the complexities of cell immortalisation.

Evidence for a role for telomere length and telomerase in human biology is observed in individuals with dyskeratosis congenita. This condition is characterised by abnormal skin pigmentation, nail dystrophy, and mucosal leukoplakia as well as bone marrow failure[221]. X-linked and autosomal dominant forms are recognised that encode for mutations affecting dyskerin[222] and TER respectively[223]. These patients have reduced telomerase activity and short telomeres for their age[223;224]. The majority of individuals eventually develop aplastic anaemia and die from infection in the second decade of life[221].

Telomerase, therefore, appears to play an important role in determining replicative capacity, although the induction of senescence probably reflects interplay between telomerase activity and telomere length[169;212;225]. Indeed, some TERT transfected cells have been found to have shorter telomeres than senescent control cells[173;226] suggesting that telomerase may have a direct protective effect against the induction of senescence. It is thought that the telomere-protein complex exists in equilibrium between capped and uncapped states[169]. Long telomeres favour the capped

conformation whether or not telomerase is present, but with shortening the telomeric-protein complex is more likely to become uncapped. This allows telomerase to access the telomere-protein complex and protect the uncapped chromosome either by mediating telomere elongation resulting in recapping or through an as yet unknown protective mechanism[169]. Telomere erosion in telomerase negative cells is, therefore, more likely to result in uncapping and senescence than telomerase positive ones.

Telomere length and immunosenescence

Aging is associated with an increased incidence of infections and autoimmunity coupled with increased morbidity and mortality[227]. This reflects a progressive decline in immune function, which has been referred to as immunosenescence[228]. This deterioration appears to predominantly involve the adaptive immune system and in particular affects T cells[228]. Thymic tissue becomes progressively replaced with adipose tissue with increasing age and there is an associated decline in naive T cell output although the thymus remains capable of immune reconstitution albeit more slowly[229]. The decline in thymic function is also reflected by an increase in $CD45RO^+$ memory T cells with a more differentiated $CD28^-$ phenotype, which is particularly evident in the $CD8^+$ subset. Expansion of the memory T cell pool is additionally characterised by an increasingly oligoclonal pattern of diversity[112;230]. These changes are associated with a decline in T cell mediated immunity *in vivo*[231-233], although there is a lack of quality studies to confirm these findings.

The role that telomere shortening and senescence play in the decline of T cell function is unknown. Certainly, it is recognised that T cells manifest only limited replicative capacity *in vitro* and usually cannot be expanded beyond 20 to 40 population doublings[234]. Evidence that immune responses *in vivo* impact on the telomere length of lymphocytes is provided by the observation that the telomeres in naive $CD4^+$ and $CD8^+$ T cells are longer than those in memory cells[193;235;236]. A consequence of this telomere erosion is a reduction in T cell replicative capacity *in vitro* and

memory $CD4^+$ T cells have been shown on average to achieve 7 fewer population doublings than naive cells[193]. Telomeres in $CD28^+CD8^+$ T cells have also been shown to be longer than those in the $CD28^-$ subset, providing further evidence that telomeres shorten with increasing cellular differentiation[237]. Interestingly, naive and memory B cells in humans have similar telomere lengths whilst tonsil germinal centre B cells actually having longer telomeres than either of these two subsets[211]. High levels of telomerase activity have been found in the germinal centre B cells, indicating that telomerase plays an active role in the maintenance and elongation of telomeres in activated B cells *in vivo* [211].

Telomere shortening has also been observed in T and B cells with increasing age[193;235;238]. The rate of telomere erosion, however, is most pronounced during infancy, particularly in the memory $CD4^+$ T cell subset[235]. The decline in telomere length thereafter is more gradual and overall ranges from 34 to 54 bp per year according to the T cell subset[235]. Both naive and memory T cell subsets are affected by telomere shortening with increasing age, but memory T cells exhibit a higher rate of telomere loss than naive T cells (51-54 and 34-39 bp per year respectively)[235].

Telomere shortening by 50bp per year would result in the loss of 2.5kb of telomeric DNA over 50 years[235]. It is still unknown what effect this has on immune function, but some authors have questioned whether at this rate of loss if T cell telomeres would actually become critically shortened during the lifetime of the average human[239]. The role that telomeres may play in the development of immunosenescence should become more apparent by studying specific subsets of cells, but to date only a limited number of studies have looked at antigen-specific populations of cells[240-244] and none has examined cells isolated from a non-lymphoid tissue.

Regulation of telomerase activity in lymphocytes

Telomerase activity in T and B lymphocytes is limited to activated cells. Induction of telomerase activity in T cells *in vitro* depends on activation

through the TCR (anti-CD3) with or without CD28 costimulation or via stimulation with phorbol myristate acetate (PMA) and ionomycin[207-210]. Telomerase activity is detected as early as one day after activation, peaks around day 3 and declines to basal levels thereafter[208;210;245]. The molecular mechanisms that regulate telomerase activity have yet to be elucidated, but appear to be dependent on protein kinase C (PKC) activity[207]. TER expression is increased following T cell activation, but it is also detectable in resting cells[207;245]. Similarly, expression of TERT is increased following activation, but is also present in resting cells when telomerase activity is negligible[246;247]. More recently, it has been demonstrated that T cell activation results in the phosphorylation of TERT which leads to its translocation into the nucleus coincident with increasing telomerase activity, whereas in resting T cells TERT was only detected in the cytoplasm[247]. The induction of telomerase activity following T cell activation is, therefore, associated with increases in TER and TERT expression and appears to depend upon the phosphorylation and nuclear translocation of cytoplasmic TERT.

A number of *in vivo* studies in mice and humans have demonstrated the induction of telomerase activity and maintenance of telomere length in antigen-specific T cells during acute immune responses[240-244]. The induction of telomerase *in vivo* can, therefore, maintain the telomere length of proliferating cells and consequently sustain replicative capacity during an acute immune response. These studies, however, have focused on lymphocytes isolated from the blood and secondary lymphoid organs. It is unknown whether the telomeres of cycling T cells that have migrated into an inflamed non-lymphoid tissue such as the skin are maintained. Interestingly, TER was not detected in lymphocytes migrating into the lesional skin of individuals with inflammatory skin conditions like psoriasis or allergic contact dermatitis[248]. In contrast, peripheral blood T cells isolated from patients with atopic eczema and psoriasis demonstrated increased telomerase activity and shorter telomeres compared to healthy volunteers[249;250]. In the long-term, it is likely that the maintenance of

telomere length in antigen-specific memory T cells is not sustained. Indeed, shortening has been observed in antigen-specific cells isolated over one year after acute Epstein-Barr virus infection[241]. This virus, however, results in persistent infection following the acute phase. It is unknown what happens to the telomere length of antigen-specific cells in the long-term following an infection in which antigen is completely cleared.

The potential functional importance of telomerase in T cell biology is highlighted by studies, which demonstrate that the lifespan of T cells can be extended by the ectopic expression of TERT[251-253]. Conversely, the inhibition of endogenous telomerase in T cells has been shown to result in the accumulation of cytogenetic abnormalities and a shortened lifespan[254]. Interestingly, the inhibition of telomerase did not result in generalised telomere shortening, but led to an increase in the frequency of very short telomeres in metaphase chromosomes[254]. This suggests that the prime targets for telomerase are the shortest telomeres, which are the least likely to be folded into a T-loop. Ectopic expression of TERT in T cells has also been shown to confer resistance to oxidative stress, which can induce telomere erosion[253]. Telomerase activity, therefore, appears to play an important role in determining the lifespan of T cells at least *in vitro*. It remains likely that the maintenance of telomere length following the induction of telomerase in activated T cells *in vivo* delays replicative senescence.

The level of telomerase activity induced does, however, decrease with repeated rounds of stimulation[254-256]. Indeed, as T cells in culture become close to senescence, very little telomerase activity is induced in comparison to the magnitude of telomerase up-regulation that is observed with the initial stimulation[255;256]. The decline in telomerase inducibility appears to be more pronounced in $CD8^+$ T cells than $CD4^+$ T cells. This decline correlates with decreased in CD28 expression[256], which may play a role in mediating optimal telomerase induction[208;256]. T cell telomerase

inducibility also declines with age *in vivo*[257;258], although this finding has not been consistently reported[259]. Telomerase activity may, therefore, only provide a limited extension to T cell lifespan so that the failure of telomerase inducibility with increasing differentiation represents an intrinsic cellular constraint on replicative capacity.

Telomerase activity can also be regulated by extrinsic factors such as cytokines. IL-7 has been shown *in vitro* to directly induce high telomerase activity in cord blood T cells independent of TCR activation[260]. On the other hand, IFN-α can inhibit telomerase in T cells *in vitro*[261]. TERT expression and telomerase activity in malignant T cell lines, leukaemic cells and activated normal T cells *in vitro* were down-regulated by more than 50-75% within 72 hours of exposure to IFN-α[261]. This effect was independent of any effects on proliferation. The mechanism of this inhibitory action is unknown, but it is of interest that type 1 IFNs, which include interferon-α, can mediate the translocation of other functional molecules such as protein kinase C delta (PKC-δ) from the nucleus back into the cytoplasm[262]. The effect of IFN-α on telomerase activity in T cells *in vivo* is unknown. IFN-γ, TGF-β and IL-4 have also been shown to inhibit telomerase activity in human tumour cell lines, but their effect on T cells is unknown[216;263-267].

Type 1 interferons and plasmacytoid dendritic cells

Type 1 interferons comprise of a number of different subtypes of interferon-α, as well as interferons β, (-δ), (-τ), -ω, -κ and a factor known as limitin[268-270]. These encompass a large group of closely related cytokines that exert their activity through a common heterodimeric receptor known as the IFN-α/β receptor, which is formed by two chains referred to as IFNAR1 and 2[270]. The type 1 IFNs exhibit potent anti-viral, anti-proliferative and anti-tumour properties. They also have immunoregulatory effects, which include increased $CD8^+$ T cell MHC class I expression, the enhancement of T and NK cell cytotoxicity and promotion of T_H1 cytokine polarisation[268;269;271] as well as rescuing T cells from apoptosis[78;79]. It is

thought that each type 1 IFN subtype interacts differently with the IFN-α/β receptor components leading to different signalling outcomes[270].

Whilst virtually all cells can secrete type 1 IFNs in response to viral infection, leucocytes represent the predominant source of IFN-α whereas IFN-β is secreted in particular by fibroblasts[271]. The key subset of leucocytes that produce IFN-α are plasmacytoid dendritic cells. They represent a distinct lineage of dendritic cells (DC) identified by the $CD14^-CD11c^-$, $CD123^+$ (interleukin-3 receptor α chain), $HLA\text{-}DR^+$, $BDCA\text{-}2^+$ (blood DC antigen-2) phenotype and constitute approximately 0.2-0.4% of peripheral blood mononuclear cells[268;272-275]. Plasmacytoid DCs are found in the bone marrow and lymphoid organs, but are virtually absent from normal skin[274;276-278]. This may be explained by their insignificant migratory response to chemokines that are constitutively expressed on dermal vascular endothelium[279]. Sizeable numbers, however, are present in the skin of a number of inflammatory dermatoses such as lupus erythematosus and allergic contact dermatitis[274;276;277;280], but interestingly are absent in atopic eczema[274]. Histamine has recently been shown to down-regulate IFN-α secretion by plasmacytoid DCs, which may provide an explanation for the low levels of type 1 interferons frequently found in the serum of atopic individuals[281].

Toll-like receptors (TLR) constitute a family of molecules that recognise distinct conserved microbial structures, which mediate DC activation and the induction of adaptive immune responses[1]. Plasmacytoid DCs express TLR7 and TLR9, which recognise viral single-stranded RNA[282] and bacterial DNA containing unmethylated CpG motifs respectively[283;284]. Indeed, plasmacytoid DCs have been shown to produce large amounts of IFN-α in response to a variety of pathogens such as herpes simplex virus, *Staphylococcus aureus* and *Mycobacteria tuberculosis*[273]. In addition, recent evidence suggests that the underlying inflammatory milieu may regulate the relative production of IFN-α by plasmacytoid DCs and thereby

dictate the polarisation of the resulting T cell response[285]. Plasmacytoid DCs, therefore, may play a role in not only initiating adaptive immune responses, but also in influencing its nature.

1.3.2 Regulatory T cells

In the past decade, it has become increasingly apparent that a subset of $CD4^+$ T cells has pronounced suppressive activity. These cells play an important role in not only maintaining tolerance to self antigens, but also in the regulation of immune responses to infection, tumours and transplants[148;286-288]. Attention has in particular focused on a naturally occurring subset of $CD4^+$ T cells that constitutively express CD25, although TGF-β secreting T_H3 and IL-10 secreting Tr1 $CD4^+$ regulatory T cell phenotypes have also been identified. Sakaguchi and colleagues were the first to demonstrate that organ-specific autoimmune disease could be induced in mice either by the adoptive transfer of $CD4^+$ T cells depleted of $CD4^+CD25^+$ T cells into athymic nude recipients[146] or by day 3 thymectomy[289]. Co-transfer or reconstitution of these mice with $CD4^+CD25^+$ T cells prevented the development of autoimmunity[146;289]. More recently, $CD4^+CD25^+$ regulatory T cells (T_{regs}) have been identified in humans[147;290-296]. Similarly to mice, they constitute 5-15% of the $CD4^+$ T cell subset and can be isolated from the peripheral blood, thymus and tonsils[147;290-296]. Activation of $CD4^+CD25^+$ T cells with polyclonal[147;291-296], allogeneic[293-296] or antigen-specific[290] stimuli results in the suppression of co-cultured $CD4^+CD25^-$ responder T cells.

$CD4^+CD25^+$ regulatory T cell phenotype

No definitive marker has yet been described for T_{regs}, although expression of CD25 remains the most practicable way to enrich for cells with regulatory activity[148]. The main limitation with CD25 as a marker is that it is transiently up-regulated on recently activated $CD4^+$ T cells[144;145;297]. T_{regs}, however, express CD25 constitutively and at higher levels than recently activated responder cells[292;298]. On the other hand, it is likely that regulatory activity is not entirely exclusive to the CD25 fraction. Indeed,

although CD25 expression on T_{regs} is lost following their transfer and expansion in severe combined immune deficiency (SCID) mice, the newly derived $CD25^-$ cells exhibit preserved suppressive actvity[299]. CD25, however, probably plays an indispensable role in the generation and maintenance of T_{regs}, since the development of spontaneous severe autoimmunity is observed in CD25 deficient, IL-2 deficient and CD122 (IL2-R β-chain) deficient mouse models as well as following the *in vivo* neutralisation of IL-2[288]. CD122 is constitutively expressed in human T_{regs}, but is also up-regulated following T cell activation[291-293;295].

T_{regs} in mice and humans are recognised to exhibit a differentiated $CD45RB^{low}$ and $CD45RA^-CD45RO^+CD45RB^{low}$ phenotype respectively[147;292;293;298;300;301]. In addition, T_{regs} in humans have been shown to have shorter telomeres than $CD4^+CD45RO^+$ T cells highlighting their highly differentiated state and indicating that they have experienced many rounds of division[290]. Human T_{regs} also express CD95 in conjunction with low levels of Bcl-2, suggesting that they are prone to apoptosis[147]. Indeed, T_{regs} are susceptible to apoptosis in culture, which can be prevented by IL-2 or IFN-β[147].

CTLA-4 (CD152) is constitutively expressed on T_{regs} in mice[300;302] and humans[147;291;293;294], but is also up-regulated on activated T cells. GITR (glucocorticoid-induced tumour necrosis factor receptor) represents another activation marker that is constitutively expressed on nearly all T_{regs}[303-306]. Interestingly, signalling through this molecule in mice abrogates suppressive activity[303;304]. In contrast in humans, ligation of GITR appears to have minimal or no effect in attenuating suppressive function[305;306]. Other non-specific markers that show preferential expression on T_{regs} include OX-40 (CD134)[147;303], CCR4 and CCR8[307].

More recently, the transcription factor *Foxp*3 has been identified as a possible discriminative marker for identifying T_{regs}[308-311]. *Foxp*3 encodes

Scurfin, which is a member of the forkhead/winged-helix family of transcription factors. Mutation of the *Foxp*3 gene in mice results in the Scurfy mouse phenotype, which exhibits X-linked recessive lethal autoimmune $CD4^+$ T cell hyperactivation[312]. The homologous X-linked recessive condition in humans is IPEX (immune dysregulation, polyendocrinopathy, enteropathy, X-linked syndrome), which is characterised by mutation of the *Foxp*3 gene and autoimmune disease of multiple endocrine organs, inflammatory bowel disease (IBD), atopic eczema and fatal infections[313;314]. *Foxp3* is specifically expressed in T_{regs} and $CD4^+CD8^-CD25^+$ thymocytes, but not in activated responder $CD4^+CD25^-$ T cells in mice[308-310]. Transduction of *Foxp*3 into naive $CD4^+CD25^-$ T cells converted them into $CD4^+CD25^+$ T_{reg}-like cells. F*oxp*3 has, therefore, become regarded as the master control gene for the development and function of T_{regs} in mice. In contrast to mouse studies, stimulation of human $CD4^+CD25^-$ T cells *in vitro* has been reported to result in the expression of *Foxp*3 in a proportion of the activated cells, although this did correlate with the development of suppressive function[311]. *Foxp3* is a nuclear protein and it is, therefore, of limited value as a tool to isolate T_{regs}. Analysis of genes linked to *Foxp3,* however, has identified neuropilin-1 as potentially useful marker of $CD4^+CD25^+$ T_{reg} cells[315].

On the basis of *in vitro* experiments, murine and human T_{regs} had been regarded until recently as having an anergic phenotype, because they failed to proliferate following TCR stimulation and secreted little or no IL-2[147;291;294;316;317]. The anergic/suppressive state, however, could be reversibly abrogated *in vitro* by TCR stimulation in the presence of IL-2, CD28 co-stimulation and/or allogeneic mature DC[292;295;295;316;318], although not consistently so[293;294]. In addition, murine studies indicated that T_{regs} could undergo homeostatic expansion in lymphopenic hosts, suggesting that they might behave differently *in vivo*[299;319]. More recently, $CD4^+CD25^+$ T_{regs} have been shown to actively proliferate *in vivo* in response to antigenic stimulation and consequently acquire enhanced suppressive

activity[320-323]. It remains unclear whether T_{regs} can proliferate in humans *in vivo*.

Mechanism of $CD4^+CD25^+$ regulatory T cell mediated suppression

The precise mechanism by which T_{regs} suppress the activation and proliferation of other T cells is currently unknown and remains a matter of debate. Conflicting findings have implicated roles for cytokines, cell contact–dependent mechanisms and/or T_{reg}–mediated modification of APCs. Variable findings have been reported depending on whether studies have been performed *in vitro* or *in vivo*[288]. T_{regs}, however, do display a number of recognised cellular characteristics that relate to their suppressive function. Polyclonal or antigen-specific TCR stimulation is required in order for T_{regs} to exert suppressive function *in vitro*[290;301;316]. Indeed, TCR Vβ expression is diverse amongst T_{regs} and similar to $CD4^+CD25^-$ T cells, suggesting that T_{regs} can respond to a wide variety of antigens[290;316]. Once T_{regs} have been activated, they mediate suppression in an antigen non-specific manner[317]. Finally, T_{regs} not only block the expansion of $CD4^+CD25^-$ responder T cells, but also suppress their transcription and secretion of IL-2[291;292;301].

Human *in vitro* studies suggest that cell-contact dependent mechanisms are required in order for T_{regs} to exert their suppressive effects on $CD4^+$ and $CD8^+$ T cells[147;291-293]. This finding has been reciprocated in mouse studies[301;316]. The cell contact dependent suppressive mechanism may involve the down-regulation of expression of CD80 and CD86 on DCs[324]. More recently, it has been proposed that T_{regs} may render DCs tolerogenic by promoting DC tryptophan catabolism through the induction of endogenous indoleamine 2,3-dioxygenase in a CTLA-4 dependent manner[325;326]. Indeed, blockade of CTLA-4 in mice abrogates the suppressive effects of T_{regs} *in vivo*[300;302;327] and CTLA-deficient mice are characterised by a lethal lymphoproliferative and autoimmune syndrome[328]. Attenuation of suppression by anti-CTLA-4 in murine experiments *in vitro*, however, is not consistently observed[302], and CTLA-4

blockade has demonstrated no effect on the suppressive effect of human T_{regs} *in vitro*[292;294;295].

A role for IL-10 in mice *in vivo* has been demonstrated[319;327;329], but this has not been consistently supported by *in vitro* studies[301;330]. The production of IL-10 in cultures of human T_{regs} has been documented[291;293], but blocking studies resulted in no attenuation of suppressive effect[147;293;295;296]. Data on the role of TGF-β (transforming growth factor) are also conflicting[287;288;300;301;330;331;331-333], but human studies overall have failed to demonstrate a clear role for TGF-β in mediating suppression by T_{regs}[147;293;295;296]. It has, however, been suggested that T_{regs} in humans and mice may exert immunosuppressive effects by cell-cell interactions involving cell surface TGF-β1[331;334], although this mechanism has not received support from other authors[333]. Interestingly, recent *in vitro* studies have shown that human T_{regs} could mediate 'infectious tolerance' leading to the induction of a suppressive phenotype in $CD4^+CD25^-$ responder T cells. This process was cell contact dependent, whereas the anergised cells acted independently of cell contact by secreting IL-10 or TGF-β and were likened to Tr1 and T_H3 regulatory cells respectively[335;336]. These findings may provide a unifying mechanism, by which the discrepant data on cell contact and soluble factor mediated suppression may be explained[286;337].

Generation of $CD4^+CD25^+$ regulatory T cells

Strong evidence supports the thymic generation of T_{regs}[288;338], although accumulating data now suggests that these cells can also be generated in the periphery[339]. A number of lines of evidence support the involvement of the thymus. Firstly, mice that have been thymectomised 3 days after birth have reduced numbers of peripheral T_{regs} and develop spontaneous autoimmunity[289]. Interestingly, humans with thymic hypoplasia as a consequence of DiGeorge syndrome have been reported to have reduced numbers of $CD4^+CD25^+$ T cells[340]. In healthy mice and humans, approximately 5-10% of $CD4^+CD8^-$ thymocytes are $CD25^+$ and exhibit

suppressive function[291;341]. It has also been demonstrated that the adoptive transfer of $CD4^+CD8^-$ thymocytes that have been depleted of the $CD25^+$ fraction can also result in autoimmunity, which can be prevented by the co-transfer of $CD25^+$ thymocytes[341]. Lastly, the differentiation of $CD25^+CD4^+CD8^-$ thymocytes towards a regulatory phenotype is also supported by the observation that the *Foxp*3 expression in the thymus is specifically limited to this population[308;310].

The additional peripheral generation of T_{regs} overcomes a number of possible restrictions imposed by thymic generation. Firstly, the thymic selection of T_{regs} is driven by interactions with self-peptides and class II MHC, which might preclude responsiveness to exogenous antigens and endogenous antigens that are not thymically expressed. Secondly, involution of the thymus with aging might result in a progressive decrease in T_{reg} numbers. Thymically generated T_{regs} might, therefore, be supplemented by peripherally generated ones, which would ensure a full repertoire of T_{reg} specificities capable of preventing immunopathology. The same pioneering mouse studies that demonstrated the importance of the thymus in the generation of T_{regs}, also provides evidence for their peripheral generation. $CD4^+CD25^+$ T cells were initially absent during the first week after thymectomy, but progressively reappeared, indicating the peripheral development of T_{regs} from $CD4^+CD25^-$ T cells[289] Indeed, subsequent studies have confirmed that $CD4^+CD25^+$ T_{regs} can be generated *in vivo* from $CD4^+CD25^-$ T cells independent of the thymus[330;332;342]. Furthermore, recent *in vitro* studies show that the stimulation of murine $CD4^+CD25^-$ T cells through the TCR and CD28 in the presence of TGF-β results in the induction *Foxp*3 expression and development of $CD4^+CD25^+$ T cells with a T_{reg}-phenotype[343].

Recently, our group has postulated that $CD4^+CD25^+$ regulatory T cells can be generated in the periphery in humans[290;339]. Our findings suggested that T_{regs} in humans are highly differentiated antigen-specific T cells that

encompass a diverse repertoire of specificities. Indeed, we showed that anergic/suppressive CTLA-4$^+$ CD4$^+$CD25$^+$ T cells could be generated *in vitro* from highly differentiated T cell clones upon non-professional antigen presentation (T-T presentation)[290]. We consequently proposed that, in addition to thymic generation, human T_{regs} might be generated in the periphery when highly differentiated cells encounter antigen presented in a non-professional manner[290;339] (Figure 1.6). The differentiation of T cells during an immune response could theoretically, therefore, result in the generation of T_{regs}, which might then contribute to the down-modulation of inflammation during resolution.

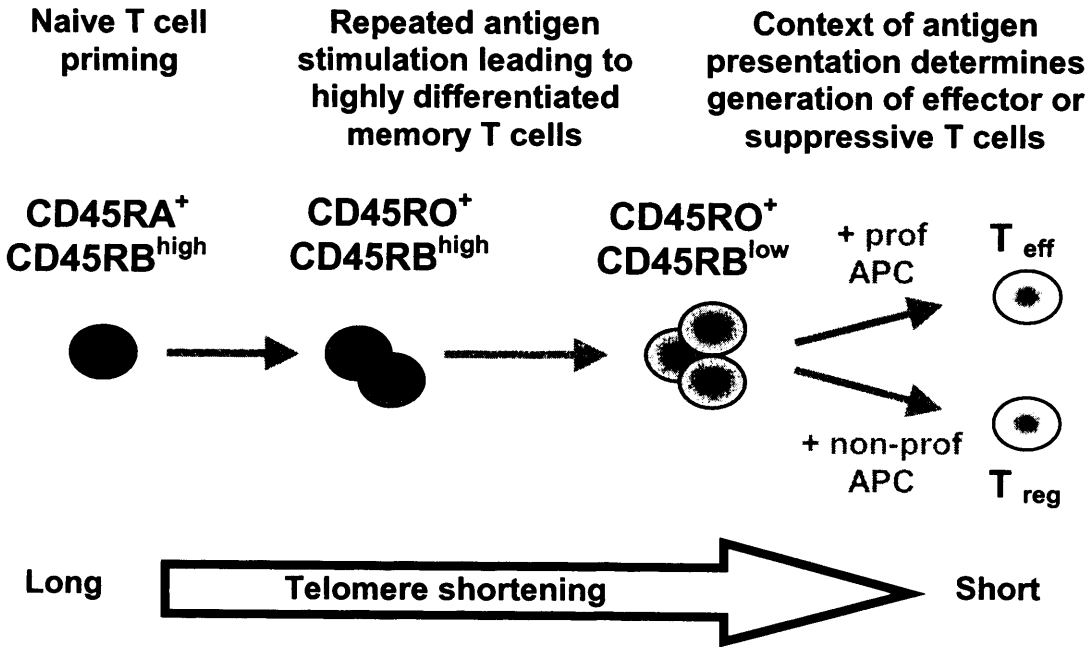

Figure 1.6 Model of T cell differentiation and generation of suppressive CD4$^+$CD25$^+$ T cells.

Naive T cells primed by antigen and APC lose CD45RA and acquire CD45RO expression. Primed cells are initially CD45RB^{high} and can secrete IL-2. Repeated stimulation by antigen leads to the generation of highly differentiated T cells with shortened telomeres and a CD45RB^{low} phenotype. Highly differentiated CD4$^+$ T cells exhibit diminished IL-2 secretion and are susceptible to apoptosis[73]. These cells may become effector (T_{eff}) or regulatory (T_{reg}) T cells depending on the context in which they encounter antigen.

$CD4^+CD25^+$ regulatory T cell function

T_{regs} are now believed to influence immunity in a number of different ways. One of the principle functions of T_{regs} is to prevent the development of autoimmunity resulting from the activation of self-reactive T cells that have escaped negative selection in the thymus[288]. T_{regs} have also been shown to mediate transplant tolerance[146;148] and maternal tolerance to the foetus[344]. In humans, they may be involved in maintaining tolerance to allergens such as nickel[345]. Interestingly, increasing evidence in mouse models suggests that T_{regs} may also play an important role in controlling immune responses to pathogens including viruses, bacteria and parasites. Indeed, T_{regs} may act to counter pathogen-induced immunity and limit the resulting immunopathology[346-349], but conversely may also mediate persistent infection[350;351], which may be necessary to maintain T cell memory[350]. On the other hand, T_{regs} may be used by pathogens to escape host immune responses[352]. From a therapeutic angle, some reports suggest that T_{regs} can suppress an on-going immune response[353;354] whereas others do not[355]. Finally, recent indirect evidence points to a possible role for T_{regs} in mediating the resolution of an immune response[346]. The functional role of T_{regs} during an on-going immune response in humans *in vivo* has yet to be determined.

1.4 Cutaneous immunity

The skin forms the body's largest interface with the environment and it therefore plays an important role in host defence. This is dependent not only on the mechanical structure of the skin as a physical barrier, but also on the dedicated cutaneous immune system that is involved in immunosurveillance and its protection. The importance of the immune component is highlighted by the increase in cutaneous malignancies and infections that is observed in immunodeficiency disorders[356] or in individuals that are receiving immunosuppressants[357]. Cutaneous immunity, however, like other aspects of the immune system, depends on tight regulation to prevent the development of inflammatory dermatoses,

many of which are T cell mediated e.g. psoriasis, atopic eczema and vitiligo[358].

The human skin is composed of four distinct immune compartments: 1) the epidermis, 2) dermis, 3) dermal lymphatic vessels and 4) dermal post-capillary venules (Figure 1.7)[358]. The epidermis is predominantly composed of keratinised epithelial cells known as keratinocytes (KC), but also contains resident intraepithelial lymphocytes and specialised DCs called Langerhans cells (LC). LCs are bone marrow derived DCs that contain tennis racket-shaped Birbeck granules and express Langerin, class II MHC, CD1a and E-cadherin, which mediates the attachment of LCs to contiguous KCs[359]. It is now recognised that KCs can also express class II MHC and produce IL-1α, TNF and anti-microbial peptides like β-defensins in response to various physical and pathogenic stimuli[360].

The dermis is mainly composed of connective tissue produced by fibroblasts, but also contains RFD1$^+$ and Factor XIIIa$^+$ dermal DCs, CD14$^+$CD68$^+$ macrophages, mast cells and occasional CD45RO$^+$ T cells most of which are located perivascularly[361;362]. Very few of the dermal or epidermal T cells express the $\gamma\delta$ chain TCR[363]. The dermis also contains a plexus of blood and lymphatic vessels.

Dermal lymphatic vessels play an important role in directing the migration of APCs and recirculation of lymphocytes from the skin to draining lymph nodes[364-366]. Distingushing the lymphatic vessels from the blood microvasculature has until recently been hampered by the lack of specific markers. For instance, the endothelial cell marker CD31 is expressed in both blood and lymphatic vessels. More recently, podoplanin, the vascular endothelial cell growth factor (VEGF)-C receptor, VEGFR-3 and in particular the hyaluronate receptor LYVE-1 have all been shown to be preferentially expressed in lymphatic endothelial cells as opposed to blood endothelial cells[364;367].

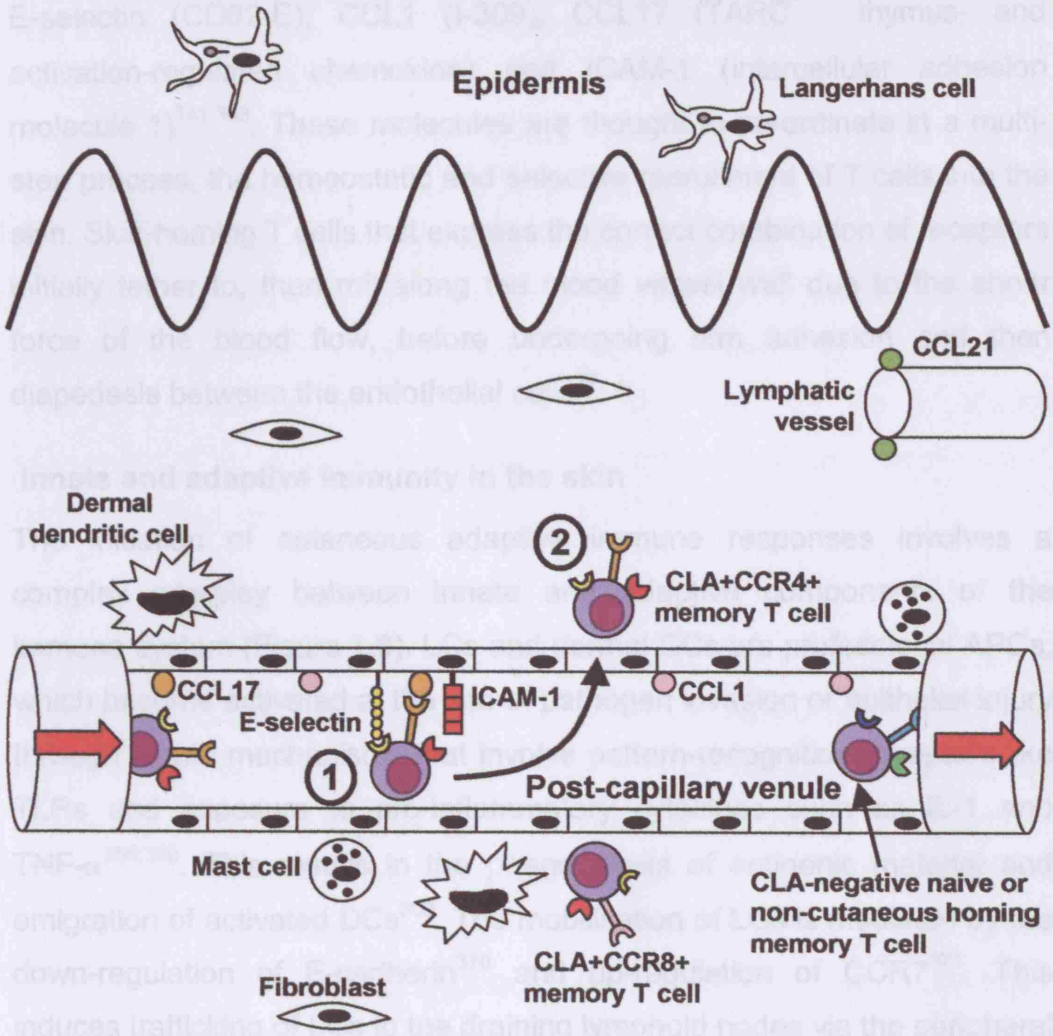

Figure 1.7 Schematic representation of the immune system in normal non-inflamed skin.

Immune cells resident in the epidermis include Langerhans cells and intraepithelial lymphocytes. The dermis contains dermal dendritic cells, mast cells and a few cutaneous lymphocyte antigen (CLA)-positive memory T cells. Endothelial cells of the dermal post-capillary venule constitutively express E-selectin, CCL1 / CCL17 and ICAM-1 at low levels. These factors mediate the (1) rolling, adhesion, arrest and diapedesis of $CCR8^+$ and $CCR4^+$ CLA^+ memory T cells into non-inflamed skin. This system controls the (2) homeostatic trafficking of skin-homing memory T cells into the dermis. CLA^- naive and non-cutaneous homing memory T cells pass through the dermal post-capillary venule. Gut-homing $\alpha4\beta7^+CCR9^+$ memory T cells lack the combined expression CLA and CCR4 or CCR8, and are unable to roll and adhere to the dermal vascular endothelium.

Dermal post-capillary venules constitutively express low levels of E-selectin (CD62-E), CCL1 (I-309), CCL17 (TARC – thymus- and activation-regulated chemokine) and ICAM-1 (intercellular adhesion molecule 1)[141;368]. These molecules are thought to co-ordinate in a multi-step process, the homeostatic and selective recruitment of T cells into the skin. Skin-homing T cells that express the correct combination of receptors initially tether to, then roll along the blood vessel wall due to the shear force of the blood flow, before undergoing firm adhesion and then diapedesis between the endothelial cells[27].

Innate and adaptive immunity in the skin

The initiation of cutaneous adaptive immune responses involves a complex interplay between innate and adaptive components of the immune system (Figure 1.8). LCs and dermal DCs are professional APCs, which become activated at the site of pathogen invasion or epithelial injury through innate mechanisms that involve pattern-recognition receptors like TLRs and exposure to pro-inflammatory cytokines such as IL-1 and TNF-α[358;359]. This results in the phagocytosis of antigenic material and emigration of activated DCs[369]. The mobilisation of LCs is mediated by the down-regulation of E-cadherin[370] and up-regulation of CCR7[371]. This induces trafficking of LCs to the draining lymphoid nodes via the peripheral lymphatics, which constitutively express CCL21 (SLC, secondary lymphoid-tissue chemokine), the ligand for CCR7[367;371;372]. Dermal lymphatic endothelial cells activated by exposure to TNF-α and IL-1 in fact upregulate CCL21 expression as well as CCL20 (MIP-3α, macrophage-inflammatory protein) and CCL2 (MCP-2, monocyte chemotactic protein), which are the ligands for CCR6 and CCR2 respectively[367;373]. It has been proposed that CCL21 and CCL20 derived from lymphatic endothelial cells may respectively serve to promote the recruitment of $CCR7^+$ and $CCR6^+$ T cells into inflamed skin[367]. Activated DCs undergo a process of maturation that enhances antigen processing and increases the expression of MHC class II, ICAM-1 and co-stimulatory molecules[359;374]. This ensures that antigenic peptides are optimally presented to antigen-specific T cells in the draining lymph node.

The capacity of primed memory and effector T cells to migrate into non-lymphoid tissues reflects their acquired expression of tissue-specific homing receptors that include selectins, selectin ligands, chemokine receptors and integrins[6]. The DCs and local microenvironment within cutaneous secondary lymphoid organs differentially direct the expression of these adhesion molecules and chemoattractant receptors, selectively targeting the effector T cells back to inflamed skin[20;375-377]. Cutaneous homing to inflamed skin is principally controlled by the combined expression of the cutaneous lymphocyte antigen (CLA), the integrin $\alpha 4\beta 1$ and chemokine receptors CCR4 or CCR10[378].

Cutaneous lymphocyte antigen

CLA identifies a subset of circulating primed T that can selectively localise to the skin. CLA is present on 10-15% of peripheral blood T cells and is restricted to the memory / effector subset[379]. In non-cutaneous tissues only about 5% T cells express CLA, whereas the vast majority (80-90%) of T cells infiltrating into inflamed skin are positive[380]. Indeed, CLA has been shown to be expressed on most T cells infiltrating the skin in atopic eczema, psoriasis, allergic contact dermatitis, erythema multiforme, cutaneous graft-versus-host disease, cutaneous T cell lymphoma and the Mantoux test[20;23;380-382]. Furthermore, circulating allergen-specific T cells from individuals with atopic eczema and allergic contact dermatitis are predominantly confined to the CLA^+ subset[381], as are virus-specific $CD8^+$ T cells in cutaneous viral infections[383]. CLA is also expressed on the majority of T cells in skin-draining lymphatics[384].

CLA expression has been previously demonstrated to be important in mediating interactions with E-selectin and the rolling of lymphocytes on the vascular endothelium[385-387]. The CLA epitope is an inducible cell surface post-translational glycosylation of P-selectin glycoprotein ligand-1 (PSGL-1), which is modified by the activity of $\alpha(1,3)$-fucosyltransferase VII (FucT-VII)[388]. Recent evidence, however, suggests that CLA is not the

ligand for E-selectin, but instead represents a marker for on-going or previous FucT-VII expression, which is pre-requisite for E-selectin ligand activity[389-392]. CLA expression on activated naive T cells is first observed after 3 days, reaches a maximum at day 5 and is maintained up to day 10 *in vitro*[20]. The expression of CLA, however, can be easily influenced by the *in vitro* culture conditions used[388;391;393;394]. TCR activation in the presence of TGF-β1, IL-6 or IL-12 have been reported to enhance CLA expression *in vitro*[20;393;395]. The mechanisms regulating CLA expression *in vivo* are unknown.

Skin-related chemokine receptors

A number of chemokines and their receptors are associated with the homing of T cells to the skin[138-140;396;397]. Specific interactions between chemokines expressed on the dermal endothelium and chemokine receptors on rolling T cells induces a rapid increase in the affinity of integrins resulting in the firm adherence of T cells and the initiation of transmigration across the endothelium[398;399]. Non-intestinal homing T cells express high levels of the α4β1 integrins, which interact with vascular cell adhesion marker-1 (VCAM-1) expressed on dermal endothelium[378].

CCR4 is the principal skin-homing chemokine receptor and is expressed on the vast majority of CLA^+ T cells, but not on $\alpha_4\beta_7^+$ intestinal homing cells[140]. The ligands for CCR4, CCL17 and CCL22 (MDC, macrophage-derived chemokine), are secreted by keratinocytes, DCs and macrophages in the skin[400;401], but only CCL17 has so far been identified on dermal endothelial cells[140;368]. CCR10 is expressed on approximately 30% of CLA^+CCR4^+ T cells[138;139;396], and its ligand CCL27 (CTACK, cutaneous T cell-attracting chemokine) is secreted by keratinocytes and may be displayed on the dermal vascular endothelium[138;402]. CCR4 and CCR10 seem to play overlapping and redundant roles in mediating the recruitment of T cells into inflamed skin[397]. In addition to CCR4 and CCR10, CCR8 and its ligand CCL1 have recently also been recognised to mediate the homeostatic traffic of T cells into normal non-inflamed human

skin[141]. CCL1 is expressed on endothelial cells as well as by Langerhans cells and melanocytes. CCR8 is present on 55 and 77% of $CD4^+$ and $CD8^+$ T cells in the skin respectively, and is absent on T cells in the intestine. Interestingly, cutaneous $CCR8^+$ T cells display a pre-activated inflammatory $CD69^+$ phenotype[141]. It is unclear whether CCL1 and CCR8 play a role in mediating T cell recruitment into inflamed skin. A number of other chemokines and their receptors may play a secondary relatively non-specific role in mediating T cell entry into inflammed skin e.g. CCR5, CCR6 and CXCR3[403-405].

Entry of T cells into cutaneous tissues is, therefore, determined by the combined expression of several molecules[358;378]. This mechanism results in the recruitment of skin-specific T cells in an antigen non-specific manner. Some authors, however, have proposed that MHC-peptide complexes expressed on endothelial cells may have a potential role for mediating the recruitment of antigen-specific cells or even the initiation of a secondary response[406].

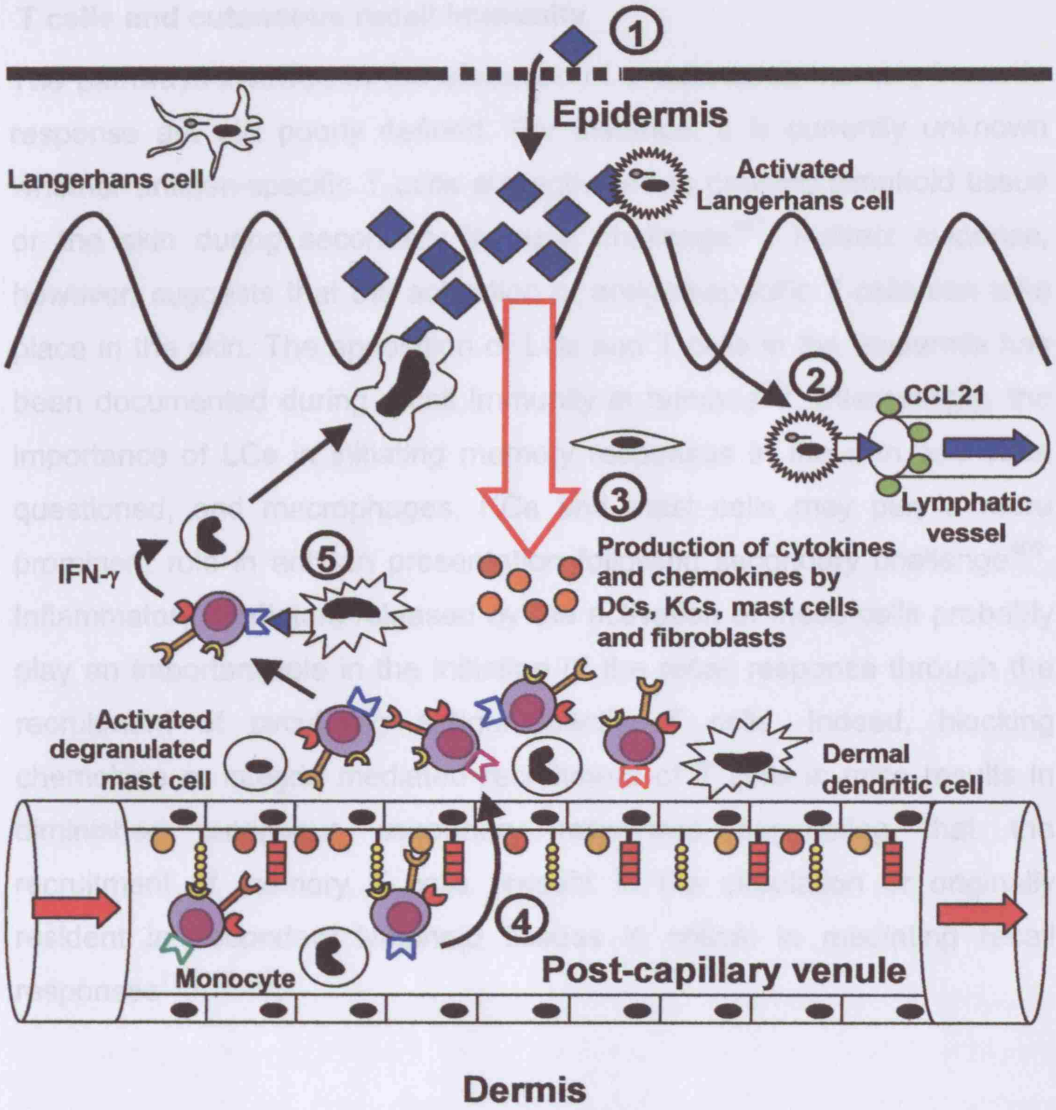

Figure 1.8 Schematic representation of an adaptive immune response in the skin.

(1) Antigenic infection of the skin results in resident innate immune cells (Langerhans cells, dermal dendritic cells and mast cells) becoming activated through Toll-like receptors, surface bound immunoglobulin and exposure to pro-inflammatory cytokines (IL-1 and TNF-α) that are released in response to epithelial cell damage. Activated LCs and dermal dendritic cells phagocytose and process antigenic material. (2) This results in their maturation and CCR7-CCL21 mediated emigration to draining lymph nodes where antigen is presented to naive or memory T cells. (3) The release of pro-inflammatory cytokines within the skin promotes endothelial up-regulation of E-selectin and ICAM-1 expression. (4) In addition, the production and presentation of chemokines (CCL17, CCL22 and CCL27) on dermal endothelium results in the recruitment of antigen non-specific CLA^+ T cells. (5) Antigen presented by local DCs as well as activated macrophages, KCs and mast cells leads to the activation of antigen-specific T cells. (5) These mediate effector responses, including the activation of macrophages, which participate in the clearance of antigen.

T cells and cutaneous recall immunity

The pathways involved in the elicitation of a cutaneous memory immune response are still poorly defined. For instance, it is currently unknown whether antigen-specific T cells are activated in draining lymphoid tissue or the skin during secondary immune challenge[407]. Indirect evidence, however, suggests that the activation of antigen-specific T cells can take place in the skin. The apposition of LCs and T cells in the epidermis has been documented during recall immunity in humans[408]. Interestingly, the importance of LCs in initiating memory responses in the skin has been questioned, and macrophages, KCs and mast cells may play a more prominent role in antigen presentation following secondary challenge[409]. Inflammatory mediators released by the activation of these cells probably play an important role in the initiation of the recall response through the recruitment of circulating antigen-specific T cells. Indeed, blocking chemokine or integrin mediated recruitment of T cells in mice results in diminished cutaneous secondary responses suggesting that the recruitment of memory T cells present in the circulation or originally resident in secondary lymphoid tissues is critical in mediating recall responses[138;397;410].

Recent evidence in mice suggests that memory cells can persist in non-lymphoid tissues including the skin and confer protective immunity[11;101-104]. The presence of memory cells of a particular specificity in the skin, however, may be limited to the site of antigenic challenge[411]. Repeated allergen exposure on the site of a previous allergic contact dermatitis reaction in guinea pigs leads to a more rapid clinical response, which is not reciprocated at other non-exposed sites (retest reactivity)[412]. Resident cutaneous memory T cells, therefore, are likely to be confined to the site of previous antigen exposure. It is still to be determined whether memory cells can persist in non-lymphoid tissues in humans following an immune response. In support of their localisation and persistence in the skin, IFN-γ producing $CD8^+$ T cells have been identified in the epidermis of fixed drug eruptions before and after secondary challenge[413].

Overall, it would seem that memory T cells resident in normal non-inflamed skin, that has not been previously exposed to antigen, are unlikely to be responsible for the initiation of a recall immune response at that site. In addition, very few T cells are present in normal non-inflamed skin[407], and it is, therefore, doubtful that an adequate number of T cells with a sufficiently broad spectrum of specificities is present at any given time or site in the skin to mediate an effective recall immune response. Furthermore, as previously mentioned, evidence suggests that recall immunity in the skin appears to be dependent on the recruitment of T cells from the blood[138;397;410;414]. It is likely that memory T cells activated in the draining lymphoid tissue also contribute to the overall response, perhaps in a redundant fashion, since activated LCs emigrate to draining lymph nodes[369-371]. Indeed, evidence has demonstrated that T cell activation does in part take place in draining lymph nodes during secondary challenge, although at a diminished rate compared with the primary response[415]. Recall immune responses in humans can, however, be maintained despite compromised afferent lymphatics vessels[416]. Recall cutaneous immune responses are, therefore, in most cases probably mediated by the recruitment of antigen-specific T cells from the blood, some of which will have been pre-activated in the draining lymphoid tissue.

1.5 The Mantoux test

The Mantoux test (MT) is a classical delayed-type hypersensitivity (DTH) response to the intradermal injection of tuberculin purified protein derivative (PPD)[417]. It represents a cutaneous T cell mediated recall immune response. PPD consists of a sterile aqueous solution of purified proteins prepared from human strains of *Mycobacterium tuberculosis*. The test is typically used to determine immunity to tuberculosis in humans and positive reactions develop not only in individuals previously exposed to *Mycobacterium tuberculosis*, but also in those previously immunised with

the Bacillus of Calmette and Guérin (BCG) vaccine[417]. The BCG is in fact prepared from live attenuated strains of *Mycobacterium bovis*[418]. Clinically, the reaction may start a few hours after the injection of PPD with white or rose-coloured induration of the skin then peaks by 48-72 hours and resolves by 10 to 14 days. The height of the response is characterised by a localised red and indurated area of skin, occasionally associated with petechiae and rarely vesicles or even ulceration[417].

The cellular infiltrate up to 12-24 hours is characterised by an initial non-specific infiltrate consisting predominantly of neutrophils, but also macrophages and DCs[22;419;420]. Increased T cell numbers are apparent perivascularly from 12 hours after challenge[419] with $CD4^+$ T cells predominating throughout the response[25;419-421]. Maximal activated infiltrating macrophages have been reported to be present at 24 hours[419], but by 48 hours the vast majority of cells are T cells[22;419;421]. Only a minority of the infiltrating cells are B cells[419-421]. Most cells are located perivascularly, although some T cells and macrophages are situated within the interstitium and occasional T cells may be seen infiltrating the epidermis[419-421]. The proportion of T cells within the skin that are antigen-specific during the MT is unknown, but previous estimates in other DTH models using limiting dilution analysis suggest that they account for less than 1% of the infiltrating T cells[422;423].

Previous studies have used the MT to investigate the regulation of $CD4^+$ T cell mediated cutaneous inflammation and have demonstrated the preferential migration of $CLA^+CD45RO^+$ $CD4^+$ T cells into the skin[20;23;24]. These studies, however, only studied the response up to 96 hours. We have previously examined this model for up to 14 days after induction[25;26]. This allowed us to demonstrate that the peak of T cell infiltration was actually at day 7. Furthermore, the increase in T cell numbers was mediated in part by localised proliferation in the skin[25]. This expansion was balanced by an increase in T cell apoptosis from day 7, which presumably

mediated the clearance of the redundant expanded population of cells during resolution[25]. The death of T cells at the peak of the T cell response was linked to activation-induced cell death, associated with elevated expression of CD95L, whereas apoptosis during the resolution phase was linked to cytokine deprivation associated with down-regulation of the anti-apoptotic molecule Bcl-2[25].

1.6 Aims of project

The presence of cycling T cells in the skin during the MT is in direct contrast to studies in mice, which have demonstrated that antigen-specific T cells do not proliferate in non-lymphoid tissues, including the skin, during primary[8;9] and secondary immune responses[10-12]. We therefore speculated that T cells undergo differentiation within the skin during the Mantoux test, and that this would result in functional and regulatory sequelae. Hence, the aims of this project were to:

1. Establish a technique for isolating inflammatory cells from the skin of MT responses for cell culture and flow cytometric analysis.
2. Determine the extent of T cell differentiation and telomere erosion in the skin during the MT.
3. Examine for the possible development and role of $CD4^+CD25^+$ regulatory T cells during the MT.
4. Study the regulation of telomerase during the MT.

2 Materials and Methods

2.1 Volunteer Recruitment and Sample Collection

Normal healthy volunteers, previously immunised with the BCG vaccine were recruited from hospital staff or their associates. Subjects were medically assessed prior to entry into the study and informed consent was obtained. Exclusion criteria included pregnancy, breast-feeding, and previous hypersensitivity to any of the study drugs. The approval of the Ethics Committee of the Royal Free Hospital was obtained before recruitment was commenced.

2.1.1 Mantoux tests

Mantoux tests were performed on the volar aspect of each forearm by the intradermal injection of tuberculin purified protein derivative (PPD) (Evans Vaccines Ltd., Liverpool, UK) 0.1ml 100units/ml (Figure 2.1a). Individuals at risk of hyper-responsiveness to the Mantoux test (MT) due to past significant exposure to tuberculosis or previous pronounced Mantoux test reactions were injected with 0.1ml 10units/ml solution.

Baseline skin erythema was measured using a DermaSpectrometer (Cortex Technology, Hadsund, Denmark) (Figure 2.1b). This is a portable handheld device, which allows the measurement of the skin erythema-index (EI) by measuring light absorption coefficients[424]. The mean of 3 measurements was recorded. Skin EI, size of induration and palpability were also recorded 3 days after MT induction and at the time of sampling (if different). The change in skin EI was calculated by subtracting the baseline from the MT measurement. The size of induration was determined by calculating the mean of 2 measured perpendicular planes. The change in erythema-index, size of induration and palpability were scored and the sum of these scores then used to give an overall clinical

score at 3 days and the time of sampling (Figure 2.1c). Non-responding individuals were defined as having a clinical score of less than 1 at 3 days.

A

B

C

Clinical Score	0	1	2	3	4	5	MT score
Erythema-index (EI)	0	1-5	6-10	11-15	>16		
Size of induration (mm)	0	1-5	6-10	11-15	16-20	>21	
Palpability	Nil	Just palpable	Easily palpable	Marked	Very marked		
						Total	

Figure 2.1 Clinical measurement of the Mantoux test

(A) The Mantoux test is characterised clinically by the presence of a localised area of erythematous indurated oedematous skin. MTs were induced on the volar aspect of the forearm. The MT peaks clinically 2-3 days after induration. (B) The erythema-index was measured at baseline, on day 3 and at the time of sampling using a DermaSpectrometer. The mean of 3 measurements was recorded. (C) The change in EI from baseline, size of induration and palpability were scored and added together to give an overall clinical score

The experimental protocol involved either raising a skin suction blister over the Mantoux test and/or taking a 5mm punch biopsy (Figure 2.2). Samples were collected between 2 and 19 days after Mantoux test induction during

the induction, peak or resolution phases of the immune response. Each volunteer was allotted to a specific sample time-point.

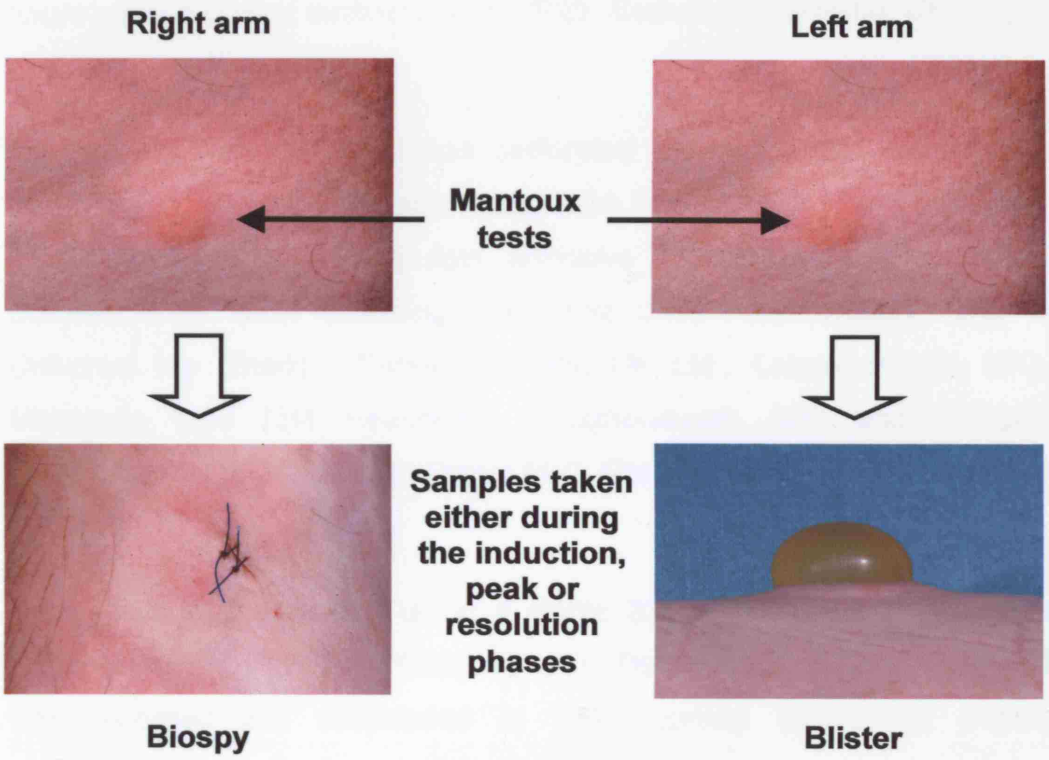

Figure 2.2 The experimental protocol for sample collection

A Mantoux test was induced on the flexor aspect of each forearm. Each volunteer was allotted to a sample time-point between 2 and 19 days after MT induction. A skin suction blister was raised over one MT primarily to obtain cutaneous leucocytes and the other MT was biopsied. Venous blood was also collected for PBMC isolation.

2.1.2 Suction blisters

Suction blister induction

Skin suction blister induction involves splitting the epidermis from the dermis at the lamina lucida by the application of prolonged negative pressure. Suction blisters were raised over normal or MT skin 18-24 hours prior to sampling. This was undertaken to ensure maximum cell recovery. Skin suction chambers (Medical Engineering, Royal Free Hospital, UK) were centred over the test skin. The size of MT induration determined the aperture of the suction cup template i.e. 15mm diameter template if

>15mm induration, 12.5mm diameter template if 10-15mm, and 10mm diameter template if <10mm. A negative pressure of 25-40kPa (200-300mmHg) below atmospheric pressure was applied to the skin for 2-4 hours using a clinical suction pump (VP25, Eschmann, Lancing, UK) (

Figure 2.3). The procedure was performed at warm room temperature (~22°C) until a single unilocular blister was formed. The blister was then protected overnight with a rigid adhesive dressing assembled using Comfeel Plus Ulcer Dressing (Coloplast Ltd., Peterborough, UK), a Universal top (Sterilin, Fisher Scientific UK Ltd., Loughborough, UK), Micropore tape (3M Healthcare, Loughborough, UK) and Tubigrip bandaging (Seton Healthcare Group PLC, Oldham, UK).

Blister fluid was aspirated using a sterile 23G needle and 2ml syringe (Tyco Healthcare UK Ltd., Gosport, UK). The volume of fluid recovered was recorded and suspended in 1.5ml conical microtubes (Alpha Laboratories Ltd., Eastleigh, UK). The aspirated blister was dressed with Betadine dry powder spray (Seton Healthcare Group PLC, Oldham, UK) and a Mepore dressing (Mölnlycke Health Care Ltd., Dunstable, UK). Volunteers were advised to keep this covered and dry for 24-48 hours before leaving open to the air. Suction cups were dismantled and disinfected in Barrycidal 36 for at least 24 hours after use (Heraeus Instruments Ltd., Brentwood, Essex, UK).

Suction blister cell isolation

The blister fluid was microcentrifuged at 650 ×g (3000rpm) for 4 minutes (MicroCentaur, MSE Sanyo) to pellet the cellular contents. The supernatant was removed and aliquotted into 1ml cryogenic tubes (Nalge Europe Ltd., Hereford, UK) and stored at –70°C. The blister cell pellet was then re-suspended in 1ml RPMI (GIBCO, BRL Life Technologies, Paisley, UK) containing 10% human serum supplemented with 100U/ml penicillin, 100μg/ml streptomycin and 2mM L-glutamine (all from Sigma-Aldrich, Gillingham, Dorset, UK) until analysed.

A

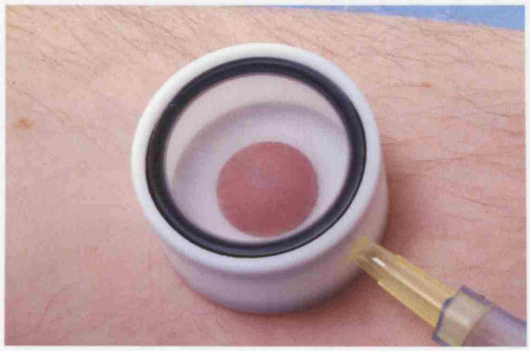

B

Figure 2.3 Suction blister induction

(A) A clinical grade suction pump was used for skin suction blister induction. The pump has a gauge allowing a consistent negative pressure to be applied to the skin. The VP25 Eschmann suction pump has sterile disposable tubing and liners that can be changed between volunteers. (B) The suction cup is applied to the skin and connected to the pump using a cut down pipette tip.

Estimation of blister cell peripheral blood contamination

Blister red and white blood cell numbers were quantified using a haemocytometer and viability was assessed by trypan blue exclusion. An estimation of the percentage of peripheral blood (PB) white cells that were contaminating the blister leucocytes was performed. In order to do this the peripheral red and white cell counts were determined from a sample of venous blood by the Department of Haematology, Royal Free Hospital, UK. The estimate was calculated as follows:

$$\frac{\text{Blister red cell count} \times (\text{PB white cell count} \div \text{PB red cell count})}{\text{Blister white cell count}} \times 100$$

Blister cell cytospins

Cytospin production involves carefully controlled centrifugation of a cell suspension resulting in the separation and deposition of a thin layer of cells onto glass slides whilst maintaining cell integrity. The prepared blister cells were centrifuged at 650 ×g for 5 minutes then resuspended in PBS at a concentration of 0.25×10^6 cells/ml. The cytospins were produced using a Cytospin 3 in conjunction with glass slides, filter cards and cytobuckets held together by a cytobracket (all from Shandon Inc., Pittsburgh, Pennsylvania, USA). The glass slide and filter card were initially prepared by placing 100μl PBS into the cytobucket and centrifuging at 20 ×g for 3 minutes. 100μl of cell suspension (25,000 cells) was then placed in each cytobucket and centrifuged at 20 ×g for 3 minutes. The slides were then air-dried at room temperature for 2 hours then fixed with acetone:chloroform (1:1) for 10 minutes (both from BDH Laboratory Supplies, Poole, UK). The cytospins were air-dried for 10 minutes then wrapped in cling-film and stored at −70°C.

2.1.3 Skin biopsy

Biopsy procedure

A single 5mm punch biopsy was taken from normal skin or the centre of the Mantoux test. The surrounding skin was infiltrated with 2% lignocaine / 1:80000 adrenaline local anaesthetic (Astra Pharmaceuticals Ltd., Kings Langley, UK) prior to biopsy. The wound was closed with 4/0 Surgipro polypropylene suture (Tyco Healthcare UK Ltd., Gosport, UK). The skin sample was transported to the laboratory in sterile phosphate buffered saline (PBS) (GIBCO, BRL Life Technologies, Paisley, UK).

Biopsy storage and sectioning

All biopsies were mounted in Cryo-M-Bed (Bright Instrument Company Ltd., Huntingdon, UK) on cork disks and then snap frozen in isopentane (Sigma-Aldrich, Gillingham, Dorset, UK) cooled in a bath of liquid nitrogen. The samples were stored in liquid nitrogen. 6μm frozen sections were cut

using a Bright 5040 microtome (Bright Instrument Company Ltd., Huntingdon, UK) onto poly-L-lysine (Sigma-Aldrich, Gillingham, Dorset, UK) coated glass slides. Poly-L-lysine is polycationic and interacts with anionic sites on the tissue sections promoting strong adhesion to the slide. Two sections were mounted onto each slide. Sections were air-dried overnight then fixed in absolute alcohol (Hayman Ltd, Witham, Essex, UK) for 5 minutes followed by acetone (BDH Laboratory Supplies, Poole, UK) for 5 minutes. The sections were air-dried for 10 minutes then wrapped in cling-film and stored at –70°C.

2.1.4 Blood samples

Blood was also collected from volunteers at the time of sampling for the isolation of peripheral blood mononuclear cells (PBMC), serum separation and analysis of the full blood count. The serum sample was refrigerated for 30 minutes then centrifuged for 20 minutes at 800 ×g. The resulting supernatant was aliquotted into 1ml cryogenic tubes and stored at –70°C.

PBMC isolation

Heparinised blood was mixed 1:1 with Hanks Balanced Salt Solution (HBSS) (GIBCO, BRL Life Technologies, Paisley, UK) and layered onto Ficoll-Paque (Amersham Biosciences U.K. Ltd., Chalfont St. Giles, UK). This was centrifuged for 20 minutes at 800 ×g with no brake. The buffy coat at the interface was then harvested and washed for 10 minutes in excess HBSS by centrifugation at 650 ×g for the first wash and 300 ×g for the second wash. Typically $1\text{-}2\times10^6$ PBMC are isolated per 1ml of venous blood. The PBMCs were finally resuspended in complete medium (CM). This consisted of RPMI (GIBCO, BRL Life Technologies, Paisley, UK) containing 10% normal human serum (NHS) supplemented with 100U/ml penicillin, 100μg/ml streptomycin and 2mM L-glutamine (all from Sigma-Aldrich, Gillingham, Dorset, UK) until analysed.

2.2 Purification of lymphocyte subsets

2.2.1 Cell purification using MACS separation columns

Magnetic Cell Sorting (MACS) (Miltenyi Biotec, Bisley, Surrey, UK) allows the purification of cell subsets from complex cell mixtures. Cells can be specifically labelled using MACS MicroBeads. These are extremely small biodegradable super-paramagnetic beads that do not activate or influence cell function or viability. After magnetic labelling, the cells are passed through a separation column, which is placed in a strong permanent magnetic field. The column matrix serves to create a high-gradient magnetic field. The magnetically labelled cells are retained in the column, while non-labelled cells pass through. After removal of the column from the magnetic field, the magnetically retained cells can be eluted. Purified cells can be used for *in vitro* cell culture or flow cytometry. MACS MicroBeads are submicroscopic and therefore the light scatter characteristics of labelled cells are unaffected. There are two general approaches to magnetic cell sorting: depletion and positive selection.

$CD4^+$ T cell isolation by depletion

This protocol involves the magnetic labelling of the unwanted cells so that they can be depleted from the cell suspension leaving a pure population of 'untouched' $CD4^+$ T cells. PBMC can be magnetically depleted of B cells, $CD8^+$ T cells, NK cells, monocytes, dendritic cells, early erythroid cells, platelets and basophils by using a cocktail of CD8, CD11b, CD16, CD19, CD36 and CD56 antibodies, which forms part of a $CD4^+$ T cell isolation kit. PBMCs in CM were centrifuged at 650 ×g for 5 minutes. The supernatant was completely removed and the cell pellet was resuspended in 80μl of MACS buffer (PBS containing 0.5% foetal calf serum (FCS) and 2mM EDTA (both from Sigma-Aldrich, Gillingham, Dorset, UK)) per 10^7 PBMC plus 20μl Hapten-Antibody Cocktail ($CD4^+$ T cell isolation kit, Miltenyi Biotec, Bisley, Surrey, UK) per 10^7 PBMC. Cold and degassed MACS buffer was used for all stages. The cells were vortexed and incubated for 10 minutes at 4°C, then washed with MACS buffer by adding 10× the labelling volume and centrifuging at 650 ×g for 5 minutes. The pellet was

resuspended in 80μl of MACS buffer per 10^7 PBMC plus 20μl of MACS Anti-Hapten Microbeads per 10^7 PBMC. The cells were vortexed, incubated for 10 minutes at 4°C and then washed in MACS buffer as before. The cell pellet was resuspended in 1ml of MACS buffer per 10^8 PBMC. LS separation columns were used, which allow up to 10^8 labelled cells to be positively selected. The column was prepared by applying 3ml of MACS buffer, which was allowed to run through. The cell suspension was then applied to the column, after which the column was washed 3 times with 3ml of MACS buffer. The effluent unlabelled fraction representing enriched $CD4^+$ T cells was collected.

Positive selection of cell subsets

This involves the isolation of target cells as the positive magnetically labelled fraction and was used to purify $CD25^+$ and $CD45RO^+$ $CD4^+$ T cells. PB $CD4^+$ T cells were isolated as described above. The cells were washed in MACS buffer centrifuging at 650 ×g for 5 minutes. For $CD25^+$ purification, the cell pellet was resuspended in 90μl of MACS buffer per 10^6 total cells, to which 10μl of CD25 Microbeads per 10^6 total cells was added. For $CD45RO^+$ purification, the cell pellet was resuspended in 80μl of MACS buffer per 10^6 total cells, to which 20μl of CD45RO Microbeads per 10^6 total cells was added. The cells were vortexed and incubated for 10 minutes at 4°C before washing with MACS buffer by adding 10× the labelling volume and centrifuging at 650 ×g for 5 minutes. MS and LS columns were used for the positive selection of up to 10^7 and 10^8 labelled cells respectively. MS columns were used for $CD25^+$ cell selection and LS columns for $CD45RO^+$ cell selection. The cell pellet was resuspended in 500μl or 1000μl of MACS buffer per 10^7 or 10^8 $CD4^+$ T cells respectively. MS columns were prepared by applying 500μl of MACS buffer. The cell suspension was applied to the column, after which the column was washed 3 times with 500μl of MACS buffer. The effluent unlabelled fraction representing enriched $CD25^-CD4^+$ T cells was collected. The column was then removed from the magnet and 1ml of MACS buffer was flushed through the column using a plunger. This effluent was also

collected and consisted of the positive magnetically labelled fraction representing enriched $CD25^+$ $CD4^+$ T cells. For $CD45RO^+CD4^+$ T cell isolation, only the positive fraction was collected.

2.2.2 Purification of blister $CD4^+$ T cells by panning

This method was employed for purifying blister cells in view of the low number of cells isolated i.e. generally $<1\times10^6$, which makes purification by MACS unfeasible. The same principle of depletion applies, but a cocktail of unconjugated antibodies is used to label the unwanted cells. The labelled cells are then depleted by incubating the cells in wells to which rabbit anti-mouse immunoglobulin is immobilised.

250μl of polyclonal rabbit anti-mouse immunoglobulin (DAKO A/S, Glostrup, Denmark) 50μg/ml in sterile PBS was added to 1 well in a 24 well plate and incubated overnight at 4°C. The residual volume was aspirated and the well was carefully washed twice with 1ml of sterile PBS. The blister cells were microcentrifuged at 650 ×g (3000rpm) for 4 minutes. The supernatant was completely removed and the cell pellet resuspended in the depleting antibody cocktail (Table 2.1). The cells were incubated for 20 minutes at room temperature then washed with 1ml CM. The cell pellet was resuspended with 250μl CM, which was then added to the labelled well and incubated for 2 hours at 37°C in a humidified 5% CO_2 atmosphere. The residual volume was carefully collected as well as the 250μl of CM used to wash the well. This residual cell suspension represented an enriched blister $CD4^+$ T cell population.

Table 2.1 Antibodies used in panning cell depletion

Specificity	Clone	Isotype	Volume (µl)	Source
CD8	RFT8	IgG1	100	RFH
CD14	UCHM-1	IgG1	40	RFH
CD16	3GB	IgG1	4 (0.2mg/ml)	Coulter
CD19	RFB9	IgG1	4	RFH
Glycophorin A / CD235a (sialo-glycoprotein on RBCs)	11E4B7.11	IgG1	10 (0.2mg/ml)	Coulter
± CD25	CD25-3G10	IgG1	10	Caltag

RFH Royal Free Hospital

2.3 Flow cytometry

Flow cytometry is a technique that allows the rapid measurement of individual cells as they flow in a fluid stream one by one through a laser beam. In addition to the measurement of cell size and granularity, the use of antibodies conjugated to different fluorochromes also permits the identification and analysis of specific subsets of cells.

A FACSCalibur flow cytometer (Becton Dickinson, Oxford, UK) was used for all experiments. This machine has 2 lasers (488nm and 600-650nm), which allows for the simultaneous measurement of 4 different coloured fluorochromes (channels FL-1 – FL-4). Acquisition and analysis of all data was undertaken using CellQuest software (Becton Dickinson, Oxford, UK). Instrument settings and sensitivity were monitored before each experiment using CaliBRITE beads and FACSComp software (Becton Dickinson, Oxford, UK). Additionally, DAKO FluoroSpheres (DAKO A/S, Glostrup, Denmark) were used to ensure standardisation of the flow cytometer between experiments when fluorescent intensity was being measured. This corrects for fluctuations in the cytometer that occur either intrinsically or following servicing. Single colour fluorochrome controls were used to compensate between different channels to correct for overlapping emission spectra that can occur between different fluorochromes.

Analysis was performed by gating on the live lymphocyte population using forward and side scatter profiles. This excludes dead cells and debris. Isotype and negative controls were used to delineate positive populations, where positive and negative populations were not clearly distinguishable. The antibodies used in flow cytometry experiments are shown in Table 2.2. The optimum concentration for each antibody was determined by preliminary titration. Isotype matched control antibodies to irrelevant antigens were sourced from the same company where possible and were used at the same concentration as the test antibody.

Table 2.2 Antibodies used for flow cytometry

Staining method	Specificity# / fluorochrome	Clone	Isotype / (Species)*	Source
Membrane / direct	CD3-APC	SK7	IgG1	BD Biosciences
	CD3-PECy5.5	S4.1	IgG2a	Caltag Laboratories
	CD3-PerCP	SK7	IgG1	BD Biosciences
	CD3-RPE-Cy5	UCHT1	IgG1	DAKO
	CD4-APC	MT310	IgG1	DAKO
	CD4-PerCP	SK3	IgG1	BD Biosciences
	CD4-PECy5.5	S3.5	IgG2a	Caltag Laboratories
	CD25-FITC	M-A261	IgG1	BD Pharmingen
	CD45-FITC	T29/33	IgG1	DAKO
	CD45RA-FITC	L48	IgG1	BD Biosciences
	CD45RA-PE	4KB5	IgG1	DAKO
	CD45RB-FITC	PD7/26	IgG1	DAKO
	CD69-PE	L78	IgG1	BD Biosciences
	TCR$\alpha\beta$-FITC	WT31	IgG1	BD Biosciences
	TCR$\gamma\delta$-PE	11F2	IgG1	BD Biosciences
Membrane / indirect	CLA	HECA-452	IgM (Rat)	BD Pharmingen
	CCR5	45531.111	IgG2b	R&D Systems
	CCR7	2H4	IgM	BD Pharmingen
	CXCR4	12G5	IgG2a	R&D Systems
Second layer / indirect	Anti-mouse IgG2a+b-PerCP	X57	IgG1 (Rat)	BD Biosciences
	Anti-mouse IgM-PE	P/C	(Goat)	Southern Biotechnology
	Anti-mouse IgG2b-FITC	P/C	(Goat)	Southern Biotechnology
Intracellular / direct	Ki67-FITC	B56	IgG1	BD Pharmingen
	Interferon γ-FITC	25723.11	IgG1	BD Biosciences
	Interferon γ-APC	B27	IgG1	BD Pharmingen
	Interleukin 2-FITC	5344.111	IgG1	BD Biosciences

* Murine unless specified
\# Anti-human unless specified
P/C Polyclonal
FITC Fluoroscein isothiocyanate
PE Phycoerythrin
PerCP Peridinin chlorophyll protein
PECy5.5 Phycoerythrin-cyanin 5.5
APC Allophycocyanin

2.3.1 Surface staining by direct and indirect immunofluorescence

Direct immunofluorescence

This involves the use of antibodies that are directly conjugated to a specific fluorochrome and therefore only a single incubation stage is required. The use of a combination of different fluorochromes such as FITC, PE, PerCP or PECy5.5 and APC allows the detection of up to 4 different antigens simultaneously. 100μl of blister or PBMC cell suspensions were aliqotted into 5ml FACS test tubes (Falcon®, Becton Dickinson Labware, New Jersey, USA) together with an equal volume of PBSA (1% w/v bovine serum albumin and 0.02% sodium azide (both Sigma-Aldrich, Gillingham, Dorset, UK) in PBS) and optimal concentrations of directly conjugated antibodies. The tubes were vortexed and incubated in the dark at 4°C for 30 minutes. The cells were then washed in excess PBSA and centrifuged at 650 ×g for 5 minutes. The supernatant was carefully decanted and cells resuspended in the residual PBSA by vortexing the tubes. The cells were then fixed with 200μl of 2% paraformaldehyde (Sigma-Aldrich, Gillingham, Dorset, UK) in PBS and stored for at least 1 hour in the dark at 4°C until analysed.

Indirect immunofluorescence

This method was used if the primary antibody was only available in a purified form that was unconjugated to a fluorochrome. A fluorochrome conjugated second layer antibody is then used to detect the unconjugated primary antibody that was bound to the cells. This second layer antibody is raised in another animal host and is specific to the primary antibody species and isotype. The primary incubation was carried out as for the direct immunofluorescence technique. After the wash, the cell pellet was resuspended in the residual PBSA and the appropriate concentration of second layer fluorochrome conjugated antibody was added. The second layer antibody was pre-diluted in PBSA with 4% normal human serum (NHS) (Sigma-Aldrich, Gillingham, Dorset, UK). This was undertaken to minimise non-specific staining. The tubes were vortexed and incubated in

the dark at 4°C for 30 minutes. The cells were then washed and fixed as described in the direct immunofluorescence protocol.

2.3.2 Intracellular staining

The detection of intracellular antigens such as Ki67 or cytokines requires cells to be fixed and permeabilised to facilitate access of the antibody to intracellular structures whilst preserving the morphological scatter characteristics. A modified protocol of the Caltag Fix & Perm® Cell Permeabilisation Kit (Caltag Laboratories, Burlingame, California, USA) was used. 100μl of blister or PBMC cell suspensions were aliqotted into 5ml FACS test tubes with 100μl of reagent A (Fixation medium, which contains formaldehyde). The tubes were vortexed and incubated at room temperature (RT) for 15 minutes. The cells were washed with PBSA and centrifuged at 650 ×g for 5 minutes. The supernatant was aspirated and the cell pellet resuspended with 100μl of reagent B (Permeabilisation medium). The tubes were vortexed and incubated at RT for 15 minutes. The cells were then washed again with PBSA and centrifuged at 650 ×g for 5 minutes. The supernatant was aspirated and optimal concentrations of directly conjugated antibodies to surface and intracellular antigens were added. The tubes were vortexed and incubated in the dark at 4°C for 30 minutes. The cells were then washed and fixed as described in the direct immunofluorescence protocol.

2.3.3 Enumeration of antigen-specific cells

$CD4^+$ and $CD8^+$ antigen-specific T cells were identified using flow cytometry to detect the intracellular accumulation of effector cytokines following short term *in vitro* stimulation with antigen in the presence of brefeldin A. Brefeldin A is a fungal metabolite that interferes with vesicular transport from the rough endoplasmic reticulum to the Golgi complex. This enhances the staining by preventing the secretion of cytokines produced in antigen-activated T cells.

PBMCs (1×10^6/ml) or blister cells in CM were added to sterile FACS polypropylene tubes (Kendall, Tyco Healthcare Group, Mansfield, Massachusetts, USA). The cells were stimulated with PPD (Statens Serum Institut, Copenhagen, Denmark) at a final concentration of 10μg/ml and incubated for 15 hours at 37°C in a humidified 5% CO_2 atmosphere. Brefeldin A (Sigma-Aldrich, Gillingham, Dorset, UK) at a final concentration of 5μg/ml was added after 2 hours. Following the incubation, the cells were washed with PBSA and centrifuged at 650 ×g for 5 minutes. The cells were then fixed and permeabilised as described in section 2.3.2. After washing, optimal concentrations of directly conjugated antibodies to CD3, CD4 and intracellular cytokines (interferon-γ and interleukin-2) were added. The tubes were vortexed and incubated in the dark at 4°C for 30 minutes. The cells were finally washed and fixed as described in the direct immunofluorescence protocol. Unstimulated PBMC and blister cell controls were undertaken to determine background staining. Isotype-matched negative controls in conjunction with the unstimulated controls were used to verify the staining specificity and as a guide for setting markers to delineate positive and negative populations. Purified tetanus toxoid (Aventis Pasteur MSD Ltd, Maidenhead, UK) was used as a control antigen at a final dilution of 1:1000. Gating was set on the live lymphocyte population using forward and side scatter profiles to include lymphocytic blasts.

2.3.4 Enumeration of T lymphocytes

Absolute cell counts of T lymphocytes in PBMCs and blister cells were performed using TruCOUNT™ tubes (BD Biosciences, San Jose, California, USA). These were performed to determine the absolute number of lymphocytes analysed in the TRAP assay, heteroduplex analysis and antigen-specific cell enumeration experiments. The technique relies on a known volume of cell suspension been added to a TruCOUNT™ tube that contains a known number of fluorescent beads. During analysis the

absolute number of cells in a sample can be determined by comparing gated cellular events to gated bead events. If fluorescent antibodies are added to the tube absolute numbers of positively labelled cells can be calculated.

A known volume of the PBMC or blister cell samples was carefully pipetted into a TruCOUNT™ tube to which 50µl PBSA and 10µl TriTEST™ (CD3-PerCP, CD4-FITC, CD8-PE; BD Biosciences, San Jose, California, USA) had been added. The tube was vortexed gently and incubated at RT in the dark for 15 minutes. After incubation, 400µl of 1× FACS Lysing Solution (BD Biosciences, San Jose, California, USA) was added and gently vortexed. The sample was stored overnight at 4°C in the dark before analysis. The absolute count of cells was calculated using the following equation:

$$\frac{X \text{ gated cell events} \times Y \text{ beads per TruCOUNT}^{TM} \text{ tube} \times \text{sample volume}}{Z \text{ gated bead events} \times \text{TruCOUNT}^{TM} \text{ volume}}$$

2.4 Measurement of telomere length by flow-FISH

Flow-fluorescence in situ hybridisation (flow-FISH) can be used to measure the telomere length of large numbers of individual cells. Flow-FISH measures the total telomeric signal of a cell i.e. the sum of all the telomeres in each cell. The technique depends on the hybridisation of a fluorescent probe that is specific for the repeated telomere sequence TTAGGG. The fluorescent intensity of an individual cell then provides a measure of the total cellular telomere length. Previously described Flow-FISH protocols were modified to allow the determination of telomere length in $CD4^+$ and PPD-specific $CD4^+$ T cell subsets[126;236;241].

2.4.1 Assessment of telomere length in $CD4^+$ T cells using two colour flow-FISH

PBMCs and blister cells were initially washed with excess PBSA by centrifuging at 650 ×g for 5 minutes. The supernatant was decanted and cells resuspended in 100μl PBSA. The cells were then incubated with anti-CD4 biotin (Immunotech, Marseille, France) 2μg/ml for 15 minutes at RT. After washing with 1ml PBSA, the cells were mixed with streptavidin-Cy5 (Southern Biotechnology Associates, Birmingham, Alabama, USA) at a final concentration of 5μg/ml and incubated for 15 minutes at RT. The cells were then washed in 1ml PBS and the supernatant was decanted to leave a dry cell pellet. The pellet was resuspended in 100μl PBS and 100μl BS^3 solution (Pierce Biotechnology, Rockford, Illinois, USA) in PBS was then added whilst vortexing to give a final concentration of 2mM. BS^3 is an amine-reactive cross-linking fixative. The tubes were incubated at 4°C in the dark for 30 minutes, after which the BS^3 was quenched by adding 1ml of 50mM Tris in PBS pH7.2 and incubating for a further 20 minutes at RT in the dark. The tubes were then washed with 1ml PBS and the cell pellet was resuspended by adding 1ml of hybridisation buffer (70% deionised formamide (BDH Laboratory Supplies, Poole, UK), 1% bovine serum albumin (BSA), 20mM Tris hydrochloride and 150mM sodium chloride (all from Sigma-Aldrich, Gillingham, Dorset, UK) whilst vortexing. The cells were then centrifuged at 800 ×g for 7 minutes and the supernatant decanted leaving a dry cell pellet. The pellets were resuspended in 200μl of hybridisation buffer containing no probe or 0.3μg/ml peptide nucleic acid (PNA) probe $(C_3TA_2)_3$ conjugated to FITC. PNA probes were obtained from Perseptive Biosystems, Framingham, Massachusetts, USA. PNA probes have a peptide-like backbone consisting of repeating glycine units linked by amine bonds. Nucleobases are attached to the backbone by methylene carbonyl linkages. The neutral backbone of the PNA probe allows faster hybridisation with stronger binding and enhanced specificity compared to an oligonucleotide probe. The samples were vortexed and incubated at 82°C for 10 minutes then rapidly cooled in ice water for 5 minutes before incubating at RT for 60 minutes in the dark. The cells were

washed twice with 1ml of post-hybridisation buffer (70% deionised formamide, 0.1% BSA, 10mM Tris hydrochloride, 150mM sodium chloride and 0.1% Tween 20 (Sigma-Aldrich, Gillingham, Dorset, UK) centrifuging at 800 ×g for 7 minutes followed by two further washes in 1ml PBSA centrifuging at 650 ×g for 5 minutes. The cells were resuspended in 500µl PBSA and stored at 4°C in the dark for 30 minutes before being analysed by flow cytometry that same day. The flow cytometer was standardised for each experiment using DAKO FluoroSpheres (DAKO A/S, Glostrup, Denmark) in conjunction with control reference human PBMC and bovine thymocytes. Telomere length was measured in terms of median fluorescent intensity (MFI) by gating on live $CD4^+$ lymphocytes, but excluding lymphocyte blasts. Channel values were converted to MEF values using a calibration curve based on the MFI values obtained using Dako Fluorosphere Calibration Beads, which were acquired during each experiment. This permitted the control no probe sample MEF to be subtracted from the telomeric probe MEF. The final MEF value was then converted back to MFI using the calibration curve.

2.4.2 Assessment of telomere length in antigen-specific $CD4^+$ T cells using three colour flow-FISH

PBMCs and blister cells were stimulated with PPD in the presence of brefeldin A as described in section 2.3.3 for 15 hours at 37°C in a humidified 5% CO_2 atmosphere. Unstimulated controls were also prepared. The cells were washed with 1ml PBSA and centrifuged at 650 ×g for 5 minutes. The cell pellet was resuspended in PBSA containing CD4 biotin antibody (Immunotech, Marseille, France) at a final concentration of 2µg/ml for 15 minutes at RT. The cells were then washed and incubated with streptavidin-Cy3 (Cedarlane Laboratories Ltd, Hornby, Ontario, Canada) at a final concentration of 25µg/ml for 15 minutes at RT in the dark. After washing, the cells were fixed and permeabilised using Caltag Fix & Perm® Cell Permeabilisation Kit as described in section 2.3.2, except that the cells were incubated with interferon-γ-FITC (IFN-γ) (BD

Biosciences, San Jose, California, USA) at the same time as reagent B. All incubations were carried out at RT in the dark. The cells were washed with PBSA then hybridisation buffer, after which they were processed as described in section 2.4.1, except that the PNA probe used was conjugated with Cy5 instead of FITC. The flow cytometer was standardised using control reference human PBMC. Telomere length was measured in terms of MFI by gating on live IFN-$\gamma^{+}CD4^{+}$ lymphocytes, but excluding lymphocyte blasts.

2.5 Telomerase activity assay

Telomerase activity was detected by the Telomeric Repeat Amplification Protocol (TRAP) using the TRAPeze® Detection Kit (Intergen Company, Oxford, England). Telomerase directs telomeric repeats onto the 3' end of existing telomeres using its RNA component as a template. The first step of the protocol involves allowing sample telomerase to mediate the addition of telomeric repeats (GGTTAG) onto the 3' end of a substrate oligonucleotide (TS) (Figure 2.4). In the second step, the extended products are amplified by polymerase chain reaction (PCR) using TS and reverse primers (RP). This generates a ladder of products with 6 base increments starting at 50 nucleotides i.e. 50, 56, 62, etc. Each sample tested includes a 36 base pair internal standard positive control making it possible to quantify telomerase activity. Telomerase is an RNase sensitive ribonucleoprotein and therefore gloves were used when handling all samples and equipment. Additionally, RNase-free materials and conditions were employed. To avoid PCR carry-over contamination protein extraction, PCR amplification and gel preparation were performed in separate laboratories.

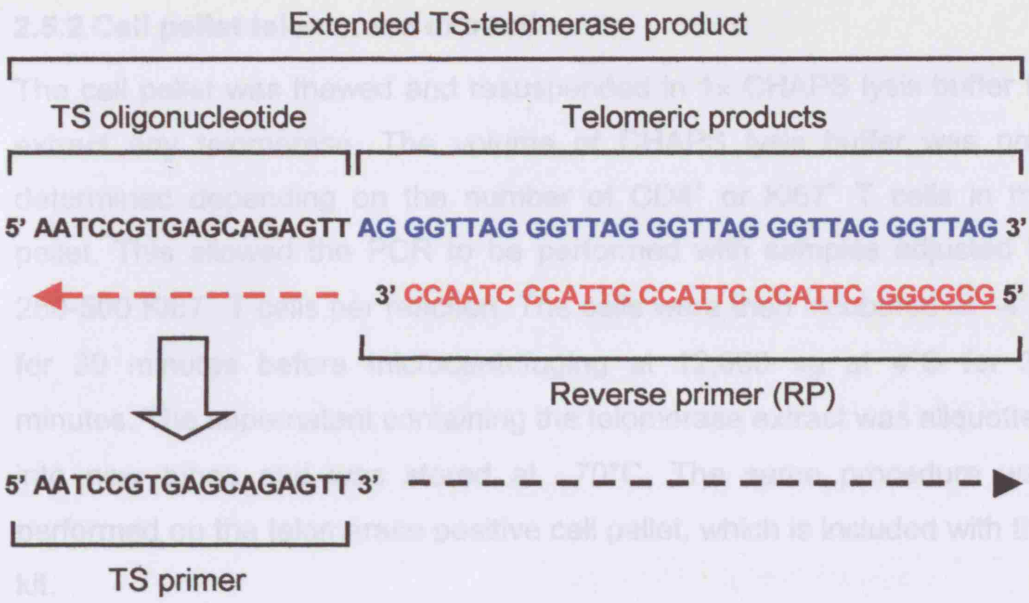

Figure 2.4 TRAP assay scheme

In the first step, sample telomerase activity mediates the addition of telomeric repeats (GGTTAG) shown in blue onto the 3' end of a substrate oligonucleotide (TS). In the second step, the extended products are amplified by polymerase chain reaction (PCR) using reverse (RP) and TS primers. This generates a ladder of products with 6 base increments starting at 50 nucleotides i.e. 50, 56, 62, etc. Underlined nucleotides on the reverse primer (shown in red) indicate designed mismatches to reduce primer interaction and primer dimer artefacts.

2.5.1 Cell pellet preparation

PBMC and blister cell samples were aliquotted into in 1.5ml conical microtubes (Alpha Laboratories Ltd., Eastleigh, UK). The number of cells in each aliquot was determined as described in section 2.3.4. The cells were microcentrifuged at 12,000 ×g for 1 minute. The pellet was resuspended in 1ml sterile PBS and microcentrifuged at 12,000 ×g for 1 minute. The PBS was completely aspirated and the cell pellet frozen in liquid nitrogen before storing at –70°C until analysis.

2.5.2 Cell pellet telomerase extraction

The cell pellet was thawed and resuspended in 1× CHAPS lysis buffer to extract any telomerase. The volume of CHAPS lysis buffer was pre-determined depending on the number of $CD4^+$ or $Ki67^+$ T cells in the pellet. This allowed the PCR to be performed with samples adjusted to 250-500 $Ki67^+$ T cells per reaction. The cells were then incubated at –4°C for 30 minutes before microcentrifuging at 12,000 ×g at 4°C for 30 minutes. The supernatant containing the telomerase extract was aliquotted into new tubes and was stored at –70°C. The same procedure was performed on the telomerase positive cell pellet, which is included with the kit.

2.5.3 Telomerase assay and PCR amplification

Radiolabelling was used to detect the reaction products. This involved end-labelling the TS primer with γ32-ATP prior to performing the telomerase assay. The TS primer was incubated with γ32-ATP in the presence of T4 polynucleotide kinase in 1× kinase buffer at 37°C for 20 minutes then 85°C for 5 minutes (Table 2.3). This method is more quantitative than non-radioactive detection. A 'master mix' of reagents for the extension and PCR reactions was prepared as shown in Table 2.4. The deoxynucleotide triphosphate (dNTP) mix contains equal volumes of dATP, dTTP, dGTP and dCTP. The *Taq* polymerase (thermophilic DNA polymerase) was obtained from Amersham Biosciences U.K. Ltd., Chalfont St. Giles, England.

Table 2.3 Reagents used for end-labelling of TS primer

	Amount required for 10 assays at 2μl per TRAP assay reaction (μl)
γ^{32}-ATP (10mCi/ml)	2.5
TS primer	10
10× kinase buffer	2
T4 polynucleotide kinase (10U/μl)	0.5
Distilled H_20	5
Total	**20**

Table 2.4 Reagents used for master mix for extension and PCR reactions

	Amount required for each sample (μl)
10× TRAP reaction buffer	5.0
50× dNTP mix	1.0
γ^{32}-ATP-TS primer	2.0
TRAP primer mix	1.0
Taq polymerase (5 units/μl)	0.4
Distilled H_20	35.6
Total	**45.0**

Each sample was prepared by adding 5μl of sample or control extract with 45μl of master mix to RNase-free PCR tubes (Eppendorf U.K. Ltd., Cambridge, UK). The following controls were used in the assays:

1. PCR amplification control: Cell extracts can contain inhibitors of *Taq* polymerase, which can produce false negative results. The TRAP primer mix contains internal control oligonucleotides K1 and TSK1, which in combination with TS produce a 36bp band in every lane. This band can be used as a control for amplification efficiency in each reaction and was used to quantitatively analyse the TRAP products.
2. Heat inactivation control: Telomerase is a heat sensitive enzyme. An aliquot of each sample was heated at 85°C for 10 minutes and 5μl used as a comparative negative control. The internal control band is the only band that should be visible in the heat inactivated control.

3. Telomerase positive control: A sample of telomerase positive cells is included in the kit and 5μl of stock positive control cell extract was run with each assay.
4. Primer-Dimer/PCR contamination control: Primer-dimer PCR artefacts are PCR products that arise in the absence of the DNA template. This control is performed with each assay by adding 5μl of 1× CHAPS lysis buffer instead of cell extract. No product should be detected except for the 36bp internal control band. The presence of products indicates sub-optimal PCR conditions or the presence of PCR contamination carried over from another assay.
5. Telomerase quantification control template: TSR8 is an oligonucleotide, which consists of a TS primer sequence extended with 8 telomeric repeats $AG(GGTTAG)_7$. Each assay was performed by adding 2μl of TSR8 template plus 3μl distilled water into one tube and 1μl of TSR8 template plus 4μl distilled water into another. This served as a standard for estimating the amount of TS primers with telomeric repeats extended by telomerase in a given extract.

The sample and control tubes were placed in a thermocycler block and incubated at 30°C for 30 minutes. This allows any telomerase present to extend the TS primer with added telomere units. This was followed by 2-step PCR at 94°C for 30 seconds then 59°C for 30 seconds for 25 cycles in a thermocycler. The first phase denatures the double-stranded DNA and second phase allows the RP primers to anneal and DNA polymerase to function. The samples were then stored at 4°C until gel electrophoresis was performed.

2.5.4 Gel electrophoresis and data analysis

Each reaction tube was mixed with 5μl of loading dye containing bromophenol blue and xylene cyanol (both from Sigma-Aldrich,

Gillingham, Dorset, UK) (0.25% of each in 50% glycerol / 10% 50mM EDTA in deionised water). 25µl of each sample mixture was loaded onto a 12.5% non-denaturing polyacrylamide gel electrophoresis (PAGE) gel (40% polyacrylamide stock solution, *N,N,N',N'*-tetramethyletylenediamine (TEMED), 25% ammonium persulphate (all from Amersham Biosciences U.K. Ltd., Chalfont St. Giles, UK)) in 0.5× TBE buffer pH 8.1-8.5 (Tris-base, boric acid, 0.5mM EDTA; all from BDH Laboratory Supplies, Poole, UK) on a cooled vertical gel electrophoresis apparatus. The gel was run for 90 minutes at 500 volts until the loading dye had run 75% of the gel length. The gel was then dried in a gel dryer (Bio-Rad Laboratories, Hemel Hempstead, UK) on Whatman chromatography paper for 90 minutes. The reaction products were visualised by autoradiography using Hyperfilm MP (Amersham Biosciences U.K. Ltd., Chalfont St. Giles, UK).

Telomerase activity in the sample determines the amount of TRAP product generated and this can be quantified by densitometric analysis. The signal from the region of the TRAP product ladder of each of the following lanes was measured: all of the non-heat treated (x) and heat treated samples (x_o), the primer-dimer/PCR contamination control (r_o) and the TSR8 telomerase quantification control (r). Additionally the signal from the region of the internal standard control in non-heat treated samples (c) and TSR8 telomerase quantification control (c_R) was measured. The amount of TRAP product can be quantified using the following formula:

$$\frac{(x - x_o) / c}{(r - r_o) / c_R} \times 100$$

2.6 Heteroduplex analysis

Heteroduplex analysis (HDA) is a sensitive global method of analysis of TCR heterogeneity that can detect clonal T cell expansions at a frequency of 1:10,000 cells [42;425;426]. This technique depends on the fact that when similar DNA strands are denatured and allowed to re-anneal

heteroduplices are formed that contain mismatched sequences. Heteroduplices are retarded compared to homoduplices when the products are separated by polyacrylamide gel electrophoresis such that the degree of retarded migration correlates with the extent of mismatching. The inclusion of an excess of extended C-region monoclonal 'carrier' DNA specific for the variable region of a particular TCR Vβ chain family increases the probability that sample strands will pair with the carrier DNA forming sample / carrier heteroduplices (Figure 2.5). This allows the use of a probe specific for the extended C-region to detect carrier DNA thereby increasing the sensitivity of the technique and reducing the background polyclonal TCR smear[426;427].

In practice, RNA is extracted from the sample T cell population and reverse transcribed using random primers. Aliquots of sample complimentary DNA (cDNA) are then amplified by PCR using primers specific for each Vβ family. Monoclonal carrier DNA is also amplified using a primer that generates a product with extended TCR C-region end. An excess of monoclonal carrier specific for a Vβ family is mixed with the amplified test sample of the same Vβ specificity. This is then denatured and allowed to anneal. Four types of duplices are generated:

1. Carrier homoduplex: is identified as a strong band running furthest in the gel.
2. Sample TCR and carrier heteroduplices: these are identified as multiple weaker bands, which are retarded in the gel and indicate clonally expanded populations. They are set against a background smear representing the polyclonal populations within the Vβ family.
3. Sample TCR homoduplex: is not visualised.
4. Heteroduplices between 2 different sample TCR: are not visualised.

The excess of monoclonal carrier minimises the formation of the last 2 types.

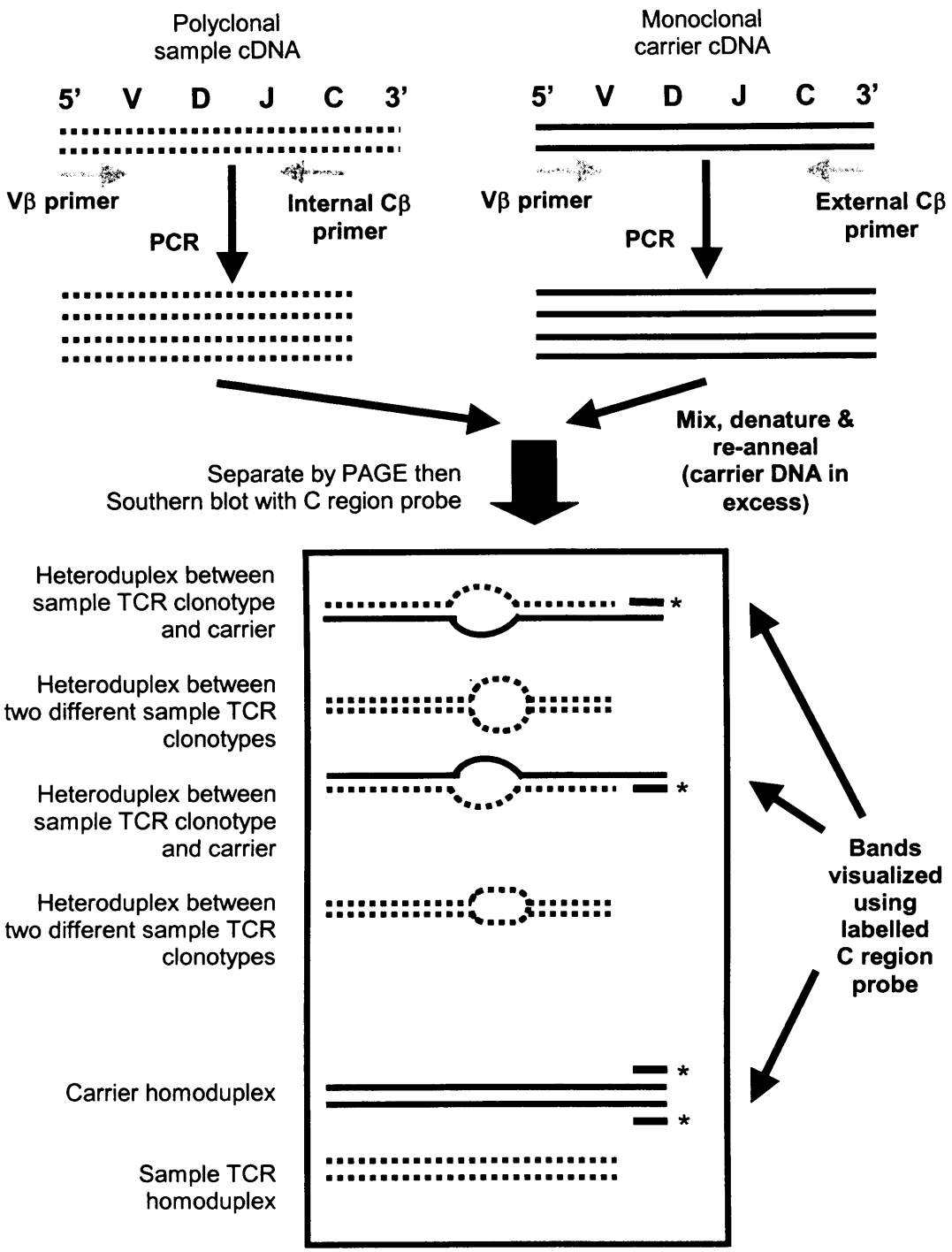

Figure 2.5 Schematic representation of heteroduplex analysis.

Monoclonal 'carrier' DNA is shown by the black solid lines and polyclonal sample DNA is shown in black dotted lines. The short thicker black line with an asterix represents the digoxigenin labelled C region oligonucleotide probe that was used to visualise the carrier homoduplex and carrier/sample heteroduplices.

2.6.1 RNA extraction and cDNA synthesis

Heteroduplex analysis was kindly performed by Joanne Cook and Professor Peter Beverley at the Edward Jenner Institute for Vaccine Research, Compton, UK. Total RNA was extracted from cells using Tri Reagent (Sigma-Aldrich, Poole, UK). This lyses the cells and disrupts the nucleoprotein complexes. Intact RNA was purified by chloroform extraction. The aqueous phase was transferred to a new Eppendorf tube and the RNA was precipitated with isopropanol containing glycogen 20mg/ml at 4°C for 15 minutes before centrifuging. The RNA was then washed in 75% ethanol, centrifuged, air-dried and resuspended in 20μl diethyl pyrocarbonate (DEPC) (Sigma-Aldrich, Poole, UK) treated distilled water. Samples were stored at –70°C.

The RNA was reverse transcribed to produce cDNA using Moloney murine leukaemia virus reverse transcriptase (M-MLV RT) and an oligo(dT) primers (Invitrogen, Paisley, UK). 20μl of sample RNA was combined with 30μl of master mix containing (per sample) 10μl 5× first strand buffer, 4μl dNTP (2.5mM) (Amersham Biosciences U.K. Ltd., Chalfont St. Giles, UK), 5μl oligoDT (0.5μg/μl), 0.5μl dithiothreitol (DTT) (0.1M), 1μl RNasin (40U/μl), 2μl M-MLV RT made up to 30μl with DEPC treated distilled water. The reaction mix was incubated for 1-2 hours at 37°C and cDNA concentration determined by spectrophotometry.

2.6.2 Heteroduplex analysis

PCR with *Taq* polymerase was carried out for each of the 26 human Vβ families (i.e. Vβ1-24 including Vβ 8.1 / 8.2 and Vβ 13.1 / 13.2) using 500ng of sample cDNA in a final volume of 50μl with Vβ-specific and $C\beta_{int\ (internal)}$ reverse primers[42]. A master mix was prepared containing (per reaction) 5μl 10x *Taq* buffer, 4μl 25mM $MgCl_2$, 4μl 2.5mM dNTP, 0.5μl *Taq* polymerase mixed with distilled H_2O to a final volume of 50μl. Hot start PCR on a thermocycler (GeneAmp 9700; Applied Biosystems, Foster City,

California, USA) was performed under the following conditions: 94°C for 3 minutes then 35 cycles of 94°C for 30 seconds, 58°C for 30 seconds, 72°C for 1 minute and a final extension period at 72°C for 10 minutes. Amplification was assessed by analysing the PCR product using 1% agarose gel electrophoresis. Monoclonal carrier cDNA for each of the 26 Vβ genes were cloned from T cell clones or lines and was obtained from Dr Mala Maini (RFUCMS)[42]. Carrier cDNA was amplified using *Pfu* (*Pyrococcus furiosus*) Turbo polymerase (Stratagene, Amsterdam, Netherlands) under the same conditions as sample cDNA. Vβ-specific and $C\beta_{ext\ (external)}$ reverse primers were used.

20 μl of Vβ-specific amplified sample cDNA was mixed with 1μl of matched Vβ-specific cDNA carrier PCR product. The mixed DNA was denatured at 95°C for 5 minutes in a thermocycler and then allowed to anneal at 50°C for 1 hour. The mixtures were separated against a 1kb DNA ladder on a 12% non-denaturing polyacrylamide gel for 16 hours at 10 mA and 4°C. Gels were stained in 5μg/ml ethidium bromide in 0.5× TBE for 20 minutes to visualise DNA, then destained with 0.5× TBE.

The gels were blotted onto a Hybond N^+ membrane (Amersham Biosciences U.K. Ltd., Chalfont St. Giles, UK) in 0.5x TBE using a Trans-blot SD (Bio-Rad Laboratories, Hemel Hempstead, UK). The membranes were washed with 0.5× TBE and the DNA was then fixed by ultraviolet cross-linking (0.12 J) using a Stratalinker 2400 (Stratagene, Amsterdam, Netherlands).

The Cβ external oligonucleotide probe was end-labelled with digoxigenin (Roche Diagnostics, Lewes, UK). $C\beta_{ext}$ oligonucleotide (1μg/μl), digoxigenin-11-ddUTP (1mM), terminal transferase (50U/μl) and cobalt chloride (25mM) in 5x reaction buffer (8μl) were mixed and made up to

40μl with distilled H_2O. The reaction mix was incubated at 37°C for 15-60 minutes.

Membranes were pre-hybridised for 30 minutes in Rapid-Hyb buffer (Amersham Biosciences U.K. Ltd., Chalfont St. Giles, UK) at 57°C, and 20μl of the purified digoxigenin-labelled probe was then hybridised at 57°C for 2.5 hours. They were washed twice in 2x saline sodium citrate (SSC) buffer containing 0.1% sodium dodecyl sulphate (SDS) (Invitrogen Ltd, Paisley, UK) for 5 minutes, then twice in 0.1x SSC containing 0.1% SDS for 5 min. The membranes were incubated with anti-digoxigenin–AP Fab fragments for 30 minutes with constant rocking at RT and were then washed with wash buffer (Roche Diagnostics, Lewes, UK). The labelled probes were then detected by the addition of CDP-Star substrate (Roche Diagnostics, Lewes, UK). Chemoluminescence was detected by autoradiography using a Fluor-S Max (Bio-Rad Laboratories, Hemel Hempstead, UK) and Compact X4 (Xograph Imaging Systems Ltd., Tetbury, UK).

2.7 *In vitro* cell culture

2.7.1 Standard cell culture conditions

Cells were suspended in complete medium (CM): RPMI (GIBCO, BRL Life Technologies, Paisley, UK) containing 10% human serum supplemented with 100U/ml penicillin, 100μg/ml streptomycin and 2mM L-glutamine (all from Sigma-Aldrich, Gillingham, Dorset UK). The cell concentration was adjusted to $0.5\text{-}2\times10^6$ cells/ml. Aliquots of cell suspension were pipetted into the wells of cell culture plates and incubated at 37°C in a humidified 5% CO_2 atmosphere. If purified populations of cells were being stimulated, antigen presentation was provided by co-culture with autologous PBMC irradiated at 4000 rads.

2.7.2 Long-term cell culture

Long-term cell culture was used to assess the i*n vitro* proliferative capacity of PBMC and blister cell samples. Cells were cultured in complete medium (CM) in round-bottomed 96-well plates at a concentration of 1×10^6 cells/ml and stimulated with PPD (Statens Serum Institut, Copenhagen, Denmark) at a final concentration of 1μg/ml. Cell lines were maintained in CM supplemented with interleukin-2 (IL-2) (R&D Systems, Abingdon, UK) at a final concentration of 1-5ng/ml and re-stimulated with PPD-pulsed (1μg/ml) autologous irradiated PBMC every 10-14 days. The cells were sub-cultivated every 3-7 days and viability was determined by trypan blue exclusion. Numbers of $CD4^+$ T cells were quantified using TruCOUNT™ tubes. Population doublings (PD) were determined by comparing the total number of cells at the start and end of each sub-cultivation using the equation: $\log10 \times (\text{cell total}_{end} / \text{cell total}_{start}) / \log2$.

2.7.3 Assessment of cell viability

The trypan blue exclusion test was used to determine the number of viable cells. An aliquot of cell suspension was mixed 1:1 with trypan blue (Sigma-Aldrich, Gillingham, Dorset, UK) and viable non-stained cells were counted using a haemocytometer.

2.7.4 Measurement of cellular proliferation by [^{3}H] thymidine incorporation

Cells were cultured in CM in the wells of 96 well round bottomed cell culture plates (Falcon®, Becton Dickinson Labware, New Jersey, USA) in the presence of appropriate stimuli. Experiments were performed in triplicate. The cells were incubated for 4-6 days before adding 10μl of 0.0025MBq [^{3}H] thymidine (Amersham Biosciences U.K. Ltd., Chalfont St. Giles, UK) to each well and incubating for an additional 16 hours. Cells were then harvested onto glass microfibre filter strips using a cell harvester (Cambridge Technology, Watertown, Massachusetts, USA) and

counts per minute (cpm) from incorporated [^{3}H] thymidine were determined by liquid scintillation counting.

2.7.5 Indirect and direct suppression assays

For indirect suppression assays, the proliferative responses of equal numbers of PB $CD4^+$, PB $CD4^+CD25^+$, PB $CD4^+CD25^-$ or blister $CD4^+$ T cells to stimulation with PPD and autologous irradiated PBMC were compared. For direct suppression assays, PB $CD4^+CD25^-$ T cells or blister $CD4^+$ T cells were cultured alone or co-cultured with an equal number of either PB $CD4^+CD25^-$ or $CD4^+CD25^+$ T cells and stimulated with PPD and autologous irradiated PBMC. Proliferative responses were assessed as described.

2.7.6 Induction of anergy and suppressive function experiments

The PPD-specific $CD4^+$ T cell line was established using day 19 MT blister cells as described in section 2.7.2. Cells for these experiments were harvested after 4 rounds of stimulation with PPD (1μg/ml) and autologous irradiated PBMC *in vitro*. Induction of anergy and suppressive function experiments were kindly performed by Padraic Dunne, RFUCMS. Fibroblast-conditioned medium (FCM) was harvested from confluent human embryonic lung fibroblasts (HELF) and used at a working dilution of 1:1 with CM. Anti-CD3 antibody (OKT-3 purified from hybridoma supernatant, ECACC, Salisbury, UK) was immobilised by incubating diluted antibody (0.005-0.1 μg/ml) in 24 well plates for 2 hours at 37°C. The cells (1×10^6/ml) were incubated in the 24 well plates with FCM in the absence or presence of the increasing concentrations of immobilised anti-CD3 OKT-3 antibody (0.005-0.1 μg/ml) for 18-24 hours at 37°C in a humidified 5% CO_2 atmosphere. Following this stimulation, the cells were washed and stimulated in a 1:1 ratio with autologous irradiated PPD-pulsed (1μg/ml) PBMC in 96 well round bottomed plates. To assess suppressive function, the same cells were instead washed and stimulated

with an equal number of autologous non-anergised responder PPD cell line cells and autologous irradiated PPD-pulsed PBMC in 96 well round bottomed plates. The cells were cultured for 3 days and the proliferative response was measured by [^{3}H]-thymidine incorporation (cpm) during the last 16 hours of culture.

2.7.7 Type 1 interferon inhibition experiments.

To investigate the effect of blister fluid on telomerase induction *in vitro*, fresh day 3 blister fluid (50% final dilution) was added to PPD stimulated (0.5μg/ml) autologous PBMC. In addition, autologous serum diluted 1:1 in RPMI (25% final dilution) was added to PPD-stimulated PBMC as a control. To block the effects of type 1 interferon (IFN), anti-CD118 antibody (anti-IFNAR 2, Calbiochem, Nottigham, UK) or isotype control antibody (Mouse IgG2a, Sigma-Aldrich, Gillingham, Dorset UK) were added at 2.5μg/ml to parallel cultures containing fresh day 3 MT blister fluid. Samples for the measurement of proliferation and telomerase activity were collected on day 3 after PPD stimulation.

To investigate the direct inhibition of telomerase activity by type 1 IFN *in vitro*, a PPD-specific CD4$^+$ T cell line was re-stimulated with PPD (0.5μg/ml) and autologous irradiated PBMC in the presence of various doses of recombinant interferon-α (subtype 2a; R and D systems, Abingdon, UK) or Roferon, a clinically used preparation of IFN-α (subtype 2a; Roche Pharmaceuticals, Welwyn Garden City, Hertfordshire, UK). After 4 days, the cells were sampled to assay for telomerase activity. Samples were adjusted so that 500 Ki67$^+$ T cells were assayed in each lane.

2.7.8 CFSE cell labelling

Carboxy-fluorescein diacetate succinimidyl ester (CFSE) staining detected by flow cytometry was used to distinguish one population of cells from

another e.g. irradiated autologous PBMC from blister cells. CFSE diffuses freely into cells and intracellular esterases cleave the acetate groups converting it to a membrane impermeable fluorescent dye. Intracellular CFSE is detected in the FL-1 channel by FACS. The cell population to be labelled were washed in warm RPMI medium (37°C) containing 100U/ml penicillin, 100μg/ml streptomycin and 2mM L-glutamine, but no serum. The cells were centrifuged at 650 ×g for 5 minutes and resuspended in 1ml of medium. They were then incubated for 10 minutes at 37°C in 1μM CFSE (Molecular Probes Inc., Oregon, USA) diluted in warm medium. Cold CM (4°C) (10ml) was added to stop the CFSE-labelling and the cells were then centrifuged before resuspending in CM.

2.8 Cytokine assays

2.8.1 Multiple cytokine assay by multiplex bead immunoassay

The multiplex assay of cytokines and chemokines in blister fluid was performed by Dr John Curnow, Division of Immunity and Inflammation, MRC Centre for Immune Regulation, University of Birmingham, UK. A Luminex 100 and cytokine Beadlyte assay kit were used (both from Upstate Biotechnology, Lake Placid, New York, USA). The assay kit is capable of the simultaneous detection of multiple cytokines: IL-1β, IL-2, IL-4, IL-6, IL-8, IL-10, IL-12, tumour necrosis factor-α (TNF-α), IFN-γ, granulocyte monocytes-colony stimulating factor (GM-CSF), CCL5 (RANTES), CCL11 (eotaxin), CCL2 (MCP-1). The technique combines enzyme linked immuno-absorbant assay (ELISA) and flow cytometry technology. It is based on sets of polystyrene microspheres, which are internally dyed with precise ratios of two spectrally distinct fluorochromes. This ratio confers a distinct signature to each set of microspheres. Each set of microspheres is conjugated with a specific cytokine capture antibody. The captured cytokine is detected by a second biotinylated antibody that binds to streptavidin labelled with a third fluorochrome. The Luminex 100 flow cytometer and software can be used to separate a pool of microspheres with different specificities into individual bead sets and

determine the proportion of analyte bound to the surface of each microsphere. In this way, multiple assays can be performed simultaneously on small samples with high specificity and sensitivity.

2.8.2 Measurement of type 1 interferon by anti-viral assay

The amount of type 1 interferon in blister fluid was assayed by standard anti-viral assay[428]. This work was carried out by Professor Graham Foster at the Royal London Hospital, London, England. Duplicate serial three-fold dilutions of the blister fluids were prepared in 100μl DMEM (Dulbecco's modification of Eagle's medium) plus 10% foetal calf serum (FCS) and added to 96-well plates containing confluent cultures of A549 cells (human lung adenocarcinoma cell line). The cells were cultured for 24 hours before the medium was removed and murine encephalomyelitis virus in DMEM plus 10% FCS was added for 1 hour. The viral suspension was then removed and the cells washed before incubating in DMEM plus 10% FCS for a further 18 hours. Cell viability was assessed by staining with 0.25% methyl violet in 2% formaldehyde and the OD540 measured by spectrophotometry in an automated plate reader. The concentration of type 1 IFN was determined by comparison with a standard curve prepared using IFN-α at known concentrations (IFNαN1, Wellferon; GlaxoSmithKline, Uxbridge, UK) and the antiviral activity of the original sample calculated from the dilution. Using this technique 15-200 IU/ml IFN-α can be detected.

2.9 Immunohistochemistry

2.9.1 Biotin / streptavidin alkaline phosphatase

An indirect biotin / streptavidin alkaline phosphatase technique was used to identify the distribution of interferon-α expression in skin sections. The primary unconjugated antibody is allowed to bind with specific antigen in the tissue sections. A secondary biotinylated antibody is then applied. This is raised in a different species to the primary antibody, but is specific to the

primary antibody species and immunoglobulin class. Finally the third layer containing streptavidin conjugated to alkaline phosphatase is added. Alkaline phosphatase hydrolyses naphthol phosphate esters to phenolic compounds and phosphate. The phenolic compounds couples to the chromogen (Fast Red) to produce a soluble coloured precipitate or azo dye. Several isoenzymes of alkaline phosphatase are recognised in humans and are characteristic for different tissues. All the endogenous isoforms, except the intestinal one can be blocked by the inclusion of levamisole in the final substrate medium. The alkaline phosphatase streptavidin conjugate used in this protocol was prepared from calf intestine. The precipitant is soluble so an aqueous mounting medium was used.

Stored frozen sections were thawed for 30 minutes then placed in PBS for 5 minutes. The sections were ringed with polysiloxane, which acts as a water repellent and prevents solutions from mixing between adjacent sections. The sections were then incubated for 18 hours at 4°C with 50µl unconjugated interferon-α (Clone: C10F5; murine IgG1; Serotec Ltd., Oxford, UK) 25µg/ml in PBS. All incubations were carried out in a humidified chamber to prevent the sections from drying out. Sections were then washed in excess PBS for 5 minutes. 50µl of affinity purified horse biotinylated anti-mouse IgG (Vector Laboratories Inc., Burlingame, California, USA) 37.5µg/ml in PBS was added to each of the sections and incubated at room temperature (RT) for 1 hour. Sections were then washed again in excess PBS for 5 minutes before adding 50µl of alkaline phosphatase streptavidin (Vector Laboratories Inc., Burlingame, California, USA) 25µg/ml in PBS for 1 hour at room RT. The sections were then washed two times in Tris buffered saline (TBS) (8g sodium chloride, 0.605g Tris hydrochloride, 3.8ml 1M HCl (all from BDH Laboratory Supplies, Poole, UK) in 500ml distilled water, made up to 1l) at pH7.6 for 5 minutes each. The substrate solution was prepared using Fast Red TR/Napthol AS-MX phosphate tablets (Sigma-Aldrich, Gillingham, Dorset, UK). This comprised Fast Red TR 1.0mg/ml, napthol AS-MX 0.4mg/ml and

levamisol 0.15mg/ml in 0.1M Tris buffer. The solution was filtered with a 0.2µm filter prior to use. 200µl of substrate solution was added to each section and left to develop for 15 minutes at RT. The slides were then washed in tap water for 2 minutes before counterstaining with fresh filtered Mayer's haematoxylin (Sigma-Aldrich, Gillingham, Dorset, UK) for 5 minutes. The sections were finally rinsed with tap water and washed in distilled water for 5 minutes before mounting with PBS:glycerol (1:9). Isotype controls were performed using a matched isotype antibody to an irrelevant antigen at the same concentration as the primary antibody.

2.9.2 Indirect double immunofluorescence

This technique was used for the simultaneous detection of two different antigens i.e CD4 and Ki67. These experiments were performed by Cate Orteu, RFUCMS. The primary unconjugated antibody is allowed to bind with the specific antigen in the tissue sections. A secondary FITC or tetramethylrhodamine isothiocyanate (TRITC) conjugated antibody is then applied and allowed to bind to the primary antibody. The secondary antibody is raised in a different species to the primary antibody, but is specific to the primary antibody species and immunoglobulin class. The simultaneous detection of two different antigens can be achieved by using primary antibodies of different isotype. This allows the identification of single and double immunofluorescent stained cells.

Sections were initially prepared as described in section 2.9.1. The sections were incubated for 45 minutes in a humidified chamber at RT with 50µl of appropriate combinations of primary antibodies diluted in PBS. For the antibodies used see Table 2.5. The slides were washed in PBS for 5 minutes before applying 50µl of appropriately combined species and isotype specific FITC and TRITC conjugated secondary antibodies diluted in PBS. The slides were incubated in the dark for 45 minutes at RT and then washed twice in PBS for 5 minutes. Finally, the sections were mounted in Citifluor AF1 (Citifluor Ltd, London, Ltd). This is a PBS glycerol

solution containing an anti-bleaching agent, which retards the fading of the fluorochromes during fluorescence microscopy. Controls were performed with isotype and negative controls for the primary antibodies.

Table 2.5 Antibodies used for indirect double immunofluorescence

	Specificity# / fluorochrome	**Clone**	**Isotype / (Species)***	**Source**
Primary antibody	CD4	S3.5	IgG2a	Caltag Laboratories
	Ki67	Ki67	IgG1	DAKO
Secondary antibody	Anti-mouse IgG1-TRITC	P/C	(Goat)	Southern Biotechnology
	Anti-mouse IgG2a-FITC	P/C	(Goat)	Southern Biotechnology

* Murine unless specified
\# Anti-human unless specified
P/C Polyclonal

2.9.3 Indirect immunoperoxidase

This technique was used for the identification of cell subsets on blister cell cytospins and to determine the number of $CD3^+$ T cells within perivascular infiltrates of skin sections of MTs. The secondary antibody consists of a horseradish-peroxidase conjugate, which converts the substrate, 3,3'-diaminobenzidine tetrahydrochloride (DAB), to an insoluble brown precipitate. Non-specific binding of the secondary antibody was minimised by a preliminary incubation with serum species-matched to the secondary antibody i.e. normal rabbit serum (NRS)

Cytospins were initially prepared as described in section 2.9.1. The sections were then incubated with NRS diluted 1:100 in PBS for 10 minutes at RT. The excess was removed before adding 50μl primary antibody diluted in PBS and incubating in a humidified chamber for 60 minutes at RT. The primary antibodies used are shown in Table 2.6. The sections were washed in PBS and then incubated for 60 minutes at RT with 50μl peroxidase conjugated rabbit anti-mouse immunoglobulins (P260; DAKO A/S, Glostrup, Denmark) diluted 1:25 with PBS containing

10% NHS. The slides were then washed in PBS and 100μl DAB (1mg/ml) solution containing 0.045% hydrogen peroxide was added to each section for 5-10 minutes. The reaction was stopped by washing in distilled water for 5 minutes. The sections were counterstained with Harris's haematoxylin (Sigma-Aldrich, Gillingham, Dorset, UK) for 2 minutes then washed in distilled water for 2 minutes. The sections were then dehydrated by washing in 70% ethanol for 1 minute, twice in 90% ethanol for 1 minute, twice in absolute ethanol for 1 minute and twice in Citroclear for 1 minute. The sections were then mounted in DPX mountant (BDH Laboratory Supplies, Poole, UK).

Table 2.6 Antibodies used for indirect immunoperoxidase

	Specificity	Clone	Isotype	Source
Primary antibody	CD1a	RFT6	IgG1	RFH
	CD3	UCHT1	IgG1	DAKO
	CD68	EBM11	IgG1	DAKO
	Interdigitating dendritic cells	RFD1	IgM	RFH
	Macrophages	RFD7	IgG1	RFH

RFH Royal Free Hospital

2.9.4 Quantification of immunohistology

All measurements were carried out by a single observer using coded slides. The slides were visualised using a light microscope and an Axiocam digital camera (both from Carl Zeiss Ltd, Welwyn Garden City, UK). Fluorescence microscopy was performed using fluorescence filters and a high-energy arc lamp adaptor on the same microscope. Digital images of the slides were analysed using KS300 software (Image Associates, Bicester, UK). A predetermined circular framed area (100μm diameter) was centred on 5 of the largest perivascular inflammatory cell infiltrates in the upper and mid dermis. This then allowed the number of positive and negative cells to be then quantified. The mean of the 5 counts was recorded

2.10 Statistics

Statistical analysis was performed using GraphPad Prism version 3.00 for Windows (GraphPad Software, San Diego, California, USA). Dr Richard Morris, Department of General Practice and Population Sciences, Royal Free and University College Medical School provided statistical advice. Non-parametric tests were predominantly used. The Kruskal-Wallis test was used to compare three or more unpaired groups and the Mann-Whitney was used when comparing only two unpaired groups. The Wilcoxon matched pairs test was used when comparing two groups of paired data. The used of parametric tests such as one-way analysis of variance, unpaired and paired t tests were only used if the data passed a Normality test. The chi-squared test was used for analysing the sex ratio in different groups.

3 Isolation of skin lymphocytes using the skin suction blister technique

3.1 Introduction

Immunohistochemistry and flow cytometry are complementary techniques that are often used to study lymphocytes that are resident in tissues. Immunohistochemistry permits morphological interpretation, whereas flow cytometry allows more accurate quantification and multi-parameter analysis on a single cell basis. A pre-requisite for flow cytometry consequently is the generation of a single cell suspension from the tissue of interest. In the skin, however, the harvesting of lymphocytes is complicated by its rigid structure. The epidermis consists of tightly adhering keratinocytes and the dermis of connective tissue composed of collagen and elastin fibres with variable numbers of cells embedded in a viscous amorphous ground substance[429]. Investigators have, therefore, developed a number of isolation procedures in order to release viable lymphocytes from the skin. Enzymatic digestion and mechanical disaggregation can yield large numbers of lymphocytes, but concerns have been raised regarding the effects this can have on the phenotypic and functional characteristics of the isolated cells[430-432]. Collagenase, DNase and Dispase are enzymes commonly used in enzyme digestion protocols. However, reduced or undetectable expression of CD3, CD4, CD8 and CD25 as well as certain cell integrins and selectins on lymphocytes has been reported with the use of these enzymes on PBMC and tonsillar lymphocytes[430-432]. This is thought to be the result of impurities in the enzymes and the use of ultrapure collagenase or proteinase inhibitors has, therefore, been recommended. This prevents the loss of some markers, but CD25 and integrins were still affected under

these conditions[430;432]. The natural re-expression of markers has been reported[433], but this is not consistently recognised and requires an *in vitro* rest period of at least 12 hours[431;432]. Furthermore, cell viability can be affected following enzyme digestion so that approximately 70-90% of cells remain viable[433;434], although viability as low as 15% has been reported[435]. Lymphocytes can also be isolated from skin explants, but this requires up to 5 days or longer of *in vitro* culture[436;437]. Both of the above techniques require skin biopsies to be performed, which often result in scarring.

The accessibility of the skin allows an alternative technique to be used to isolate resident lymphocytes. The skin suction blister technique is a relatively simple technique, which is non-scarring and allows the study of both cells and soluble mediators contained within the blister fluid. Furthermore, it allows skin lymphocytes to be used immediately for phenotypical and functional studies with the minimum of *in vitro* exposure. The aim of this work was to examine the characteristics of lymphocytes resident in the skin during a human cutaneous T cell mediated immune response and in view of this we decided to use the suction blister technique to isolate inflammatory cells from the skin. The use of this technique to isolate T lymphocytes from non-inflamed and inflamed skin will be examined in this chapter.

3.2 Skin suction blister technique

The main objective of inducing skin suction blisters on normal and inflamed skin was to isolate the leucocytes, and in particular the T cells resident within the skin. Published data suggests that the number of cells obtained from normal non-inflamed and MT skin can be maximised if the suction blister is raised and left for up to 24 hours before aspirating the blister fluid[22;438;439]. We, therefore, decided that we would raise skin suction blisters 18-24 hours prior to samples being collected i.e. for a volunteer allotted to have samples collected on day 3, the skin suction blister would be raised 2 days after the induction of the MT.

Skin suction blister induction involves applying prolonged negative pressure to the skin. We used a negative pressure of 25-40 kPa (200-300 mmHg) below atmospheric pressure as it minimises trauma to the skin whilst ensuring a relatively short blister induction time. Higher pressures were initially tried, but were associated with macroscopic haemorrhage. We also performed the procedure at warm room temperature (~22°C), as cooler temperatures were associated with a prolonged induction time (up to 6 hours). Any hairs that were present at the site of blister induction were removed by gentle shaving.

Blister induction was initially attempted using a disposable 10ml syringe connected to a water-jet vacuum pump with pressure gauge. A blister was successfully induced, but the procedure was uncomfortable in view of the instability of the syringe on the forearm. Additionally, this method was judged to be inconvenient for volunteers since the vacuum pump had to be connected to continuously running water. We, therefore, decided to use specifically designed suction cups assembled from Nylon and Perspex components (Figure 3.1). The aperture of the suction cup can be changed by using templates with different diameters. The negative pressure was generated using a portable VP25 clinical grade suction pump. This has a pressure gauge, which allows a controlled constant pressure to be applied to the skin.

Figure 3.1 Suction cups for skin suction blister induction

Suction cups consisted of 3 main components: a template and cup made of Nylon plus a see-through Perspex lid. Rubber O-rings fit around the lid and template so that the 3 components fit together forming airtight seals. The size of template used can be changed according to the size of MT induration i.e. 15mm diameter template if >15mm induration, 12.5mm diameter template if 10-15mm, and 10mm diameter template if <10mm. The template apertures have bevelled edges. This is to ensure that skin is comfortably drawn into the suction cup during blister induction. The see-through lid allows the induction process to be observed and monitored.

Suction cups were centred on the sample skin and negative pressure was then applied. A 'nipple' of skin is drawn up into the chamber of the suction cup and this produced firm attachment of the cup to the forearm (Figure 3.2a,b). The suction cup was then stabilised on the forearm with Micropore tape. This meant that although the volunteers were restricted in the amount they could move about, they could use the arm to undertake other activities. This method of blister induction was judged to be more comfortable and superior to the original used.

The onset of blister formation was evidenced by mild paraesthesiae and the appearance of clear vesicles on the skin in the suction chamber. This usually occurred within 1-2 hours of the onset of the blister induction process. The vesicles progressively enlarged then coalesced forming a single unilocular blister (Figure 3.2c). Fully developed skin suction blisters formed on average in 3 hours (range 1.5-6 hours). The blister was protected overnight using a rigid adhesive dressing. This was constructed by placing a trimmed Universal container top on to a piece of soft padded dressing positioned around the blister and secured with Micropore tape and Tubigrip bandaging (Figure 3.2d-h). This was generally found to be comfortable.

Aspiration of the blister fluid the following day was generally perceived by the volunteers as being painless (Figure 3.2i,j). Occasional 'stinging' discomfort was experienced as the roof of the blister came into contact with the dermis, but this was alleviated once the site was dressed with a Mepore dressing. The mean volume of blister fluid recovered from skin suction blisters raised over inflamed Mantoux test skin and normal non-inflamed skin was 874μl (standard deviation (SD) ± 498μl) with a range from 50 to 2500μl. No adverse events were encountered. The blisters healed within 7-10 days with the exfoliation of the blister roof leaving an area of post-inflammatory erythema. No scarring was encountered, although some individuals developed variable post-inflammatory hyperpigmentation and this was more common, as would be expected, in darker skin types.

Skin suction blister induction on normal or inflamed Mantoux test skin was successfully achieved in 100% of the volunteers. Attempts, however, to extend this to the skin of patients with atopic eczema were less successful. The epidermis of lesional atopic eczema is often damaged by scratching, but is also scaly, lichenified and oedematous[440]. An intact epidermis is pre-requisite for suction blister induction. We, therefore,

decided to induce suction blisters on both peri-lesional and non-lesional skin. Out of 6 volunteers who were recruited, however, only 3 peri-lesional and 5 non-lesional skin suction blisters were successfully induced. The time taken for blisters to be induced was increased (mean 5 hours; range 3-6 hours) making the procedure unpopular with patients. Additionally, the blisters induced were smaller (peri-lesional skin mean volume 267μl SD ± 58μl, range 200-300μl; non-lesional skin mean volume 470μl, SD ± 427μl, range 100-1000μl. The induction process was also often associated with the leakage of copious amounts of watery fluid from the skin into the suction chamber. This produced excessive condensation on the chamber window, which made assessing the progress of the induction process very difficult. The skin suction blister technique was, therefore, less reliable and more problematic to perform in volunteers with atopic eczema. We consequently decided not to use this technique to pursue the analysis of cutaneous lymphocytes in atopic eczema.

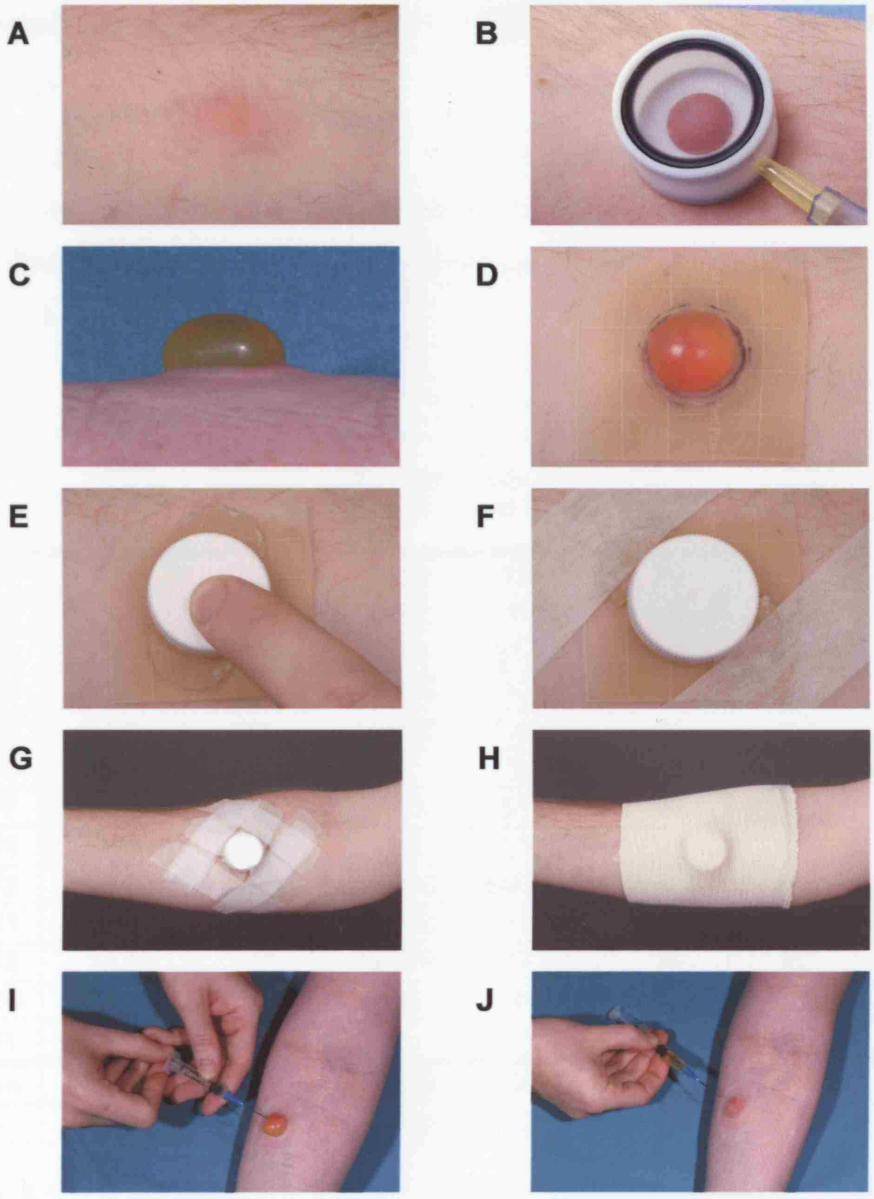

Figure 3.2 Skin suction blister induction, dressing and aspiration

(A) Skin suction blisters were raised on Mantoux tests or normal skin 18-24 hours prior to sampling. (B) A suction cup was centred on the Mantoux test and a negative pressure of 25-40 kPa (200-300 mmHg) below atmospheric pressure was applied to the skin until (C) a unilocular blister was formed. The blister was dressed with (D) a 5×5cm piece of Comfeel Plus Ulcer Dressing, (E) a trimmed Universal container top, (F,G) Micropore tape and (H) a Tubigrip bandage. (I) Blister fluid was aspirated the following day using a sterile 23G needle and 2ml syringe. (J) The deflated blisters occasionally refilled in the 24-72 hours after aspiration. Blisters dried-up within 7 days and the epidermal roofs exfoliated 7-10 days after aspiration. This left an area of post-inflammatory erythema or hyperpigmentation, but no scarring.

3.3 Analysis of skin suction blisters induced on normal skin

Optimisation of the skin suction blister technique was carried out on normal non-inflamed skin. Data relating to parameters measured during the collection of blister fluid from these experiments are shown below in Table 3.1.

	Blister diameter (mm)	Volume blister fluid (μl)	Number of RBC	Number of WBC	RBC/μl blister fluid	WBC/μl blister fluid	% PB WBC contamin.
JR#1	7.5	50	3000	12600	50	252	0.02
JR#2	10	150	16800	31200	112	208	0.05
JR#3	11	200	8000	217500	40	1088	0.004
JR#4	11.5	350	14400	40800	41	117	0.04
JR#5	11.5	250	20800	134400	83	538	0.02
JR#6	12	400	0	3600	0	9	0
JR#7	13.5	700	17500	51300	25	73	0.03
PD#1	12.5	350	4200	21600	12	62	0.02
PD#2	15.5	750	46200	98400	62	131	0.05
KB#1	10	250	11000	13000	44	52	0.09
KB#2	14.5	750	57000	72000	76	96	0.08
AC#1	12	250	600	10200	2	41	0.006
BT#1	13	500	0	5500	0	11	0
Mean	**11.88**	**380.77**	**15346**	**54777**	**42**	**206**	**0.03**
SD	**2.07**	**231**	**17707**	**62876**	**35**	**300**	**0.03**

Table 3.1 Parameters measured on skin suction blisters induced on normal control skin

The diameter and volume of fluid recovered from each blister were measured. The total blister leucocyte and red cell count was determined using a haemocytometer. Peripheral blood RBC and WBC counts were also measured. This allowed an estimate of the percentage of peripheral blood leucocytes contaminating the blister due to microhaemorrhages to be made.

3.3.1 Leucocyte and RBC numbers

The skin suction blister technique is regarded as causing relatively little trauma, especially with small blisters on non-inflamed skin that are immediately harvested[438;441]. Our intention was to induce suction blisters

on inflamed skin to obtain as many skin leucocytes as possible, which meant delaying the aspiration of the blister fluid for up to 24 hours. The presence of red blood cells (RBC) in the perivascular and interstitial regions of the dermis is not a histological feature of non-inflamed skin or the Mantoux test in normal individuals[419;421]. Their presence in blister fluid, therefore, points to haemorrhage from the underlying dermal blood vessels. This may allow peripheral blood leucocytes to directly enter the suction blister, by-passing the selective recruitment of leucocytes that occurs across cutaneous post-capillary venules with inflammation. This would consequently result in the dilution of leucocytes selectively recruited into the inflammatory microenvironment of the skin, which might possibly mask any detectable difference between skin and PB leucocytes. Previous studies that have examined lymphocytes isolated from delayed-type hypersensitivity responses using skin suction blisters have not routinely monitored RBC contamination[20;23;24;442]. We considered that an assessment of RBC contamination should be made. The total number of red and white cells in the aspirated fluid of each blister was therefore quantified using a haemocytometer. Additionally, PB RBC and white blood cell (WBC) counts were measured by the Department of Haematology, Royal Free Hospital. This then allowed an estimation of the percentage of peripheral blood (PB) white cells that were contaminating the blister white cells. Simplistically, there are 1000 fold more RBC than WBC in the peripheral blood of healthy volunteers. Therefore, for every 1000 RBC in the blister fluid one can estimate that there would be 1 contaminating peripheral blood WBC that was not part of the underlying cutaneous inflammatory infiltrate. The estimate was calculated as follows:

$$\frac{\text{Blister red cell count} \times (\text{PB white cell count} \div \text{PB red cell count})}{\text{Blister white cell count}} \times 100$$

The mean number of leucocytes isolated per blister raised on normal skin was 54777 SD ± 62876 (range 3600-217500). The number of red blood cells isolated per blister was consistently lower than the number of

leucocytes (mean 15346 SD ± 17707 (range 0-57000)). Overall, this meant that the estimated percentage of contaminating PB WBC in the blister leucocytes was very low in suction blisters raised on normal non-inflamed skin (mean 0.03% SD ± 0.03 (range 0-0.09)) (Table 3.1). Additionally, leucocyte viability as assessed by trypan blue exclusion was greater than 95%.

The diameter of the blisters varied from 7.5 to 15.5mm and this allowed an assessment of the effect of blister size on cell recovery to be made. Increasing blister diameter was associated with a trend of increasing RBCs and leucocytes isolated, but this correlated poorly (r_s=0.28 and 0.14, p=0.35 and 0.65 respectively) (Figure 3.3a,b). Additionally, increasing blister diameter appeared to have little effect on the percentage of contaminating PB leucocytes in the blister leucocytes isolated (r_s=–0.05, p=0.88) (Figure 3.3c).

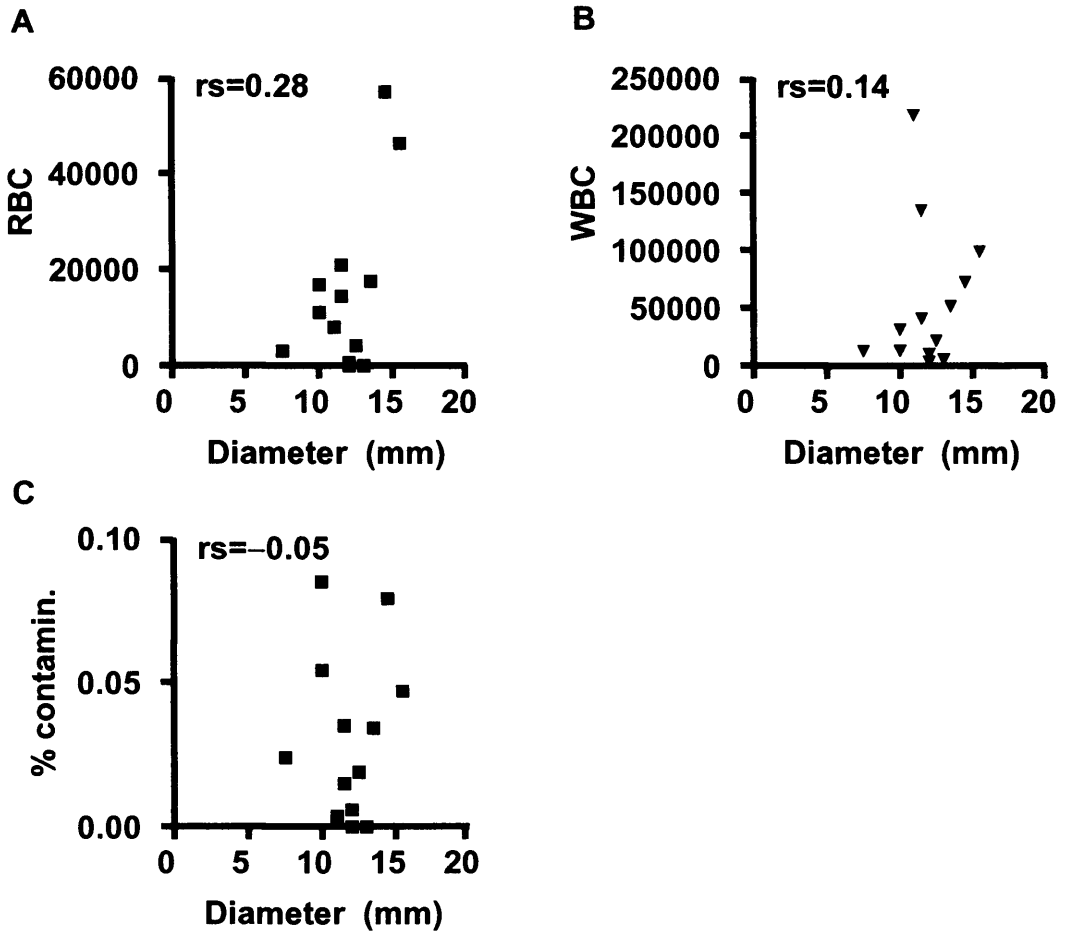

Figure 3.3 Leucocyte and RBC numbers in skin suction blisters raised on normal skin

Blister fluid was aspirated from skin suction blisters 18-24 hours after being raised on normal non-inflamed skin. RBC and leucocyte numbers were determined using a haemocytometer. The size of the blister was determined by calculating the mean of 2 measured perpendicular planes. The relationship between blister diameter and (A) RBC and (B) leucocyte numbers isolated is shown. (C) The effect of blister size on the percentage of contaminating blood WBC in blister leucocytes isolated. The graphs illustrate the results of 13 skin suction blisters raised on normal skin. The Spearman rank correlation (rs) for each graph is shown.

3.3.2 Skin-homing inflammatory T cells in suction blisters

Lymphocytes in inflamed skin predominantly display a skin-homing phenotype i.e. CLA and CCR4 or CCR10[20;138;139]. Additionally, it is recognised that memory / effector T cells in the skin express the non-specific inflammatory chemokine receptor CCR5[403;442-444]. We, therefore,

undertook a preliminary assessment to determine whether lymphocytes isolated in a skin suction blister were of a skin-homing effector phenotype.

The expression of CLA and CCR5 on $CD3^+$ lymphocytes in PBMC and blister cells isolated from normal skin was determined using flow cytometry. In the PB 20.58% of $CD3^+$ T cells were CLA positive. This compared with 77.71% of $CD3^+$ T cells in skin suction blisters raised on normal skin (Figure 3.4). The proportion of PB and skin blister $CD4^+$ T cells positive for CLA expression was very similar to $CD3^+$ T cells (24.83% and 76.79%). The difference in expression observed between the PB and skin suction blisters corresponds to that previously reported in PBMC and MT skin sections[380]. This indicates that T cells that migrate into skin suction blisters do so from the skin microenvironment and are therefore representative of the underlying resident T cells

The percentage of T cells expressing CCR5 was also enriched in the skin suction blisters compared to the PB (Figure 3.5). In the blood 37.76% of $CD3^+$ T cells were $CCR5^+$ whereas in the skin suction blister the proportion increased to 76.01%. The intensity of expression on positively gated cells appeared to be unchanged (MFI 8.58 versus 9.39 in PB and blister respectively). This lends additional support to the assertion that the lymphocytes isolated from a skin suction blister are representative of cells that have migrated into the skin microenvironment in a cutaneous-specific manner and that these cells are also of an inflammatory effector phenotype. On the basis of the results gained in these preliminary experiments on non-inflamed normal skin, it was decided to extend the skin suction blister technique to isolating cells from the inflamed skin of Mantoux tests.

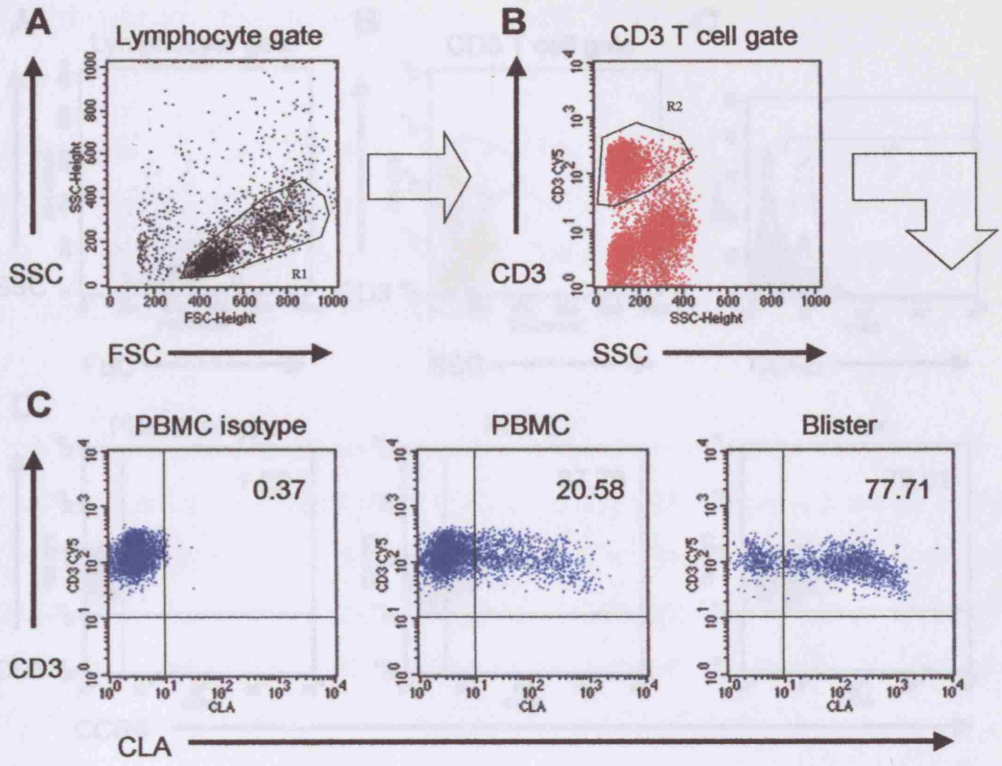

Figure 3.4 CLA expression on peripheral blood and normal skin blister $CD3^+$ T cells

PB and blister cells from non-inflamed normal skin were isolated and stained with anti-CD3-RPE-Cy5, anti-CD4-FITC and anti-CLA as described in Materials and Methods. CLA was detected by indirect immunofluorescence staining using goat anti-mouse IgM-PE. The cells were analysed by flow cytometry. 10000 events were collected and gated as shown. (A) A live lymphocyte gate was used to exclude cell debris, but include lymphocyte blasts (R1). (B) $CD3^+$ T cell gate (R2). (C) Dot-plots showing CLA expression on $CD3^+$ T cells isolated from the PB and a suction blister raised on normal skin. The number in each dot-plot refers to the percentage of $CD3^+$ T cells positive for CLA expression. The PB isotype control was used to set the quadrant position to delineate negative and positive events.

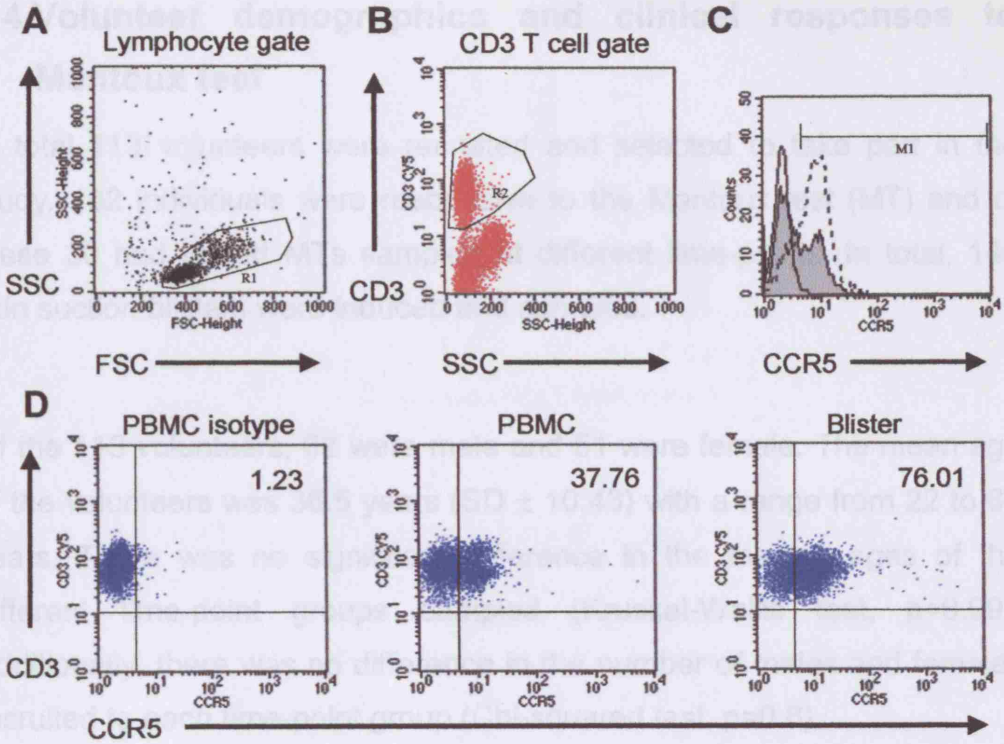

Figure 3.5 CCR5 expression on peripheral blood and normal skin blister $CD3^+$ T cells

PB and blister cells from non-inflamed normal skin were isolated and stained for anti-CD3-RPE-Cy5 and anti-CCR5 as described in Materials and Methods. CCR5 was detected by indirect immunofluorescence staining using goat anti-mouse IgG2b-FITC. The cells were analysed by flow cytometry. 10000 events were collected and gated as shown. (A) A live lymphocyte gate was used to exclude cell debris, but include lymphocyte blasts (R1). (B) $CD3^+$ T cell gate (R2). (C) Histogram of CCR5 expression on PB and skin T cells in suction blisters. The M1 gate was used to determine the intensity of CCR5 expression in terms of the median fluorescent intensity (MFI) on $CCR5^+$ cells. Expression of CCR5 in the PB is shown by the filled grey histogram and in the blister by the open broken lined histogram. The PB isotype control is shown by the open solid lined histogram. (D) Dot-plots showing CCR5 expression on $CD3^+$ T cells isolated from the PB and a suction blister raised on normal skin. The number in each dot-plot refers to the percentage of $CD3^+$ T cells positive for CCR5 expression. The PB isotype control was used to set the quadrant position to delineate negative and positive events.

3.4 Volunteer demographics and clinical responses to Mantoux test

In total 113 volunteers were recruited and selected to take part in the study. 102 individuals were responsive to the Mantoux test (MT) and of these 30 had paired MTs sampled at different time-points. In total, 149 skin suction blisters were induced and sampled.

Of the 113 volunteers, 62 were male and 51 were female. The mean age of the volunteers was 36.5 years (SD ± 10.43) with a range from 22 to 69 years. There was no significant difference in the median ages of the different time-point groups sampled (Kruskal-Wallis test, p=0.99). Additionally, there was no difference in the number of males and females recruited to each time-point group (Chi-squared test, p=0.6).

Figure 3.6 shows the clinical kinetics of the Mantoux test, which was determined by measuring the responses at the time of sampling. The clinical peak of the immune response occurs 3 days after the induction of the MT and resolution is evident from day 7 onwards (day 3 versus day 7; Mann-Whitney test, p=0.0006). All volunteers additionally had the clinical response to the MT measured at the clinical peak on day 3, to ensure that the intensity of response was similar between the sample time-point groups. There was no difference in responsiveness to the Mantoux test between the time-points (Kruskal-Wallis test, p=0.42) (Figure 3.7). Based on the clinical characteristics this, therefore, implies that the groups were comparable.

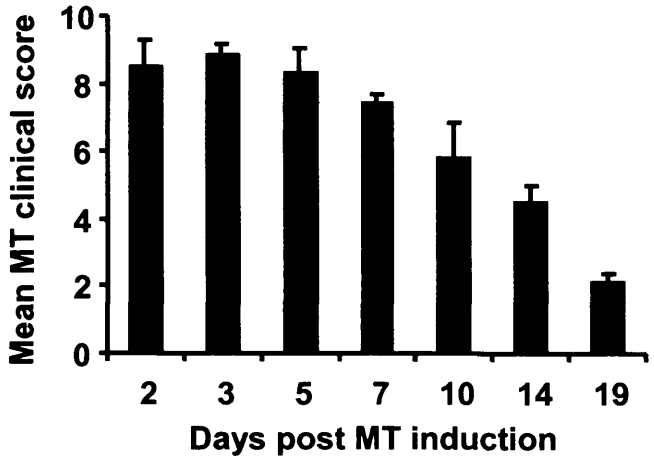

Figure 3.6 The clinical response kinetics to the Mantoux test

Each response was measured clinically at the time of sampling. The change in erythema-index from baseline, size of induration and palpability were scored and the sum of these scores then used to give an overall clinical score for each MT measured. The mean clinical score ± standard error of the mean (SEM) for each time-point group is shown and represents a minimum of at least 6 MTs measured per time-point group. The variation observed between the different time-points was statistically significant (Kruskal-Wallis test, $p<0.0001$).

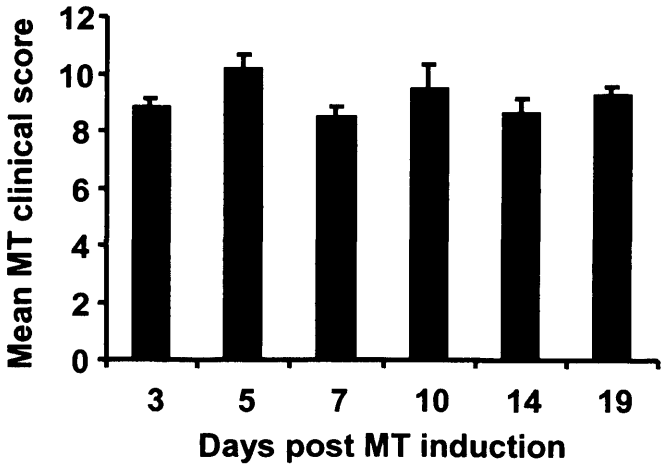

Figure 3.7 Comparative Mantoux test responsiveness between sample time-point groups

Each response was measured clinically 3 days after induction. The mean MT clinical score ± SEM is shown for each time-point group and represents a minimum of at least 6 MTs measured per time-point group. The variation observed between the different time-points was not statistically significant (Kruskal-Wallis test, $p=0.42$).

3.5 Analysis of skin suction blisters raised over Mantoux tests

3.5.1 Leucocyte and RBC numbers

Skin suction blisters were raised over a total of 132 MTs at various time-points. The mean number of leucocytes isolated from skin suction blisters raised on normal skin was 50830 (range 2100 to 217500). In comparison, the number of leucocytes obtained from suction blisters raised on inflamed MT skin was markedly higher than in normal skin suction blisters (339000 per blister; range 5000 to 9.7×10^6). This was true for all the different MT time-point groups analysed (Mann-Whitney test, p=0.019-0.0001). The peak for isolating leucocytes from skin suction blisters was 2 days after MT induction (Figure 3.8a). To control for variations in blister size, the number of leucocytes isolated per microlitre of blister fluid was also analysed. This was again significantly higher at all time-points during the MT compared to control normal skin (Mann-Witney test; 0.0178-0.0351) except at day 5 (Figure 3.8b). Leucocyte viability as assessed by trypan blue exclusion was greater than 95% at all time-points.

The number of RBC contaminating the suction blisters during the MTs was significantly elevated at all time-points during the MT compared to normal control skin (Mann-Whitney test, p=0.0004-<0.0001) (Figure 3.8c). This was reflected in the estimated percentage of PB WBC contaminating the blister leucocytes, which was significantly higher at all time-points during the Mantoux test compared to normal control skin (Mann-Whitney test, p=0.0029-<0.0001). In general, however, the percentage of PB WBC contaminating the blister leucocytes was about 1% or less during the Mantoux test (Figure 3.8d). This means that approximately only 1 in 100 leucocytes isolated from suction blisters had migrated into the blister directly from damaged dermal blood vessels rather than the skin microenvironment.

We also analysed the effect of clinical responsiveness to the MT on cell recovery. The data obtained from the day 7 MT volunteers are presented as a representative example. Larger clinical responses generally allowed bigger suction blisters to be induced (Figure 3.9a) (r_s=0.44, p=0.015). On this background, a trend of increasing numbers of leucocytes isolated from suction blisters was observed with increasing clinical responsiveness (r_s=0.49, p=0.0056) (Figure 3.9b). Despite this trend, a larger clinical response did not necessarily assure the isolation of a large number of leucocytes. When the number of leucocytes isolated per microlitre of blister fluid was analysed to control for blister size the correlation with clinical response was less predictive (r_s=0.27, p=0.16) (Figure 3.9c). Overall, however, larger MT responses generally resulted in more leucocytes being isolated.

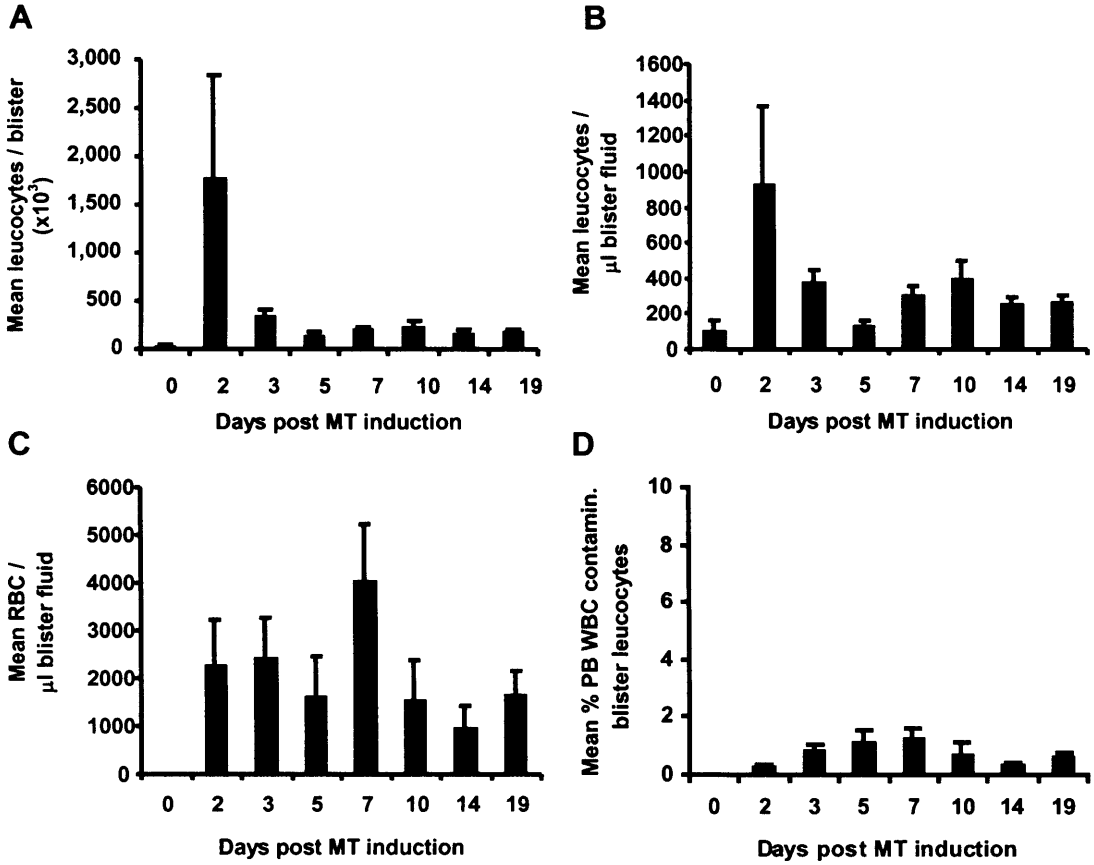

Figure 3.8 Skin suction blister RBC and leucocyte numbers isolated during Mantoux tests

(A) The mean number of leucocytes isolated from skin suction blisters raised over Mantoux tests at different time-points after MT induction. (B) The mean number of leucocytes isolated per microlitre (µl) of blister fluid in skin suction blisters raised over Mantoux tests at different time-points after MT induction. (C) The mean number of RBC isolated per microlitre (µl) of blister fluid in skin suction blisters raised over Mantoux tests at different time-points after MT induction. (D) The mean percentage of PB WBC contaminating isolated blister leucocytes in skin suction blisters raised over Mantoux tests at different time-points after MT induction. The mean ± SEM is shown for each time-point group and represents a minimum of at least 6 experiments per time-point group.

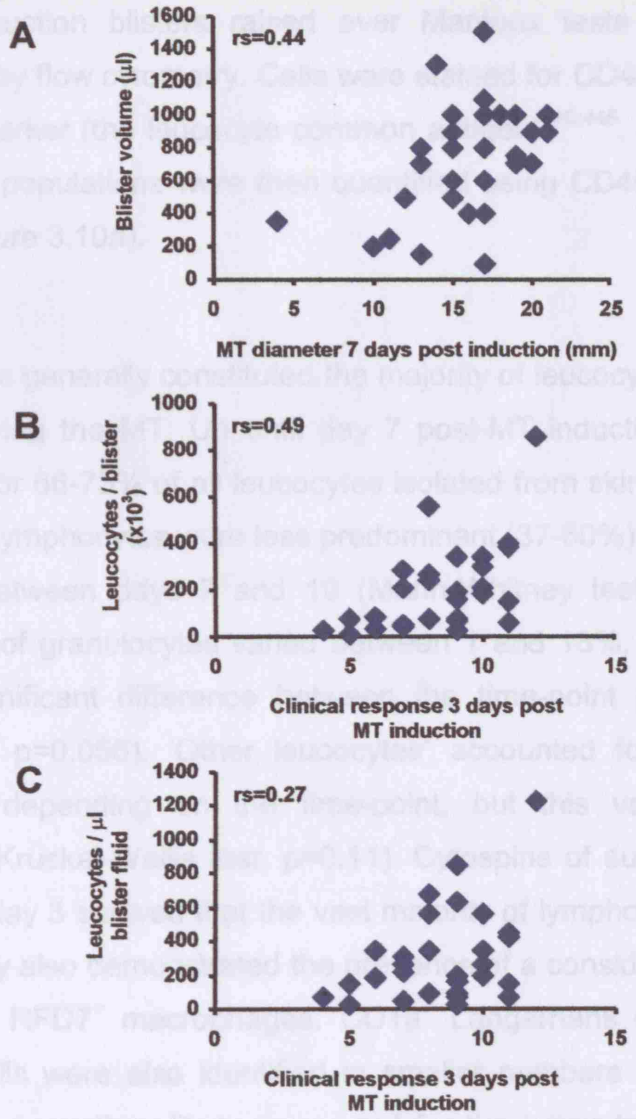

Figure 3.9 Blister volumes and leucocyte numbers isolated from skin suction blisters raised over Mantoux tests 7 days after induction

Figures show data collected from 30 skin suction blisters raised over MTs in volunteers allotted to the day 7 time-point group. (A) Blister fluid volume aspirated compared to MT induration diameter (mm) at day 7. (B) Number of leucocytes isolated from skin suction blisters at day 7 compared to the clinical response measured at day 3. (C) Number of leucocytes isolated per microlitre (µl) of skin suction blister fluid at day 7 compared to the clinical response measured at day 3. The Spearman rank correlation (rs) for each graph is shown.

3.5.2 Leucocyte subsets in MT skin suction blisters

The focus of our interest in the skin suction blisters was the T lymphocytes. The proportion of lymphocytes in the leucocytes isolated

from skin suction blisters raised over Mantoux tests was, therefore, determined by flow cytometry. Cells were stained for CD45, which is a pan leucocyte marker (the leucocyte common antigen)[120;445]. Lymphocyte and granulocyte populations were then quantified using CD45-FITC and SSC profiles (Figure 3.10a).

Lymphocytes generally constituted the majority of leucocytes isolated from the skin during the MT. Up until day 7 post-MT induction, lymphocytes accounted for 66-73% of all leucocytes isolated from skin suction blisters. Thereafter, lymphocytes were less predominant (37-50%) with a significant decrease between days 7 and 10 (Mann-Whitney test, $p=0.036$). The percentage of granulocytes varied between 1 and 18%, but overall there was no significant difference between the time-point groups (Kruskal-Wallis test, $p=0.056$). 'Other leucocytes' accounted for 20-53% of all leucocytes depending on the time-point, but this variation was not significant (Kruskal-Wallis test, $p=0.11$). Cytospins of suction blister cells isolated at day 3 showed that the vast majority of lymphocytes were $CD3^+$ T cells. They also demonstrated the presence of a considerable number of $CD68^+$ and $RFD7^+$ macrophages. $CD1a^+$ Langerhans cells and $RFD1^+$ dendritic cells were also identified in smaller numbers (Figure 3.10b-e). These cells more than likely accounted for the 'other leucocytes' subset identified by flow cytometry in Figure 3.10a. Cytospin staining was verified by comparison with cytospin negative controls and with positive MT skin or tonsil controls depending on the target antigen being examined.

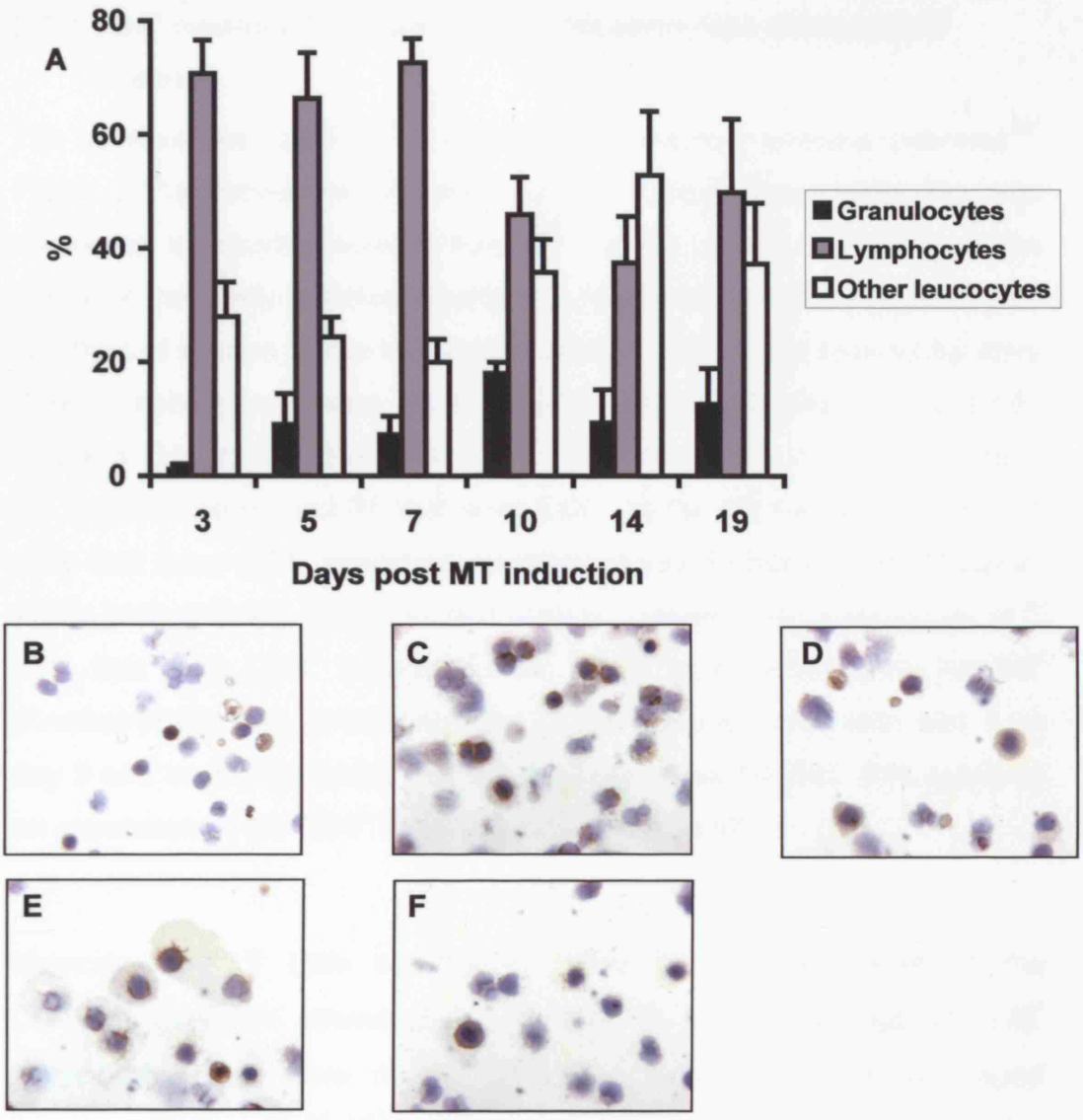

Figure 3.10 Composition of leucocytes isolated from skin suction blisters raised on Mantoux tests

(A) Percentage of granulocytes (black bars, ■), lymphocytes (grey bars, ■) and other leucocytes (white bars, □) isolated from skin suction blisters raised on MTs at different time-points. Lymphocyte and granulocyte percentages were determined by flow cytometry gating on specific populations using CD45-FITC and SSC profiles. The mean ± SEM is shown for each time-point group. The data for each group represents 3-6 experiments per time-point group. (B-E) Indirect immunoperoxidase staining of cytospins of blister cells isolated from Mantoux tests 3 days after induction (×40 magnification). (B) $CD3^+$ T cells. (C) $CD68^+$ macrophages. (D) $RFD7^+$ macrophages. (E) $RFD1^+$ dendritic cells. (F) $CD1a^+$ Langerhans cell. The figure shows representative photomicrographs taken from 1 of 3 experiments.

3.5.3 $CD4^+$ memory T lymphocytes in Mantoux test skin suction blisters

The Mantoux test is a $CD4^+$ T cell mediated memory immune response[25]. Figure 3.11a shows the proportion of $CD4^+$ lymphocytes within the total number of leucocytes isolated from MT suction blisters. Surprisingly, this remained relatively constant during the course of the MT. Approximately one third of suction blister leucocytes isolated at different time-points were $CD4^+$ lymphocytes (mean 23.57-40.87%) (Kruskal-Wallis test, p=0.56). Figure 3.11b on the other hand shows the percentage of $CD3^+$ T cells in MT suction blisters and PB that were $CD4^+$. In the PB the percentage of T cells that were $CD4^+$ remained relatively stable during the MT (Kruskal-Wallis test, p=0.49). In the suction blisters, however, the percentage of T cells that were $CD4^+$ increased from 57.71 to 87.97% during the MT (Kruskal-Wallis test, p=0.0006). The CD4:CD8 ratio in the skin was 3 on day 3 and increased during the MT peaking at day 14 (58). This points to an expansion of the $CD4^+$ T cell subset during the MT.

Memory $CD4^+$ T cells can be identified by the expression of the $CD45RO^+CD45RA^-$ phenotype[7;73]. In the PB, the percentage of $CD4^+$ lymphocytes that were of the $CD45RA^-$ memory phenotype ranged between 40.76 and 50.02% during the MT (Figure 3.11). In contrast, the vast majority of $CD4^+$ lymphocytes isolated from suction blisters raised on normal skin or MTs were of the $CD45RA^-$ memory phenotype (mean 94.87-98.33%). The difference between the blood and skin was significant at all time-points (Wilcoxon signed rank test, p=0.016-0.031). This points to the selective recruitment and retention of $CD4^+$ memory T cells in the skin during the immune response. Furthermore, it lends additional support to the supposition that the cells migrating into skin suction blisters are representative of the underlying infiltrate.

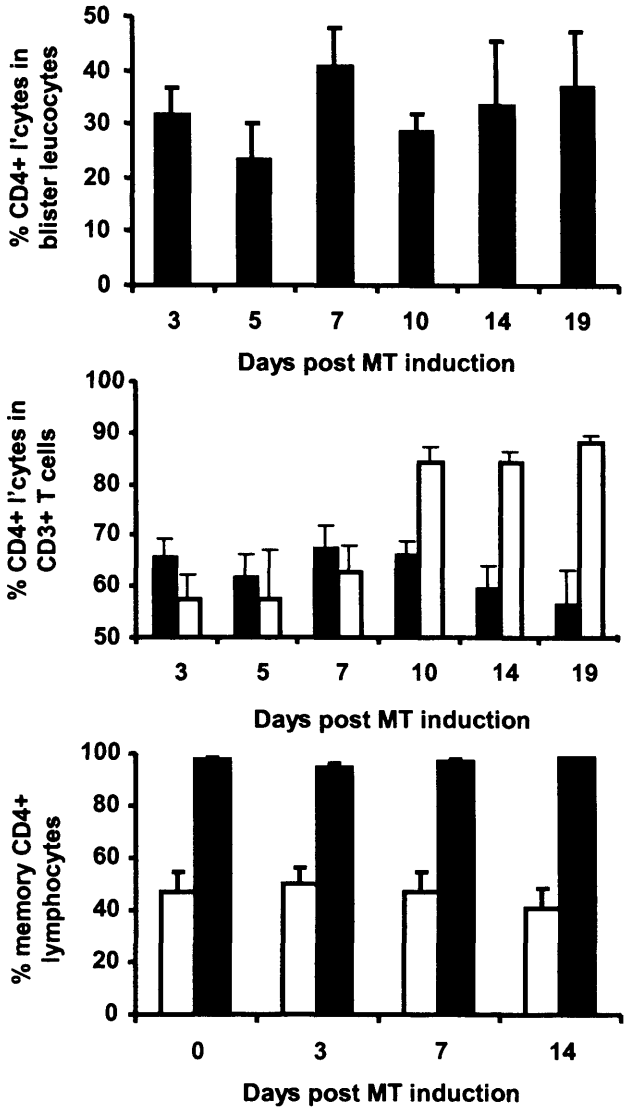

Figure 3.11 The proportion of lymphocytes in the blood and skin suction blisters with the $CD4^+$ and $CD45RA^-$ memory phenotype during the Mantoux test

(A) The mean percentage (± SEM) of $CD4^+$ lymphocytes within leucocytes isolated from MT blisters 3-19 days after induction. This was determined by flow cytometry after gating on the lymphocyte population using CD45 and SSC profiles. 3-6 volunteers were studied per time-point. (B) The mean percentage (± SEM) of $CD3^+$ T cells expressing CD4 isolated from the PB and MT suction blisters at different time-points after MT induction. PB and blister cells were stained with anti-CD3-PerCP and anti-CD4-APC then analysed by flow cytometry. 4-6 volunteers were studied per time-point. Open bars (□) represent the PB and black bars (■) the skin suction blisters. (C) The mean percentage (± SEM) of $CD4^+$ lymphocytes with the $CD45RA^-$ memory phenotype isolated from the PB and MT suction blisters 0-14 days after MT induction. PB and blister cells were stained for anti-CD4-APC and anti-CD45RA-FITC then analysed by flow cytometry. Open bars (□) represent the PB and black bars (■) the skin suction blisters. 6-7 volunteers were studied per time-point

3.5.4 CLA$^+$ T cells in MT skin suction blisters

In section 2.3, we showed that CD3$^+$ T cells isolated from a suction blister raised on normal skin were enriched with the CLA$^+$ skin-homing phenotype. This was also observed in the CD4$^+$ T cell subset. Figure 3.12 shows that a high proportion of CD4$^+$ and CD8$^+$ T cells isolated from suction blisters raised on MTs 3 days after PPD challenge were also CLA$^+$. In the blood, the percentage of CD4$^+$ T cells positive for CLA expression was 21.62%, whereas in suction blisters this was increased to 76.02% (p=0.012). In the CD8$^+$ T cell subset the percentage positive for CLA expression in the PB was 10.67%, whereas in suction blisters this was increased to 58.75% (p=0.007). These results correspond with previous reports comparing CLA expression on T cells in the blood with MT skin sections[380].

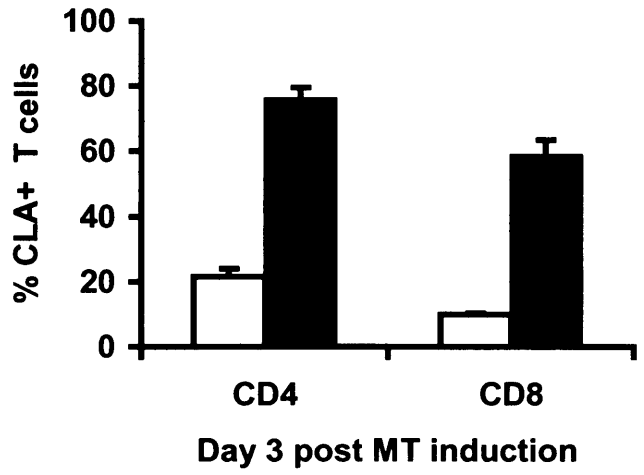

Figure 3.12 CLA expression on T cells in the blood and skin 3 days after Mantoux test induction

The mean percentage (± SEM) of CD4$^+$ and CD8$^+$ T cells expressing CLA in PB and MT suction blisters sampled at day 3. PBMC and blister leucocytes were stained with anti-CD3-PerCP, anti-CD4-APC and anti-CLA antibodies. Anti-CLA antibody was detected by indirect immunofluorescence staining using goat anti-mouse IgM-PE. Samples were analysed by flow cytometry, gating on the CD3$^+$CD4$^+$ and CD3$^+$CD4$^-$ (CD8$^+$) subsets. An isotype control staining with PBMC was used to set the quadrant position in order to delineate negative and positive expression of CLA (as shown in Figure 3.4). Open bars represent the PB (□) and black bars (■) the skin suction blisters. 3 volunteers were studied per time-point

3.6 Discussion

The isolation of lymphocytes from peripheral tissues can be problematic and this is particularly true of the skin with its rigid cohesive structure. Ideally, an isolation method should yield all of the resident lymphocytes in a viable state whilst maintaining their phenotypic and functional characteristics. The use of the suction blister technique to isolate T lymphocytes from non-inflamed and inflamed skin has been examined in this chapter. This technique was chosen, because it allows the *ex vivo* isolation of cutaneous lymphocytes without resorting to the use of enzymatic digestion or *in vitro* culture. This means that once the cells have been removed from the *in vivo* setting they can be analysed immediately with the minimum of *in vitro* manipulation. Furthermore, leucocytes isolated using this technique demonstrate good viability and the nominal exposure to *in vitro* conditions would be expected to minimise any changes on phenotypic and functional characteristics. Data presented in later chapters will demonstrate that cells isolated from Mantoux tests using this technique remain functionally active. Another additional benefit of this technique is that it allows for the analysis of soluble mediators such as cytokines and chemokines that are present in the blister fluid.

The technique is relatively non-invasive and this is reflected in the fact that no serious complications were encountered. Additionally, the procedure is non-scarring, although post-inflammatory hyperpigmentation was observed and this was more common in darker skin types. Overall the induction of suction blisters on inflamed and non-inflamed skin involved minimal discomfort, although it was time-consuming for volunteers. This is one of the drawbacks of the technique. A number of factors are recognised to effect suction blister induction time. Increasing skin temperature has been noted to accelerate suction blister induction[446;447]. The suction blister technique described in this chapter was generally performed at warm room temperature (~22°C) and increased induction times were noted with cooler conditions. To minimise the induction time, other investigators have used water baths[446], infrared lamps[442;448], heated

suction chambers[449;450] and warm (50°C) saline soaks[451] to ensure a skin temperature of at least 37°C. Active skin warming was not adopted in this study in order to maintain the portability of the technique and minimise the effects the overall procedure might have on cutaneous lymphocytes. In addition to skin temperature, increasing age[446;452-454], pressure[447;452;455] and suction cup aperture diameter[456] have all been noted to reduce the blister induction time. Other authors, however, have found no variation in blister induction time with changing aperture diameter[455]. In this study, the diameter of MT induration measured at the time of sampling determined the aperture of the suction cup used. This was to ensure that only inflamed skin was blistered and not the surrounding non-inflamed skin. High negative pressures of 90-100 kPa (~700-760mmHg) below atmospheric pressure have in the past been used for the rapid induction of skin suction blisters (reviewed by Falabella[457]). However, lower pressures of 25-40 kPa (200-300 mmHg) below atmospheric pressure are now generally used since this minimises damage to the skin and associated haemorrhage[438;441]. We adopted this pressure range in this study so as to minimise the risk of haemorrhage in suction blisters.

Two novel developments were made to the skin suction blister technique in this study. The first was the regular assessment of RBC contamination in suction blisters. Haemorrhage from the dermal blood vessels may allow peripheral blood WBC to by-pass the physiological selective recruitment of skin-homing leucocytes from the blood across the endothelium into the skin microenvironment. The inflamed skin of the Mantoux test demonstrated significantly higher RBC contamination in suction blisters compared to non-inflamed skin. This more than likely reflects the vasodilatation and vascular proliferation that is associated with inflammation. As a result of the higher RBC contamination the estimated percentage of PB WBC contaminating the blister leucocytes was significantly higher at all time-points during the Mantoux test compared to normal control skin, but overall was about 1% or less. This degree of

contamination, however, would not be sufficient to mask any detectable difference when comparing skin and blood lymphocytes.

The second development was the use of the skin suction blister technique to isolate leucocytes from MTs up to 19 days after the induction of the immune response. Previous studies examining the Mantoux test using skin suction blisters have only followed the immune response up to 96 hours[20-24]. This represents the phase of the immune response when the clinical peak occurs, whereas the kinetics of lymphocytic infiltration actually differs and these will be examined in the next chapter. On average over 300,000 leucocytes, regardless of suction blister size, were isolated from each blister during the course of the Mantoux test. Even 19 days after the induction of the immune response, when clinically there is usually little to detect except for residual increased erythema, on average almost 200,000 leucocytes per suction blister could be recovered. This was sufficient to undertake a range of experimental analyses involving flow cytometry and cell culture. A limitation of the technique, however, is the relatively poor predictability of cell numbers that can be recovered. A trend of increasing leucocytes isolated was noted with increasing blister size and MT clinical response, but a definitive correlation was not observed. This not only reflected variability occurring between individuals, but also variability observed in suction blisters raised under identical conditions in the same individual. It remains unclear as to the reasons responsible for this.

T lymphocytes, macrophages and other antigen presenting cells were isolated in suction blisters raised over Mantoux tests. This reflects the histological composition of the MT as a delayed type hypersensitivity reaction[25;419;458;459]. Up to 7 days after MT induction lymphocytes predominated in suction blisters, whereas later in the response there was an increased proportion of 'other leucocytes', which more than likely consisted predominantly of macrophages. The MT is a $CD4^+$ memory T

cell mediated cutaneous immune response[25;419;421] and the vast majority of $CD4^+$ T lymphocytes isolated from suction blisters during the MT were of a memory / effector phenotype. Furthermore, the T lymphocytes isolated from suction blisters at day 3 were predominantly of the CLA^+ skin-homing phenotype. This points to the selective recruitment of skin-homing memory / effector T lymphocytes into the skin microenvironment and suction blisters overlying MTs. These findings are consistent with those previously published in studies using suction blisters to examine the immunology of the MT[20;21;24].

The proportion of T cells in skin suction blisters that were $CD4^+$ increased during the course of the response and this points to the expansion of the $CD4^+$ T cell subset within the skin. This is consistent with the MT being a $CD4^+$ T cell mediated immune response. Furthermore, this may reflect the selective recruitment and/or localised proliferation of $CD4^+$ T cells within the skin during the immune response. Importantly, these observations made using suction blisters over MTs are similar to those previously reported using immunohistology on section of MTs up to 14 days post-induction[25]. This suggests that the composition of the cells in the blister fluid accurately reflects the cellular infiltrate in the underlying dermis.

In summary, the suction blister technique represents a simple technique for isolating viable T lymphocytes from the skin of Mantoux tests. The T cells isolated also appear to be representative of the underlying inflammatory infiltrate. Importantly, this method does not involve prolonged *in vitro* culture or enzymatic digestion, which is known to result in phenotypic changes on T lymphocytes including decreased expression of CD4, CD8 and CD25[430-432]. Data presented in the following chapters will demonstrate that the suction blister technique and Mantoux test model can be used to explore questions of cellular differentiation and functionality during a cutaneous immune response.

4 Lymphocyte differentiation during the Mantoux test

4.1 Introduction

Adaptive immune responses are dependent on the proliferation and clonal expansion of antigen-specific T cells[6]. It is generally accepted that this occurs in draining lymph nodes to which activated and mature dendritic cells have migrated following the uptake of antigen in peripheral non-lymphoid tissues. Antigen-specific T cells that recognise processed antigen in the context of peptide-MHC complexes then become activated, proliferate and undergo a process of differentiation whereby they gain effector function with modified cytokine secretion, signalling and migratory properties[6;7;460]. This allows the activated antigen-specific T cells to migrate back into the inflamed non-lymphoid tissue to carry out effector functions, which lead to the clearance of the antigen. In primary murine immune responses, there is increasing evidence in mice that the proliferation of antigen-specific T cells occurs principally in the lymph node environment[8;9]. The expansion of cell numbers in non-lymphoid tissues appears to be dependent on the recruitment and retention of cells that have undergone clonal expansion within the lymph node rather than as a result of *in situ* proliferation. It is as yet unclear whether this is also true of secondary immune responses particularly in light of evidence suggesting the persistence of memory cells in non-lymphoid tissues[101;102]. However, various adoptive transfer experiments using either *in vitro* activated transgenic $CD4^+$ T cells or *in vivo* priming strategies have demonstrated a similar preferential proliferation in lymphoid tissues[10-12]. Proliferation in non-lymphoid tissues, however, was not completely excluded in two of these studies and in fact was evident later in the immune response in the remaining study, albeit to a lesser extent compared to lymphoid tissue[11]. It

is unknown whether this pattern of T cell expansion applies to a localised immune response in humans.

$CD4^+$ T cell differentiation is characterised by the acquisition of CD45RO expression, loss of CD45RA expression and gradual decrease in CD45RB expression combined with telomere shortening[7;73;193;290]. Previous *in vivo* studies in humans and mice have shown that telomere length is actually maintained in T cells isolated from the blood or lymphoid tissues during acute primary and secondary immune responses as result of the induction of telomerase activity[240-244]. The effect of a localised immune response on telomere length in T cells that have migrated into a non-lymphoid tissue is unknown. We have, therefore, used the MT model to investigate whether extra-lymphoidal T cell expansion and differentiation occurs in the skin following secondary immune challenge in humans *in vivo*.

4.2 Kinetics of the clinical versus the cutaneous T cell response

In chapter 3, we demonstrated that the Mantoux test peaks clinically at day 3 and that resolution of the response is evident from 7 days, so that by 19 days after induction residual increased erythema is often all that can be detected clinically. Interestingly, when the course of the clinical response is compared to the kinetics of T cell infiltration into the skin, it can be seen that the clinical and cellular peaks are asynchronous (Figure 4.1). The peak of T cell infiltration into the skin lags the clinical peak by 4 days. This peak of T cell infiltration indicates that a significant expansion and contraction of T cell numbers takes place in the skin during the MT (Kruskal-Wallis, $p<0.0001$). Based on these observations, we were able to define 2 main phases of the cellular immune response: the induction phase up to day 7 and resolution phase from day 7 onwards.

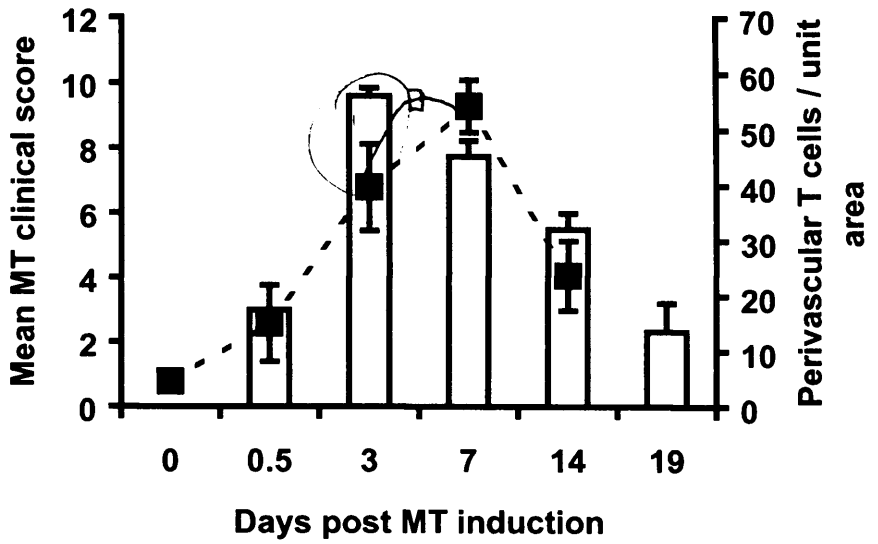

Figure 4.1 Comparison of the Mantoux test clinical course with the kinetics of T cell infiltration

MTs were measured clinically at the time of sampling. The change in erythema-index from baseline, size of induration and palpability were scored. The sum of these scores was then used to give an overall clinical score for each MT measured (□, left-hand y-axis). The mean number of T cells per unit area of dermal perivascular infiltrates in tissue sections of Mantoux test is shown (■, right-hand y-axis). T cells were detected by indirect immunoperoxidase staining and quantified within a 100μm diameter circular frame centred on the 5 largest perivascular infiltrates by image analysis. The mean ± SEM for each time-point group is shown and represents at least 5 MTs examined per time-point.

4.3 αβ and γδ T cell subsets in the blood and skin during the Mantoux test

Evidence suggests that, in addition to the established importance of αβ T cells, γδ T cells may also play an important role in mediating immunity to *Mycobacteria tuberculosis*[461-463]. Furthermore, patients with active pulmonary tuberculosis (TB), who are non-responsive to the MT have a selective loss of γδ T cells compared to MT positive TB patients and healthy controls[464]. We were, therefore, interested in determining the relative proportions of αβ and γδ T cells in the blood and skin during the Mantoux test, and whether there was evidence of selective expansion of either subset. Greater than 95% of T cells isolated from SBs raised over MTs were TCR $\alpha\beta^+$ with no significant change in the proportion during the

course of the response (Mann-Whitney test, p=0.1) (Figure 4.2). γδ T cells accounted for less than 5% of the T cells and although there was an increasing trend in the proportion of these cells, this was not significant (1.38% on day 3 compared with 3.71% on day 19) (Mann-Whitney test, p=0.2). There was no change in the proportion of αβ and γδ T cells in the blood during the MT (Mann-Whitney, p=0.2 and 0.7 respectively). The αβ TCR subset of T cells, therefore, accounts for the vast majority of T cells in the skin during the MT with the relative proportion of αβ and γδ T cells remaining unchanged.

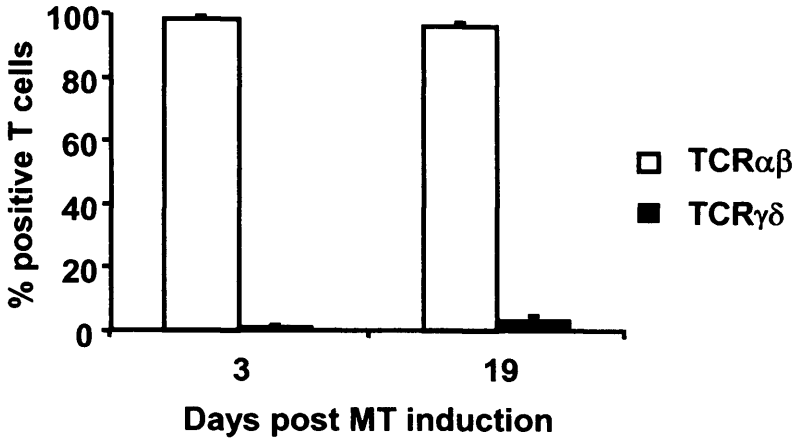

Figure 4.2 The proportion of αβ and γδ T cells in the skin during the Mantoux test

The proportion of αβ (□) and γδ (■) positive T cells isolated from SBs raised over MTs was determined by flow cytometry. SB cells were stained with CD3-APC, then washed, before staining with TCRαβ-FITC and TCRγδ-PE. The percentage of $CD3^+$ T cells that were $TCR\alpha\beta^+$ and $TCR\gamma\delta^+$ in day 3 and 19 MT SBs is shown. The data represent the mean of 3 experiments per time-point ± SEM.

4.4 Kinetics of antigen-specific cell infiltration into the skin of Mantoux tests

The increase in T cell numbers in the skin during an immune response should really be viewed in the context of antigen-specific cell infiltration. The proportion of T cells that are antigen-specific during a cutaneous DTH response, however, is unclear as these have been variably reported to comprise either the majority or less than 1% of the infiltrating T cells[422;465].

These studies represented only 'snap-shots' of the immune responses analysed and the kinetics of antigen-specific cell infiltration during the course of a memory immune response in humans are, therefore, unknown. Antigen-specific T cells can be identified using tetramers, but MHC class II tetramer technology is as yet not well-established. PPD is also a complex antigen that consists of multiple epitopes, which would necessitate the use of tetramers of different specificities to identify the distinct populations of antigen-specific cells. We, therefore, adapted an established technique that uses flow cytometry to detect the intracellular accumulation of an effector cytokine i.e. IFN-γ following short term *in vitro* stimulation with specific antigen in the presence of brefeldin A to identify antigen-specific cells (Figure 4.3). This allowed us to examine the kinetics of antigen-specific T cell infiltration into the skin during the MT.

Figure 4.4a shows the proportion of PPD-specific $CD4^+$ T cells that are present in the blood and skin at different time-points during the course of the MT. The proportion of blood $CD4^+$ T cells that expressed IFN-γ following stimulation with PPD remained less than 0.75% during the course of the MT, although a peak of expression was observed on day 14 (Kruskal-Wallis, $p=0.01$). In contrast, the proportion of blister $CD4^+$ T cells that expressed IFN-γ following stimulation with PPD showed a significant increase during the course of the MT (Kruskal-Wallis test, $p<0.0001$). Background IFN-γ expression in $CD4^+$ T cells in the unstimulated blister control samples was low and remained relatively constant during the course of the MT (range of means 0.05-0.72%) (Kruskal-Wallis, $p=0.22$) (Figure 4.3). Furthermore, stimulation of cells with tetanus toxoid as a control antigen resulted in minimal IFN-γ expression in SB $CD4^+$ T cells (generally < 1%) (Figure 4.4a). This indicates that the SB $CD4^+$ T cells that expressed IFN-γ following stimulation with PPD were antigen-specific. Interestingly, during the clinical peak of the Mantoux test, the percentage of cutaneous PPD-specific IFN-γ^+ $CD4^+$ T cells was relatively low (1.35% at day 3). Indeed, the percentage of PPD-specific IFN-γ^+ $CD4^+$ T cells was low throughout the induction phase, although it progressively increased

from 0.14% at day 2 to 1.50% at day 5 (Mann-Whitney test, p=0.04). Two days after the induction of the MT, there was no significant difference in the proportion of PPD-specific $CD4^+$ T cells in the PB and skin (0.15% and 0.14% respectively; Wilcoxon signed rank test, p=0.8), but from day 3 onwards a detectable difference between the PB and skin was evident (0.25% and 1.35% respectively at day 3; Wilcoxon signed rank test, p=0.005). On day 7 there was a dramatic increase in the proportion of PPD-specific IFN-γ^+ $CD4^+$ T cells (13.14%) in the skin. The proportion of skin blister PPD-specific $CD4^+$ T cells increased further during the resolution phase peaking 14 days after the induction of MT (32.04%).

The absolute number of PPD-specific IFN-γ^+CD4^+ T cells within SBs was also determined in order to characterise the expansion and contraction of antigen-specific cells during the MT(Figure 4.4b). In order to control for variations in blister size, the number of PPD-specific cells is expressed as the number of cells per microlitre of blister fluid. During the induction phase and clinical peak of the MT low numbers of PPD-specific $CD4^+$ T cells were isolated from the skin blisters. A striking increase in the number of PPD-specific $CD4^+$ T cells was observed on day 7 with the peak at day 10. This was followed by a marked decrease in numbers by day 19 post-MT induction. Overall, a significant expansion and contraction of PPD-specific $CD4^+$ T cell numbers was observed in the skin during the MT (Kruskal-Wallis test, p=0.04).

To ensure that the low level of IFN-γ expression observed during the induction phase was not an effect of insufficient antigen-presentation, we performed additional experiments with day 3 SB cells to which autologous irradiated CFSE-labelled PBMC were added. The addition of supplementary APCs to the SB cells did not augment IFN-γ expression. This suggests that the low number of SB IFN-γ^+ $CD4^+$ T cells observed during the clinical peak was a true reflection of the number of infiltrating PPD-specific T cells (Figure 4.5).

We also examined the extent to which PPD-specific $CD8^+$ T cell infiltrated into the skin during the MT. This was determined by analysing the expression of IFN-γ on the $CD4^-$ population of $CD3^+$ T cells. There was no significant increase in the proportion of skin blister $CD8^+$ T cells expressing IFN-γ following stimulation with PPD during the course of the MT (<2% at all time-points; Kruskal-Wallis, p=0.2). The expansion of PPD-specific T cells in the skin is, therefore, essentially confined to the $CD4^+$ T cell subset. This highlights the fact that the MT is predominantly a $CD4^+$ T cell mediated immune response.

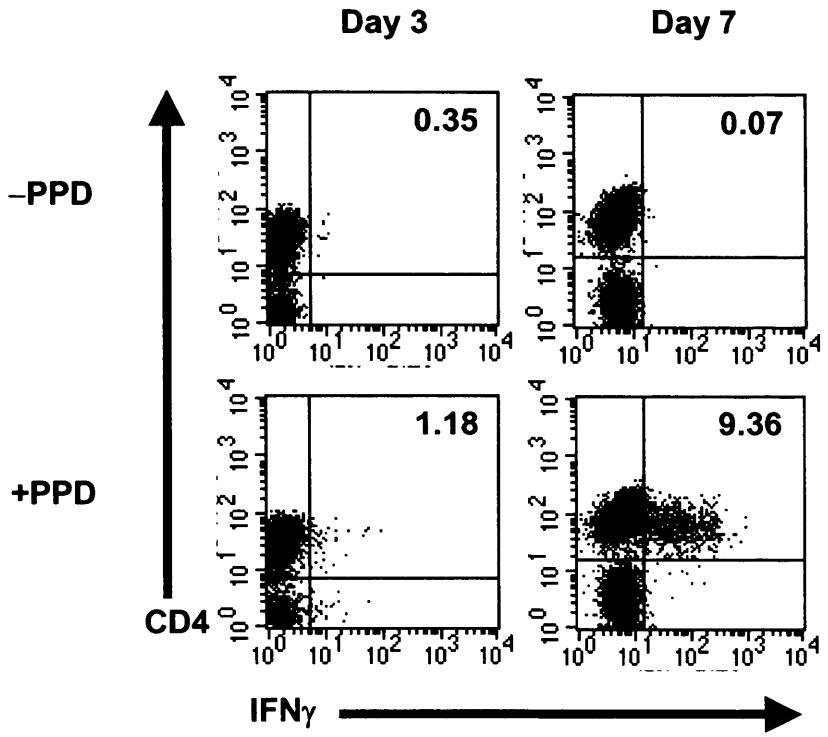

Figure 4.3 T cell intracellular IFN-γ expression in day 3 and 7 Mantoux test blister cells

MT blister cells were incubated for 15 hours with or without PPD in the presence of Brefeldin A, which was added after the first 2 hours of culture. The cells were then stained with CD3-PerCP, CD4-PE and IFNγ-APC following fixation and permeabilisation. The cells were then examined by flow cytometry for intracellular IFN-γ expression by gating on live $CD3^+$ T lymphocytes to include lymphocyte blasts. Representative dot-plots show expression of IFN-γ in $CD4^+$ and $CD4^-$ $CD3^+$ T cells isolated from SBs 3 and 7 days after MT induction. Unstimulated (–PPD) and PPD stimulated (+PPD) dot-plots are shown for each time-point. The figure in the right upper quadrant represents the percentage of $CD4^+$ T cells positive for IFN-γ expression.

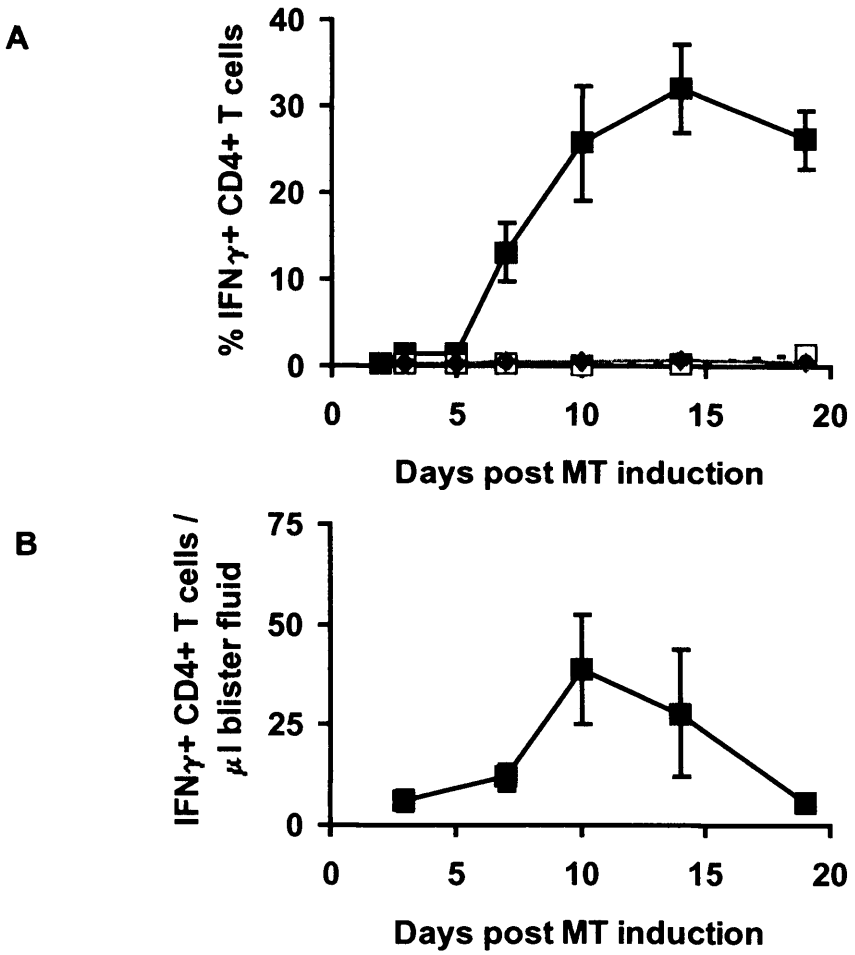

Figure 4.4 The kinetics of PPD-specific T cell infiltration in the skin during the Mantoux test.

The percentage and number of PPD-specific $CD4^+$ T cells in the PB and skin was determined by examining for intracellular cytokine staining using flow cytometry. SB cells and PBMC were stimulated with PPD or tetanus toxoid *in vitro* and were incubated for 15 hours in the presence of Brefeldin A. Unstimulated controls were also performed. Live $CD4^+CD3^+$ T cells were gated to include lymphocyte blasts. At least 10,000 $CD4^+$ T cell events were acquired. (A) The graph shows the percentage of $CD4^+$ T cells positive for IFN-γ expression during the MT. Data for SB cells stimulated with PPD (■) or tetanus toxoid (□) and PBMC stimulated with PPD (◆) are shown. The graph shows the mean ± SEM of 3-11 experiments performed at each time-point. (B) The number of IFN-γ^+CD4^+ T cells per μl of blister fluid following stimulation with PPD *in vitro* was also determined. The number of $CD4^+$ T cells isolated from MT skin blisters was enumerated using TruCOUNT™ tubes as described in the Materials and Methods (section 2.3.4). The volume of blister fluid was recorded at the time of SB aspiration. This allowed the number of $CD4^+$ T cells per μl of blister fluid positive for IFN-γ expression to be calculated. The graph shows the mean ± SEM of 3-5 experiments performed at each time-point.

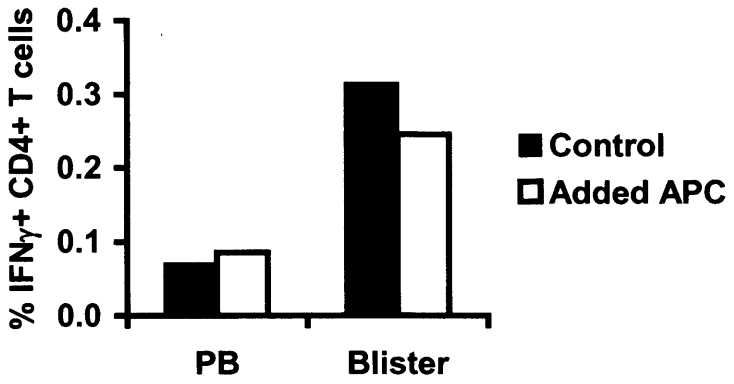

Figure 4.5 The effect of supplementary antigen presenting cells on day 3 Mantoux test blood and skin $CD4^+$ T cell IFN-γ expression

PBMC and SB cells collected at day 3 from MT volunteers were incubated for 15 hours with PPD in the presence of Brefeldin A. 2×10^5 irradiated autologous CFSE-labelled PBMC were added to duplicate tubes. The cells were stained with CD3-PerCP, CD4-PE and IFNγ-APC following fixation and permeabilisation. Unstimulated controls were also performed. The cells were then examined by flow cytometry for intracellular IFN-γ expression by gating on live $CD4^+CD3^+$ T lymphocytes to include lymphocyte blasts. CFSE labelled cells were gated out using FSC and FL-1 channel profiles. At least 10000 $CD4^+$ T cell events were acquired. Data for control samples (■) and samples with added irradiated autologous CFSE-labelled PBMC (□) are shown. The graph shows the mean of 2 experiments.

4.5 T cell proliferation during the Mantoux test

The increase in antigen-specific $CD4^+$ T cells observed in the skin during the MT may not only result from the recruitment of T cells from the blood, but also from the localised proliferation of activated T cells in the skin. Evidence in mice, however, suggests that expansion of antigen-specific T cells in non-lymphoid tissues is predominantly mediated by proliferation in lymphoid tissues[8-12]. We, therefore, examined PBMC, skin sections and SB cells isolated from MT volunteers for Ki67 expression. Ki67 represents a marker of cell proliferation, which is exclusively expressed in the G1, S, G2 and M phases of the cell cycle[466]. Minimal blood $CD4^+$ or $CD8^+$ T cells (<1%) were in cycle during the MT. Interestingly, proliferating $Ki67^+$ $CD4^+$ T cells were identified in skin sections and SB cells during the MT (Figure 4.6). Indeed, the dramatic expansion of PPD-specific $CD4^+$ T cells

observed on day 7 coincided with a peak of $CD4^+$ T cell proliferation when approximately 20% of cells were in cycle. In contrast, the proportion of cutaneous $CD4^+$ T cells proliferating on day 3 during the clinical peak of the MT was markedly lower and similar to that observed during resolution on day 14. Importantly, similar proportions of proliferating $CD4^+$ T cells were identified by both immunohistochemistry on skin sections and flow cytometry of blister cells taken at different time-points during the MT. This lends support to the assertion that the composition of cells contained in SBs is representative of the underlying inflammatory infiltrate[442]. Minimal proliferation was identified in SB $CD4^-$ ($CD8^+$) T cells (<2%) throughout the course of MT. This once again highlights that the MT is essentially a $CD4^+$ T cell mediated immune response. Overall, this data suggests that the expansion of antigen-specific $CD4^+$ T cells in the skin during the MT is in part mediated by proliferation *in situ*.

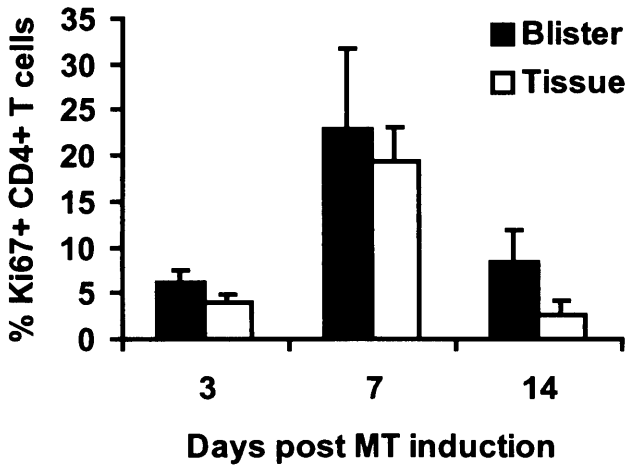

Figure 4.6 T cell proliferation in the skin during the Mantoux test

The percentage of proliferating ($Ki67^+$) $CD4^+$ T cells in the skin after PPD challenge was determined by flow cytometry using blister cells (■) and by double immunofluorescence in skin sections (□). The mean ± SEM of 3-5 experiments performed at each time-point is shown. Double immunofluorescence experiments were performed by Cate Orteu, RFUCMS.

4.6 Clonality

The increase in antigen specific cell numbers during the MT is dependent on the clonal expansion of T cells activated by PPD. Changes in the clonal composition of T cells during an immune response may be reflected by changes in the phenotypic and functional characteristics of lymphocytes being studied. The evolution in clonality of $CD4^+$ T cells during an immune response in the skin has not previously been determined. We, therefore, used heteroduplex analysis to determine what effect $CD4^+$ T cell proliferation in the skin had on the clonal composition of $CD4^+$ T cells during the MT. Heteroduplex analysis was kindly performed by Dr Joanne Cook and Professor Peter Beverley at the Edward Jenner Institute for Vaccine Research, Compton, UK.

SB cells were isolated from the sites of paired MTs in the same individuals 7 and 19 after challenge with PPD. In view of the relatively small numbers of cells isolated from SBs, $CD4^+$ T cells were purified by means of negative depletion by panning as described in section 2.2.2. The purity of $CD4^+$ cells was assessed by flow cytometry and was routinely greater than 70% (mean at day 7 82.81% and at day 19 91.87%).

PBMC were also isolated from the volunteers at days 0, 7 and 19 post-MT induction. Unstimulated blood $CD4^+$ T cells showed a polyclonal smear after HDA (Figure 4.7). Clonal bands were, however, detected when these cells were stimulated with PPD *in vitro* for 6 days. These were identified as bands above the dense carrier homoduplex band. $CD4^+$ T cells isolated from blisters on days 7 and 19 after PPD challenge showed a highly oligoclonal distribution (Figure 4.7 and Figure 4.8). Virtually all the clones identified in the blister samples at days 7 and 19 were also found in PPD stimulated PBMC from the same individuals (93-96%) indicating that the clonal bands in blister samples represented PPD-specific clones. Interestingly, of the clones identified in PPD stimulated PBMC, only 66% (range 44-85%) and 56% (range 49-71%) were present in the skin on days

7 and 19 after PPD challenge respectively (Table 4.1). This suggests that not all PPD clones that are present in the blood could enter, expand and/or survive in the skin.

We then determined the total number of clones that were identified in the 26 different Vβ families of $CD4^+$ T cells isolated from the paired skin blisters raised over MTs on day 7 and day 19 in the same individual. We identified 44 ± 14 clonal bands on day 7 (mean ± SD of 4 individuals) and 40 ± 15 at day 19 highlighting the polyclonal nature of the MT (Table 4.2). Generally, the number of clones identified at day 19 was less than that at day 7. Clonality during the MT remained relatively stable with the vast majority of clones identified at day 7 still present at day 19 (mean 71%; range 57-92%) (Figure 4.8). Of those clones present at day 19, however, 20% were not identifiable at day 7 post-MT induction suggesting that these represented recently expanded clonal populations. Conversely, of those clones identified at day 7, 29% were not present later in the immune response at day 19. This points to a dynamic evolving clonal picture, in which the vast majority of PPD-specific clones are maintained during the course of the immune response, but where a minority fail to succeed in competing with rival clones and others become newly established.

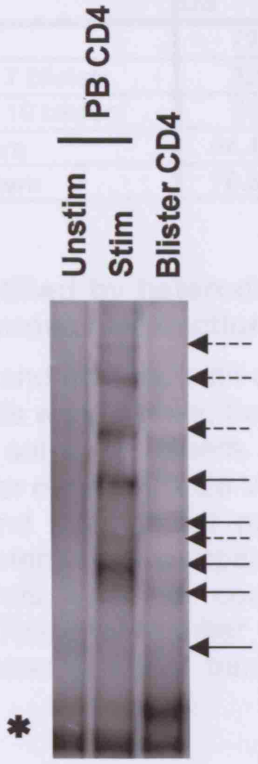

Figure 4.7 Heteroduplex analysis of blood and blister CD4$^+$ T cells isolated during the Mantoux test

Unstimulated blood CD4$^+$ T cells (Unstim), blood CD4$^+$ T cells stimulated with PPD *in vitro* for 6 days (Stim) and purified blister CD4$^+$ T cells from a day 7 Mantoux test (Blister CD4) collected from the same individual were compared. Solid arrows indicate clonal bands shared between PPD-stimulated blood and blister CD4$^+$ T cells. Dashed arrows indicate clonal bands that are only present in the PPD-stimulated blood CD4$^+$ T cells. One representative Vβ family out of 26 analysed from 1 out of 4 volunteers that were investigated is shown. The asterisk (✱) denotes the position of the monoclonal carrier homoduplex on the gel.

	DS	DW	KB	TST	Mean
Number of PPD clones in PBMC	72	39	59	69	**60**
Number of PBMC PPD clones in day 7 blisters	32	25	50	49	**39**
Number of PBMC PPD clones in day 19 blisters	51	20	29	37	**34**
% of PB PPD clones in day 7 blisters	**44.4**	**64.1**	**84.7**	**71.0**	**66.08**
% of PB PPD clones in day 19 blisters	**70.8**	**51.3**	**49.2**	**53.6**	**56.22**

Table 4.1 Clonal bands identified by heteroduplex analysis in PBMC stimulated with PPD and Mantoux test suction blisters

PBMC were isolated at day 0 and cultured with or without PPD *in vitro* for 6 days. In addition, $CD4^+$ T cells were purified from SBs raised over paired MTs at days 7 and 19 in the same volunteers. Heteroduplex analysis of the cells was then performed for each of the 26 Vβ families. The number of clonal bands was counted and the number present in PPD-stimulated PBMC and days 7 and 19 blisters were compared. Clonal bands present in unstimulated PBMC controls were not counted. A single observer performed this assessment. The total number of clonal bands for each volunteer and the mean number of clonal bands for all 4 volunteers is shown.

	DS	DW	KB	TST	Mean
Number of clones in day 7 blisters	37	28	60	51	**44**
Number of clones in day 19 blisters	60	23	39	37	**40**
Number of clones in both blisters	34	19	34	35	**31**
% of day 7 clones present in day 19 blisters	**91.9**	**67.9**	**56.7**	**68.6**	**71.26**
% of day 19 clones present in day 7 blisters	**56.7**	**82.6**	**87.2**	**94.6**	**80.26**

Table 4.2 Clonal bands identified by heteroduplex analysis in $CD4^+$ T cells in Mantoux test skin suction blisters

$CD4^+$ T cells purified from SBs raised over paired MTs 7 and 19 days after PPD challenge were analysed by heteroduplex analysis. Analysis on each sample was carried out for each of the 26 human Vβ families. The number of clonal bands identified on each day and on both days was counted. A single observer performed the assessment. The total number of clonal bands for each volunteer and the mean number of clonal bands for all 4 volunteers is shown.

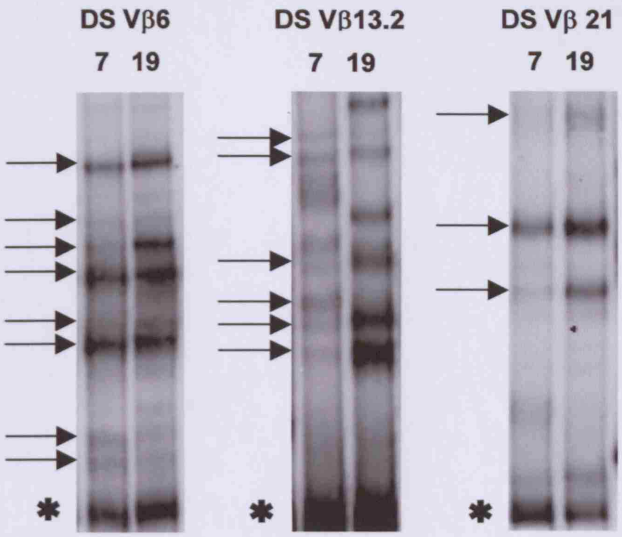

Figure 4.8 Heteroduplex analysis of CD4$^+$ T cells isolated from Mantoux test skin suction blisters

CD4$^+$ T cells purified from SBs raised over paired MTs in the same individual at days 7 and 19 following PPD challenge were analysed by heteroduplex analysis. The black arrows indicate clonal bands that are present in the skin at both time-points. Three different representative Vβ families out of the 26 analysed from the same volunteer are shown. The asterisks (✱) denote the position of the monoclonal carrier homoduplex in each gel.

4.7 Markers of cellular differentiation

The proliferation of CD4$^+$ T cells in the skin coupled with their preserved clonality and the associated expansion of PPD-specific CD4$^+$ T cells point to the on-going differentiation of CD4$^+$ T cells during the MT. We, therefore, next examined CD4$^+$ T cells isolated at different time-points during the course of the MT to determine telomere length and the expression of cell markers associated with differentiation.

4.7.1 CLA expression

CLA is expressed on a subset of memory T cells that home to the skin[20;23;380-382]. In section 3.5.4, we demonstrated the selective recruitment of CLA$^+$ T cells into SBs raised over MTs 3 days after their induction. We next examined the peak and resolution phases of the MT to see if the

localised expansion of T cells affected CLA expression. Figure 4.9 shows the percentage of $CD4^+$ memory T cells in the PBMC and SB cells that were positive for CLA expression during the course of the MT. Since the vast majority of $CD4^+$ T cells in SBs are of the $CD45RA^-$ memory / effector phenotype, PB $CD4^+$ T cells of the same phenotype were compared to those in the skin.

No significant change in the percentage of CLA positivity was observed on PB $CD4^+$ memory T cells during the course of the MT (Kruskal-Wallis test, $p=0.3$). Intriguingly in SBs the percentage of CLA expression on $CD4^+$ memory T cells decreased during the course of the Mantoux test (Kruskal-Wallis test, $p=0.03$). At 3 days post MT induction, 76.04% of skin $CD4^+$ memory T cells were CLA positive, but by day 14 this had decreased to 27.06%. Additionally, the MFI of CLA positive cells was found to decrease during the MT (544.22 and 233.77 on days 3 and 19 respectively). In contrast, there was no significant change in the percentage of $CD8^+$ ($CD4^-CD3^+$) T cells in the PB or SBs expressing CLA during the MT (Kruskal Wallis test, $p=0.88$ and 0.86 respectively). The data is consistent with the recruitment of skin-homing CLA^+ T cells into the skin during the induction phase of the immune response. This is subsequently followed by the progressive loss of CLA expression on $CD4^+$ T cells coinciding with the proliferation and clonal expansion of PPD-specific $CD4^+$ T cells. This argues against the skin microenvironment being the site of CLA up-regulation on the skin-homing subset of T cells.

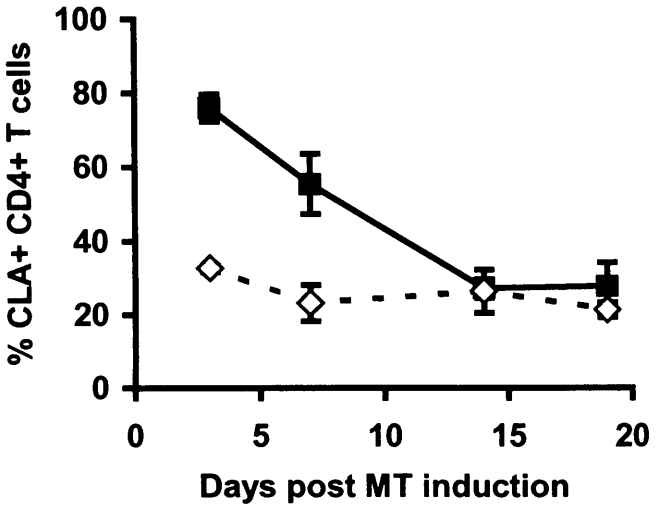

Figure 4.9 CLA expression on CD4$^+$ memory T cells during the Mantoux test

PBMC (◇) and SB (■) cells isolated from MT volunteers were analysed using flow cytometry for the percentage of CD4$^+$ memory T cells positive for CLA expression. PBMC and blister cells were stained with anti-CD3-PerCP, anti-CD4-APC, anti-CD45RA-FITC and anti-CLA antibodies. Bound anti-CLA antibody was detected by indirect immunofluorescence staining using goat anti-mouse IgM-PE. Samples were analysed by gating on the CD3$^+$CD4$^+$ CD45RA$^-$ subset of cells within the live lymphocyte / lymphoblast gate. The mean ± SEM of 3 experiments per time-point is shown.

4.7.2 CCR7 expression

CCR7 has been proposed as marker of lymphocyte differentiation by Sallusto *et al*, with negative expression correlating with a more highly differentiated subset of cells[89]. Sallusto *et al* also suggested that CCR7$^+$ memory T cells represent a population of cells that primarily migrate to lymphoid organs[89], although the finding that approximately 50% of CD4$^+$ T cells in normal skin are CCR7$^+$ argues against this[136]. We, therefore, next used the MT model to determine CCR7 expression on memory CD4$^+$ T cells in the blood and skin during the course of the immune response.

CCR7 expression on PB CD4$^+$ memory (CD45RA$^-$) T cells showed no significant change during the course of the MT (range 73.42-78.91%; Kruskal-Wallis test, p=0.5). In contrast, expression on CD4$^+$ memory T

cells in SBs varied significantly during the MT (Kruskal-Wallis test, 0.0002) (Figure 4.10). CCR7 expression on SB $CD4^+$ memory T cells was significantly lower than the PB cells at all time-points (Wilcoxon signed rank test, p=0.016-0.031). This points to a bias in the selective recruitment of $CCR7^-$ cells into the skin microenvironment. In SBs raised over normal (day 0) skin 22.49% of $CD4^+$ memory T cells were CCR7 positive, whereas on day 3 following the induction of the MT this was 46.05%. Interestingly, CCR7 expression decreased during the course of the MT so that by day 14 during resolution only 12.32% of $CD4^+$ memory T cells were positive for CCR7 expression. The progressive loss of CCR7 on $CD4^+$ memory T cells points to the on-going differentiation of lymphocytes during the immune response resulting in the generation of cells with a primed highly differentiated phenotype.

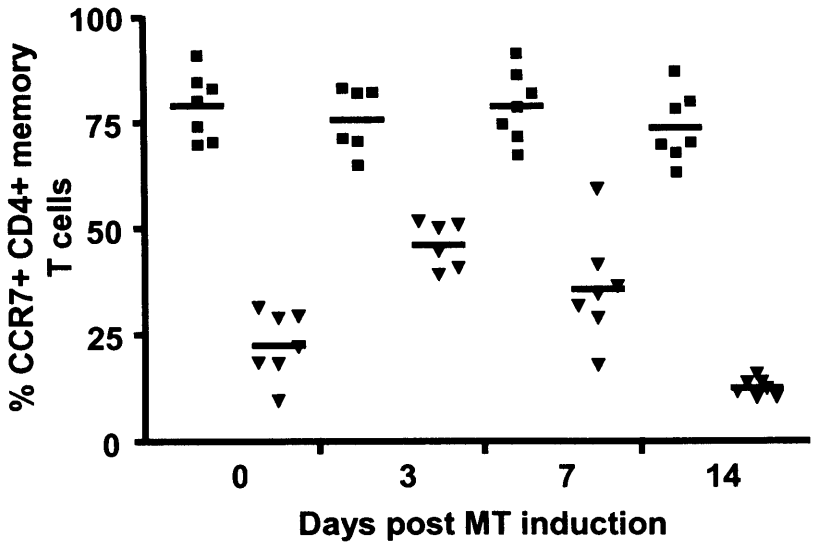

Figure 4.10 CCR7 expression on $CD4^+$ memory T cells during the Mantoux test

PBMC (■) and SB (▼) cells isolated from MT volunteers were analysed using flow cytometry for the percentage of $CD4^+$ $CD45RA^-$ memory T cells positive for CCR7 expression. PBMC and SB cells were stained with anti-CD4-APC, anti-CD45RA-FITC and anti-CCR7 antibodies. Bound anti-CCR7 antibody was detected by indirect immunofluorescence staining using goat anti-mouse IgM-PE. Samples were analysed by gating on the $CD4^+CD45RA^-$ subset of cells within the live lymphocytes gate. The horizontal black bar denotes the mean.

4.7.3 CD45RB expression

CD45RB expression can also be used as a marker of lymphocyte differentiation[73]. Naive T cells express high levels of CD45RB, but expression is progressively lost on memory T cells following repeated rounds of stimulation (Figure 4.11a)[73]. $CD45RA^-CD45RO^+$ memory T cells that express low levels of CD45RB consequently represent a highly differentiated subset of lymphocytes. Ongoing differentiation of lymphocytes during an immune response should accordingly lead to an increase in the proportion of memory cells with low expression of CD45RB. We, therefore, examined the expression of CD45RB on blister $CD4^+$ memory T cells to further assess the differentiation of T cells in the skin (Figure 4.11a,b).

The dot-plots shown in Figure 4.11a, as already described in section 3.5.3, illustrate that virtually all $CD4^+$ T cells isolated from the skin were of the $CD45RA^-$ memory phenotype in contrast to cells isolated from the blood of the same individuals. When we analysed CD45RB expression on $CD4^+$ memory T cells isolated from the blood and skin of the same individuals, there was no significant change in CD45RB expression in blood during the course of the MT, whereas in the skin there was a definite increase the proportion of $CD45RB^{low}$ cells (Kruskal-Wallis test, p=0.51 and 0.017 respectively). At 3 days post-MT induction 65.56% of skin $CD4^+$ memory T cells were $CD45RB^{low}$, but by day 19 this had increased to 87.12% (Mann-Whitney test, p=0.0095). The difference between PB and skin was clearly divergent during the course of MT, but this was not significant until day 19 (Wilcoxon signed rank test, p=0.03). The increase in proportion of $CD4^+$ memory T cells with low expression of CD45RB in the skin during the MT further indicated that there is a process of on-going differentiation occurring *in situ* within the skin microenvironment.

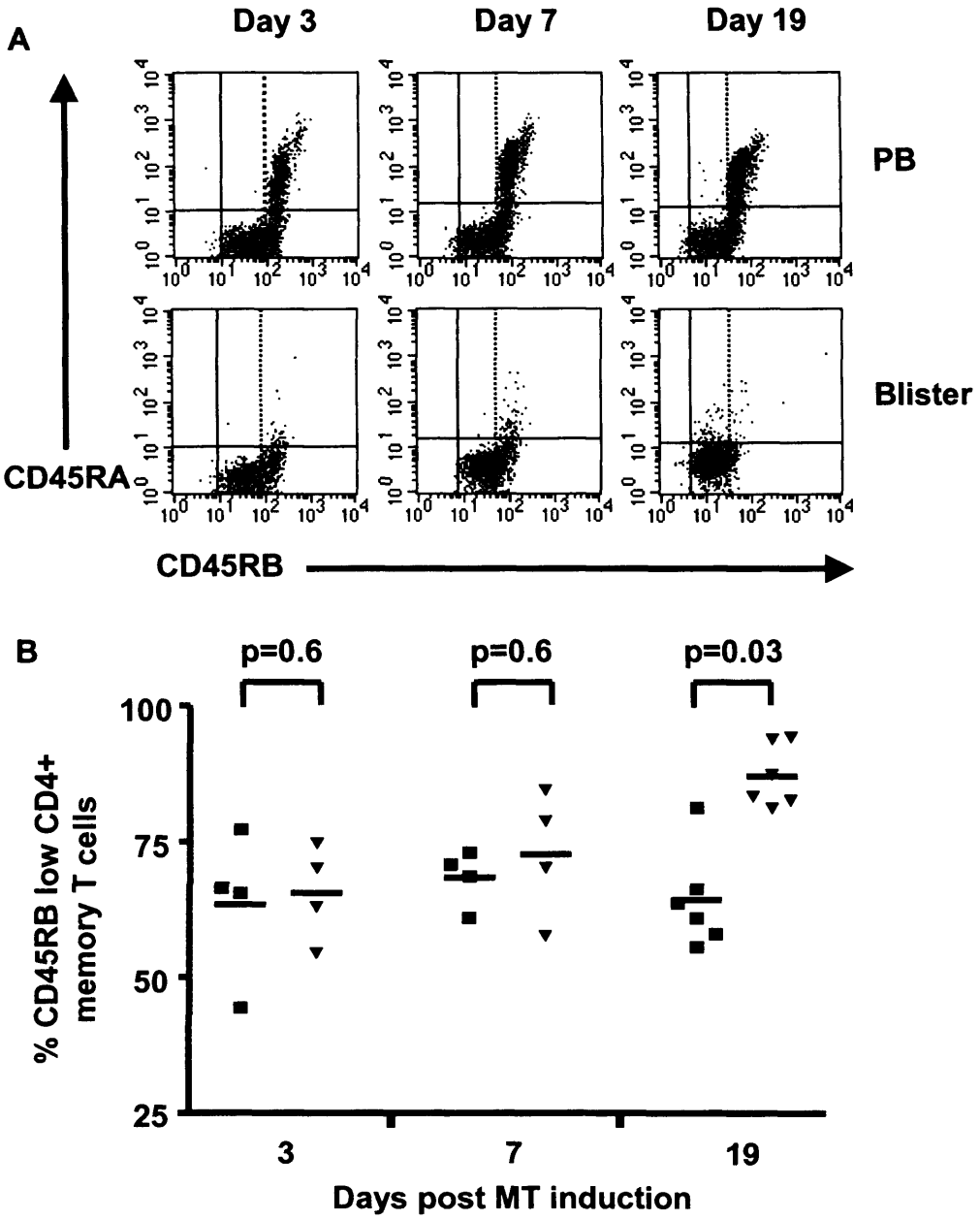

Figure 4.11 The proportion of CD4$^+$ memory T cells with low expression of CD45RB in the peripheral blood and skin during the Mantoux test

(A) Representative dot-plots showing CD45RA and CD45RB profiles of PB and SB CD4$^+$ T cells isolated from 3 different volunteers at different time-points. PBMC and SB cells were analysed by flow cytometry after staining with anti-CD4-APC, anti-CD3-PerCP, anti-CD45RA-PE and CD45RB-FITC. CD45RA and CD45RB profiles of PB CD4$^+$ T cells were used to delineate high and low expression of CD45RB as denoted by the vertical dotted line in each dot-plot. (B) The percentage of CD4$^+$ memory T cells with low expression of CD45RB in PBMC (■) and SB cells (▼) isolated from volunteers during the MT. The horizontal black bar denotes the mean.

4.7.4 Telomere length

T cell differentiation is associated with telomere shortening and this occurs as a consequence of proliferation[193;239]. In the short-term, however, during acute immune responses activated T cells can up-regulate telomerase and maintain telomere length. This has been demonstrated in a number of *in vivo* studies of cells isolated from the PB and lymphoid tissues[240-244]. Therefore, although telomeres shorten in T cells as they become more differentiated, compensatory mechanisms may obscure the true state of cellular differentiation. The effect of a secondary immune response on telomere length in T cells within the skin has not previously been studied.

We, therefore, used 2- and 3-colour flow-FISH techniques to examine telomere length in $CD4^+$ T cells during the MT. As previously demonstrated, blister $CD4^+$ T cells are predominantly (>95%) of memory phenotype, and so for comparison we purified $CD4^+CD45RO^+$ memory T cells from PBMC using MACS beads. Blood and blister samples were collected from volunteers either 7 or 19 days after the induction of the MT. Importantly the median ages of these two time-point groups were similar (Mann-Whitney test, p=0.6) since it is recognised that telomeres in T cells shorten with increasing age[193;235;238]. There was no significant change in telomere length in blood $CD4^+$ memory T cells during the course of the MT (Mann-Whitney, p=0.6). In contrast, significant telomere shortening was observed in blister $CD4^+$ T cells between days 7 and 19 (Mann-Whitney, p=0.04). On day 7, during the peak of $CD4^+$ T cell proliferation in the skin, the telomere length of blood and skin $CD4^+$ T cells were similar (Wilcoxon signed rank test, p=0.8), whereas by day 19 during resolution skin $CD4^+$ T cells had significantly shorter telomeres than PB $CD4^+$ T cells (Wilcoxon signed rank test, p= 0.03). The telomeres of $CD4^+$ T cells present within the skin at the site of PPD challenge, therefore, become significantly shortened during the course of the MT. It is possible to determine the length of telomeric DNA lost in terms of kilobases (kB) using a correlation curve of telomere length measured by flow-FISH versus Southern Blot measurement that has been previously performed within the research

group[241]. The decrease in MFI observed equates to a loss of 0.44kB of telomeric DNA (range +0.08 to −1.1kB). Intriguingly, the greatest erosion occurred in the 2 oldest volunteers (45 and 54 years old). The telomere shortening observed in skin $CD4^+$ T cells confirms that these cells became more differentiated during the course of the MT, but also points to the failure of mechanisms that compensate for the telomere erosion that occurs with cell proliferation.

We next developed a novel 3-colour flow-FISH technique to measure the telomere length of PPD-specific $CD4^+$ T cells in PBMC and SB cells isolated during the MT. This involved stimulating PBMC and MT SB cells with PPD in the presence of Brefeldin A as in section 4.4, then examining telomere length by flow-FISH by gating on the IFN-γ^+ $CD4^+$ subset of lymphocytes (Figure 4.12). When blood and blister $CD4^+$ lymphocytes isolated 19 days after MT induction were examined, telomere length in the PPD-specific IFN-γ^+ subset was shorter in the skin compared to blood (86.82 versus 132.16 and 82.42 versus 104 respectively). This indicates that telomere shortening occurred in the PPD-specific $CD4^+$ T cells in the skin rather than the blood during the MT. These dindings are in direct contrast to previous *in vivo* studies on lymphoid and blood antigen-specific T cells demonstrating the maintenance of telomere length during an acute immune response[240-244].

Overall, these data show that $CD4^+$ T cells undergo a process of differentiation as a consequence of localised proliferation in the skin during the course of the MT, so that by day 19 a high proportion of $CD4^+$ T cells are PPD-specific with low expression of CCR7 and CD45RB in association with shortened telomeres. This is consistent with the development of a highly differentiated phenotype.

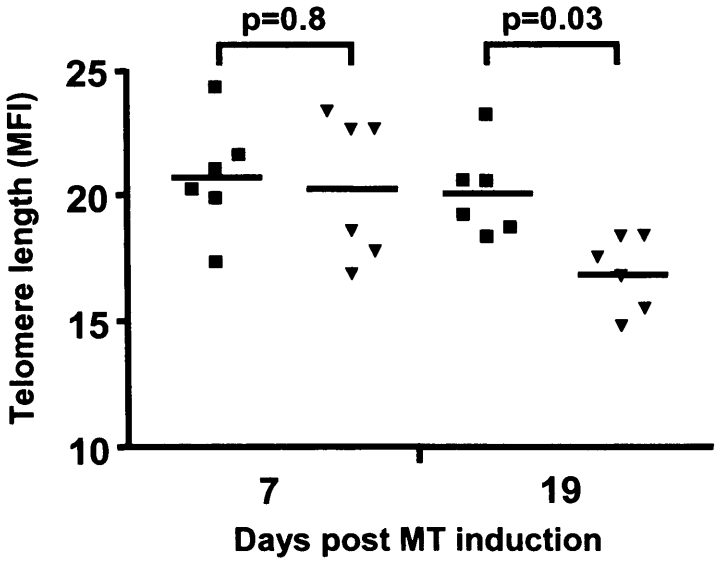

Figure 4.12 Telomere length in peripheral blood and skin suction blister $CD4^+$ memory T cells during the Mantoux test

The telomere length of PB (■) and SB (▼) $CD4^+$ memory T cells isolated from volunteers during the course of the MT is shown. SB cells and positively selected PB $CD45RO^+$ $CD4^+$ T cells were stained with anti-CD4-biotin followed by streptavidin-Cy5. The cells were then fixed and processed for 2-colour flow-FISH by hybridising with a telomeric PNA-FITC probe. Gating was set on the live $CD4^+$ lymphocytes to exclude doublets. The flow cytometer was standardised for each experiment using DAKO FluoroSpheres in conjunction with control reference human PBMC and bovine thymocytes. Channel values were converted to MEF values using a calibration curve based on the MFI values obtained using Dako Fluorosphere Calibration Beads, which were acquired during each experiment. This permitted the control no probe sample MEF to be subtracted from the telomeric probe MEF. The final MEF value was then converted back to MFI using the calibration curve. The black horizontal bar denotes the mean.

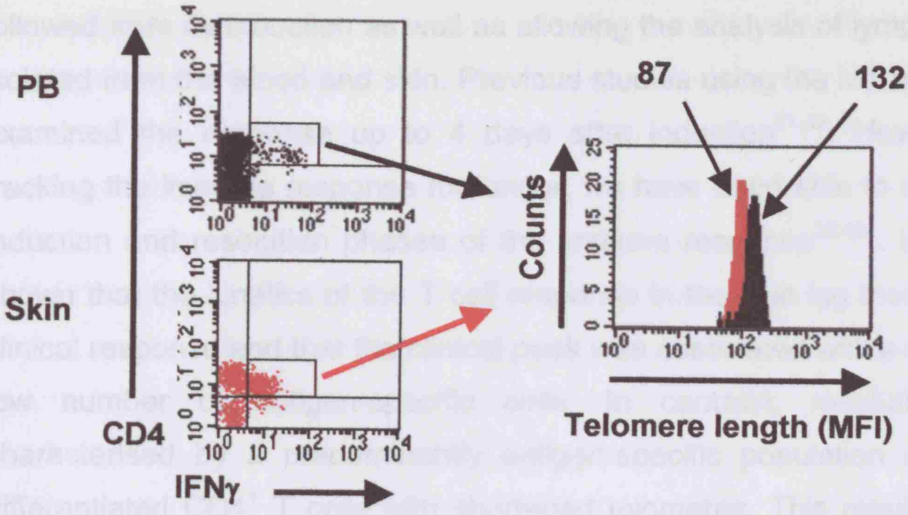

Figure 4.13 Telomere length in PPD-specific CD4$^+$ T cells isolated from peripheral blood and skin suction blisters during Mantoux tests

The telomere length of PB and SB PPD-specific IFN-γ$^+$CD4$^+$ T cells during the course of the MT. PBMC and MT SB cells isolated 19 days after MT induction were incubated with PPD (1μg/ml) for 15 hours in the presence of Brefeldin A. The cells were stained with anti-CD4-biotin followed by streptavidin-Cy3, then fixed and permeabilised in the presence of anti-IFNγ-FITC. The cells were hybridised for flow-FISH with a telomeric PNA-Cy5 probe. No probe and unstimulated controls were performed. The figure shows representative PB and SB dot-plots of CD4 and IFN-γ profiles gated on live lymphocytes but excluding doublets. An overlay histogram of the telomere length (MFI) of gated IFN-γ$^+$CD4$^+$ lymphocytes in the PB and skin is also shown. Representative dot-plots and histogram from 1 of 2 experiments are shown.

4.8 Discussion

In this chapter, we have used the MT as a human *in vivo* model of an immune response to examine the kinetics of antigen-specific cell infiltration and differentiation of CD4$^+$ T cells in the non-lymphoid environment of the skin. Human models are often limited by the difficulty in determining the exact timing of antigenic inoculation. An attempt to circumvent this quandary has been previously made by examining primary CMV infection in the sero-negative recipients of a sero-positive renal transplant[467]. However, these authors only analysed PB CD4$^+$ T cells and the possible effect of concomitant immunosuppressants could not be completely excluded. The MT model has the advantage that it can be

followed from its induction as well as allowing the analysis of lymphocytes isolated from the blood and skin. Previous studies using the MT have only examined the response up to 4 days after induction[21-23]. However by tracking the immune response for longer, we have been able to study the induction and resolution phases of the immune response[25;468]. We have shown that the kinetics of the T cell response in the skin lag those of the clinical response and that the clinical peak was associated with a relatively low number of antigen-specific cells. In contrast, resolution was characterised by a predominantly antigen-specific population of highly differentiated $CD4^+$ T cells with shortened telomeres. This resulted from the expansion of antigen-specific $CD4^+$ T cells, which was at least in part mediated by localised proliferation within the skin. Our results highlight that there is significant T cell activity long after the perceived clinical course of the skin test reaction. The continued T cell reactivity in the skin between days 7 and 19 may reflect the continued presence of residual antigen and expansion of cells by cytokines that are present *in situ*[25]. In addition, activated PPD-specific T cells may become committed to undergo a pre-determined number of divisions as has been observed with both antigen-specific $CD4^+$ and $CD8^+$ T cells[35-38].

We decided to use intracellular cytokine staining in order to identify antigen-specific cells in view of the lack of suitable class II tetramers and the complex antigenic nature of PPD. This assay identifies antigen-specific cells based on the capacity of cells to produce effector cytokines upon stimulation with cognate antigen. Some authors have found a strong correlation between intracellular cytokine staining and tetramer staining[43;47], whereas others have observed that intracellular cytokine staining only detects between 30 and 90% of tetramer positive cells possibly because a proportion of cells are refractory to re-stimulation or are functionally heterogeneous[469;470]. It therefore remains possible that the frequency of PPD-specific cells that we observed during the MT represents an underestimate.

The kinetics of PPD-specific T cell infiltration into the skin that we have demonstrated are similar to the kinetics of antigen-specific T cell expansion and infiltration into non-lymphoid organs that have been previously described in a variety of mouse models[8;9;471;472]. This, however, is the first time that a detailed study of the kinetics of antigen-specific infiltration into a non-lymphoid tissue during all of the phases of an immune response in humans has been performed. Furthermore, by examining a cutaneous immune response we have been able to correlate the T cell response with the clinical response. Previous estimates of the numbers of antigen-specific T cells within the skin in other DTH models using limiting dilution analysis have suggested that they account for less than 1% of the infiltrating T cells[422;423]. These studies represented only snapshots of the immune response and we have highlighted the need to study all phases of a response.

The finding of a low percentage of antigen-specific T cells in the skin during the peak of the clinical response is intriguing. The most likely explanation for the low percentage of antigen-specific T cells during the clinical peak is that antigen non-specific mechanisms mediate the recruitment of T cells into the skin[378]. The antigen non-specific recruitment of memory T cells has been recently demonstrated in the lungs of mice [12;473]. The likely advantage of this is that it means a large number of specificities can be screened by DCs for reactivity within the skin.

The expansion of PPD-specific cells in the skin appeared in part to be mediated by localised $CD4^+$ T cell proliferation. Proliferating $CD4^+$ T cells were identified in MT tissue sections and blister cells by the expression of Ki67. The peak of $CD4^+$ T cell proliferation in the skin at day 7 coincided with the marked increase in frequency of PPD-specific $CD4^+$ T cells that was observed. Although T cells that have divided within the draining lymph nodes may partly play a role in the expansion of this population, the marked increase in Ki67 positive $CD4^+$ T cells within the skin is strongly

suggestive that proliferation *in situ* mediates T cell expansion. This is in direct contrast to murine studies that suggest that T cell expansion in antigen-bearing non-lymphoid tissues is predominantly mediated by proliferation in lymphoid tissues[8-12]. The inability of T cells to divide in these studies appeared to be a function of the non-lymphoid environment, since the cells could divide extensively when activated *in vitro*[10]. It must be noted that most of these studies were carried out on T cells isolated from the lungs and it has been proposed that the pulmonary microenvironment may actively suppress T cell division[10]. The study by Reinhardt *et al* did, however, examined the proliferative behaviour of T cells during cutaneous immune responses and demonstrated that the accumulation of T cells in the skin was not mediated by local proliferation[8]. These authors, however, only examined a primary immune response.

The contradictory findings between these studies and ours may reflect inter-species differences, but might also be a consequence of differences in primary and secondary immune responses. The proliferative behaviour of T cells in non-lymphoid tissues in mice during a true memory immune response has yet to be determined. However, it has been reported that recall immune responses induced after various adoptive transfer strategies demonstrate a similar pattern of preferential proliferation in lymphoid tissues[10-12]. Proliferation of T cells in non-lymphoid tissues, however, was not completely excluded in these reports and was in fact evident to some degree in two of the studies[10;11]. It, therefore, seems likely that T cell expansion in cutaneous recall immune responses in humans can probably take place in both lymphoid and non-lymphoid compartments. Indeed recall responses can be maintained in humans even when afferent lymphatics are compromised[416]. This is of particular interest considering the increasing evidence, which suggests that memory T cells can be maintained in non-lymphoid tissues[8;101;102]. It appears, therefore, that a significant proportion of T cell expansion during secondary cutaneous immune responses in humans takes place in the non-lymphoid environment of the skin.

The increase in the proportion of PPD-specific $CD4^+$ T cells from day 7 may, in part, also be accounted for by the active retention of antigen-specific cells as non-specific T cells that have not been activated pass through the tissue back to the lymphatics. This would lead to a relative enrichment of the antigen-specific population. Apoptosis may also result in the clearance of some of the antigen non-specific T cells that are recruited into the skin particularly if they have been activated in a bystander fashion. Indeed, we have previously demonstrated an increase in the apoptosis of T cells within MTs from day 7 onwards[25].

The clonality of $CD4^+$ T cells in the skin remained relatively preserved during the MT despite the dramatic expansion and contraction of PPD-specific $CD4^+$ T cells. Although the vast majority of clonal populations persisted throughout the course of the immune response, a minority did however either newly emerge or disappear during the MT. This points to possible selective pressures influencing the clonal composition with some clones failing to compete successfully and others becoming either newly established or exhibiting better survival characteristics. Interestingly, it appears that not all PPD clonotypes identified in the blood could establish clonal expansions in the skin during the MT. This implies that some PPD clones either fail to expand within the skin microenvironment or are excluded from inflamed skin. It is possible that not all PPD clones present in the blood express the correct combination of homing receptors that is necessary for entry into the skin[131].

The preserved clonality coupled with proliferation *in situ* corresponded with the increasing differentiation of $CD4^+$ T cells during the MT. Virtually all $CD4^+$ T cells recruited into the skin during the MT were of a memory / effector phenotype and these cells exhibited a progressive loss of CD45RB expression. Low expression of CD45RB has previously been shown to correlate with an increasingly differentiated apoptosis prone

population of cells that have undergone multiple rounds of activation[73]. Furthermore, expression of CCR7 and CLA also decreased on $CD4^+$ T cells in the skin during the MT.

CCR7 has recently been widely used a potential marker of differentiation in memory T cell populations. Sallusto *et al* originally proposed that $CCR7^+$ (central memory) T cells expressed lymph node homing receptors and lacked immediate effector function e.g. IFNγ production, whereas $CCR7^-$ (effector memory) cells represented a more highly differentiated subset that expressed receptors for migration to inflamed tissues and displayed immediate effector function[89]. The implication of this model was that $CCR7^+$ cells are incapable of migrating into inflamed non-lymphoid tissues. Only about a quarter of blood $CD4^+$ memory T cells are $CCR7^-$, so the finding that greater than half of the $CD4^+$ T cells in the skin were $CCR7^-$ supports the preferential migration of this subset of cells into non-lymphoid tissues. However, up to 46% of cells at day 3 were $CCR7^+$ demonstrating that this subset is not excluded from the skin. This finding corresponds with those of Campbell *et al*, who demonstrated that approximately half of T cells in normal skin and synovial tissues were $CCR7^+$[136]. In contrast, in the gut, lung and liver virtually all $CD4^+$ T cells were found to be $CCR7^-$. The migratory characteristics of these two subsets, therefore, appear to be less clear-cut than originally proposed[89]. Furthermore, there is increasing evidence that CCR7 is not a good marker for distinguishing effector function[85;92;133-135]. CCR7 can be up-regulated on activated T cells and this may partly explain the high proportion of $CCR7^+$ cells at day 3, although as only a small fraction of $CD4^+$ T cells at this time-point are actually PPD-specific this characteristic may not be of relevance[137]. In fact, CCR7 expression on $CD4^+$ T cells decreased during the MT so that by day 14 virtually all cells were $CCR7^-$. This can be interpreted as indicating the development of a highly differentiated effector population of T cells, which is supported by the loss of CD45RB expression and telomere erosion. A possible alternative explanation is that during resolution $CCR7^+$ cells in the inflammatory infiltrate emigrate from

the skin via the peripheral lymphatics. It is recognised that CCR7 is up-regulated on activated DCs[371;474;475] and that CCL21 is expressed by the lymphatic endothelium in non-lymphoid tissues[371;372]. Furthermore, the *in vivo* emigration of mature skin-derived DCs has been shown to be dependent on CCL21 expression[371]. The mechanisms that control lymphocyte emigration are unknown. However, if they are similar to those controlling DC emigration then the $CCR7^-$ population of $CD4^+$ T cells observed during resolution may represent a population of highly differentiated cells that in essence are trapped in the skin. The vast majority of these cells are probably cleared by the increased levels of apoptosis observed in T cells in the skin during resolution[25].

The decrease in CLA expression on $CD4^+$ T cells during the MT is intriguing. CLA represents a post-translational modification of P-selectin glycoprotein ligand-1 (PSGL-1) and is expressed on primed skin-homing T cells[20;380;388]. It denotes the expression of functional E-selectin ligands that mediate rolling on the dermal post-capillary venules[388]. The vast majority of $CD4^+$ T cells in the skin during the induction phase of the MT were CLA positive, which is consistent with previously published data[20;23;380]. CLA expression, however, unexpectedly decreased thereafter so that by day 19 only a minority of cells were positive. Acquisition of skin-homing function has been shown to occur preferentially in cutaneous rather than mucosal draining lymph nodes[20;375] and is probably influenced by the local lymphoid cytokine microenvironment[20;393;395]. The skin microenvironment may, therefore, not promote the maintenance of CLA expression so that the proliferation of $CD4^+$ T cells consequently leads to the progressive loss of CLA expression. Another possible explanation is the selective expansion of PPD-specific cells that might partly comprise the CLA^- subset of $CD4^+$ T cells that constitute a minority of skin-infiltrating T cells. Interestingly, the majority of T cells in afferent lymphatic vessels draining the skin in humans have been shown to be CLA^+ for up to 10 days after the induction of allergic contact dermatitis[384]. This suggests that CLA^- cells may be retained within the skin. Further investigation is obviously required to

determine the mechanism influencing the expression of CLA in the skin during inflammatory responses.

The finding of significant telomere shortening in antigen-specific $CD4^+$ T cells in the skin during the MT confirms that these cells undergo differentiation *in situ* following PPD challenge. It is of considerable interest that an average loss of 400 base pairs of telomeric DNA was observed in the $CD4^+$ T cells in the skin during the 3 weeks after the PPD injection. Since telomeres in human $CD4^+$ T cells have been shown to decrease by an average of 50 base pairs per year[193;235], this loss of telomeric DNA is equivalent to that expected after 8 years of normal ageing *in vivo*. At this rate of telomere erosion, one prediction would be that cells that proliferate continuously in the skin would reach senescence rapidly. Interestingly, this telomere erosion contrasts directly with previous reports showing the maintenance of telomere length in T cells during acute immune responses *in vivo*[240-244]. These studies, however, were performed on cells isolated from the blood and lymphoid tissue. This points to a possible difference in the regulation of telomere biology of T cells infiltrating into the non-lymphoid environment of the skin.

The accelerated differentiation and telomere shortening in T cells proliferating in the skin may, therefore, lead to the accumulation of an increasingly terminally differentiated and senescent population of cells. This may act as an immunoregulatory mechanism to limit the extent of T cell expansion within the skin. It would also have implications for memory cell formation if they do reside appreciably in non-lymphoid tissues as has been shown in mice[101;102]. In the next chapters, we will examine the mechanisms that regulate telomere length and investigate the consequences of the accelerated T cell differentiation in the skin during the MT.

5 The consequences of T cell differentiation in the skin during the Mantoux test

5.1 Introduction

In the previous chapter, we demonstrated that $CD4^+$ T cells recruited into the skin during the course of the Mantoux test proliferate *in situ* and undergo a process of cellular differentiation. A significant proportion of the $CD4^+$ T cells isolated from the skin during the resolution of the immune response were antigen-specific and the vast majority had a highly differentiated phenotype with low expression of CD45RB and shortened telomeres. The increasing preponderance of this phenotype in the skin during the MT is consistent with the generation of a highly differentiated population of memory $CD4^+$ T cells[54;73;89;193]. Interestingly, $CD4^+CD25^+$ regulatory T cells (T_{regs}) are recognised as having a similar highly differentiated phenotype[148;287;338;339]. T_{regs} purified from the blood also have significantly shortened telomeres compared to PB $CD4^+CD45RO^+$ T cells[290] and this corresponds to the pattern observed during the resolution of the MT. It is, therefore, possible that T_{regs} form a significant fraction of the $CD4^+$ T cell population in the skin during the resolution of the MT. Human T_{regs} are suppressive[147;290-296] and therefore might participate in down-regulating inflammation thereby mediating the resolution of the immune response. Furthermore, it has been argued that T_{regs} may be generated in the periphery as antigen-specific $CD4^+$ T cells approach end-stage differentiation[287;290;339]. We, therefore, hypothesized that T_{regs} might be generated in the skin during the MT as a result of on-going differentiation and consequently be involved in mediating resolution.

Another possible outcome of the differentiation process is the induction of replicative senescence in a subset of the antigen-specific $CD4^+$ T cells, which have undergone telomere shortening. The induction of this state of growth arrest would have serious implications for the generation of T cell memory, but would also limit the expansion of antigen-specific T cells recruited into the skin, and might therefore play an additional role in the resolution process. These issues will be addressed during the course of this chapter.

5.2 The suppressive activity of $CD4^+CD25^+$ T cells

No definitive marker has yet been described for T_{regs}, although expression of CD25, the α-subunit of the IL-2 receptor (IL-2R), is the most practicable way to enrich for cells with regulatory activity[146-148]. We purified $CD4^+CD25^+$ T cells from PB $CD4^+$ T cells by magnetic cell sorting using anti-CD25 magnetic beads. $CD4^+CD25^+$ T cells constitute 5-15% of peripheral blood $CD4^+$ T cells in humans[147;290-296] (Figure 5.1). The purity of the $CD25^+$ fraction after positive selection of $CD25^+$ $CD4^+$ T cells routinely exceeded 60%. In addition, following the depletion of $CD4^+CD25^+$ T cells, the $CD25^-$ fraction contained a markedly reduced proportion of $CD25^+$ cells with decreased expression of this molecule.

The proliferative responsiveness of these fractions was then investigated. PB $CD4^+CD25^+$ T cells were unresponsive / anergic to stimulation with PPD and irradiated APC in comparison with the $CD4^+$ and $CD4^+CD25^-$ fractions (Figure 5.2). The depletion of $CD4^+CD25^+$ T cells from the $CD4^+$ fraction resulted in enhanced responsiveness in the $CD4^+CD25^-$ fraction. This suggests that the $CD4^+CD25^+$ T cells can suppress the responsiveness of other $CD4^+$ T cells. To investigate this further, co-culture experiments using $CD4^+CD25^+$ and responder $CD4^+CD25^-$ T cells were performed (Figure 5.3). The responsiveness of $CD4^+CD25^-$ T cells to stimulation with PPD and irradiated APC was suppressed by almost 50% by the addition of an equal number of $CD4^+CD25^+$ T cells. In contrast,

when $CD4^+CD25^-$ T cells were co-cultured with $CD4^+CD25^-$ T cells the response was enhanced by over 70%. This implies that the suppression was not due to competition for space or nutrients at high cell concentrations. Overall, this indicates that the $CD4^+CD25^+$ T cell fraction is enriched with cells that are anergic and suppressive *in vitro*.

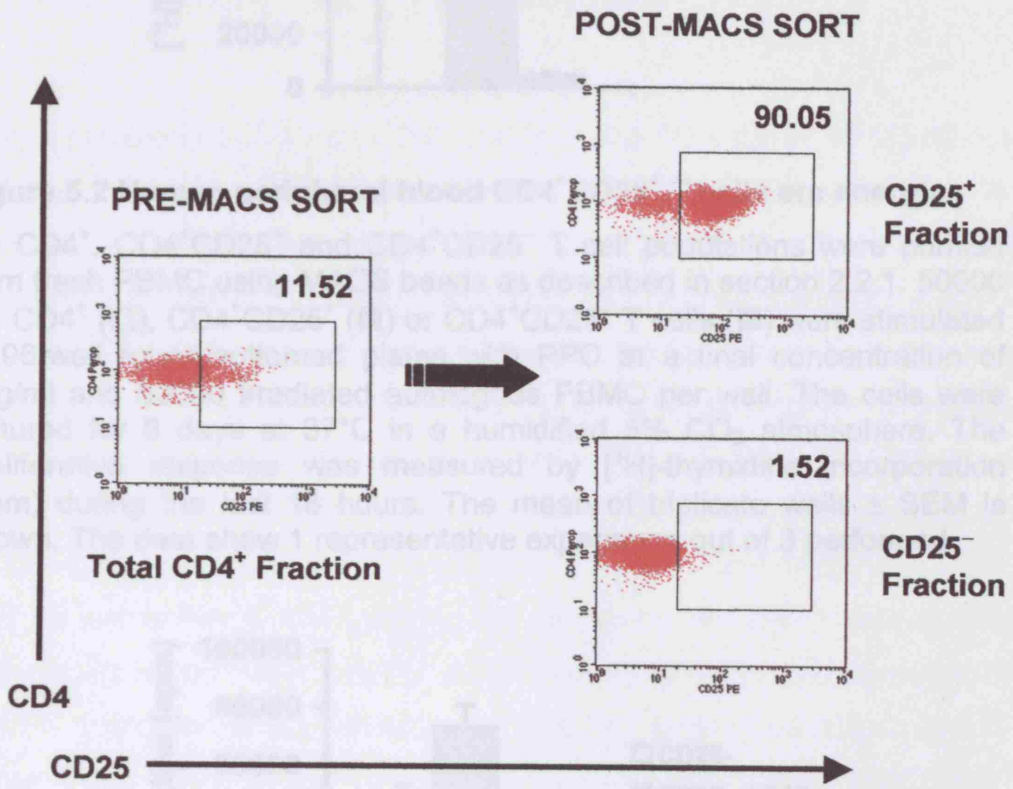

Figure 5.1 Purification of peripheral blood $CD4^+CD25^+$ T cells

A purified population of PB $CD4^+$ T cells was isolated from fresh PBMC by negative selection. $CD25^+$ cells were enriched from PB $CD4^+$ T cells by magnetic positive selection using anti-CD25 MACS Microbeads (Miltenyi Biotec, Bisley, Surrey, UK) (See section 2.2.1 for more details). The negatively selected unlabelled fraction representing $CD25^-CD4^+$ T cells was also collected. Purity of both fractions was routinely assessed by flow cytometry. Dot-plots of CD4 and CD25 expression in total $CD4^+$, $CD25^+$ and $CD25^-$ T cell fractions from 1 representation purification are shown. The $CD25^+$ gate was positioned using an isotype control. The figure in the top right-hand corner of each dot-plot represents the percentage of $CD4^+$ T cells expressing CD25.

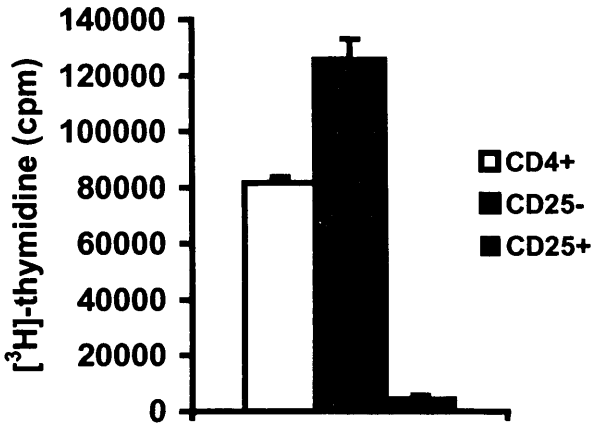

Figure 5.2 Human peripheral blood $CD4^+CD25^+$ T cells are anergic.

PB $CD4^+$, $CD4^+CD25^+$ and $CD4^+CD25^-$ T cell populations were purified from fresh PBMC using MACS beads as described in section 2.2.1. 50000 PB $CD4^+$ (□), $CD4^+CD25^+$ (■) or $CD4^+CD25^-$ T cells (■) were stimulated in 96-well round-bottomed plates with PPD at a final concentration of 1μg/ml and 50000 irradiated autologous PBMC per well. The cells were cultured for 6 days at 37°C in a humidified 5% CO_2 atmosphere. The proliferative response was measured by [^{3}H]-thymidine incorporation (cpm) during the last 18 hours. The mean of triplicate wells ± SEM is shown. The data show 1 representative experiment out of 3 performed.

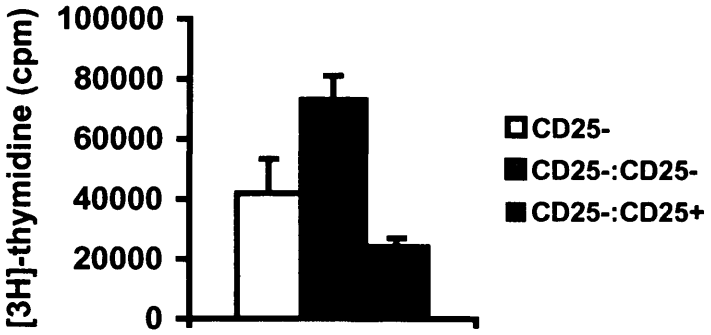

Figure 5.3 Human peripheral blood $CD4^+CD25^+$ T cells are suppressive

50000 PB $CD4^+CD25^-$ T cells were cultured alone (□) or co-cultured with equal numbers of PB $CD4^+CD25^-$ (■) or $CD4^+CD25^+$ T cells (■) in 96-well round-bottomed plates with PPD at a final concentration of 1μg/ml and 50000 irradiated autologous PBMC per well. The cells were cultured for 6 days at 37°C in a humidified 5% CO_2 atmosphere. The proliferative response was measured by [^{3}H]-thymidine incorporation (cpm) during the last 18 hours. The mean of triplicate wells ± SEM is shown. The data show 1 representative experiment out 3 performed.

5.3 CD25 expression during the Mantoux test

The main limitation with CD25 as a marker for T_{regs} is that it is transiently up-regulated on recently activated $CD4^+$ T cells[144;145]. T_{regs} on the other hand express CD25 constitutively[292;298]. With this proviso in mind, we sought to determine the expression of CD25 on $CD4^+$ T cells and analyse the phenotype of $CD4^+CD25^+$ T cells during the MT.

The expression of CD25 on $CD4^+$ T cells in the PB showed no significant change during the MT (Mann-Whitney test, p=0.2) (Figure 5.4a). In contrast to the PB, the proportion of $CD4^+$ T cells positive for CD25 expression in SBs at day 3 was markedly increased (Wilcoxon signed rank test, p=0.02). The proportion of positive cells in SBs, however, decreased during the MT (Mann-Whitney test, p=0.005), although it remained significantly greater than that observed in the PB (Day 19, Wilcoxon signed rank test, p=0.03). Furthermore, the MFI of CD25 expression on $CD25^+$ gated cells decreased during the MT (22.77 and 14.90 on days 3 and 19 respectively). Interestingly, the proportion of $CD4^+$ T cells in SBs expressing the activation marker CD69 was higher during the resolution of the MT compared to the induction (35.08% and 76.94% on days 3 and 19 respectively; Mann-Whitney test, p=0.002). The percentage of $CD4^+CD25^+$ T cells expressing CD69 showed a similar increase during the MT (36.20% and 59.50% on days 3 and 19 respectively; Mann-Whitney test, p=0.03) (Figure 5.4b). The presence of $CD4^+CD25^+$ T cells with an activated phenotype during resolution, however, does not necessarily imply that these cells are non-regulatory, since activated $CD4^+CD25^+$ $T_{regs,}$ as observed in tonsils, are CD69 positive and still display suppressive activity[147]. CD45RB expression is lower on $CD4^+CD25^+$ regulatory T cells compared to the $CD25^-$ responder population[147;290]. Expression of CD45RB decreased similarly in $CD25^+$ and $CD25^-$ populations of $CD4^+$ T cells during the MT (Figure 5.4c). Overall, this shows $CD4^+CD25^+$ T cells do not accumulate in the skin during the MT and that the majority of $CD4^+CD25^+$ T cells during resolution demonstrate an increasingly differentiated but activated phenotype.

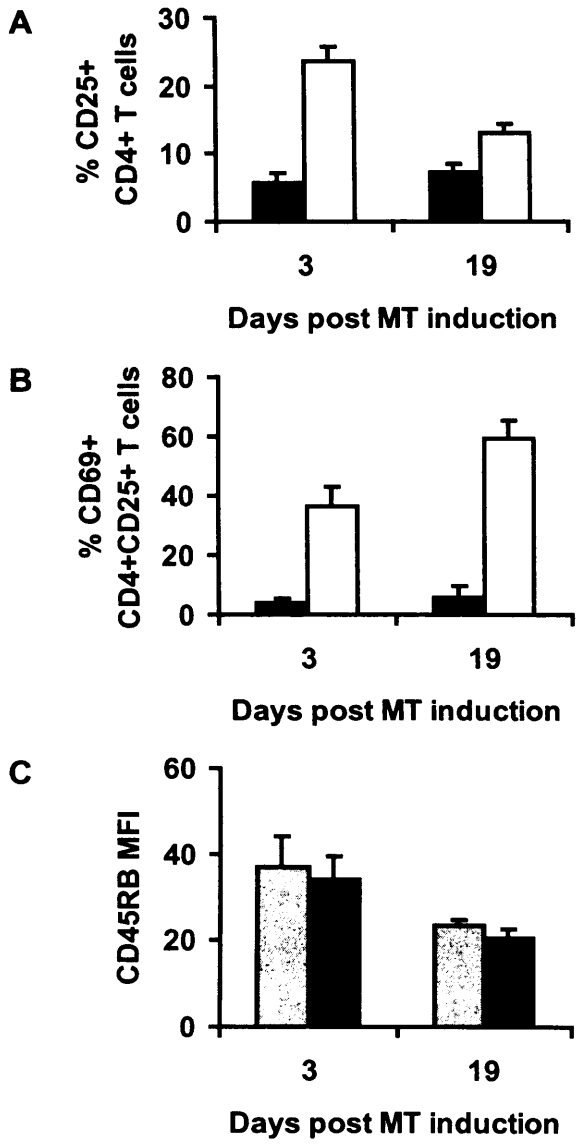

Figure 5.4 Expression of CD25 on $CD4^+$ T cells and phenotype of $CD4^+CD25^+$ T cells during the Mantoux test

CD25, CD69 and CD45RB expression on $CD4^+$ T cells isolated from the blood and skin during the MT was determined by flow cytometry. (A) The percentage of $CD4^+$ T cells expressing CD25 in the PB (■) and skin (□) during the MT. (B) The percentage of $CD4^+CD25^+$ T cells expressing CD69 in the PB (■) and skin (□) during the MT. (C) CD45RB expression (MFI) on $CD4^+CD25^+$ (▒) and $CD4^+CD25^-$ (■) T cells in the skin during the MT. The mean ± SEM of 4-6 experiments per time-point is shown.

5.4 Interleukin-2 production of $CD4^+$ T cells during the Mantoux test

Another characteristic of T_{regs} is that they produce little or no IL-2 upon activation[291;293-295]. We, therefore, next examined the capacity of cutaneous $CD4^+$ T cells isolated from MTs to produce IL-2 following re-stimulation with PPD *ex vivo*. Minimal IFN-γ or IL-2 was produced in the absence of PPD re-stimulation. The kinetics of infiltration of PPD-specific $CD4^+$ T cells into the skin during the MT was similar irrespective of whether expression of IL-2 or IFN-γ was analysed (Figure 5.5). The proportion of PPD-specific $CD4^+$ T cells capable of producing IL-2 was low during the clinical peak at day 3 (0.31%), but showed a marked increase at day 7 (8.81%) that was maintained during resolution at day 19 (9.82%) (Kruskal-Wallis test, p=0.01). Virtually all IL-2 producing $CD4^+$ T cells also expressed IFN-γ. Interestingly the proportion of PPD-specific IFN-γ^+CD4^+ T cells that could produce IL-2 showed no significant change during the MT (Kruskal-Wallis test, p=0.6). Therefore, despite their highly differentiated phenotype, cutaneous PPD-specific $CD4^+$ T cells during resolution remain capable of IL-2 production. It must be noted, however, that $CD4^+CD25^+$ T_{regs} are recognised to produce low levels of IFN-γ[292-296], so IFN-γ intracellular cytokine staining may identify only a limited number of any PPD-specific T_{regs} that are present in the skin. The continued presence of IFN-γ and IL-2 producing $CD4^+$ T cells during resolution, therefore, suggests that T_{regs} do not accumulate in the skin during the MT

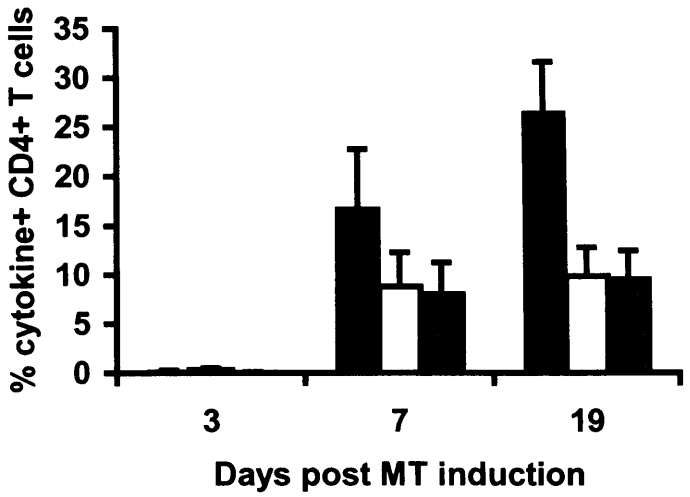

Figure 5.5 CD4$^+$ T cell interleukin-2 production during the Mantoux test

Blister cells were stimulated with PPD *ex vivo* for 15 hours in the presence of Brefeldin A. CD4$^+$ T cells were then examined for intracellular IFN-γ and IL-2 expression by flow cytometry. The percentage of CD4$^+$ T cells expressing IFN-γ (■), IL-2 (□) and both IFN-γ and IL-2 (■) are shown. The mean ± SEM of 3-4 experiments per time-point is shown.

5.5 Proliferative and suppressive capacity

5.5.1 Proliferative capacity

If T_{regs} were to constitute a significant proportion of the CD4$^+$ T cell population in the skin during resolution then their anergic behaviour[147;291-295] would be expected to affect the *in vitro* responsiveness of these cells. Furthermore, telomere shortening in cutaneous CD4$^+$ T cells during the MT would be expected to limit their residual proliferative potential. We, therefore, compared the proliferative capacity of blood and skin CD4$^+$ T cells isolated from MTs to re-stimulation with PPD in short- and long-term cultures *in vitro*.

In view of the comparatively low number of cells isolated from SBs raised over MTs, cutaneous CD4$^+$ T cells were again purified by negative selection using panning (see section 2.2.2). Interestingly, purified SB CD4$^+$ T cells isolated from day 3 and 19 MTs showed increased proliferative

responses to PPD in the short-term compared to PB $CD4^+$ or $CD4^+CD25^-$ responder T cells (Figure 5.6). Indeed, SB $CD4^+$ T cells isolated during resolution at day 19 were hyper-responsive compared to those isolated at day 3. This was apparent not only in terms of the proliferative response, but also with regard to the speed of onset of proliferation as judged by daily visual examination. Clumps of proliferating cells were evident in cultures of day 19 SB $CD4^+$ T cells within 24-48 hours, whereas it would take 72-96 hours for the same appearance to be manifest in day 3 SB $CD4^+$ T cell cultures. This resulted in [^{3}H]-thymidine incorporation been measured in the day 19 cultures 24-48 hours before the day 3 cultures. SB $CD4^+$ T cells isolated during resolution are, therefore, still capable of short-term *in vitro* proliferation despite their shortened telomeres and highly differentiated state. This argues against the presence of a significant population of anergic suppressive T_{regs}. The hyper-responsive character of the skin $CD4^+$ T cells probably reflects the increased proportion of antigen-specific cells present at day 19 compared to day 3. It might also reflect the on-going differentiation process, which may permit cells to cycle more rapidly following TCR stimulation[108].

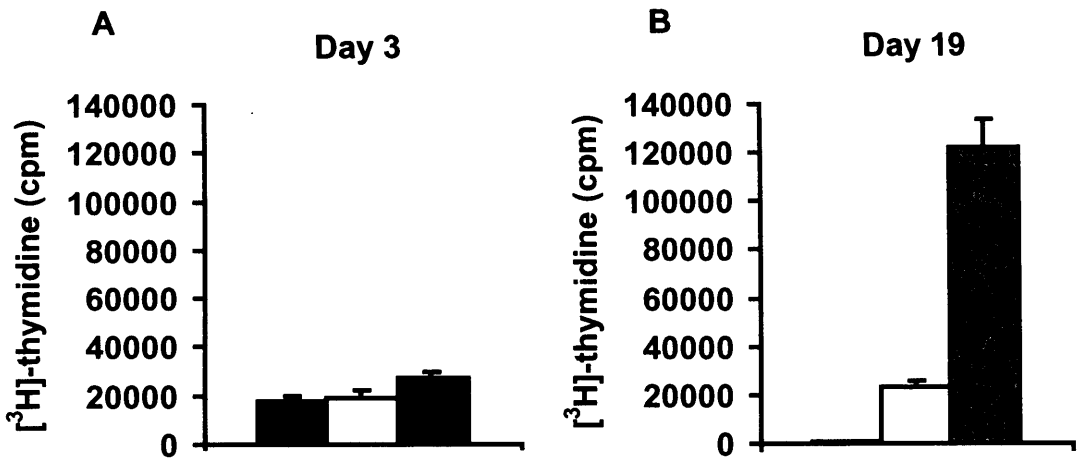

Figure 5.6 *In vitro* proliferative response to PPD of blood and skin $CD4^+$ T cells isolated during the Mantoux test

12500 PB $CD4^+$ T cells (■), PB $CD4^+CD25^-$ T cells (□) or purified SB $CD4^+$ T cells (■) isolated at (A) day 3 or (B) day 19 after MT induction were incubated in round bottomed 96-well plates and stimulated with PPD at a final concentration of 0.2μg/ml and 25000 irradiated autologous PBMC. The cells were then incubated for 4-6 days at 37°C in a humidified 5% CO_2 atmosphere. The proliferative response was measured by [^{3}H]-thymidine incorporation (counts per minute (cpm)) during the last 18 hours. The mean of triplicate wells ± SEM is shown. Representative data from 1 out of 3 experiments performed at each time-point are shown.

To assess whether telomere shortening affected the residual proliferative capacity of skin $CD4^+$ T cells, we looked at the long-term proliferative capacity of MT SB cells isolated from healthy young volunteers at day 19 compared to day 0 and day 19 PBMC. SB cells stimulated with PPD and irradiated autologous PBMC surprisingly continued to proliferate as well as day 0 and day 19 PBMC for up to 50 days (Figure 5.7). Intriguingly, the telomere length of the SB PPD-specific $CD4^+$ T cell subset was maintained during the course of this experiment despite almost 10 population doublings being achieved (MFI day 0 and 50: 87 and 91 respectively).

The capacity of day 19 MT SB cells to expand further was then examined. These cells were able to expand *in vitro* for almost another 50 days i.e. 100 days in total (Figure 5.8). At this stage, no further expansion occurred

despite optimal re-stimulation suggesting that the cells had reached replicative senescence. Day 19 skin PPD-specific $CD4^+$ T cells, therefore, are capable of further, albeit limited, long-term expansion *in vitro* despite significantly shortened telomeres.

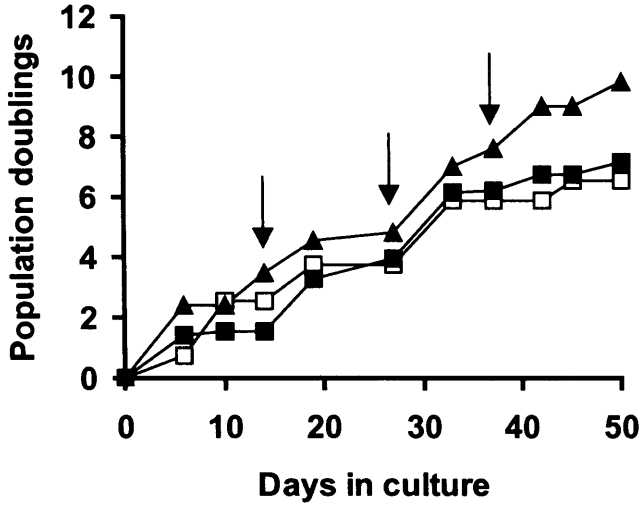

Figure 5.7 Comparative long-term *in vitro* proliferative capacity of blood and skin PPD-specific cells isolated during the Mantoux test.

The proliferative capacity of MT day 19 SB cells (▲), day 19 PBMC (■) and thawed cryo-preserved day 0 (□) PBMC isolated from the same volunteer was assessed in long-term *in vitro* cell culture. Cells were cultured in complete medium (CM) in round-bottomed 96-well plates at a concentration of 1×10^6 cells/ml and stimulated with PPD at a final concentration of 1μg/ml. After 5-7 days, the CM was supplemented with IL-2 at a final concentration of 1-5ng/ml. The cells were sub-cultivated every 3-7 days and cell numbers were quantified using TruCOUNT™ tubes. The arrows indicate when the cultures were re-stimulated with PPD and irradiated autologous PBMC (approximately every 14 days). Population doublings (PD) were determined by comparing the total number of cells at the start and end of each sub-cultivation using the equation: log10 × (cell $total_{end}$ / cell $total_{start}$) / log2. The cumulative PDs versus days in culture are shown. The data are representative of 1 out of 2 experiments performed.

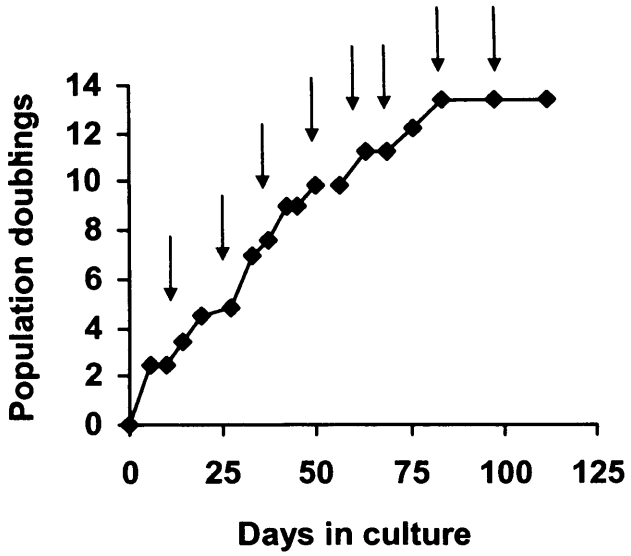

Figure 5.8 Induction of replicative senescence in day 19 Mantoux test cutaneous PPD-specific cells

The proliferative capacity of day 19 MT SB cells (◆) isolated from the same volunteer as depicted in Figure 5.7 was assessed in long-term *in vitro* cell culture. Cells were cultured and population doublings determined as described in Figure 5.7. The arrows indicate when the cultures were re-stimulated with PPD and irradiated autologous PBMC.

5.5.2 Suppressive activity

We next assessed whether cutaneous PPD-specific $CD4^+$ T cells isolated from MTs could mediate direct suppressive activity. To address this, we co-cultured purified SB $CD4^+$ T cells with PB $CD4^+CD25^-$ T cells in parallel with the short-term cultures performed in section 5.5.1. Skin $CD4^+$ T cells isolated from MTs at day 19 failed to exhibit any direct suppressive activity when co-cultured 1:1 with PB $CD4^+CD25^-$ responder T cells. Indeed, as previously shown, they exhibited pronounced hyper-responsiveness (Figure 5.9). It was possible that any T_{regs} present in the blister $CD4^+$ T cells at day 19 were not detectable, because they were out-numbered by responder cells. PPD stimulated SB $CD4^+$ T cells were, therefore, compared with SB $CD4^+$ T cells that had been relatively depleted of $CD25^+$ cells by panning to see if this led to any accentuation in the proliferative response (Figure 5.10). CD25 depleted SB $CD4^+$ T cells showed a small (17%) increase in the proliferative response compared to the undepleted SB cells, but this difference was not significant (Wilcoxon signed rank test,

p=0.25). Overall, it therefore appears that the highly differentiated $CD4^+$ T cells isolated from the skin during resolution of the MT at day 19 are predominantly of a primed memory / effector phenotype that does not exhibit significant suppressive activity.

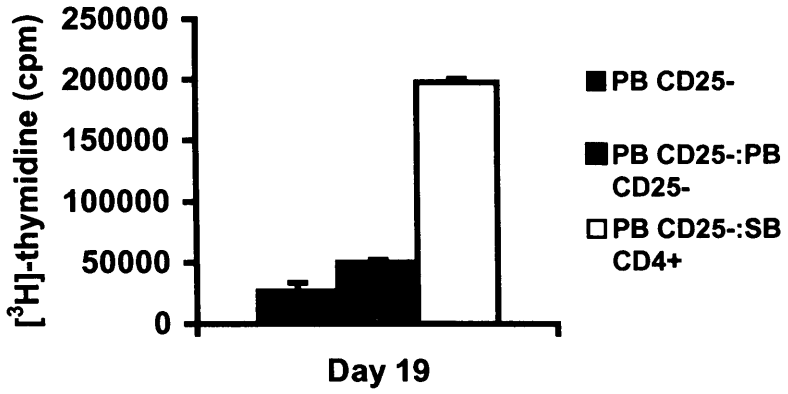

Figure 5.9 Day 19 suction blister $CD4^+$ T cells lack suppressive activity.

PBMC and SB cells were isolated at day 19 from volunteers undergoing MTs. 12500 PB $CD4^+CD25^-$ T cells were cultured alone (■) or co-cultured with equal numbers of PB $CD4^+CD25^-$ (■) or SB $CD4^+$ T cells (□) in round bottomed 96-well plates and stimulated with PPD at a final concentration of 0.2μg/ml and 25000 irradiated autologous PBMC. The cells were incubated for 4 days at 37°C in a humidified 5% CO_2 atmosphere. The proliferative response was measured by $[^3H]$-thymidine incorporation (cpm) during the last 18 hours. The mean of triplicate wells ± SEM is shown. The data show 1 representative experiment out of 3 performed.

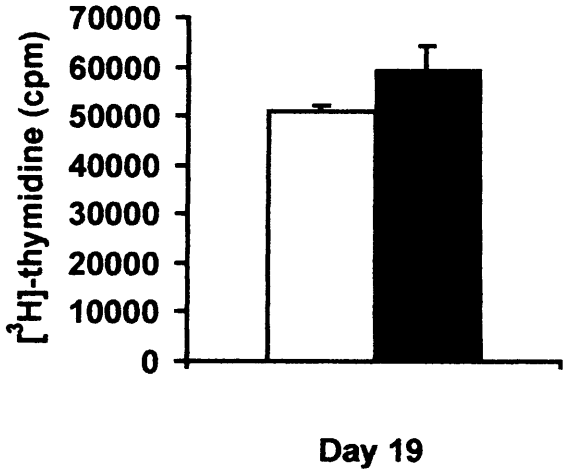

Figure 5.10 The effect on proliferative responsiveness to PPD *in vitro* of depleting $CD25^+$ cells from blister $CD4^+$ T cells.

SB cells were isolated from MTs at day 19. 12500 purified SB $CD4^+$ T cells undepleted (□) or depleted (■) of $CD25^+$ cells by panning were incubated in round bottomed 96-well plates and stimulated with PPD at a final concentration of 0.1μg/ml with 25000 irradiated autologous PBMC. The cells were then incubated for 4 days at 37°C in a humidified 5% CO_2 atmosphere. The proliferative response was measured by $[^3H]$-thymidine incorporation (cpm) during the last 18 hours. The mean of triplicate wells ± SEM is shown.

5.6 Suppressive effect of regulatory T cells on suction blister cells

Collectively, these data suggest that T_{regs} do not play a significant role in mediating the resolution of the MT. This may in part be a consequence of their numbers being overwhelmed by the predominant expansion of effector T cells, but also as a result of the on-going inflammatory microenvironment abrogating the suppressive effects any regulatory T cells present in the skin. Indeed, it has recently been shown that IL-6 secreted by dendritic cells can block the suppressive activity of T_{regs}[476]. Interestingly, IL-6 was present in SB fluid in significant quantities during the MT with a peak of expression on day 3 (Kruskal-Wallis test, $p<0.0001$) (Figure 5.11). Additionally, IL-2 is capable of reversing the anergic state of T_{regs} and may also inhibit their suppressive function[147;291;292;296;301;477]. IL-2 expression was just detectable in SB fluid during the MT and peaked at

day 7 (Figure 5.11). The inflammatory microenvironment of the skin during the MT may, therefore, inhibit the suppressive function of T_{regs}. In particular, the marked expression of IL-6 in the skin during the MT may be of critical importance, since it may render antigen-specific T cells refractory to the suppressive effect of T_{regs}[476].

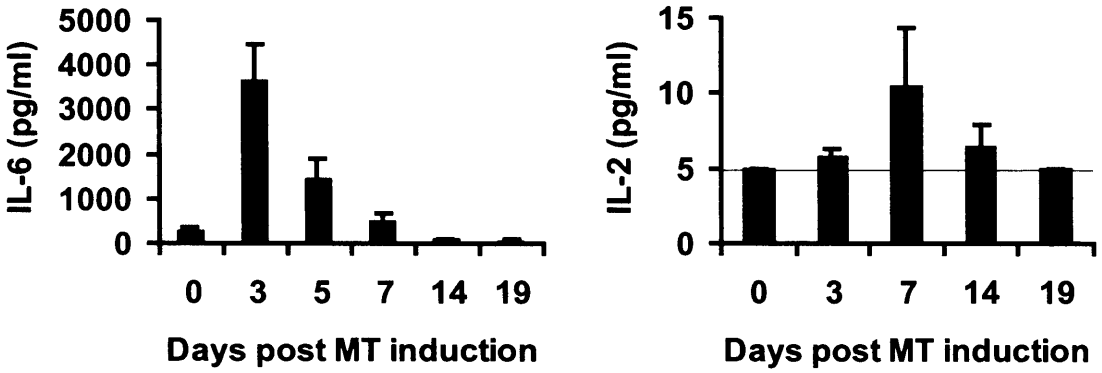

Figure 5.11 Suction blister fluid interleukin-2 and interleukin-6 expression during the Mantoux test.

IL-2 and IL-6 expression in SB supernatants was assayed by multiplex bead immunoassay using a Luminex 100 and cytokine Beadlyte assay kit. The assay was kindly performed by Dr John Curnow, University of Birmingham. The graph shows the mean ± SEM of 3-18 experiments per time-point. The dotted line on the graph showing IL-2 data denotes the lower limit of detection in the assay.

We next examined whether cutaneous $CD4^+$ T cells isolated from MTs at different time-points were sensitive to suppressive activity mediated by freshly isolated PB $CD4^+CD25^+$ regulatory T cells in 1:1 co-cultures. For each experiment performed, control parallel cultures of PB $CD4^+$, $CD4^+CD25^-$, $CD4^+CD25^+$ and 1:1 co-cultures of PB $CD4^+CD25^-$ with PB $CD4^+CD25^+$ T cells were established to confirm that the PB $CD4^+CD25^+$ T cells were anergic and suppressive. PB $CD4^+CD25^+$ T cells were able to partially suppress the proliferation of SB $CD4^+$ T cells isolated early in the immune response at day 3, but demonstrated no suppressive effect on day 19 SB cells (Figure 5.12). $CD4^+$ T cells isolated from the skin during the induction phase of the immune response, therefore, are partially

sensitive to T_{reg} mediated suppression, but this sensitivity appears to diminish during the course of the MT. This probably partly reflects the increase in the proportion of PPD-specific $CD4^+$ T cells during the MT.

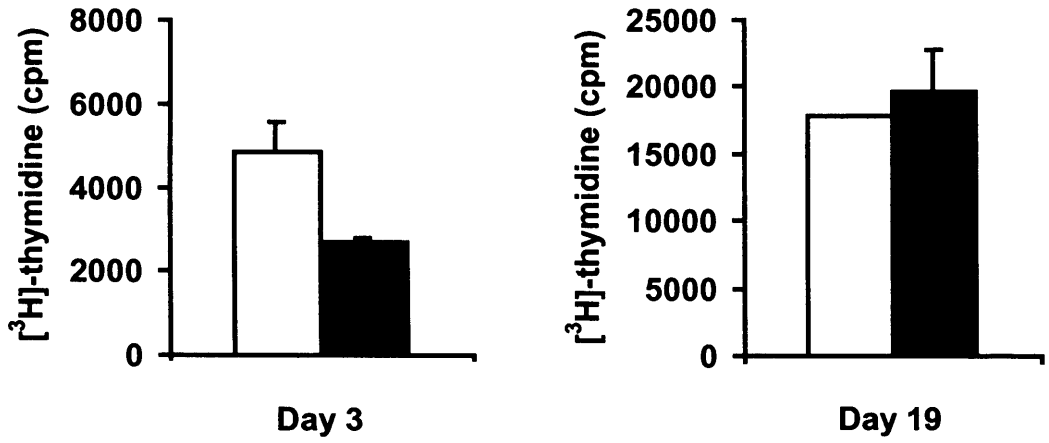

Figure 5.12 Suppressive effect of autologous peripheral blood $CD4^+CD25^+$ regulatory T cells on suction blister $CD4^+$ T cells isolated from Mantoux tests

SB cells and PBMC were isolated either 3 or 19 days after MT induction. SB $CD4^+$ T cells were purified by negative selection using panning and PB $CD4^+CD25^+$ T cells were prepared from fresh PBMC using MACS beads. 12500 SB $CD4^+$ T cells cultured alone (□) or co-cultured 1:1 with 12500 PB $CD4^+CD25^+$ T cells (■) were stimulated in 96-well round-bottomed plates with PPD at a final concentration of 0.5μg/ml and 25000 irradiated autologous PBMC. The cells were cultured for 4-6 days at 37°C in a humidified 5% CO_2 atmosphere. The proliferative response was measured by [^{3}H]-thymidine incorporation (cpm) during the last 18 hours. The mean of triplicate wells ± SEM is shown. The data are representative of 1 out of 3 experiments performed at each time-point.

5.7 Induction of anergy and suppressive function in skin PPD-specific $CD4^+$ T cells

We have shown that highly differentiated day 19 MT skin $CD4^+$ T cells are hyper-responsive to PPD, non-suppressive and have relatively preserved long-term proliferative capacity to stimulation with PPD *in vitro*. Previous studies have shown that highly differentiated $CD4^+$ T cell clones can be easily anergised by TCR stimulation in the absence of co-stimulation or by peptide presented by T cells to each other (T-T presentation)[290;478;479]. Importantly, these anergised cells acquire the ability to suppress the proliferation of other responsive cells[290;478;480]. We, therefore, hypothesized that the hyper-responsive day 19 MT cutaneous PPD-specific $CD4^+$ T cells could acquire suppressive activity when stimulated under appropriate conditions. To this end, we explored whether a cell line raised from day 19 MT blister $CD4^+$ T cells could be rendered suppressive following the induction of anergy. These experiments were kindly performed by Dr Padraic Dunne, RFUCMS.

Cells from a day 19 MT cell line were stimulated in the presence of immobilised anti-CD3 antibodies in the absence of co-stimulation for 18-24 hours. AICD was prevented by performing the cultures in the presence of 50% fibroblast-conditioned medium (FCM). The main pro-survival factor in FCM is IFN-β[480]. Induction of anergy was assessed by measuring the proliferative response to re-stimulation with PPD-pulsed autologous APC. We found that PPD-specific $CD4^+$ T cells were rendered increasingly anergic following stimulation with increasing concentrations of anti-CD3 antibodies in the absence of co-stimulation (Figure 5.13). We then investigated whether these anergic cells could suppress the responsiveness of non-anergised responder cells. Figure 5.14 shows that anergised PPD-specific $CD4^+$ T cells can suppress the proliferative response of responder cells to stimulation with PPD-pulsed APC. Indeed, the more the cells had been rendered anergic the more they became suppressive. The induction of anergy in highly

differentiated PPD-specific $CD4^+$ T cells, therefore, resulted in the acquisition of suppressive function.

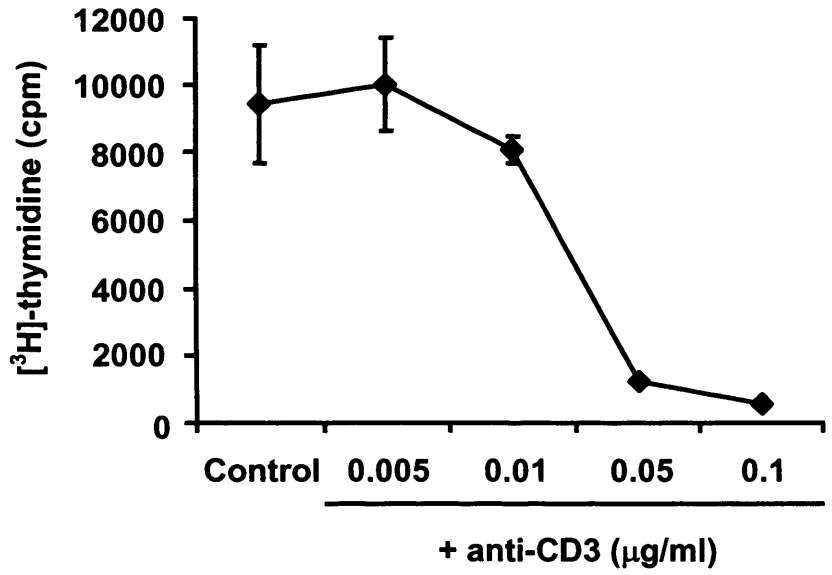

Figure 5.13 Induction of anergy in skin derived PPD-specific $CD4^+$ T cells

Day 19 MT skin PPD-specific $CD4^+$ T cell line cells rescued from anti-CD3-induced apoptosis by fibroblast conditioned medium (FCM) are unresponsive to subsequent re-challenge with PPD-pulsed autologous APC. The PPD-specific $CD4^+$ T cell line was established using day 19 MT blister cells as described in section 2.7.2. Cells for anergy induction experiments were harvested after 4 rounds of stimulation with PPD (1μg/ml). Cells were then incubated in 24 well plates with 50% FCM in the absence or presence of increasing concentrations of immobilised anti-CD3 (OKT-3) for 18-24 hours at 37°C in a humidified 5% CO_2 atmosphere. The cells were then washed and stimulated in a 1:1 ratio with autologous irradiated PPD-pulsed (1μg/ml) PBMC in 96 well round bottomed plates. The cells were cultured for 3 days and the proliferative response was measured by $[^3H]$-thymidine incorporation (cpm) during the last 16 hours of culture. The mean of triplicate wells ± SEM is shown. The data are representative of 1 out of 3 experiments performed. These experiments were kindly performed by Padraic Dunne, RFUCMS.

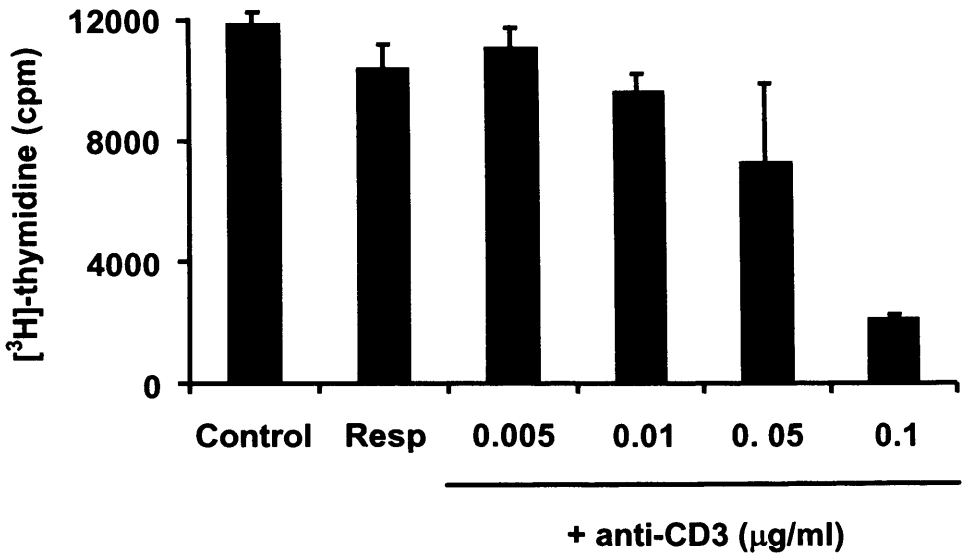

Figure 5.14 Suppressive function of anergised skin PPD-specific CD4$^+$ T cells

MT day 19 skin PPD-specific CD4$^+$ T cell line cells were rendered anergic as described in Figure 5.13. The cells were co-cultured with an equal number of autologous non-anergised responder PPD cell line cells and stimulated with autologous irradiated PPD-pulsed (1μg/ml) PBMC in 96 well round bottomed plates. The cells were cultured for 3 days and the proliferative response was measured by [^{3}H]-thymidine incorporation (cpm) during the last 16 hours of culture. The mean of triplicate wells ± SEM is shown. The data are representative of 1 out of 3 experiments performed. These experiments were kindly performed by Padraic Dunne, RFUCMS.

5.8 Discussion

In this chapter we have investigated the functional consequences of the accelerated cellular differentiation that is observed in CD4$^+$ T cells infiltrating into the skin during the MT. One possible consequence is the generation of anergic regulatory CD4$^+$ T cells that have suppressive function. It has been suggested that CD4$^+$CD25$^+$ regulatory T cells may arise in the periphery from highly differentiated antigen-specific cells that are approaching end-stage differentiation[287;290;339]. We, therefore, hypothesized that the on-going differentiation of CD4$^+$ T cells in the skin during the MT might result in the accumulation of T_{regs}, which might in turn mediate the resolution of the immune response.

The investigation of T_{regs}, particularly in inflammatory settings *in vivo*, however, has been hampered by the lack of an exclusive marker[148;287;338]. Most of the markers associated with T_{regs} represent activation markers and may therefore also be expressed on activated $CD4^+$ T cells e.g. CD25, CD122, CTLA-4 (CD152) and GITR. Studies of T_{regs} have relied on the use of functional assays to detect their anergic and suppressive qualities combined with analysis for associated surface markers. The activated microenvironment of the MT was likely, therefore, to limit the specificity of data generated solely from looking at surface markers. One might expect, however, that if T_{regs} were being generated in the skin during the MT, that the proportion of $CD4^+$ T cells expressing CD25 would increase suggesting a relative accumulation. In fact, although there was a progressive increase in the proportion of $CD4^+$ T cells in the skin during the MT with an activated phenotype as determined by CD69 expression, the proportion of $CD4^+$ T cells positive for CD25 decreased. It did, however, remain higher than compared to the blood. The predominance of cells positive for CD69 expression during the resolution phase of the immune response has been reported by other authors[103;104;481]. The reasons for this are unclear, but other authors have argued against the persistence of antigen as being an explanation[103;481]. Indeed, the decrease in the proportion of proliferating $CD4^+$ T cells in the MT after day 7 would support the notion that antigen has been cleared from the skin microenvironment. This might also explain the relative decrease in CD25 expression observed on $CD4^+$ T cells in the skin during the MT.

As already stated, the fact that CD25 represents an activation marker makes interpretation of this data difficult and we therefore incorporated functional assays to further investigate the role of T_{regs} in the MT. Human T_{regs} are anergic, suppressive and produce little or no IL-2[147;290-296]. However, we found that there was no significant change in the proportion of $CD4^+$ T cells that was capable of IL-2 or IFN-γ secretion during the course of the MT. Furthermore, $CD4^+$ T cells isolated from the skin during

the resolution of the MT were in fact hyper-responsive to re-stimulation with PPD and did not exhibit suppressive activity.

These findings, however, do not necessarily exclude the generation of T_{regs} during the course of the immune response. $CD4^+CD25^+$ regulatory T cells exhibit low Bcl-2 expression and are very susceptible to apoptosis. They may, therefore, be preferentially cleared during resolution. Apoptosis of T_{regs} can be prevented by fibroblast conditioned medium (FCM) or IL-2[147]. FCM contains type 1 interferons and the anti-apoptotic effects of FCM appear to be mediated by IFN-β[480]. Increasing IFN-β expression has been detected in MT tissue sections up to day 14[26]. It is likely that T_{regs}, if present, only comprise a minority of $CD4^+$ T cells and they would have to compete extensively with the predominant population of memory / effector cells for pro-survival cytokines. IL-2 was undetectable in blister fluid by day 19 after exhibiting a peak of expression at day 7. This pattern of expression matches that previously reported in MT tissue sections[25]. The level of expression in blister fluid, however, appears to be lower than in tissue sections and this apparent difference may be explained by the autocrine mode of action by which IL-2 acts[482]. The microenvironment of the skin during resolution, therefore, may not be favourable to the long-term survival of T_{regs}. Furthermore, even if T_{regs} are generated during the MT, the likelihood that antigen has been cleared by resolution means that their activation, which is required if they are to mediate suppression, is unlikely to be promoted[293;317].

We recently proposed that human T_{regs} can be generated in the periphery when highly differentiated cells encounter antigen presented in a non-professional manner[290;339]. Although day 19 MT skin $CD4^+$ T cells exhibited no suppressive function *in vitro*, they were easily anergised and this resulted in the acquisition of prominent suppressive activity. This indirectly supports the notion that $CD4^+CD25^+$ T_{regs} can be generated in the periphery, depending on the context in which $CD4^+$ T cells become

activated. T_{regs} may, therefore, be generated in the periphery *in vivo* through mechanisms such as T-T presentation[290;480]. The techniques used to detect T_{regs} in this chapter are relatively insensitive and non-specific, so the data presented does not necessarily exclude the generation and accumulation of T_{regs} during the course of the MT. The analysis of *Foxp*3 expression in $CD4^+$ T cells will perhaps give a clearer indication as to whether T_{regs} are generated during the course of an immune response *in vivo*.

Immune non-responsiveness is in part dependent on responder antigen-specific T cells being sensitive to suppression by T_{regs}. This is obviously of critical importance when discriminating between self and non-self, since the inappropriate suppression of pathogen-specific T cells during an immune response could be detrimental. The cytokine microenvironment probably plays a critical role in determining this responsiveness. Indeed, T cell activation was recently shown to be dependent on IL-6 produced by dendritic cells and macrophages, which had been activated through the ligation of Toll-like receptors by pathogenic antigens[476]. This rendered the responder T cells refractory to suppression mediated by T_{regs}. In addition, IL-2 may also be able to partially reverse the suppressive function of T_{regs}[291;292;296;301;477]. IL-2 and IL-6 were both detected in blister fluid and tissue sections[25] at different time-points during the MT. High expression of IL-6 in tissue sections was observed up to day 14[25], whereas only low levels were detectable in blister fluid by day 14 and 19. The inflammatory microenvironment of MT skin may, therefore, be unfavourable to T_{reg}-mediated suppressive activity. Indeed, the hyper-responsiveness of skin $CD4^+$ T cells may in part be accounted for by their exposure to this microenvironment, which renders them insensitive to T_{regs}. Skin $CD4^+$ T cells isolated 3 days after the induction of the MT were, however, partially sensitive to suppression mediated by fresh PB $CD4^+CD25^+$ T cells following re-stimulation with PPD *in vitro*, whereas cells isolated after 19 days were resistant to suppression when cultured at a 1:1 ratio. This again may partly reflect the increase in the proportion of antigen-specific cells,

but could also be explained by induced refractoriness to suppression. The partial sensitivity of skin $CD4^+$ T cells to T_{reg} mediated suppression in the early part of the response suggests that the main role of T_{regs} may be to prevent the initiation of immune responses rather than regulate the on-going response. This would make sense when one considers that the principle function of T_{regs} appears to be to prevent the activation of self-reactive T cells in the periphery[148;287;483;484]. The situation, however, in chronic infections may be different, where it has been shown that T_{regs} may play a role in mediating the persistence of pathogens thereby maintaining memory and limiting damage to tissues produced by the immune system[350;351].

Another possible consequence of the accelerated differentiation process in the skin is the induction of replicative senescence in a subset of the antigen-specific $CD4^+$ T cells, which have developed critically shortened telomeres. Interestingly, $CD4^+$ T cells were capable of proliferation following re-stimulation with PPD in the short- and long-term at least *in vitro*. This suggests that the extent of telomere erosion in PPD-specific $CD4^+$ T cells does not result in the induction of replicative senescence in the expanded antigen-specific population and thereby does not act as a significant regulatory mechanism in mediating resolution. The ability of the cells to proliferate in response to re-challenge is probably of critical importance in light of the findings that suggest that memory cells can persist in non-lymphoid tissues[101;102;104]. Data relating to the long-term proliferative capacity of cells, however, need to be interpreted with caution, because the method used to assess this was performed *in vitro*. Indeed, the telomere shortening that was observed in $CD4^+$ T cells in the skin was not reciprocated *in vitro*. This suggests that factors present in the skin microenvironment, but absent *in vitro* may influence telomere maintenance. The proliferative capacity of these cells may, therefore, be more limited *in vivo*, since further expansion in the skin would presumably result in additional telomere erosion. This issue will be explored in the next chapter. Additionally, the results probably reflect the selection of the fittest

clone with the longest telomeres rather than assessing the proliferative capacity of the whole population[161;485]. It must also be noted that our studies were performed with a relatively young cohort of volunteers. Telomeres in lymphocytes shorten as we age and therefore the implications of accelerated differentiation may be more profound with aging[235;238;259;486;487].

In summary, we have shown that the accelerated differentiation of skin $CD4^+$ T cells during the MT results in a population of cells demonstrating increased responsiveness and preserved function. Furthermore, it appears that T_{regs} do not play a significant role in regulating the on-going immune response of the MT.

6 Mechanisms of regulation of telomerase activity in the skin during the Mantoux test

6.1 Introduction

We have demonstrated that the differentiation of $CD4^+$ T cells in the skin during the MT was associated with accelerated telomere shortening. Telomerase is an RNA-dependent DNA polymerase, which can synthesize terminal telomeric repeats and elongate telomeres thereby compensating for the erosion of telomeres that results from cell division[171;198;200;488]. Telomerase activity is induced in activated T cells[207-210] and has been shown to maintain telomere length in T cells in the blood and secondary lymphoid organs during acute infections *in vivo*[240-244]. However, it is unknown whether telomerase activity is normally induced in lymphocytes that are activated at the site of an immune response in non-lymphoid tissue. Our findings suggest that telomerase activity in cutaneous antigen-specific $CD4^+$ T cells is insufficient during the MT to fully compensate for the telomere erosion that is induced by proliferation *in situ*. In this chapter we will examine telomerase activity in SB T cells during the MT.

6.2 Telomerase activity in antigen-specific T cells in the skin during the Mantoux test

Telomerase activity in T cells is only detected in activated cells[207-210] and is assayed for using the Telomeric Repeat Amplification Protocol (TRAP) assay[202]. Data relating to telomerase activity in T cells has up until now been presented on the basis of the assay of a pre-determined number of T cells. This takes no account of the proportion of activated antigen-specific T cells present in the assay population, which may influence the level of

telomerase activity detected. The proportion of antigen-specific T cells in the skin changes during the MT, so we decided that this should be taken into account when analysing telomerase activity at different time-points. We, therefore, measured the number of T cells and the proportion of antigen-specific T cells present in MT SB samples, so that we could determine the level of telomerase activity on an antigen-specific cell basis (Figure 6.1). The telomerase activity per PPD-specific T cell decreased during the course of the MT. Telomerase activity was detected early in the immune response up to day 5, but from day 7 onwards negligible activity per PPD-specific cell was detected. In particular, minimal PPD-specific T cell telomerase activity was present at day 7 when T cell proliferation in the skin is maximal. This supports the hypothesis that the telomere erosion observed in $CD4^+$ T cells in the skin during the MT resulted from insufficient telomerase activity. We were concerned, however, that these results might be influenced by the dramatic increase in antigen-specific T cells at day 7 compared to earlier time-points. It is also likely that not all of the antigen-specific cells would be activated and cycling, and thereby exhibiting up-regulated telomerase activity. This would result in an underestimate of telomerase activity on a per cell basis.

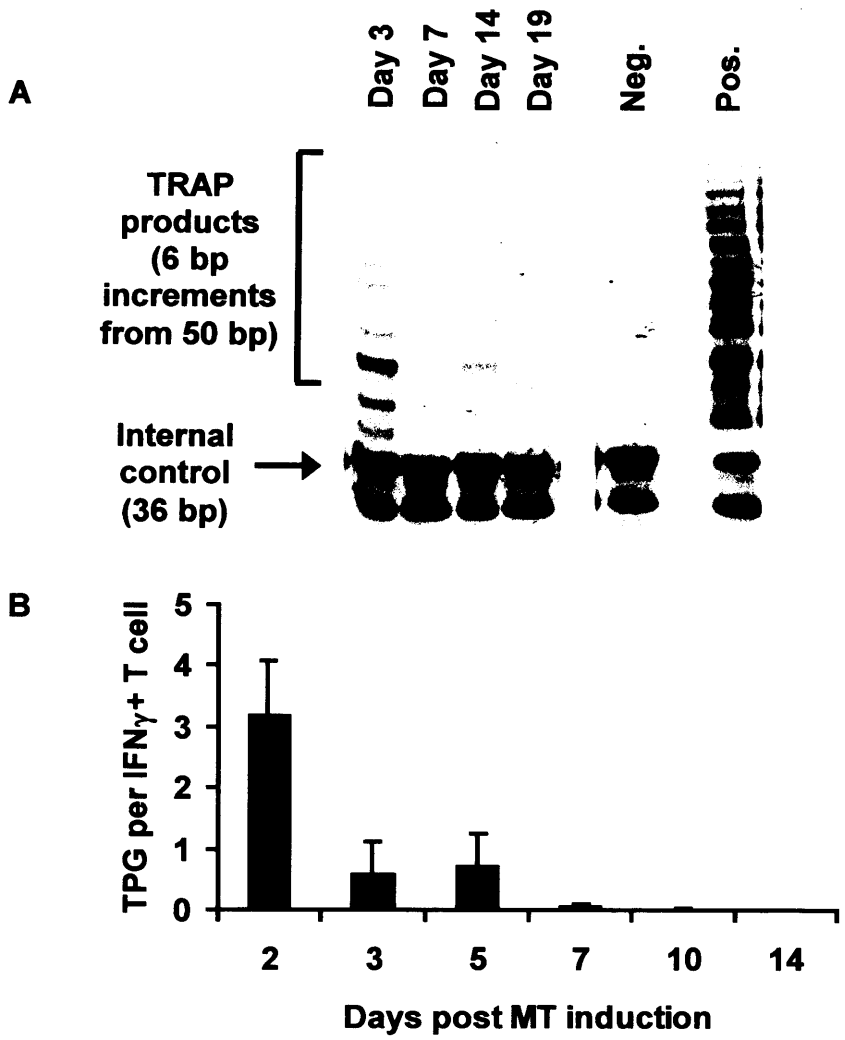

Figure 6.1 Telomerase activity in antigen-specific T cells in the skin during the Mantoux test.

(A) Telomerase activity was determined using the TRAP assay with the reaction products detected by autoradiography. Telomerase activity is visualised as a ladder of extended reaction products generated on a substrate oligonucleotide (TS primer), which is then amplified by PCR. The negative control (Neg.) contains PCR mix without cell extract. The positive control (Pos.) contains extract from a telomerase positive tumour cell line. Internal control oligonucleotides contained in the PCR mix produce a 36 bp band in each lane. The number of T cells in SB samples isolated from MTs at different time-points was enumerated using TruCOUNT™ tubes. The percentage of PPD-specific T cells was determined by intracellular cytokine (IFN-γ) staining. This allowed the number of PPD-specific T cells in each sample to be determined. Each assay was standardised to 12500 $CD4^+$ T cells. A representative gel autoradiograph is shown. (B) Telomerase activity was quantified as the total product generated (TPG). This corresponds to the number of TS primers extended with at least 4 telomeric repeats by telomerase in the extract. The TPG was divided by the number of IFN-γ^+ T cells in each sample to give the telomerase activity per PPD-specific T cell. The graph shows the mean ± SEM of 3 experiments per time-point.

6.3 Telomerase activity in proliferating T cells in the skin during the Mantoux test

One of the consequences of T cell activation is proliferation and telomerase induction is closely associated with entry into cell cycle[213-215]. In view of this, we decided to measure the level of telomerase activity at different time-points during the MT in relation to T cell proliferation. We, therefore, next determined the number of proliferating $Ki67^+$ T cells present in each sample so that we could measure the level of telomerase activity relative to a predetermined number of proliferating T cells (Figure 6.2). Each assay was standardised to 500 proliferating $Ki67^+$ T cells. Telomerase activity was detected at low levels in cycling T cells that were isolated from the skin on days 3 and 7 after PPD challenge, but was minimal in comparison to that observed in PB T cells stimulated *in vitro* with PPD for 7 days (Figure 6.2a,b). These cells demonstrated striking up-regulation of telomerase activity despite less intense T cell proliferation ($2.4 \pm 20.4\%$ and $9.7 \pm 4.0\%$ $Ki67^+$ on days 3 and 7 respectively (mean ± SEM)) compared to those isolated *ex vivo* from the MT ($7.7 \pm 2.0\%$ and $17.8 \pm 6.2\%$ $Ki67^+$ on days 3 and 7 respectively (mean ± SEM)) (Figure 6.2c). Once again though, telomerase activity was minimal on day 7 *in vivo* when T cell proliferation in the skin was maximal. Overall, this suggests that the telomere erosion in cycling PPD-specific $CD4^+$ T cells in the skin during the MT was linked to insufficient telomerase activity *in vivo*.

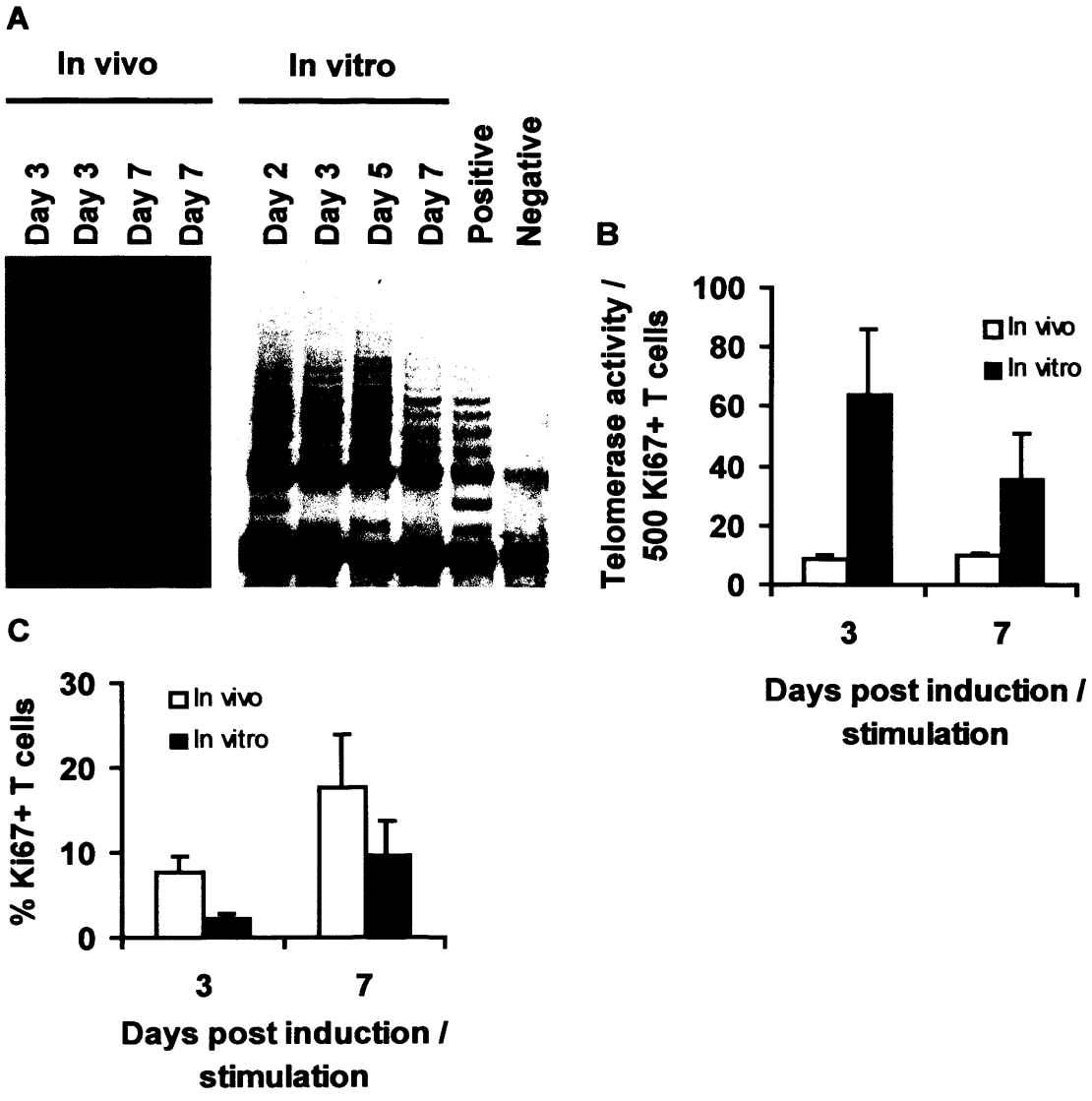

Figure 6.2 Telomerase activity in proliferating T cells in the skin during the Mantoux test and *in vitro* following PPD stimulation.

Samples were collected from SBs raised over MTs (*in vivo* (□)) at days 3 and 7, and were also harvested at different time-points up to 7 days from PBMC stimulated *in vitro* (■) with PPD at a final concentration of 1 μg/ml. The number of proliferating T cells in each sample was determined by enumerating T cells using TruCOUNT™ tubes and measuring the percentage of $Ki67^+$ T cells by FACS analysis. Telomerase activity was measured using the TRAP assay and autoradiography. Assays were standardised to 500 proliferating $Ki67^+$ T cells per lane. (A) Representative gel autoradiographs showing telomerase activity per 500 $Ki67^+$ T cells following stimulation *in vivo* (in 2 individuals) and *in vitro* (from 1 individual). (B) The graph shows telomerase activity (TPG) per 500 proliferating $Ki67^+$ T cells *in vivo* and *in vitro* at different time-points. The mean ± SEM of 3 experiments per time-point is shown. (C) The graph shows the percentage of proliferating $Ki67^+$ T cells present *in vivo* and following *in vitro* stimulation with PPD at different time-points. The mean ± SEM of 3 experiments is shown.

6.4 The reversible inhibition of telomerase in T cells in the skin during the Mantoux test

The lack of telomerase activity in T cells isolated from the skin during the MT could be either due to an inherent inability to induce this enzyme or the active inhibition of this enzyme in T cells *in situ*. We, therefore, isolated blister cells 3 days after PPD challenge and investigated their ability to up-regulate telomerase activity after re-stimulation with PPD *in vitro* (Figure 6.3a,b). As observed in section 6.3, there was minimal telomerase activity in freshly isolated cycling blister T cells. In contrast, there was an almost 5-fold increase in telomerase activity when these cells were re-stimulated with PPD *in vitro.* This suggests that telomerase is actively inhibited in the skin and that this inhibition is reversible. This was confirmed by demonstrating that telomerase activity in PB T cells stimulated with PPD *in vitro* was inhibited in the presence of fresh autologous blister fluid obtained on day 3 from the site of PPD injection (Figure 6.3c). In the absence of day 3 MT blister fluid, telomerase activity was induced normally. This suggests that factors present in the skin microenvironment reversibly inhibit the induction of telomerase activity in activated proliferating T cells.

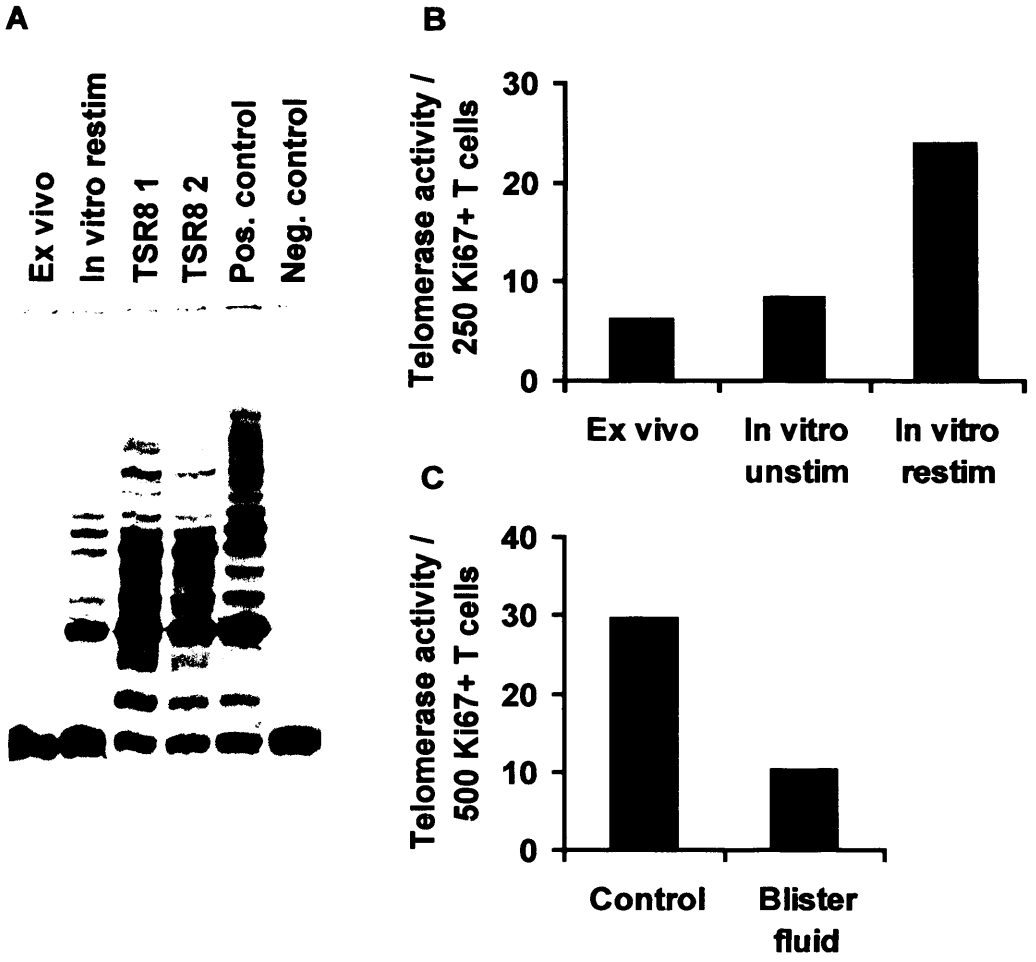

Figure 6.3 Telomerase activity in T cells is reversibly inhibited in the skin during the Mantoux test

(A & B) Skin cells were isolated from SBs raised over MTs on day 3. Telomerase activity was measured in T cells immediately upon isolation (*Ex vivo*), and in the remaining cells that were either unstimulated (In vitro unstim) or stimulated with PPD (0.5 μg/ml) *in vitro* (In vitro restim) for a further 3 days. Cells were incubated in a 5% CO_2 atmosphere at 37°C. Telomerase activity was determined using the TRAP assay and autoradiography. Assays were standardised to 250 proliferating $Ki67^+$ T cells per lane. (A) A representative gel from 1 out of 4 experiments performed is shown. TSR8 1/2 denotes the internal quantitative controls. (B) The graph shows telomerase activity (TPG) per 250 $Ki67^+$ T cells *ex vivo*, and following unstimulated and restimulated *in vitro* culture. It is representative of 1 out of 4 experiments performed. (C) Day 3 MT blister fluid suppresses telomerase activity in PB T cells. PBMC were stimulated with PPD *in vitro* in the presence fresh autologous blister fluid (50% final dilution) that was obtained from a day 3 MT (Blister fluid). Autologous serum was used as a control (Control). Telomerase activity was measured after 3 days of culture using the TRAP assay and autoradiography. Assays were standardised to 500 proliferating $Ki67^+$ T cells. The data are representative of 1 out of 3 experiments performed.

6.5 Interferon expression in the skin and suction blisters during the Mantoux test

Our previous studies indicate that type 1 IFNs (IFN-α and IFN-β) can regulate the rate of differentiation of human T cells[489]. This together with reports that IFN-α can inhibit the activity of telomerase in tumour cell lines and T cells within 72 hours of exposure *in vitro*[261], prompted us to determine whether this group of cytokines was responsible for the inhibition of telomerase activity in T cells in the skin. Analysis for type 1 interferon in blister supernatants that had been collected during the course of the MT demonstrated a peak of expression at day 3 with markedly lower levels of expression at other time-points (Kruskal-Wallis test, $p=0.007$) (Figure 6.4a). In addition, immunohistological analysis of skin sections of MTs biopsied 3 days after PPD challenge demonstrated cells that expressed high levels of IFN-α in the perivascular infiltrates (Figure 6.4b). High uniform levels of expression were also detected amongst keratinocytes. The peak of type 1 interferon and presence of IFN-α expressing cells on day 3 of the MT coincided with the time at which telomerase was greatest in PB T cells that had been stimulated with PPD *in vitro* but was minimal in cycling T cells isolated from the skin of MTs (Figure 6.2b). This, therefore, offers a possible explanation for the inhibition of telomerase activity that is observed in T cells in the skin during the MT.

IFN-γ also represents a potential additional regulatory factor. This has been shown to inhibit telomerase activity in human tumour cell lines, although it is unknown whether this effect extends to normal T cells[267]. A peak of IFN-γ in blister supernatants was observed on day 3 of the MT with minimal expression at other time-points (Kruskal-Wallis, $p<0.0001$).

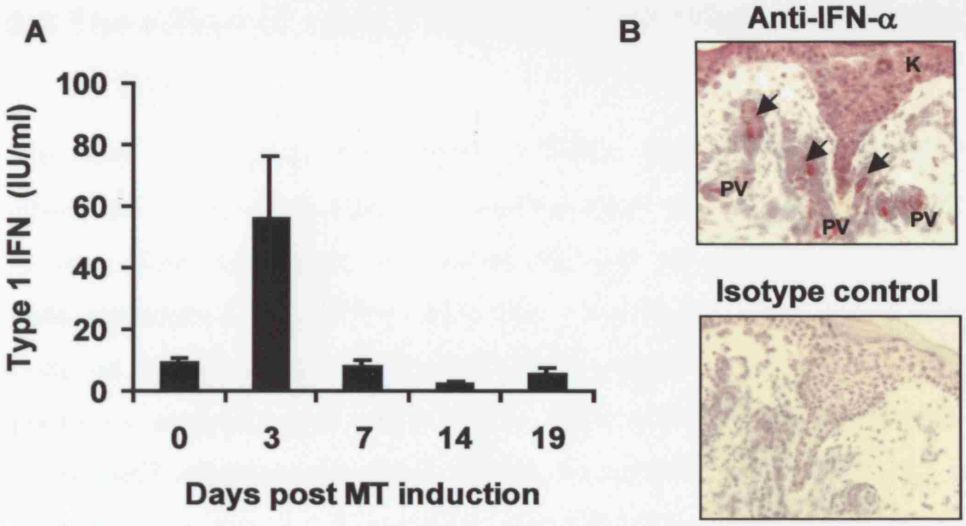

Figure 6.4 Type 1 interferon expression in suction blister fluid and the skin during the Mantoux test

(A) The concentration of type 1 interferon in blister fluid supernatants collected at different time-points during the MT was assayed using a standardised anti-viral assay. This work was kindly performed by Professor Graham Foster at the Royal London Hospital, London, UK. The data shown represent the mean ± SEM of 5 experiments performed per time-point. (B) Interferon-α producing cells present in day 3 MT skin sections were identified using indirect alkaline phosphatase staining (top panel). The bottom panel shows staining with an isotype control (×20 magnification). Keratinocytes (**K**) and isolated cells within the perivascular infiltrates (**PV;** indicated by arrows) expressed IFN-α. Representative photomicrographs from 1 out of 5 experiments are shown.

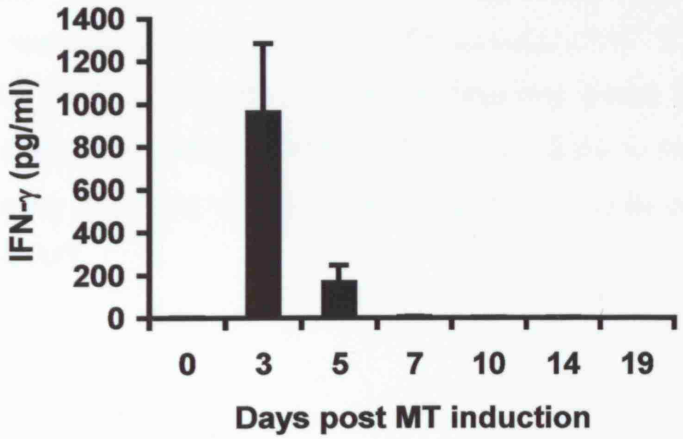

Figure 6.5 IFN-γ expression in suction blister fluid during the Mantoux test

IFN-γ expression in MT blister fluid supernatants was assayed by multiplex bead immunoassay using a Luminex 100 and cytokine Beadlyte assay kit. The assay was kindly performed by Dr John Curnow, University of Birmingham. The graph shows the mean ± SEM of 3-18 experiments per time-point.

6.6 The effect of type 1 interferon on telomerase induction in T cells

We next investigated the effect of IFN-α and the blocking of type 1 interferon receptor signalling on the induction of T cell telomerase activity *in vitro*. Consistent with our earlier findings, telomerase activity in PB T cells stimulated with PPD *in vitro* was much lower when these cells were cultured with fresh day 3 MT blister fluid compared to cells cultured in the presence of autologous serum (TPG / 500 proliferating $Ki67^+$ T cells 17 vs. 34 respectively) (Figure 6.6a). When an antibody directed to the second subunit of the type 1 IFN receptor (anti-IFNAR2), which blocks signalling to all forms of type 1 IFN, was added to cultures of PPD-stimulated PB T cells containing day 3 blister fluid, telomerase activity was enhanced 5 fold (TPG / 500 proliferating $Ki67^+$ T cells 85). Addition of an isotype control antibody to similar parallel cultures did not reverse the inhibitory effect of day 3 blister fluid on T cell telomerase activity (TPG / 500 proliferating $Ki67^+$ T cells 21) (Figure 6.6a). This suggests that type 1 IFNs present in the skin at day 3 prevent the normal induction of telomerase activity in cycling T cells. We also showed that the addition of 2 different recombinant preparations of IFN-α, at concentrations similar to those found in blister fluid, directly blocked in a dose dependent manner the induction of telomerase activity in a PPD-specific $CD4^+$ T cell line re-stimulated with PPD *in vitro* (Figure 6.6b). Together these data, indicate that type 1 interferons, and in particular IFN-α, are likely to be responsible for the reversible inhibition of telomerase activity in T cells present in the skin during the MT.

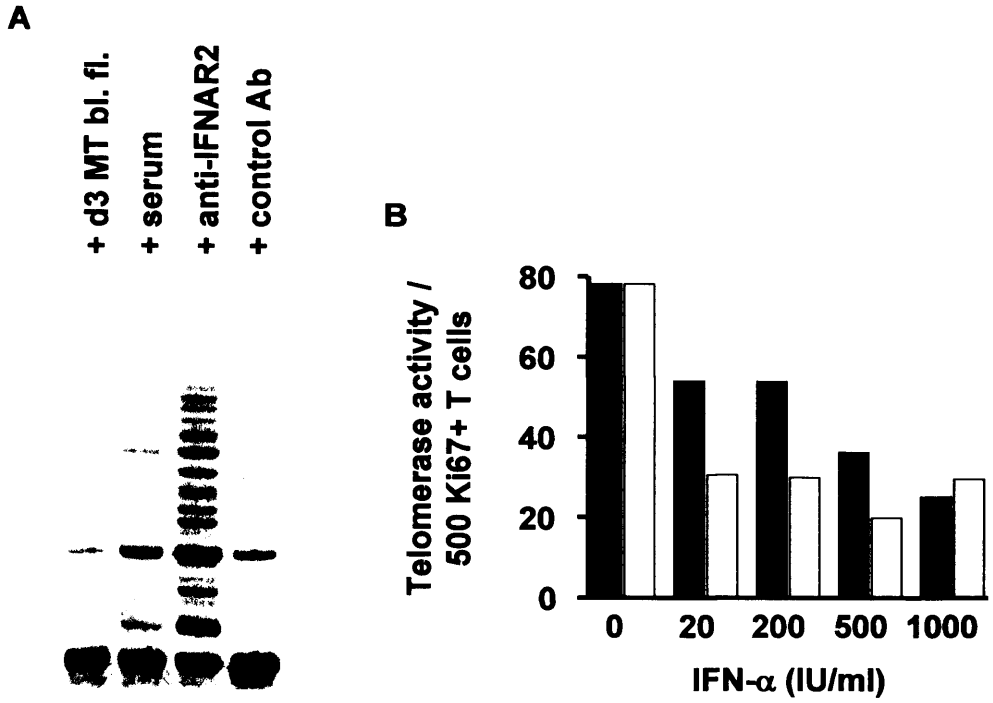

Figure 6.6 The effect of type 1 interferons on the induction of telomerase activity in peripheral blood T cells

(A) Type 1 IFN in day 3 MT blister fluid mediates the suppression of telomerase activity in T cells. PBMC were stimulated with PPD (0.5μg/ml) *in vitro* in the presence of autologous day 3 blister fluid (50% final dilution) (+ d3 MT bl. fl.) or autologous serum (25% final dilution) (+ serum). Type 1 interferon receptor blocking antibody (CD118; + anti-IFNAR2) or isotype control antibody (+ control Ab) were added to parallel cultures stimulated in the presence of day 3 MT blister fluid. Samples were collected 3 days after stimulation. Telomerase activity was measured using the TRAP assay and autoradiography. Samples were adjusted to 500 proliferating $Ki67^+$ T cells per lane. One representative experiment out of 3 is shown. (B) IFN-α directly inhibits the induction of telomerase activity in PPD $CD4^+$ T cells. A PPD-specific $CD4^+$ T cell line was re-stimulated with PPD (0.5μg/ml) in the presence of different concentrations of recombinant IFN-α (IFN-α-2a, R&D systems) (■) and Roferon (IFN-α-2a, Roche Pharmaceuticals) (□) for 4 days. Telomerase activity was measured using the TRAP assay and autoradiography. Samples were adjusted to 500 proliferating $Ki67^+$ T cells per lane. One representative experiment out of 3 performed is shown.

6.7 The effect of repeated re-stimulation *in vitro* on telomerase induction in PPD-specific $CD4^+$ T cells

In section 5.5.1, we demonstrated that despite significant telomere shortening PPD-specific $CD4^+$ T cells isolated from day 19 MT blisters could expand *in vitro* in response to repeated restimulation with PPD. These cells, however, eventually underwent replicative senescence after approximately 100 days of *in vitro* cell culture or 13 population doublings (Figure 6.7a). Previous studies have shown that the ability to induce telomerase activity protects T cells from replicative senescence[251-253]. We, therefore, finally examined whether the ability of these cells to up-regulate telomerase activity correlated with their capacity to expand upon restimulation *in vitro*. The capacity of cells to expand in culture was indeed associated with a preserved ability to up-regulate telomerase activity (Stim. 4; Figure 6.7b). In contrast, the onset of replicative senescence, after which no further expansion occurred, was associated with the loss of telomerase inducibility (Stim. 8,9; Figure 6.7b). This implies that loss of telomerase inducibility is linked with the induction of replicative senescence in T cells. In addition, this suggests that there are two independent mechanisms regulating telomerase activity in T cells. The first is an extrinsic reversible mechanism mediated by type 1 IFNs and in particular IFN-α; the second represents an intrinsic irreversible pathway of telomerase down-regulation that may be related to end-stage differentiation.

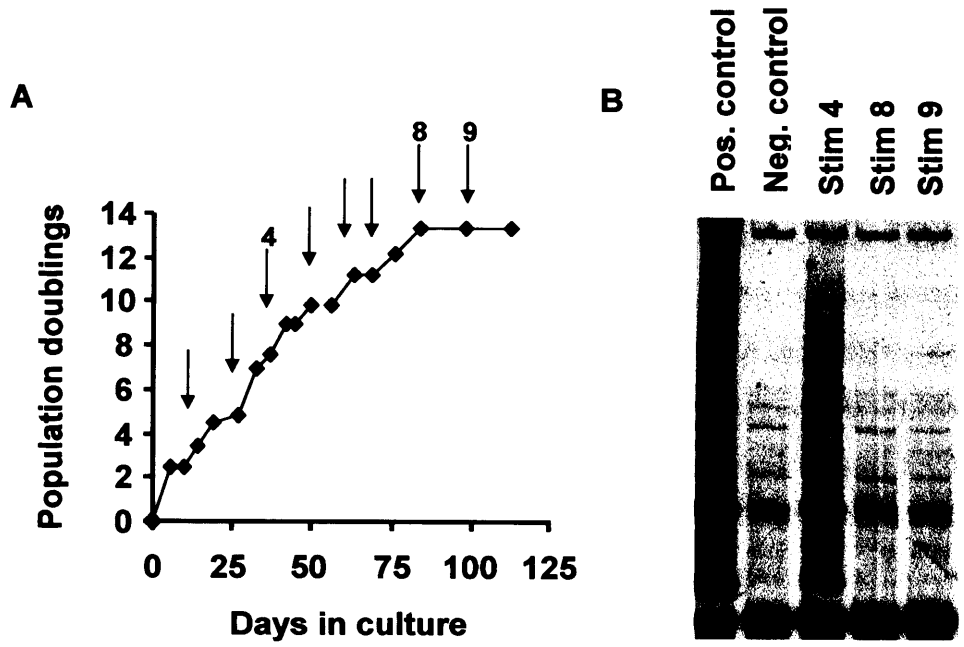

Figure 6.7 The effect of repeated restimulation *in vitro* on telomerase induction in PPD-specific CD4$^+$ T cells

(A) Cells recovered from a day 19 MT blister were repetitively stimulated *in vitro* with PPD and irradiated autologous PBMCs as APCs. Arrows indicate each point of re-stimulation. The figures indicate the simulation number and points when samples were collected to measure telomerase activity. (B) Each sample was re-stimulated with PPD (0.5 μg/ml) *in vitro* for 4 days. Telomerase activity per 500 Ki67$^+$ T cells was then determined as before. Stim 4, Stim 8 and Stim 9 indicate the 4th, 8th and 9th stimulations.

6.8 Discussion

In this chapter, we have demonstrated a number of novel findings. Firstly, we have shown that the accelerated erosion of telomeres in antigen-specific CD4$^+$ T cells in the skin during the MT occurs as a consequence of the reversible inhibition of telomerase activity in cycling T cells *in vivo*. Secondly, this inhibition appears to result from the exposure of cells to type 1 IFNs present in the skin during the MT. This mechanism of telomerase regulation differs from the inherent irreversible loss of telomerase induction that occurs as T cells reach replicative senescence and become terminally differentiated.

Previous studies examining telomerase activity in T cells have been based on the assay of a pre-determined number of cells, which took no account of the number of cells that were activated or cycling. This approach, in the dynamic setting of an immune response like the MT, would make interpretation of the data difficult. This is because the number of proliferating cells varies according to the phase of the immune response and telomerase activity is essentially only present in activated, cycling T cells[207-210;213-215]. Therefore, in a novel adaptation to the TRAP assay, we standardised the assay of each sample to a pre-determined number of proliferating $Ki67^+$ T cells. This modification, for the first time, controls for the number of activated cycling cells, and therefore provides a more accurate picture of cellular telomerase activity. It also allowed a direct comparison of the activity of this enzyme in cycling T cells from both the blood and skin at different times after stimulation.

Using this approach, we were able to demonstrate that the accelerated erosion of telomeres in antigen-specific T cells in the skin during the MT was due to low telomerase activity in cycling T cells. The induction of telomerase activity was reversibly inhibited by type 1 IFNs present in the skin. Immunohistological analysis of skin sections showed that IFN-α was a constituent of the peak of type 1 IFN, which was detected in blister fluid on day 3 after PPD challenge. This suggests that the regulatory role of IFN-α on telomerase activity that has been described *in vitro*[261] also applies to the *in vivo* setting. We were, however, unable to completely inhibit telomerase activity in T cells that were stimulated with PPD in the presence of increasing concentrations of IFN-α *in vitro* (Figure 6.6b). This suggests that other factors may be involved in regulating telomerase activity. Indeed, it remains possible that other members of the type 1 IFN family may contribute to the inhibition of telomerase in T cells in the skin, since all type 1 IFNs signal through the same receptor[270]. We have previously shown the presence IFN-β expressing cells in the skin on day 3 of the MT[26], and interestingly the number of IFN-β expressing cells actually increases during the course of the response[26]. Provisional data

suggests that IFN-β can also inhibit telomerase activity in PPD stimulated T cells *in vitro*[468].

The role of other potential inhibitory factors has yet to be determined. IFN-γ, IL-4 and TGF-β can inhibit telomerase in human tumour cell lines[216;263-266]. The expression of all three cytokines has been detected in MT skin sections[25] and IFN-γ was also detected in blister fluid at days 3 and 5 after challenge with PPD (Figure 6.5). Their effect on telomerase in normal T cells, however, is unknown and will require further investigation. Interestingly, IL-6 and IL-7 can up-regulate telomerase activity in tumour cells[490] and human T cells[260] respectively. Both are present in the skin during the MT (figure 5.11 and references [25;491]) and may partially counteract the inhibitory effects of the type 1 interferons, which may explain why telomerase activity was not completely inhibited *in vivo*. Interestingly, ceramide, a sphingolipid naturally present in the skin, has also been shown to inhibit telomerase activity in a human tumour cell line[492;493], but its effect on T cells is unknown and requires investigation. Overall, this suggests that the inflammatory microenvironment of a tissue may have a profound impact on the replicative lifespan of antigen-specific T cells.

In addition to the extrinsic cytokine mediated regulation of telomerase, we also demonstrated the intrinsic down-regulation of enzymatic activity in T cells that have been repeatedly activated. The regulation of telomerase activity by this second pathway is irreversible and may be related to end-stage differentiation[171;255], although senescence in T cells can be bypassed by telomerase transfection[251-253]. The signalling pathways that lead to telomerase down-regulation after repeated stimulation or after addition of type 1 IFN are poorly defined, but may involve inhibition of CD28 expression[256], transcriptional regulation, enzyme translocation from nucleus to the cytoplasm[247] as well as chromatin remodelling of the telomerase gene[239]. These pathways require further investigation as they

may provide targets for manipulating the retention or loss of specific T cells *in vivo*.

Previous *in vivo* studies in mice and humans have shown that telomere length is maintained during acute primary[240-244] and secondary immune responses[244] and this was linked to the induction of telomerase activity in antigen-specific T cells. These studies, however, as previously mentioned in chapter 4, were performed on cells isolated from blood and/or lymphoid tissues. This suggests that the regulation of telomere length and telomerase in T cells resident in the non-lymphoid environment of the skin may be distinct to that in lymphoid tissue. The reasons for this differential regulation are unclear, but it may act as an immunoregulatory or anti-cancer mechanism to limit the extent of expansion in the skin. In young healthy volunteers and limiting doses of antigen, as is the case in the MT, it appears that this potential regulatory mechanism does not constrain the cells functionally, at least in terms of residual proliferative capacity *in vitro*. However, one would predict that the cells would reach replicative senescence rapidly, if they continued to proliferate in the skin *in vivo* in the absence of significant telomerase activity. The relative maintenance of telomere length in lymphoid T cells during acute immune responses[240-244] may, therefore, act to ensure a 'central' population of memory cells with relatively preserved function that maximises long-term responsiveness. With increasing age, however, the combined effects of progressive telomere shortening[193;235;238], declining telomerase inducibility[257;258] and telomerase inhibition in T cells in the skin may have profound implications for cutaneous immune responsiveness in the elderly. This may partly explain why cutaneous T cell mediated immune responses *in vivo* supposedly decline with age[231-233].

In summary, we have demonstrated that the accelerated erosion of telomeres in cycling antigen-specific $CD4^+$ T cells in the skin during the MT occurs subsequent to the reversible inhibition of telomerase activity mediated by type 1 IFNs *in vivo*. In view of the ethical and practical

constraints that apply to the study of human immunity, it is likely that the investigation of antigen-specific T cells in telomerase deficient mice[217-219] and animals with short telomeres equivalent to those in humans[171] will be required to assess directly whether telomerase is differentially regulated in lymphoid and non-lymphoid tissues. Furthermore, these studies will help to determine whether telomere erosion limits uncontrolled T cell proliferation during secondary responses *in vivo.* Further human *in vivo* studies will also be required to determine the effect of aging and whether telomerase activity is similarly inhibited in T cells infiltrating into different cutaneous immune responses and inflammatory dermatoses.

7 Summary and future directions

In this thesis, we hypothesized that antigen-specific T cells differentiate in the skin as a consequence of localised proliferation at the site of secondary immune challenge in humans. Using the Mantoux Test (MT), which represents a secondary immune response, we have been able to determine the degree of cellular differentiation in the skin and its consequences during an episode of cutaneous inflammation. We have made several novel and unexpected observations. The first was that the kinetics of the clinical response and antigen-specific T cell infiltration are asynchronous. The marked antigen-specific $CD4^+$ T cell expansion with preserved clonality that was observed in the skin during the MT lagged the peak of the clinical response by 4 days. Secondly, in contrast to mouse studies[8-12], this expansion was mediated in part by the extensive proliferation of $CD4^+$ T cells within the skin. Thirdly, this was associated with substantial telomeric shortening in the antigen-specific $CD4^+$ T cells in the skin, indicating accelerated cellular differentiation. This contrasts with previous studies where telomere length was maintained during acute immune responses following the induction of telomerase in murine and human lymphocytes isolated from lymphoid tissues or the blood[240-244]. Last, telomere erosion in skin $CD4^+$ T cells appeared to be mediated by the reversible inhibition of telomerase by type 1 interferons *in vivo*. This reversible inhibition was distinct from the irreversible down-regulation of telomerase that was observed when MT skin T cells were repeatedly activated *in vitro* culminating in cell senescence.

To perform these studies, we adapted the skin suction blister technique to isolate leucocytes from the site of the Mantoux test. In a novel development, we studied the response for up to 19 days after secondary challenge with intradermal PPD. Previous studies examining the Mantoux test have only followed the immune response for up to 4 days[20-24], and in

doing so have overlooked the fact that significant cutaneous T cell reactivity occurs between days 7 and 19. We are confident that SB technique actually samples the underlying responding inflammatory infiltrate and not just those cells that are migrating away for the following reasons. First, the kinetics of $CD4^+$ T cell infiltration and phenotype of $CD4^+$ T cells in tissue sections ($CD45RO^+CD45RA^-$) closely matched those isolated from blisters. Second, the proportions of $CD4^+$ T cells that were proliferating and the kinetics of proliferation were virtually identical when these cells were analysed by flow cytometry on blister samples and histology on tissue sections, indicating that we were investigating the same responding population. In addition, numerous T cell phenotypic changes were observed in suction blisters during the course of the MT, which were not detected in the blood. Our findings, therefore, support the assertion of others that the composition of cells contained in SBs is representative of the underlying cutaneous inflammatory infiltrate[442]

The expansion of PPD-specific $CD4^+$ T cells during the MT was largely due to the *in situ* proliferation of T cell clones that were present in the skin early on in the response. This intense proliferation was balanced by an increase in T cell apoptosis indicating that there was extensive T cell turnover during the response. Previous studies in mice have shown that antigen-specific T cell proliferation occurs predominantly in lymphoid tissue and is minimal in the non-lymphoid tissue[8-12]. These conflicting results may be due to interspecies differences, but may also reflect the non-lymphoid tissue being studied. All but one of the reports in mice concerned immune responses in the lung[9-12] and it has been suggested that the pulmonary microenvironment may actively suppress T cell division[10]. Only one report was related to the skin and this described a primary response[8]. Further studies in humans and mice will be required to determine to what extent antigen-specific T cells expansion can occur in different non-lymphoid tissues following secondary immune challenge.

Extensive proliferation *in situ* coupled with inhibition of telomerase induction by type 1 IFNs resulted in significant telomere shortening in PPD-specific $CD4^+$ T cells during the MT. It is unclear whether this outcome is specific to the non-lymphoid microenvironment of the skin or nature of the immune response. Diffuse expression of IFN-α was identified amongst keratinocytes, which are known to be capable of type 1 IFN production[494], but more pronounced expression was present on focal cells in the perivascular infiltrates. The identity of these IFN-α producing cells needs to be determined, but they are most likely to be $BDCA\text{-}2^+$ plasmacytoid dendritic cells. These cells are absent in normal skin, but are present in other acute immune responses such as allergic contact dermatitis[274;276]. This raises the question as to whether a similar pattern of proliferation and telomere erosion is present in other cutaneous immune responses. This could be explored by examining different responses such as allergic contact dermatitis to nickel, the atopic patch test to house dust mite and reactions to other intradermal antigens e.g. *Candida albicans*, tetanus toxoid and *Trichophyton* species.

Ethical and practical constraints in humans make the investigation of recall immune responses in other non-lymphoid tissues difficult. The usefulness of mice in addressing this question, however, may be limited if T cell expansion is predominantly restricted to lymphoid tissue in memory immune responses as has been suggested from studies of pulmonary immune responses[10-12]. It might be possible to approach this question in humans by comparing telomere length in antigen-specific T cells in the blood and non-lymphoid tissues in a number of relatively common inflammatory diseases e.g. coeliac disease or *Helicobacter pylori* infection in the intestine and *Mycobacteria tuberculosis* infection in the lung. The impact of longer-term inflammation in these models, however, would have to be considered.

It is of considerable interest that the extent of telomeric DNA lost during the MT equates to an average of eight years of normal immune aging in the space of 3 weeks. If memory cells do reside appreciably in non-lymphoid tissues as has been shown in mice[101;102], then one would predict that this degree of telomere shortening might limit the proliferative capacity and responsiveness of memory T cells to further stimulation. We found, however, that the cells were capable of extensive further proliferation albeit *in vitro* where telomerase was normally induced. *In vivo*, at this rate of telomere erosion, it would be expected that in the context of repeated or chronic stimulation in the skin that these cells would rapidly reach senescence and growth arrest. The consequences of this degree of telomere shortening *in vivo*, however, remain unclear. The impact of replicative senescence during an acute immune response could be determined by studying the expression of markers associated with senescence such as β-galactosidase[163] and killer cell lectin-like receptor G1(KLRG1)[495]. In addition, the investigation of antigen-specific T cells in draining and non-draining lymph nodes of telomerase deficient mice[219] and animals with telomeres of equivalent length to those in humans will be required to assess directly whether telomere erosion limits uncontrolled T cell proliferation during secondary responses *in vivo.*

The impact of replicative senescence on immune responsiveness in young healthy individuals, as were used in this study, is probably negligible. It is more likely that it acts as a buffer or constraint in the skin to prevent over-expansion either in an anti-cancer or anti-inflammatory capacity to complement apoptosis in mediating resolution. Aging may be the critical factor that results in cutaneous T cell telomere shortening impacting on responsiveness[496]. It is known that all subsets of $CD4^+$ and $CD8^+$ T cells in elderly individuals have significantly shorter telomeres than young individuals[193;235;238]. Furthermore, the cells of elderly individuals have diminished replicative potential *in vitro* associated with a reduced capacity to induce telomerase[257;258]. Memory cells infiltrating into the skin in the elderly are, therefore, already compromised in terms of proliferative

capacity and this may translate into impaired responsiveness. Indeed, a number of observations point towards declining cutaneous responsiveness with increasing age. First, it is recognised that DTH responses *in vivo* diminish as we grow older[231-233]. Second, the elderly are more prone to reactivation of latent infections such as varicella zoster virus (VZV), which manifests itself on the skin as shingles. This is associated with a decline in VZV-specific T cell responses *in vitro*[497]. Third, skin cancers are not only more common in older individuals but also in the immunosuppressed[357], which suggests that responsive cell mediated immunity is necessary to prevent the emergence of tumours. The diminished responsiveness that is observed in the skin of the elderly may, therefore, be in part accounted for by the more limited replicative potential of T cells. The decline in replicative potential as we age may in turn also result in an increasingly restricted T cell repertoire, which develops as a consequence of persistent viral infections such as cytomegalovirus (CMV), further limiting T cell memory[496]. Further studies, using the MT model in the elderly, are on-going and will help determine the effect of aging on clinical responsiveness, as well as proliferation, clonality, telomere erosion and telomerase inducibility during an acute immune response in the skin.

The reversible inhibition of telomerase observed in skin T cells indicates that telomerase should be normally up-regulated in cells that emigrate from the inhibitory microenvironment of the skin. Memory T cells that emigrate from the skin would, therefore, be expected to maintain their residual proliferative capacity, in the same way that cells isolated from the blood and lymphoid tissue have been reported as doing during acute immune responses[240-244]. This suggests that memory cells may be differentially regulated in lymphoid and non-lymphoid tissues. This functional division bears a resemblance to the effector and central memory T cell model proposed by Sallusto *et al*, which is based on the differential expression of CCR7 on $CD45RA^-$ memory T cells[89]. It is of note that cutaneous $CD4^+$ T cells found 3 weeks after PPD stimulation in the skin were virtually all $CD45RA^-CCR7^-$, which is consistent with the previously

defined 'effector memory' phenotype. The extent to which memory T cells emigrate from a non-lymphoid tissue during an immune response and the mechanisms by which they do this, however, remain unknown. This could be addressed in humans by using the MT model in combination with lymphatic dissection and drainage[365].

Further work will also be required to determine whether the pattern of telomere and telomerase regulation in the MT is also observed in chronic inflammatory dermatoses. Interestingly, peripheral blood T cells isolated from patients with atopic eczema, psoriasis and mycosis fungoides demonstrate increased telomerase activity and shorter telomeres compared to healthy volunteers[249;250]. TER, however, was not detected in lymphocytes migrating into the lesional skin of individuals with psoriasis or allergic contact dermatitis[248]. Indeed, sizeable numbers of plasmacytoid dendritic cells have been identified in the skin of individuals with allergic contact dermatitis and psoriasis as well as those with lupus erythematosus[274;277]. It is interesting to speculate what effect the relative absence of these cells in lesional atopic eczema skin might have on telomerase activity in infiltrating T cells and its relationship to the persistent inflammation that characterises the condition[274]. Other inflammatory dermatoses exhibit increased cutaneous expression of IL-7[498;499], which is known to induce telomerase activity[260]. This may represent another possible mechanism, by which the normal constraint on T cell expansion in the skin is circumvented resulting in persistent inflammation. Atopic eczema is also characterised by eventual remission in most patients by their teens. An intriguing possible explanation for this is that chronically stimulated allergen-specific and other reactive T cells are lost as a result of critical telomere erosion and the induction of replicative senescence.

The inhibition of telomerase by plasmacytoid dendritic cell derived IFN-α may also play a therapeutic role in treating skin neoplasms such as basal

cell carcinoma, Bowen's disease and lentigo maligna. Imiquimod is a topical TLR-7 agonist, which is being increasingly used to treat these conditions. The exact mechanism of action is unknown, but Imiquimod is recognised to induce a pro-inflammatory cytokine environment in the skin comprising IFN-α secreted by plasmacytoid dendritic cells[500]. It, therefore, remains possible that IFN-α inhibits telomerase in neoplastic cells, thereby precipitating growth arrest and apoptosis.

Clearly further research is required to clarify the roles that telomeres and telomerase play in decreased immune responsiveness in the elderly. Indeed, increasing human life expectancy and the increased susceptibility of elderly individuals to infection suggests that this should become a priority[496]. Investigation should be aimed at further defining the signalling pathways that regulate telomerase since these may provide targets for manipulating the retention or clearance of specific T cells *in vivo*. Telomerase transfection has already been shown to extend the lifespan of T cells *in vitro*[251-253]. A possible consequence of this, however, is that there may be an increased risk of malignancy. In view of the marked difference in lifespan and telomere lengths of mice and humans, it is essential that further studies are carried out in humans as well as animals that have similar telomere lengths to humans.

In summary, we have demonstrated that antigen-specific $CD4^+$ T cells can proliferate and differentiate extensively outside of lymphoid tissue during a secondary response in humans *in vivo*. This indicates that it is essential to investigate an immune response within the context of the tissue where it is taking place. Our studies also highlight the continued need, where ethically possible, to undertake immunological research in humans to give relevance to animal studies as well as providing an opportunity to make novel observations.

8 References

1. Barton GM, Medzhitov R. Control of adaptive immune responses by Toll-like receptors. *Curr Opin Immunol* 2002; **14**: 380-3.

2. Janeway CA, Jr., Medzhitov R. Innate immune recognition. *Annu Rev Immunol* 2002; **20**: 197-216.

3. Sprent J, Tough DF. T cell death and memory. *Science* 2001; **293**: 245-8.

4. Ahmed R, Gray D. Immunological memory and protective immunity: understanding their relation. *Science* 1996; **272**: 54-60.

5. Dutton RW, Bradley LM, Swain SL. T cell memory. *Annu Rev Immunol* 1998; **16**: 201-23.

6. Sprent J, Surh CD. T cell memory. *Annu Rev Immunol* 2002; **20**: 551-79.

7. Akbar AN, Terry L, Timms A *et al.* Loss of CD45R and gain of UCHL1 reactivity is a feature of primed T cells. *J Immunol* 1988; **140**: 2171-8.

8. Reinhardt RL, Bullard DC, Weaver CT *et al.* Preferential accumulation of antigen-specific effector CD4 T cells at an antigen injection site involves CD62E-dependent migration but not local proliferation. *J Exp Med* 2003; **197**: 751-62.

9. Roman E, Miller E, Harmsen A *et al.* CD4 effector T cell subsets in the response to influenza: heterogeneity, migration, and function. *J Exp Med* 2002; **196**: 957-68.

10. Harris NL, Watt V, Ronchese F *et al.* Differential T cell function and fate in lymph node and nonlymphoid tissues. *J Exp Med* 2002; **195**: 317-26.

11. Ostler T, Hussell T, Surh CD *et al.* Long-term persistence and reactivation of T cell memory in the lung of mice infected with respiratory syncytial virus. *Eur J Immunol* 2001; **31**: 2574-82.

12. Ely KH, Cauley LS, Roberts AD *et al.* Nonspecific recruitment of memory $CD8^+$ T cells to the lung airways during respiratory virus infections. *J Immunol* 2003; **170**: 1423-9.

13. Wright WE, Shay JW. Telomere dynamics in cancer progression and prevention: fundamental differences in human and mouse telomere biology. *Nat Med* 2000; **6**: 849-51.

14. Gordon CJ, Grafton G, Wood PM *et al.* Modelling the human immune response: can mice be trusted? Commentary. *Curr Opin Pharmacol* 2001; **1**: 431-5.

15. Akbar AN, Soares MV, Plunkett FJ *et al.* Differential regulation of $CD8^+$ T cell senescence in mice and men. *Mech Ageing Dev* 2000; **121**: 69-76.

16. Sartor RB. Review article: How relevant to human inflammatory bowel disease are current animal models of intestinal inflammation? *Aliment Pharmacol Ther* 1997; **11** (Suppl 3): 89-96.

17. Birmingham DJ, Rovin BH, Yu CY *et al.* Of mice and men: the relevance of the mouse to the study of human SLE. *Immunol Res* 2001; **24**: 211-24.

18. Mestas J, Hughes CW. Of mice and not men: differences between mouse and human immunology. *J Immunol* 2004; **172**: 2731-8.

19. Bell J. A call for papers on humans subjects. *J Exp Med* 2003; **198**: 1621.

20. Picker LJ, Treer JR, Ferguson-Darnell B *et al.* Control of lymphocyte recirculation in man. II. Differential regulation of the cutaneous lymphocyte-associated antigen, a tissue-selective homing receptor for skin-homing T cells. *J Immunol* 1993; **150**: 1122-36.

21. Picker LJ, Martin RJ, Trumble A *et al.* Differential expression of lymphocyte homing receptors by human memory/effector T cells in pulmonary versus cutaneous immune effector sites. *Eur J Immunol* 1994; **24**: 1269-77.

22. Kenney RT, Rangdaeng S, Scollard DM. Skin blister immunocytology. A new method to quantify cellular kinetics in vivo. *J Immunol Methods* 1987; **97**: 101-10.

23. Pitzalis C, Cauli A, Pipitone N *et al.* Cutaneous lymphocyte antigen-positive T lymphocytes preferentially migrate to the skin but not to the joint in psoriatic arthritis. *Arthritis Rheum* 1996; **39**: 137-45.

24. Pitzalis C, Kingsley GH, Covelli M *et al.* Selective migration of the human helper-inducer memory T cell subset: confirmation by in vivo cellular kinetic studies. *Eur J Immunol* 1991; **21**: 369-76.

25. Orteu CH, Poulter LW, Rustin MH *et al.* The role of apoptosis in the resolution of T cell-mediated cutaneous inflammation. *J Immunol* 1998; **161**: 1619-29.

26. Orteu CH, Rustin MH, O'Toole E *et al.* The inhibition of cutaneous T cell apoptosis may prevent resolution of inflammation in atopic eczema. *Clin Exp Immunol* 2000; **122**: 150-6.

27. Butcher EC, Picker LJ. Lymphocyte homing and homeostasis. *Science* 1996; **272**: 60-6.

28. Mackay CR, Marston WL, Dudler L. Naive and memory T cells show distinct pathways of lymphocyte recirculation. *J Exp Med* 1990; **171**: 801-17.

29. Itano AA, Jenkins MK. Antigen presentation to naive CD4 T cells in the lymph node. *Nat Immunol* 2003; **4**: 733-9.

30. Banchereau J, Steinman RM. Dendritic cells and the control of immunity. *Nature* 1998; **392**: 245-52.

31. Watts TH, DeBenedette MA. T cell co-stimulatory molecules other than CD28. *Curr Opin Immunol* 1999; **11**: 286-93.

32. Croft M. Co-stimulatory members of the TNFR family: keys to effective T-cell immunity? *Nat Rev Immunol* 2003; **3**: 609-20.

33. Kaech SM, Wherry EJ, Ahmed R. Effector and memory T-cell differentiation: implications for vaccine development. *Nat Rev Immunol* 2002; **2**: 251-62.

34. Yashiro Y, Tai XG, Toyo-oka K *et al.* A fundamental difference in the capacity to induce proliferation of naive T cells between CD28 and other co-stimulatory molecules. *Eur J Immunol* 1998; **28**: 926-35.

35. Kaech SM, Ahmed R. Memory $CD8^+$ T cell differentiation: initial antigen encounter triggers a developmental program in naive cells. *Nat Immunol* 2001; **2**: 415-22.

36. Wong P, Pamer EG. Cutting edge: antigen-independent CD8 T cell proliferation. *J Immunol* 2001; **166**: 5864-8.

37. Lee WT, Pasos G, Cecchini L *et al.* Continued antigen stimulation is not required during $CD4^+$ T cell clonal expansion. *J Immunol* 2002; **168**: 1682-9.

38. Jelley-Gibbs DM, Lepak NM, Yen M *et al.* Two distinct stages in the transition from naive CD4 T cells to effectors, early antigen-dependent and late cytokine-driven expansion and differentiation. *J Immunol* 2000; **165**: 5017-26.

39. Schiemann M, Busch V, Linkemann K *et al.* Differences in maintenance of $CD8^+$ and $CD4^+$ bacteria-specific effector-memory T cell populations. *Eur J Immunol* 2003; **33**: 2875-85.

40. Macallan DC, Wallace DL, Irvine AJ *et al.* Rapid turnover of T cells in acute infectious mononucleosis. *Eur J Immunol* 2003; **33**: 2655-65.

41. Foulds KE, Zenewicz LA, Shedlock DJ *et al.* Cutting edge: CD4 and CD8 T cells are intrinsically different in their proliferative responses. *J Immunol* 2002; **168**: 1528-32.

42. Maini MK, Gudgeon N, Wedderburn LR *et al.* Clonal expansions in acute EBV infection are detectable in the CD8 and not the CD4 subset and persist with a variable CD45 phenotype. *J Immunol* 2000; **165**: 5729-37.

43. Homann D, Teyton L, Oldstone MB. Differential regulation of antiviral T-cell immunity results in stable $CD8^+$ but declining $CD4^+$ T-cell memory. *Nat Med* 2001; **7**: 913-9.

44. Ogg GS. Detection of antigen-specific cytotoxic T lymphocytes: significance for investigative dermatology. *Clin Exp Dermatol* 2000; **25**: 312-6.

45. Tan LC, Gudgeon N, Annels NE *et al.* A re-evaluation of the frequency of $CD8^+$ T cells specific for EBV in healthy virus carriers. *J Immunol* 1999; **162**: 1827-35.

46. Callan MF, Tan L, Annels N *et al.* Direct visualization of antigen-specific $CD8^+$ T cells during the primary immune response to Epstein-Barr virus In vivo. *J Exp Med* 1998; **187**: 1395-402.

47. Murali-Krishna K, Altman JD, Suresh M *et al.* Counting antigen-specific CD8 T cells: a reevaluation of bystander activation during viral infection. *Immunity* 1998; **8**: 177-87.

48. Bird JJ, Brown DR, Mullen AC *et al.* Helper T cell differentiation is controlled by the cell cycle. *Immunity* 1998; **9**: 229-37.

49. Richter A, Lohning M, Radbruch A. Instruction for cytokine expression in T helper lymphocytes in relation to proliferation and cell cycle progression. *J Exp Med* 1999; **190**: 1439-50.

50. Bajenoff M, Wurtz O, Guerder S. Repeated antigen exposure is necessary for the differentiation, but not the initial proliferation, of naive $CD4^+$ T cells. *J Immunol* 2002; **168**: 1723-9.

51. Agarwal S, Rao A. Modulation of chromatin structure regulates cytokine gene expression during T cell differentiation. *Immunity* 1998; **9**: 765-75.

52. Ansel KM, Lee DU, Rao A. An epigenetic view of helper T cell differentiation. *Nat Immunol* 2003; **4**: 616-23.

53. Avni O, Lee D, Macian F *et al.* T_H cell differentiation is accompanied by dynamic changes in histone acetylation of cytokine genes. *Nat Immunol* 2002; **3**: 643-51.

54. Seder RA, Ahmed R. Similarities and differences in $CD4^+$ and $CD8^+$ effector and memory T cell generation. *Nat Immunol* 2003; **4**: 835-42.

55. Kim CH, Campbell DJ, Butcher EC. Nonpolarized memory T cells. *Trends Immunol* 2001; **22**: 527-30.

56. Wang X, Mosmann T. In vivo priming of CD4 T cells that produce interleukin (IL)-2 but not IL-4 or interferon (IFN)-gamma, and can subsequently differentiate into IL-4- or IFN-gamma-secreting cells. *J Exp Med* 2001; **194**: 1069-80.

57. Iezzi G, Scheidegger D, Lanzavecchia A. Migration and function of antigen-primed nonpolarized T lymphocytes in vivo. *J Exp Med* 2001; **193**: 987-93.

58. Lund FE, Partida-Sanchez S, Lee BO *et al.* Lymphotoxin-alpha-deficient mice make delayed, but effective, T and B cell responses to influenza. *J Immunol* 2002; **169**: 5236-43.

59. Salomon B, Bluestone JA. Complexities of CD28/B7: CTLA-4 costimulatory pathways in autoimmunity and transplantation. *Annu Rev Immunol* 2001; **19**: 225-52.

60. Tivol EA, Borriello F, Schweitzer AN *et al.* Loss of CTLA-4 leads to massive lymphoproliferation and fatal multiorgan tissue destruction, revealing a critical negative regulatory role of CTLA-4. *Immunity* 1995; **3**: 541-7.

61. Waterhouse P, Penninger JM, Timms E *et al.* Lymphoproliferative disorders with early lethality in mice deficient in CTLA-4. *Science* 1995; **270**: 985-8.

62. Soares MV, Maini MK, Beverley PC *et al.* Regulation of apoptosis and replicative senescence in $CD8^+$ T cells from patients with viral infections. *Biochem Soc Trans* 2000; **28**: 255-8.

63. Akbar AN, Salmon M. Cellular environments and apoptosis: tissue microenvironments control activated T-cell death. *Immunol Today* 1997; **18**: 72-6.

64. Hildeman DA, Zhu Y, Mitchell TC *et al.* Molecular mechanisms of activated T cell death in vivo. *Curr Opin Immunol* 2002; **14**: 354-9.

65. Marsden VS, Strasser A. Control of apoptosis in the immune system: Bcl-2, BH3-only proteins and more. *Annu Rev Immunol* 2003; **21**: 71-105.

66. Jaattela M, Tschopp J. Caspase-independent cell death in T lymphocytes. *Nat Immunol* 2003; **4**: 416-23.

67. Ju ST, Panka DJ, Cui H *et al.* Fas(CD95)/FasL interactions required for programmed cell death after T-cell activation. *Nature* 1995; **373**: 444-8.

68. Refaeli Y, Van Parijs L, London CA *et al.* Biochemical mechanisms of IL-2-regulated Fas-mediated T cell apoptosis. *Immunity* 1998; **8**: 615-23.

69. Irmler M, Thome M, Hahne M *et al.* Inhibition of death receptor signals by cellular FLIP. *Nature* 1997; **388**: 190-5.

70. Refaeli Y, Van Parijs L, Alexander SI *et al.* Interferon gamma is required for activation-induced death of T lymphocytes. *J Exp Med* 2002; **196**: 999-1005.

71. Dalton DK, Haynes L, Chu CQ *et al.* Interferon gamma eliminates responding CD4 T cells during mycobacterial infection by inducing apoptosis of activated CD4 T cells. *J Exp Med* 2000; **192**: 117-22.

72. Akbar AN, Borthwick N, Salmon M *et al.* The significance of low bcl-2 expression by CD45RO T cells in normal individuals and patients with acute viral infections. The role of apoptosis in T cell memory. *J Exp Med* 1993; **178**: 427-38.

73. Salmon M, Pilling D, Borthwick NJ *et al.* The progressive differentiation of primed T cells is associated with an increasing susceptibility to apoptosis. *Eur J Immunol* 1994; **24**: 892-9.

74. Hildeman DA, Mitchell T, Kappler J *et al.* T cell apoptosis and reactive oxygen species. *J Clin Invest* 2003; **111**: 575-81.

75. Akbar AN, Borthwick NJ, Wickremasinghe RG *et al.* Interleukin-2 receptor common gamma-chain signaling cytokines regulate activated T cell apoptosis in response to growth factor withdrawal: selective induction of anti-apoptotic (bcl-2, bcl-xL) but not pro-apoptotic (bax, bcl-xS) gene expression. *Eur J Immunol* 1996; **26**: 294-9.

76. Vella AT, Dow S, Potter TA *et al.* Cytokine-induced survival of activated T cells in vitro and in vivo. *Proc Natl Acad Sci U.S.A* 1998; **95**: 3810-5.

77. Schluns KS, Lefrancois L. Cytokine control of memory T-cell development and survival. *Nat Rev Immunol* 2003; **3**: 269-79.

78. Pilling D, Akbar AN, Girdlestone J *et al.* Interferon-β mediates stromal cell rescue of T cells from apoptosis. *Eur J Immunol* 1999; **29**: 1041-50.

79. Marrack P, Kappler J, Mitchell T. Type I interferons keep activated T cells alive. *J Exp Med* 1999; **189**: 521-30.

80. Akbar AN, Lord JM, Salmon M. IFN-alpha and IFN-beta: a link between immune memory and chronic inflammation. *Immunol Today* 2000; **21**: 337-42.

81. Salmon M, Scheel-Toellner D, Huissoon AP *et al.* Inhibition of T cell apoptosis in the rheumatoid synovium. *J Clin Invest* 1997; **99**: 439-46.

82. Hou S, Hyland L, Ryan KW *et al.* Virus-specific $CD8^+$ T-cell memory determined by clonal burst size. *Nature* 1994; **369**: 652-4.

83. Hu H, Huston G, Duso D *et al.* $CD4^+$ T cell effectors can become memory cells with high efficiency and without further division. *Nat Immunol* 2001; **2**: 705-10.

84. Kaech SM, Hemby S, Kersh E *et al.* Molecular and functional profiling of memory CD8 T cell differentiation. *Cell* 2002; **111**: 837-51.

85. Wherry EJ, Teichgraber V, Becker TC *et al.* Lineage relationship and protective immunity of memory CD8 T cell subsets. *Nat Immunol* 2003; **4**: 225-34.

86. Opferman JT, Ober BT, Ashton-Rickardt PG. Linear differentiation of cytotoxic effectors into memory T lymphocytes. *Science* 1999; **283**: 1745-8.

87. Jacob J, Baltimore D. Modelling T-cell memory by genetic marking of memory T cells in vivo. *Nature* 1999; **399**: 593-7.

88. Wu CY, Kirman JR, Rotte MJ *et al.* Distinct lineages of T_H1 cells have differential capacities for memory cell generation in vivo. *Nat Immunol* 2002; **3**: 852-8.

89. Sallusto F, Lenig D, Forster R *et al.* Two subsets of memory T lymphocytes with distinct homing potentials and effector functions. *Nature* 1999; **401**: 708-12.

90. Lanzavecchia A, Sallusto F. Progressive differentiation and selection of the fittest in the immune response. *Nat Rev Immunol* 2002; **2**: 982-7.

91. Manjunath N, Shankar P, Wan J *et al.* Effector differentiation is not prerequisite for generation of memory cytotoxic T lymphocytes. *J Clin Invest* 2001; **108**: 871-8.

92. Champagne P, Ogg GS, King AS *et al.* Skewed maturation of memory HIV-specific CD8 T lymphocytes. *Nature* 2001; **410**: 106-11.

93. Appay V, Dunbar PR, Callan M *et al.* Memory $CD8^+$ T cells vary in differentiation phenotype in different persistent virus infections. *Nat Med* 2002; **8**: 379-85.

94. van Lier RA, ten Berge IJ, Gamadia LE. Human $CD8^+$ T-cell differentiation in response to viruses. *Nat Rev Immunol* 2003; **3**: 931-9.

95. Swain SL, Hu H, Huston G. Class II-independent generation of CD4 memory T cells from effectors. *Science* 1999; **286**: 1381-3.

96. Murali-Krishna K, Lau LL, Sambhara S *et al.* Persistence of memory CD8 T cells in MHC class I-deficient mice. *Science* 1999; **286**: 1377-81.

97. Kaech SM, Tan JT, Wherry EJ *et al.* Selective expression of the interleukin 7 receptor identifies effector CD8 T cells that give rise to long-lived memory cells. *Nat Immunol* 2003; **4**: 1191-8.

98. Seddon B, Tomlinson P, Zamoyska R. Interleukin 7 and T cell receptor signals regulate homeostasis of CD4 memory cells. *Nat Immunol* 2003; **4**: 680-6.

99. Zhang X, Sun S, Hwang I *et al.* Potent and selective stimulation of memory-phenotype CD8+ T cells in vivo by IL-15. *Immunity* 1998; **8**: 591-9.

100. Varga SM, Selin LK, Welsh RM. Independent regulation of lymphocytic choriomeningitis virus-specific T cell memory pools: relative stability of CD4 memory under conditions of CD8 memory T cell loss. *J Immunol* 2001; **166**: 1554-61.

101. Reinhardt RL, Khoruts A, Merica R *et al.* Visualizing the generation of memory CD4 T cells in the whole body. *Nature* 2001; **410**: 101-5.

102. Masopust D, Vezys V, Marzo AL *et al.* Preferential localization of effector memory cells in nonlymphoid tissue. *Science* 2001; **291**: 2413-7.

103. Hogan RJ, Usherwood EJ, Zhong W *et al.* Activated antigen-specific $CD8^+$ T cells persist in the lungs following recovery from respiratory virus infections. *J Immunol* 2001; **166**: 1813-22.

104. Hogan RJ, Zhong W, Usherwood EJ *et al.* Protection from respiratory virus infections can be mediated by antigen-specific $CD4^+$ T cells that persist in the lungs. *J Exp Med* 2001; **193**: 981-6.

105. Busch DH, Pilip IM, Vijh S *et al.* Coordinate regulation of complex T cell populations responding to bacterial infection. *Immunity* 1998; **8**: 353-62.

106. Berard M, Tough DF. Qualitative differences between naive and memory T cells. *Immunology* 2002; **106**: 127-38.

107. Sprent J. T memory cells: quality not quantity. *Curr Biol* 2002; **12**: 174-176.

108. Veiga-Fernandes H, Walter U, Bourgeois C *et al.* Response of naive and memory $CD8^+$ T cells to antigen stimulation in vivo. *Nat Immunol* 2000; **1**: 47-53.

109. Lauvau G, Vijh S, Kong P *et al.* Priming of memory but not effector CD8 T cells by a killed bacterial vaccine. *Science* 2001; **294**: 1735-9.

110. Veiga-Fernandes H, Rocha B. High expression of active CDK6 in the cytoplasm of CD8 memory cells favors rapid division. *Nat Immunol* 2004; **5**: 31-7.

111. Arstila TP, Casrouge A, Baron V *et al.* A direct estimate of the human αβ T cell receptor diversity. *Science* 1999; **286**: 958-61.

112. Wack A, Cossarizza A, Heltai S *et al.* Age-related modifications of the human αβ T cell repertoire due to different clonal expansions in the $CD4^+$ and $CD8^+$ subsets. *Int Immunol* 1998; **10**: 1281-8.

113. Fasso M, Anandasabapathy N, Crawford F *et al.* T cell receptor (TCR)-mediated repertoire selection and loss of TCR vβ diversity during the initiation of a $CD4^+$ T cell response in vivo. *J Exp Med* 2000; **192**: 1719-30.

114. McHeyzer-Williams MG, Davis MM. Antigen-specific development of primary and memory T cells in vivo. *Science* 1995; **268**: 106-11.

115. Busch DH, Pilip I, Pamer EG. Evolution of a complex T cell receptor repertoire during primary and recall bacterial infection. *J Exp Med* 1998; **188**: 61-70.

116. Busch DH, Pamer EG. T cell affinity maturation by selective expansion during infection. *J Exp Med* 1999; **189**: 701-10.

117. Savage PA, Boniface JJ, Davis MM. A kinetic basis for T cell receptor repertoire selection during an immune response. *Immunity* 1999; **10**: 485-92.

118. Kedl RM, Rees WA, Hildeman DA *et al.* T cells compete for access to antigen-bearing antigen-presenting cells. *J Exp Med* 2000; **192**: 1105-13.

119. Kedl RM, Schaefer BC, Kappler JW *et al.* T cells down-modulate peptide-MHC complexes on APCs in vivo. *Nat Immunol* 2002; **3**: 27-32.

120. Trowbridge IS, Thomas ML. CD45: an emerging role as a protein tyrosine phosphatase required for lymphocyte activation and development. *Annu Rev Immunol* 1994; **12**: 85-116.

121. Hermiston ML, Xu Z, Weiss A. CD45: a critical regulator of signaling thresholds in immune cells. *Annu Rev Immunol* 2003; **21**: 107-37.

122. Hermiston ML, Xu Z, Majeti R *et al.* Reciprocal regulation of lymphocyte activation by tyrosine kinases and phosphatases. *J Clin Invest* 2002; **109**: 9-14.

123. Mustelin T, Rahmouni S, Bottini N *et al.* Role of protein tyrosine phosphatases in T cell activation. *Immunol Rev* 2003; **191**: 139-47.

124. Kung C, Pingel JT, Heikinheimo M *et al.* Mutations in the tyrosine phosphatase CD45 gene in a child with severe combined immunodeficiency disease. *Nat Med* 2000; **6**: 343-5.

125. Faint JM, Annels NE, Curnow SJ *et al.* Memory T cells constitute a subset of the human $CD8^+CD45RA^+$ pool with distinct phenotypic and migratory characteristics. *J Immunol* 2001; **167**: 212-20.

126. Dunne PJ, Faint JM, Gudgeon NH *et al.* Epstein-Barr virus-specific $CD8^+$ T cells that re-express CD45RA are apoptosis-resistant memory cells that retain replicative potential. *Blood* 2002; **100**: 933-40.

127. Wills MR, Carmichael AJ, Weekes MP *et al.* Human virus-specific $CD8^+$ CTL clones revert from $CD45RO^{high}$ to $CD45RA^{high}$ in vivo: $CD45RA^{high}$ $CD8^+$ T cells comprise both naive and memory cells. *J Immunol* 1999; **162**: 7080-7.

128. Pilling D, Akbar AN, Bacon PA *et al.* $CD4^+$ $CD45RA^+$ T cells from adults respond to recall antigens after CD28 ligation. *Int Immunol* 1996; **8**: 1737-42.

129. Bell EB, Hayes S, McDonagh M *et al.* Both $CD45R^{low}$ and $CD45R^{high}$ "revertant" CD4 memory T cells provide help for memory B cells. *Eur J Immunol* 2001; **31**: 1685-95.

130. Campbell JJ, Butcher EC. Chemokines in tissue-specific and microenvironment-specific lymphocyte homing. *Curr Opin Immunol* 2000; **12**: 336-41.

131. Campbell DJ, Kim CH, Butcher EC. Chemokines in the systemic organization of immunity. *Immunol Rev* 2003; **195**: 58-71.

132. Hengel RL, Thaker V, Pavlick MV *et al.* Cutting edge: L-selectin (CD62L) expression distinguishes small resting memory $CD4^+$ T cells that preferentially respond to recall antigen. *J Immunol* 2003; **170**: 28-32.

133. Debes GF, Hopken UE, Hamann A. In vivo differentiated cytokine-producing $CD4^+$ T cells express functional CCR7. *J Immunol* 2002; **168**: 5441-7.

134. Unsoeld H, Krautwald S, Voehringer D *et al.* Cutting edge: $CCR7^+$ and $CCR7^-$ memory T cells do not differ in immediate effector cell function. *J Immunol* 2002; **169**: 638-41.

135. Kim CH, Rott L, Kunkel EJ *et al.* Rules of chemokine receptor association with T cell polarization in vivo. *J Clin Invest* 2001; **108**: 1331-9.

136. Campbell JJ, Murphy KE, Kunkel EJ *et al.* CCR7 expression and memory T cell diversity in humans. *J Immunol* 2001; **166**: 877-84.

137. Sallusto F, Kremmer E, Palermo B *et al.* Switch in chemokine receptor expression upon TCR stimulation reveals novel homing potential for recently activated T cells. *Eur J Immunol* 1999; **29**: 2037-45.

138. Homey B, Alenius H, Muller A *et al.* CCL27-CCR10 interactions regulate T cell-mediated skin inflammation. *Nat Med* 2002; **8**: 157-65.

139. Soler D, Humphreys TL, Spinola SM *et al.* CCR4 versus CCR10 in human cutaneous T_H lymphocyte trafficking. *Blood* 2003; **101**: 1677-82.

140. Campbell JJ, Haraldsen G, Pan J *et al.* The chemokine receptor CCR4 in vascular recognition by cutaneous but not intestinal memory T cells. *Nature* 1999; **400**: 776-80.

141. Schaerli P, Ebert L, Willimann K *et al.* A skin-selective homing mechanism for human immune surveillance T cells. *J Exp Med* 2004; **199**: 1265-75.

142. Kunkel EJ, Campbell JJ, Haraldsen G *et al.* Lymphocyte CC chemokine receptor 9 and epithelial thymus-expressed chemokine (TECK) expression distinguish the small intestinal immune compartment: Epithelial expression of tissue-specific chemokines as an organizing principle in regional immunity. *J Exp Med* 2000; **192**: 761-8.

143. Papadakis KA, Prehn J, Nelson V *et al.* The role of thymus-expressed chemokine and its receptor CCR9 on lymphocytes in the regional specialization of the mucosal immune system. *J Immunol* 2000; **165**: 5069-76.

144. Waldmann TA. The interleukin-2 receptor. *J Biol Chem* 1991; **266**: 2681-4.

145. Waldmann TA. The structure, function, and expression of interleukin-2 receptors on normal and malignant lymphocytes. *Science* 1986; **232**: 727-32.

146. Sakaguchi S, Sakaguchi N, Asano M *et al.* Immunologic self-tolerance maintained by activated T cells expressing IL-2 receptor α-chains (CD25). Breakdown of a single mechanism of self-tolerance causes various autoimmune diseases. *J Immunol* 1995; **155**: 1151-64.

147. Taams LS, Smith J, Rustin MH *et al.* Human anergic/suppressive $CD4^+CD25^+$ T cells: a highly differentiated and apoptosis-prone population. *Eur J Immunol* 2001; **31**: 1122-31.

148. Wood KJ, Sakaguchi S. Regulatory Lymphocytes: Regulatory T cells in transplantation tolerance. *Nat Rev Immunol* 2003; **3**: 199-210.

149. Natarajan K, Sawicki MW, Margulies DH *et al.* Crystal structure of human CD69: a C-type lectin-like activation marker of hematopoietic cells. *Biochemistry* 2000; **39**: 14779-86.

150. Testi R, D'Ambrosio D, De Maria R *et al.* The CD69 receptor: a multipurpose cell-surface trigger for hematopoietic cells. *Immunol Today* 1994; **15**: 479-83.

151. Marzio R, Mauel J, Betz-Corradin S. CD69 and regulation of the immune function. *Immunopharmacol Immunotoxicol* 1999; **21**: 565-82.

152. Ziegler SF, Ramsdell F, Alderson MR. The activation antigen CD69. *Stem Cells* 1994; **12**: 456-65.

153. Caruso A, Licenziati S, Corulli M *et al.* Flow cytometric analysis of activation markers on stimulated T cells and their correlation with cell proliferation. *Cytometry* 1997; **27**: 71-6.

154. Craston R, Koh M, Mc DA *et al.* Temporal dynamics of CD69 expression on lymphoid cells. *J Immunol Methods* 1997; **209**: 37-45.

155. Cauley LS, Cookenham T, Miller TB *et al.* Cutting edge: virus-specific $CD4^+$ memory T cells in nonlymphoid tissues express a highly activated phenotype. *J Immunol* 2002; **169**: 6655-8.

156. Hawke S, Stevenson PG, Freeman S *et al.* Long-term persistence of activated cytotoxic T lymphocytes after viral infection of the central nervous system. *J Exp Med* 1998; **187**: 1575-82.

157. Tomiyama H, Takata H, Matsuda T *et al.* Phenotypic classification of human $CD8^+$ T cells reflecting their function: inverse correlation

between quantitative expression of CD27 and cytotoxic effector function. *Eur J Immunol* 2004; **34**: 999-1010.

158. Hamann D, Kostense S, Wolthers KC *et al.* Evidence that human $CD8^+CD45RA^+CD27^-$ cells are induced by antigen and evolve through extensive rounds of division. *Int Immunol* 1999; **11**: 1027-33.

159. Rufer N, Zippelius A, Batard P *et al.* Ex vivo characterization of human $CD8^+$ T subsets with distinct replicative history and partial effector functions. *Blood* 2003; **102**: 1779-87.

160. Effros RB, Dagarag M, Valenzuela HF. In vitro senescence of immune cells. *Exp Gerontol* 2003; **38**: 1243-9.

161. Campisi J. From cells to organisms: can we learn about aging from cells in culture? *Exp Gerontol* 2001; **36**: 607-18.

162. Hayflick L, Moorhead P. The cultivation of human diploid strains. *Exp Cell Res* 1961; 585-621.

163. Sharpless NE, DePinho RA. Telomeres, stem cells, senescence, and cancer. *J Clin Invest* 2004; **113**: 160-8.

164. Sherr CJ, DePinho RA. Cellular senescence: mitotic clock or culture shock? *Cell* 2000; **102**: 407-10.

165. Rubin H. Cell aging in vivo and in vitro. *Mech Ageing Dev* 1997; **98**: 1-35.

166. Blackburn EH. Telomere states and cell fates. *Nature* 2000; **408**: 53-6.

167. Blasco MA. Telomeres and cancer: a tale with many endings. *Curr Opin Genet Dev* 2003; **13**: 70-6.

168. Hahn WC, Counter CM, Lundberg AS *et al.* Creation of human tumour cells with defined genetic elements. *Nature* 1999; **400**: 464-8.

169. Blackburn EH. Switching and signaling at the telomere. *Cell* 2001; **106**: 661-73.

170. Kanoh J, Ishikawa F. Composition and conservation of the telomeric complex. *Cell Mol Life Sci* 2003; **60**: 2295-302.

171. McEachern MJ, Krauskopf A, Blackburn EH. Telomeres and their control. *Annu Rev Genet* 2000; **34**: 331-58.

172. Sandell LL, Zakian VA. Loss of a yeast telomere: arrest, recovery, and chromosome loss. *Cell* 1993; **75**: 729-39.

173. Zhu J, Wang H, Bishop JM *et al.* Telomerase extends the lifespan of virus-transformed human cells without net telomere lengthening. *Proc Natl Acad Sci U.S.A* 1999; **96**: 3723-8.

174. Griffith JD, Comeau L, Rosenfield S *et al.* Mammalian telomeres end in a large duplex loop. *Cell* 1999; **97**: 503-14.

175. Greider CW. Telomeres do D-loop-T-loop. *Cell* 1999; **97**: 419-22.

176. Eller MS, Puri N, Hadshiew IM *et al.* Induction of apoptosis by telomere 3' overhang-specific DNA. *Exp Cell Res* 2002; **276**: 185-93.

177. Li GZ, Eller MS, Firoozabadi R *et al.* Evidence that exposure of the telomere 3' overhang sequence induces senescence. *Proc Natl Acad Sci U.S.A* 2003; **100**: 527-31.

178. d'Adda dF, Reaper PM, Clay-Farrace L *et al.* A DNA damage checkpoint response in telomere-initiated senescence. *Nature* 2003; **426**: 194-8.

179. Broccoli D, Smogorzewska A, Chong L *et al.* Human telomeres contain two distinct Myb-related proteins, TRF1 and TRF2. *Nat Genet* 1997; **17**: 231-5.

180. Smogorzewska A, van Steensel B, Bianchi A *et al.* Control of human telomere length by TRF1 and TRF2. *Mol Cell Biol* 2000; **20**: 1659-68.

181. Smith S, de Lange T. Tankyrase promotes telomere elongation in human cells. *Curr Biol* 2000; **10**: 1299-302.

182. Kim SH, Kaminker P, Campisi J. TIN2, a new regulator of telomere length in human cells. *Nat Genet* 1999; **23**: 405-12.

183. Chai W, Ford LP, Lenertz L *et al.* Human Ku70/80 associates physically with telomerase through interaction with hTERT. *J Biol Chem* 2002; **277**: 47242-7.

184. Li B, Oestreich S, de Lange T. Identification of human Rap1: implications for telomere evolution. *Cell* 2000; **101**: 471-83.

185. Colgin LM, Baran K, Baumann P *et al.* Human Pot1 facilitates telomere elongation by telomerase. *Curr Biol* 2003; **13**: 942-6.

186. Baumann P, Cech TR. Pot1, the putative telomere end-binding protein in fission yeast and humans. *Science* 2001; **292**: 1171-5.

187. Baumann P, Podell E, Cech TR. Human Pot1 (protection of telomeres) protein: cytolocalization, gene structure, and alternative splicing. *Mol Cell Biol* 2002; **22**: 8079-87.

188. Twyman RM. *Advanced molecular biology*. BIOS Scientific Publishers Ltd., 1998.

189. Levy MZ, Allsopp RC, Futcher AB *et al.* Telomere end-replication problem and cell aging. *J Mol Biol* 1992; **225**: 951-60.

190. Jacob NK, Kirk KE, Price CM. Generation of telomeric G strand overhangs involves both G and C strand cleavage. *Mol Cell* 2003; **11**: 1021-32.

191. Wei C, Price M. Protecting the terminus: t-loops and telomere end-binding proteins. *Cell Mol Life Sci* 2003; **60**: 2283-94.

192. Harley CB, Futcher AB, Greider CW. Telomeres shorten during ageing of human fibroblasts. *Nature* 1990; **345**: 458-60.

193. Weng NP, Levine BL, June CH *et al.* Human naive and memory T lymphocytes differ in telomeric length and replicative potential. *Proc Natl Acad Sci U S A* 1995; **92**: 11091-4.

194. Allsopp RC, Vaziri H, Patterson C *et al.* Telomere length predicts replicative capacity of human fibroblasts. *Proc Natl Acad Sci U.S.A* 1992; **89**: 10114-8.

195. Allsopp RC, Harley CB. Evidence for a critical telomere length in senescent human fibroblasts. *Exp Cell Res* 1995; **219**: 130-6.

196. Hemann MT, Strong MA, Hao LY *et al.* The shortest telomere, not average telomere length, is critical for cell viability and chromosome stability. *Cell* 2001; **107**: 67-77.

197. Kipling D, Cooke HJ. Hypervariable ultra-long telomeres in mice. *Nature* 1990; **347**: 400-2.

198. Collins K, Mitchell JR. Telomerase in the human organism. *Oncogene* 2002; **21**: 564-79.

199. Feng J, Funk WD, Wang SS *et al.* The RNA component of human telomerase. *Science* 1995; **269**: 1236-41.

200. Nakamura TM, Morin GB, Chapman KB *et al.* Telomerase catalytic subunit homologs from fission yeast and human. *Science* 1997; **277**: 955-9.

201. Diede SJ, Gottschling DE. Telomerase-mediated telomere addition in vivo requires DNA primase and DNA polymerases α and δ. *Cell* 1999; **99**: 723-33.

202. Kim NW, Piatyszek MA, Prowse KR *et al.* Specific association of human telomerase activity with immortal cells and cancer. *Science* 1994; **266**: 2011-5.

203. Shay JW, Bacchetti S. A survey of telomerase activity in human cancer. *Eur J Cancer* 1997; **33**: 787-91.

204. Yasumoto S, Kunimura C, Kikuchi K *et al.* Telomerase activity in normal human epithelial cells. *Oncogene* 1996; **13**: 433-9.

205. Bachor C, Bachor OA, Boukamp P. Telomerase is active in normal gastrointestinal mucosa and not up-regulated in precancerous lesions. *J Cancer Res Clin Oncol* 1999; **125**: 453-60.

206. Harle-Bachor C, Boukamp P. Telomerase activity in the regenerative basal layer of the epidermis in human skin and in immortal and carcinoma-derived skin keratinocytes. *Proc Natl Acad Sci U.S.A* 1996; **93**: 6476-81.

207. Bodnar AG, Kim NW, Effros RB *et al.* Mechanism of telomerase induction during T cell activation. *Exp Cell Res* 1996; **228**: 58-64.

208. Weng NP, Levine BL, June CH *et al.* Regulated expression of telomerase activity in human T lymphocyte development and activation. *J Exp Med* 1996; **183**: 2471-9.

209. Hiyama K, Hirai Y, Kyoizumi S *et al.* Activation of telomerase in human lymphocytes and hematopoietic progenitor cells. *J Immunol* 1995; **155**: 3711-5.

210. Igarashi H, Sakaguchi N. Telomerase activity is induced by the stimulation to antigen receptor in human peripheral lymphocytes. *Biochem Biophys Res Commun* 1996; **219**: 649-55.

211. Weng NP, Granger L, Hodes RJ. Telomere lengthening and telomerase activation during human B cell differentiation. *Proc Natl Acad Sci U S A* 1997; **94**: 10827-32.

212. Masutomi K, Yu EY, Khurts S *et al.* Telomerase maintains telomere structure in normal human cells. *Cell* 2003; **114**: 241-53.

213. Shiratsuchi M, Muta K, Umemura T *et al.* Telomerase activity in myeloma cells is closely related to cell cycle status, but not to apoptotic signals induced by interferon-α. *Leuk Lymphoma* 1999; **34**: 349-59.

214. Tanaka M, Kyo S, Takakura M *et al.* Expression of telomerase activity in human endometrium is localized to epithelial glandular cells and regulated in a menstrual phase-dependent manner correlated with cell proliferation. *Am J Pathol* 1998; **153**: 1985-91.

215. Buchkovich KJ, Greider CW. Telomerase regulation during entry into the cell cycle in normal human T cells. *Mol Biol Cell* 1996; **7**: 1443-54.

216. Zhu X, Kumar R, Mandal M *et al.* Cell cycle-dependent modulation of telomerase activity in tumor cells. *Proc Natl Acad Sci U.S.A* 1996; **93**: 6091-5.

217. Blasco MA, Lee HW, Hande MP *et al.* Telomere shortening and tumor formation by mouse cells lacking telomerase RNA. *Cell* 1997; **91**: 25-34.

218. Lee HW, Blasco MA, Gottlieb GJ *et al.* Essential role of mouse telomerase in highly proliferative organs. *Nature* 1998; **392**: 569-74.

219. Rudolph KL, Chang S, Lee HW *et al.* Longevity, stress response, and cancer in aging telomerase-deficient mice. *Cell* 1999; **96**: 701-12.

220. Gonzalez-Suarez E, Samper E, Flores JM *et al.* Telomerase-deficient mice with short telomeres are resistant to skin tumorigenesis. *Nat Genet* 2000; **26**: 114-7.

221. Dokal I. Dyskeratosis congenita in all its forms. *Br J Haematol* 2000; **110**: 768-79.

222. Heiss NS, Knight SW, Vulliamy TJ *et al.* X-linked dyskeratosis congenita is caused by mutations in a highly conserved gene with putative nucleolar functions. *Nat Genet* 1998; **19**: 32-8.

223. Vulliamy T, Marrone A, Goldman F *et al.* The RNA component of telomerase is mutated in autosomal dominant dyskeratosis congenita. *Nature* 2001; **413**: 432-5.

224. Mitchell JR, Wood E, Collins K. A telomerase component is defective in the human disease dyskeratosis congenita. *Nature* 1999; **402**: 551-5.

225. Karlseder J, Smogorzewska A, de Lange T. Senescence induced by altered telomere state, not telomere loss. *Science* 2002; **295**: 2446-9.

226. Yang J, Chang E, Cherry AM *et al.* Human endothelial cell life extension by telomerase expression. *J Biol Chem* 1999; **274**: 26141-8.

227. Wick G, Jansen-Durr P, Berger P *et al.* Diseases of aging. *Vaccine* 2000; **18**: 1567-83.

228. Franceschi C, Bonafe M, Valensin S. Human immunosenescence: the prevailing of innate immunity, the failing of clonotypic immunity, and the filling of immunological space. *Vaccine* 2000; **18**: 1717-20.

229. Douek DC, Koup RA. Evidence for thymic function in the elderly. *Vaccine* 2000; **18**: 1638-41.

230. Posnett DN, Sinha R, Kabak S *et al.* Clonal populations of T cells in normal elderly humans: the T cell equivalent to "benign monoclonal gammapathy". *J Exp Med* 1994; **179**: 609-18.

231. Castle SC, Norman DC, Perls TT *et al.* Analysis of cutaneous delayed-type hypersensitivity reaction and T cell proliferative response in elderly nursing home patients: an approach to identifying immunodeficient patients. *Gerontology* 1990; **36**: 217-29.

232. Marrie TJ, Johnson S, Durant H. Cell-mediated immunity of healthy adult Nova Scotians in various age groups compared with nursing home and hospitalized senior citizens. *J Allergy Clin Immunol* 1988; **81**: 836-43.

233. Lamoureux G, Poisson R. Letter: B.C.G. and immunological anergy. *Lancet* 1974; **1**: 989-90.

234. Effros RB, Pawelec G. Replicative senescence of T cells: does the Hayflick Limit lead to immune exhaustion? *Immunol Today* 1997; **18**: 450-4.

235. Rufer N, Brummendorf TH, Kolvraa S *et al.* Telomere fluorescence measurements in granulocytes and T lymphocyte subsets point to a high turnover of hematopoietic stem cells and memory T cells in early childhood. *J Exp Med* 1999; **190**: 157-67.

236. Rufer N, Dragowska W, Thornbury G *et al.* Telomere length dynamics in human lymphocyte subpopulations measured by flow cytometry. *Nat Biotechnol* 1998; **16**: 743-7.

237. Monteiro J, Batliwalla F, Ostrer H *et al.* Shortened telomeres in clonally expanded $CD28^{-}CD8^{+}$ T cells imply a replicative history that is distinct from their $CD28^{+}CD8^{+}$ counterparts. *J Immunol* 1996; **156**: 3587-90.

238. Frenck RW, Jr., Blackburn EH, Shannon KM. The rate of telomere sequence loss in human leukocytes varies with age. *Proc Natl Acad Sci U.S.A* 1998; **95**: 5607-10.

239. Hodes RJ, Hathcock KS, Weng NP. Telomeres in T and B cells. *Nat Rev Immunol* 2002; **2**: 699-706.

240. Soares, M. V., Plunkett, F. J., Verbeke, C. S *et al.* The integration of apoptosis and telomere erosion in virus-specific $CD8^{+}$ T cells from blood and tonsils during primary infection. *Blood* 2004; **103**: 162-7.

241. Plunkett FJ, Soares MV, Annels N *et al.* The flow cytometric analysis of telomere length in antigen-specific $CD8^{+}$ T cells during acute Epstein-Barr virus infection. *Blood* 2001; **97**: 700-7.

242. Maini MK, Soares MV, Zilch CF *et al.* Virus-induced $CD8^{+}$ T cell clonal expansion is associated with telomerase up-regulation and

telomere length preservation: a mechanism for rescue from replicative senescence. *J Immunol* 1999; **162**: 4521-6.

243. Hathcock KS, Weng NP, Merica R *et al.* Cutting edge: antigen-dependent regulation of telomerase activity in murine T cells. *J Immunol* 1998; **160**: 5702-6.

244. Hathcock KS, Kaech SM, Ahmed R *et al.* Induction of telomerase activity and maintenance of telomere length in virus-specific effector and memory $CD8^+$ T cells. *J Immunol* 2003; **170**: 147-52.

245. Weng N, Levine BL, June CH *et al.* Regulation of telomerase RNA template expression in human T lymphocyte development and activation. *J Immunol* 1997; **158**: 3215-20.

246. Liu K, Schoonmaker MM, Levine BL *et al.* Constitutive and regulated expression of telomerase reverse transcriptase (hTERT) in human lymphocytes. *Proc Natl Acad Sci U.S.A* 1999; **96**: 5147-52.

247. Liu K, Hodes RJ, Weng N. Cutting edge: telomerase activation in human T lymphocytes does not require increase in telomerase reverse transcriptase (hTERT) protein but is associated with hTERT phosphorylation and nuclear translocation. *J Immunol* 2001; **166**: 4826-30.

248. Ogoshi M, Le T, Shay JW *et al.* In situ hybridization analysis of the expression of human telomerase RNA in normal and pathologic conditions of the skin. *J Invest Dermatol* 1998; **110**: 818-23.

249. Wu K, Higashi N, Hansen ER *et al.* Telomerase activity is increased and telomere length shortened in T cells from blood of patients with atopic dermatitis and psoriasis. *J Immunol* 2000; **165**: 4742-7.

250. Wu K, Volke A, Lund M *et al.* Telomerase activity is spontaneously increased in lymphocytes from patients with atopic dermatitis and correlates with cellular proliferation. *J Dermatol Sci* 1999; **22**: 24-30.

251. Rufer N, Migliaccio M, Antonchuk J *et al.* Transfer of the human telomerase reverse transcriptase (TERT) gene into T lymphocytes results in extension of replicative potential. *Blood* 2001; **98**: 597-603.

252. Hooijberg E, Ruizendaal JJ, Snijders PJ *et al.* Immortalization of human $CD8^+$ T cell clones by ectopic expression of telomerase reverse transcriptase. *J Immunol* 2000; **165**: 4239-45.

253. Luiten RM, Pene J, Yssel H *et al.* Ectopic hTERT expression extends the life span of human $CD4^+$ helper and regulatory T-cell clones and confers resistance to oxidative stress-induced apoptosis. *Blood* 2003; **101**: 4512-9.

254. Roth A, Yssel H, Pene J *et al.* Telomerase levels control the lifespan of human T lymphocytes. *Blood* 2003; **102**: 849-57.

255. Weng NP, Palmer LD, Levine BL *et al.* Tales of tails: regulation of telomere length and telomerase activity during lymphocyte development, differentiation, activation, and aging. *Immunol Rev* 1997; **160**: 43-54.

256. Valenzuela HF, Effros RB. Divergent telomerase and CD28 expression patterns in human CD4 and CD8 T cells following repeated encounters with the same antigenic stimulus. *Clin Immunol* 2002; **105**: 117-25.

257. Mariani E, Meneghetti A, Formentini I *et al.* Different rates of telomere shortening and telomerase activity reduction in CD8 T and CD16 NK lymphocytes with ageing. *Exp Gerontol* 2003; **38**: 653-9.

258. Baerlocher GM, Mak J, Roth A *et al.* Telomere shortening in leukocyte subpopulations from baboons. *J Leukoc Biol* 2003; **73**: 289-96.

259. Son NH, Murray S, Yanovski J *et al.* Lineage-specific telomere shortening and unaltered capacity for telomerase expression in human T and B lymphocytes with age. *J Immunol* 2000; **165**: 1191-6.

260. Soares MV, Borthwick NJ, Maini MK *et al.* IL-7-dependent extrathymic expansion of $CD45RA^+$ T cells enables preservation of a naive repertoire. *J Immunol* 1998; **161**: 5909-17.

261. Xu D, Erickson S, Szeps M *et al.* Interferon α down-regulates telomerase reverse transcriptase and telomerase activity in human malignant and nonmalignant hematopoietic cells. *Blood* 2000; **96**: 4313-8.

262. Scheel-Toellner D, Pilling D, Akbar AN *et al.* Inhibition of T cell apoptosis by IFN-β rapidly reverses nuclear translocation of protein kinase C-delta. *Eur J Immunol* 1999; **29**: 2603-12.

263. Preisler HD, Li B, Yang BL *et al.* Suppression of telomerase activity and cytokine messenger RNA levels in acute myelogenous leukemia cells in vivo in patients by amifostine and interleukin 4. *Clin Cancer Res* 2000; **6**: 807-12.

264. Rama S, Suresh Y, Rao AJ. Regulation of telomerase during human placental differentiation: a role for TGFβ1. *Mol Cell Endocrinol* 2001; **182**: 233-48.

265. Cerezo A, Kalthoff H, Schuermann M *et al.* Dual regulation of telomerase activity through c-Myc-dependent inhibition and alternative splicing of hTERT. *J Cell Sci* 2002; **115**: 1305-12.

266. Yang H, Kyo S, Takatura M *et al.* Autocrine transforming growth factor β suppresses telomerase activity and transcription of human telomerase reverse transcriptase in human cancer cells. *Cell Growth Differ* 2001; **12**: 119-27.

267. Lee SH, Kim JW, Lee HW *et al.* Interferon regulatory factor-1 (IRF-1) is a mediator for interferon-γ induced attenuation of telomerase activity and human telomerase reverse transcriptase (hTERT) expression. *Oncogene* 2003; **22**: 381-91.

268. Le Bon A, Tough DF. Links between innate and adaptive immunity via type I interferon. *Curr Opin Immunol* 2002; **14**: 432-6.

269. Bogdan C. The function of type I interferons in antimicrobial immunity. *Curr Opin Immunol* 2000; **12**: 419-24.

270. Mogensen KE, Lewerenz M, Reboul J *et al.* The type I interferon receptor: structure, function, and evolution of a family business. *J Interferon Cytokine Res* 1999; **19**: 1069-98.

271. Goodbourn S, Didcock L, Randall RE. Interferons: cell signalling, immune modulation, antiviral response and virus countermeasures. *J Gen Virol* 2000; **81**: 2341-64.

272. Dzionek A, Sohma Y, Nagafune J *et al.* BDCA-2, a novel plasmacytoid dendritic cell-specific type II C-type lectin, mediates antigen capture and is a potent inhibitor of interferon alpha/beta induction. *J Exp Med* 2001; **194**: 1823-34.

273. Kadowaki N, Liu YJ. Natural type I interferon-producing cells as a link between innate and adaptive immunity. *Hum Immunol* 2002; **63**: 1126-32.

274. Wollenberg A, Wagner M, Gunther S *et al.* Plasmacytoid dendritic cells: a new cutaneous dendritic cell subset with distinct role in inflammatory skin diseases. *J Invest Dermatol* 2002; **119**: 1096-102.

275. Pascual V, Banchereau J, Palucka AK. The central role of dendritic cells and interferon-α in SLE. *Curr Opin Rheumatol* 2003; **15**: 548-56.

276. Bangert C, Friedl J, Stary G *et al.* Immunopathologic features of allergic contact dermatitis in humans: participation of plasmacytoid dendritic cells in the pathogenesis of the disease? *J Invest Dermatol* 2003; **121**: 1409-18.

277. Farkas L, Beiske K, Lund-Johansen F *et al.* Plasmacytoid dendritic cells (natural interferon-α/β producing cells) accumulate in cutaneous lupus erythematosus lesions. *Am J Pathol* 2001; **159**: 237-43.

278. Ebner S, Ehammer Z, Holzmann S *et al.* Expression of C-type lectin receptors by subsets of dendritic cells in human skin. *Int Immunol* 2004; **16**: 877-87.

279. Penna G, Sozzani S, Adorini L. Cutting edge: selective usage of chemokine receptors by plasmacytoid dendritic cells. *J Immunol* 2001; **167**: 1862-6.

280. Salazar JC, Pope CD, Sellati TJ *et al.* Coevolution of markers of innate and adaptive immunity in skin and peripheral blood of patients with erythema migrans. *J Immunol* 2003; **171**: 2660-70.

281. Mazzoni A, Leifer CA, Mullen GE *et al.* Cutting edge: histamine inhibits IFN-α release from plasmacytoid dendritic cells. *J Immunol* 2003; **170**: 2269-73.

282. Diebold SS, Kaisho T, Hemmi H *et al.* Innate antiviral responses by means of TLR7-mediated recognition of single-stranded RNA. *Science* 2004; **303**: 1529-31.

283. Hemmi H, Takeuchi O, Kawai T *et al.* A Toll-like receptor recognizes bacterial DNA. *Nature* 2000; **408**: 740-5.

284. Kadowaki N, Ho S, Antonenko S *et al.* Subsets of human dendritic cell precursors express different toll-like receptors and respond to different microbial antigens. *J Exp Med* 2001; **194**: 863-9.

285. Ito T, Amakawa R, Inaba M *et al.* Plasmacytoid dendritic cells regulate Th cell responses through OX40 ligand and type I IFNs. *J Immunol* 2004; **172**: 4253-9.

286. Jonuleit H, Schmitt E. The regulatory T cell family: distinct subsets and their interrelations. *J Immunol* 2003; **171**: 6323-7.

287. Taams L, Vukmanovic-Stejic M, Salmon M *et al.* Immune regulation by $CD4^+CD25^+$ regulatory T cells: implications for transplantation tolerance. *Transpl Immunol* 2003; **11**: 277-85.

288. Sakaguchi S. Naturally arising $CD4^+$ regulatory T cells for immunologic self-tolerance and negative control of immune responses. *Annu Rev Immunol* 2004; **22**: 531-62.

289. Asano M, Toda M, Sakaguchi N *et al.* Autoimmune disease as a consequence of developmental abnormality of a T cell subpopulation. *J Exp Med* 1996; **184**: 387-96.

290. Taams LS, Vukmanovic-Stejic M, Smith J *et al.* Antigen-specific T cell suppression by human $CD4^+CD25^+$ regulatory T cells. *Eur J Immunol* 2002; **32**: 1621-30.

291. Stephens LA, Mottet C, Mason D *et al.* Human $CD4^+CD25^+$ thymocytes and peripheral T cells have immune suppressive activity in vitro. *Eur J Immunol* 2001; **31**: 1247-54.

292. Baecher-Allan C, Brown JA, Freeman GJ *et al.* $CD4^+CD25^{high}$ regulatory cells in human peripheral blood. *J Immunol* 2001; **167**: 1245-53.

293. Dieckmann D, Plottner H, Berchtold S *et al.* Ex vivo isolation and characterization of $CD4^+CD25^+$ T cells with regulatory properties from human blood. *J Exp Med* 2001; **193**: 1303-10.

294. Jonuleit H, Schmitt E, Stassen M *et al.* Identification and functional characterization of human $CD4^+CD25^+$ T cells with regulatory properties isolated from peripheral blood. *J Exp Med* 2001; **193**: 1285-94.

295. Levings MK, Sangregorio R, Roncarolo MG. Human $CD25^+CD4^+$ T regulatory cells suppress naive and memory T cell proliferation and can be expanded in vitro without loss of function. *J Exp Med* 2001; **193**: 1295-302.

296. Ng WF, Duggan PJ, Ponchel F *et al.* Human $CD4^+CD25^+$ cells: a naturally occurring population of regulatory T cells. *Blood* 2001; **98**: 2736-44.

297. Nelson BH. IL-2, Regulatory T Cells, and Tolerance. *J Immunol* 2004; **172**: 3983-8.

298. Kuniyasu Y, Takahashi T, Itoh M *et al.* Naturally anergic and suppressive $CD25^+CD4^+$ T cells as a functionally and phenotypically distinct immunoregulatory T cell subpopulation. *Int Immunol* 2000; **12**: 1145-55.

299. Gavin MA, Clarke SR, Negrou E *et al.* Homeostasis and anergy of $CD4^+CD25^+$ suppressor T cells in vivo. *Nat Immunol* 2002; **3**: 33-41.

300. Read S, Malmstrom V, Powrie F. Cytotoxic T lymphocyte-associated antigen 4 plays an essential role in the function of $CD25^+CD4^+$ regulatory cells that control intestinal inflammation. *J Exp Med* 2000; **192**: 295-302.

301. Thornton AM, Shevach EM. $CD4^+CD25^+$ immunoregulatory T cells suppress polyclonal T cell activation in vitro by inhibiting interleukin 2 production. *J Exp Med* 1998; **188**: 287-96.

302. Takahashi T, Tagami T, Yamazaki S *et al.* Immunologic self-tolerance maintained by $CD25^+CD4^+$ regulatory T cells constitutively expressing cytotoxic T lymphocyte-associated antigen 4. *J Exp Med* 2000; **192**: 303-10.

303. McHugh RS, Whitters MJ, Piccirillo CA *et al.* $CD4^+CD25^+$ immunoregulatory T cells: gene expression analysis reveals a functional role for the glucocorticoid-induced TNF receptor. *Immunity* 2002; **16**: 311-23.

304. Shimizu J, Yamazaki S, Takahashi T *et al.* Stimulation of $CD25^+CD4^+$ regulatory T cells through GITR breaks immunological self-tolerance. *Nat Immunol* 2002; **3**: 135-42.

305. Levings MK, Sangregorio R, Sartirana C *et al.* Human $CD25^+CD4^+$ T suppressor cell clones produce transforming growth factor β, but not interleukin 10, and are distinct from type 1 T regulatory cells. *J Exp Med* 2002; **196**: 1335-46.

306. Baecher-Allan C, Viglietta V, Hafler DA. Inhibition of human $CD4^+CD25^{+high}$ regulatory T cell function. *J Immunol* 2002; **169**: 6210-7.

307. Iellem A, Mariani M, Lang R *et al.* Unique chemotactic response profile and specific expression of chemokine receptors CCR4 and CCR8 by $CD4^+CD25^+$ regulatory T cells. *J Exp Med* 2001; **194**: 847-53.

308. Fontenot JD, Gavin MA, Rudensky AY. Foxp3 programs the development and function of $CD4^+CD25^+$ regulatory T cells. *Nat Immunol* 2003; **4**: 330-6.

309. Khattri R, Cox T, Yasayko SA *et al.* An essential role for Scurfin in $CD4^+CD25^+$ T regulatory cells. *Nat Immunol* 2003; **4**: 337-42.

310. Hori S, Nomura T, Sakaguchi S. Control of regulatory T cell development by the transcription factor Foxp3. *Science* 2003; **299**: 1057-61.

311. Walker MR, Kasprowicz DJ, Gersuk VH *et al.* Induction of FoxP3 and acquisition of T regulatory activity by stimulated human $CD4^+CD25^-$ T cells. *J Clin Invest* 2003; **112**: 1437-43.

312. Brunkow ME, Jeffery EW, Hjerrild KA *et al.* Disruption of a new forkhead/winged-helix protein, scurfin, results in the fatal lymphoproliferative disorder of the scurfy mouse. *Nat Genet* 2001; **27**: 68-73.

313. Wildin RS, Ramsdell F, Peake J *et al.* X-linked neonatal diabetes mellitus, enteropathy and endocrinopathy syndrome is the human equivalent of mouse scurfy. *Nat Genet* 2001; **27**: 18-20.

314. Bennett CL, Christie J, Ramsdell F *et al.* The immune dysregulation, polyendocrinopathy, enteropathy, X-linked syndrome (IPEX) is caused by mutations of FOXP3. *Nat Genet* 2001; **27**: 20-1.

315. Bruder D, Probst-Kepper M, Westendorf AM *et al.* Frontline: Neuropilin-1: a surface marker of regulatory T cells. *Eur J Immunol* 2004; **34**: 623-30.

316. Takahashi T, Kuniyasu Y, Toda M *et al.* Immunologic self-tolerance maintained by $CD25^+CD4^+$ naturally anergic and suppressive T cells: induction of autoimmune disease by breaking their anergic/suppressive state. *Int Immunol* 1998; **10**: 1969-80.

317. Thornton AM, Shevach EM. Suppressor effector function of $CD4^+CD25^+$ immunoregulatory T cells is antigen nonspecific. *J Immunol* 2000; **164**: 183-90.

318. Godfrey WR, Ge YG, Spoden DJ *et al.* In vitro-expanded human $CD4^+CD25^+$ T-regulatory cells can markedly inhibit allogeneic dendritic cell-stimulated MLR cultures. *Blood* 2004; **104**: 453-61.

319. Annacker O, Pimenta-Araujo R, Burlen-Defranoux O *et al.* $CD25^+$ $CD4^+$ T cells regulate the expansion of peripheral CD4 T cells through the production of IL-10. *J Immunol* 2001; **166**: 3008-18.

320. Walker LS, Chodos A, Eggena M *et al.* Antigen-dependent proliferation of $CD4^+$ $CD25^+$ regulatory T cells in vivo. *J Exp Med* 2003; **198**: 249-58.

321. Oldenhove G, de Heusch M, Urbain-Vansanten G *et al.* $CD4^+$ $CD25^+$ regulatory T cells control T helper cell type 1 responses to foreign antigens induced by mature dendritic cells in vivo. *J Exp Med* 2003; **198**: 259-66.

322. Yamazaki S, Iyoda T, Tarbell K *et al.* Direct expansion of functional $CD25^+$ $CD4^+$ regulatory T cells by antigen-processing dendritic cells. *J Exp Med* 2003; **198**: 235-47.

323. Klein L, Khazaie K, Von Boehmer H. In vivo dynamics of antigen-specific regulatory T cells not predicted from behavior in vitro. *Proc Natl Acad Sci U.S.A* 2003; **100**: 8886-91.

324. Cederbom L, Hall H, Ivars F. $CD4^+CD25^+$ regulatory T cells down-regulate co-stimulatory molecules on antigen-presenting cells. *Eur J Immunol* 2000; **30**: 1538-43.

325. Fallarino F, Grohmann U, Hwang KW *et al.* Modulation of tryptophan catabolism by regulatory T cells. *Nat Immunol* 2003; **4**: 1206-12.

326. Munn DH, Sharma MD, Mellor AL. Ligation of B7-1/B7-2 by human $CD4^+$ T cells triggers indoleamine 2,3-dioxygenase activity in dendritic cells. *J Immunol* 2004; **172**: 4100-10.

327. Kingsley CI, Karim M, Bushell AR *et al.* $CD25^+CD4^+$ regulatory T cells prevent graft rejection: CTLA-4- and IL-10-dependent immunoregulation of alloresponses. *J Immunol* 2002; **168**: 1080-6.

328. Bachmann MF, Kohler G, Ecabert B *et al.* Cutting edge: lymphoproliferative disease in the absence of CTLA-4 is not T cell autonomous. *J Immunol* 1999; **163**: 1128-31.

329. Asseman C, Mauze S, Leach MW *et al.* An essential role for interleukin 10 in the function of regulatory T cells that inhibit intestinal inflammation. *J Exp Med* 1999; **190**: 995-1004.

330. Thorstenson KM, Khoruts A. Generation of anergic and potentially immunoregulatory $CD25^+CD4$ T cells in vivo after induction of peripheral tolerance with intravenous or oral antigen. *J Immunol* 2001; **167**: 188-95.

331. Nakamura K, Kitani A, Fuss I *et al.* TGF-β1 plays an important role in the mechanism of $CD4^+CD25^+$ regulatory T cell activity in both humans and mice. *J Immunol* 2004; **172**: 834-42.

332. Zhang X, Izikson L, Liu L *et al.* Activation of $CD25^+CD4^+$ regulatory T cells by oral antigen administration. *J Immunol* 2001; **167**: 4245-53.

333. Piccirillo CA, Letterio JJ, Thornton AM *et al.* $CD4^+CD25^+$ regulatory T cells can mediate suppressor function in the absence of transforming growth factor β1 production and responsiveness. *J Exp Med* 2002; **196**: 237-46.

334. Nakamura K, Kitani A, Strober W. Cell contact-dependent immunosuppression by $CD4^+CD25^+$ regulatory T cells is mediated by cell surface-bound transforming growth factor β. *J Exp Med* 2001; **194**: 629-44.

335. Dieckmann D, Bruett CH, Ploettner H *et al.* Human $CD4^+CD25^+$ regulatory, contact-dependent T cells induce interleukin 10-producing, contact-independent type 1-like regulatory T cells. *J Exp Med* 2002; **196**: 247-53.

336. Jonuleit H, Schmitt E, Kakirman H *et al.* Infectious tolerance: human $CD25^+$ regulatory T cells convey suppressor activity to conventional $CD4^+$ T helper cells. *J Exp Med* 2002; **196**: 255-60.

337. Stassen M, Schmitt E, Jonuleit H. Human $CD4^+CD25^+$ regulatory T cells and infectious tolerance. *Transplantation* 2004; **77**: S23-S25.

338. Shevach EM. $CD4^+$ $CD25^+$ suppressor T cells: more questions than answers. *Nat Rev Immunol* 2002; **2**: 389-400.

339. Akbar AN, Taams LS, Salmon M *et al.* The peripheral generation of $CD4^+$ $CD25^+$ regulatory T cells. *Immunology* 2003; **109**: 319-25.

340. Sullivan KE, McDonald-McGinn D, Zackai EH. $CD4^+$ $CD25^+$ T-cell production in healthy humans and in patients with thymic hypoplasia. *Clin Diagn Lab Immunol* 2002; **9**: 1129-31.

341. Itoh M, Takahashi T, Sakaguchi N *et al.* Thymus and autoimmunity: production of $CD25^+CD4^+$ naturally anergic and suppressive T cells as a key function of the thymus in maintaining immunologic self-tolerance. *J Immunol* 1999; **162**: 5317-26.

342. Karim M, Kingsley CI, Bushell AR *et al.* Alloantigen-induced $CD25^+CD4^+$ regulatory T cells can develop in vivo from $CD25\text{-}CD4^+$ precursors in a thymus-independent process. *J Immunol* 2004; **172**: 923-8.

343. Chen W, Jin W, Hardegen N *et al.* Conversion of peripheral $CD4^+CD25^-$ naive T cells to $CD4^+CD25^+$ regulatory T cells by TGF-β induction of transcription factor Foxp3. *J Exp Med* 2003; **198**: 1875-86.

344. Aluvihare VR, Kallikourdis M, Betz AG. Regulatory T cells mediate maternal tolerance to the fetus. *Nat Immunol* 2004; **5**: 266-71.

345. Cavani A, Nasorri F, Ottaviani C *et al.* Human $CD25^+$ regulatory T cells maintain immune tolerance to nickel in healthy, nonallergic individuals. *J Immunol* 2003; **171**: 5760-8.

346. Suvas S, Kumaraguru U, Pack CD *et al.* $CD4^+CD25^+$ T cells regulate virus-specific primary and memory $CD8^+$ T cell responses. *J Exp Med* 2003; **198**: 889-901.

347. Suvas S, Azkur AK, Kim BS *et al.* $CD4^+CD25^+$ regulatory T cells control the severity of viral immunoinflammatory lesions. *J Immunol* 2004; **172**: 4123-32.

348. Hesse M, Piccirillo CA, Belkaid Y *et al.* The pathogenesis of schistosomiasis is controlled by cooperating IL-10-producing innate effector and regulatory T cells. *J Immunol* 2004; **172**: 3157-66.

349. Hori S, Carvalho TL, Demengeot J. $CD25^+CD4^+$ regulatory T cells suppress CD4- T cell-mediated pulmonary hyperinflammation driven by Pneumocystis carinii in immunodeficient mice. *Eur J Immunol* 2002; **32**: 1282-91.

350. Belkaid Y, Piccirillo CA, Mendez S *et al.* $CD4^+CD25^+$ regulatory T cells control Leishmania major persistence and immunity. *Nature* 2002; **420**: 502-7.

351. Dittmer U, He H, Messer RJ *et al.* Functional impairment of $CD8^+$ T cells by regulatory T cells during persistent retroviral infection. *Immunity* 2004; **20**: 293-303.

352. Hisaeda H, Maekawa Y, Iwakawa D *et al.* Escape of malaria parasites from host immunity requires $CD4^+$ $CD25^+$ regulatory T cells. *Nat Med* 2004; **10**: 29-30.

353. Mottet C, Uhlig HH, Powrie F. Cutting edge: cure of colitis by $CD4^+CD25^+$ regulatory T cells. *J Immunol* 2003; **170**: 3939-43.

354. Liu H, Hu B, Xu D *et al.* $CD4^+CD25^+$ regulatory T cells cure murine colitis: the role of IL-10, TGF-β, and CTLA-4. *J Immunol* 2003; **171**: 5012-7.

355. Foussat A, Cottrez F, Brun V *et al.* A comparative study between T regulatory type 1 and $CD4^+CD25^+$ T cells in the control of inflammation. *J Immunol* 2003; **171**: 5018-26.

356. Uthayakumar S, Nandwani R, Drinkwater T *et al.* The prevalence of skin disease in HIV infection and its relationship to the degree of immunosuppression. *Br J Dermatol* 1997; **137**: 595-8.

357. Bordea C, Wojnarowska F, Millard PR *et al.* Skin cancers in renal-transplant recipients occur more frequently than previously recognized in a temperate climate. *Transplantation* 2004; **77**: 574-9.

358. Kupper TS, Fuhlbrigge RC. Immune surveillance in the skin: mechanisms and clinical consequences. *Nat Rev Immunol* 2004; **4**: 211-22.

359. Kimber I, Cumberbatch M, Dearman RJ *et al.* Cytokines and chemokines in the initiation and regulation of epidermal Langerhans cell mobilization. *Br J Dermatol* 2000; **142**: 401-12.

360. Steinhoff M, Brzoska T, Luger TA. Keratinocytes in epidermal immune responses. *Curr Opin Allergy Clin Immunol* 2001; **1**: 469-76.

361. Nestle FO, Zheng XG, Thompson CB *et al.* Characterization of dermal dendritic cells obtained from normal human skin reveals phenotypic and functionally distinctive subsets. *J Immunol* 1993; **151**: 6535-45.

362. Buckley CC, Ivison C, Poulter LW *et al.* Fc epsilon R11/CD23 receptor distribution in patch test reactions to aeroallergens in atopic dermatitis. *J Invest Dermatol* 1992; **99**: 184-8.

363. Dupuy P, Heslan M, Fraitag S *et al.* T-cell receptor-γ/δ bearing lymphocytes in normal and inflammatory human skin. *J Invest Dermatol* 1990; **94**: 764-8.

364. Podgrabinska S, Braun P, Velasco P *et al.* Molecular characterization of lymphatic endothelial cells. *Proc Natl Acad Sci U.S.A* 2002; **99**: 16069-74.

365. Yawalkar N, Hunger RE, Pichler WJ *et al.* Human afferent lymph from normal skin contains an increased number of mainly memory / effector $CD4^+$ T cells expressing activation, adhesion and co-stimulatory molecules. *Eur J Immunol* 2000; **30**: 491-7.

366. Brand CU, Hunger RE, Yawalkar N *et al.* Characterization of human skin-derived CD1a-positive lymph cells. *Arch Dermatol Res* 1999; **291**: 65-72.

367. Kriehuber E, Breiteneder-Geleff S, Groeger M *et al.* Isolation and characterization of dermal lymphatic and blood endothelial cells reveal stable and functionally specialized cell lineages. *J Exp Med* 2001; **194**: 797-808.

368. Chong BF, Murphy JE, Kupper TS *et al.* E-selectin, thymus- and activation-regulated chemokine/CCL17, and intercellular adhesion molecule-1 are constitutively coexpressed in dermal microvessels: a foundation for a cutaneous immunosurveillance system. *J Immunol* 2004; **172**: 1575-81.

369. Hunger RE, Yawalkar N, Braathen LR *et al.* CD1a-positive dendritic cells transport the antigen DNCB intracellularly from the skin to the regional lymph nodes in the induction phase of allergic contact dermatitis. *Arch Dermatol Res* 2001; **293**: 420-6.

370. Jakob T, Udey MC. Regulation of E-cadherin-mediated adhesion in Langerhans cell-like dendritic cells by inflammatory mediators that mobilize Langerhans cells in vivo. *J Immunol* 1998; **160**: 4067-73.

371. Saeki H, Moore AM, Brown MJ *et al.* Cutting edge: secondary lymphoid-tissue chemokine (SLC) and CC chemokine receptor 7 (CCR7) participate in the emigration pathway of mature dendritic cells from the skin to regional lymph nodes. *J Immunol* 1999; **162**: 2472-5.

372. Gunn MD, Tangemann K, Tam C *et al.* A chemokine expressed in lymphoid high endothelial venules promotes the adhesion and chemotaxis of naive T lymphocytes. *Proc Natl Acad Sci U.S.A* 1998; **95**: 258-63.

373. Eberhard Y, Ortiz S, Ruiz LA *et al.* Up-regulation of the chemokine CCL21 in the skin of subjects exposed to irritants. *BMC Immunol* 2004; **5**: 7.

374. Schuler G, Steinman RM. Murine epidermal Langerhans cells mature into potent immunostimulatory dendritic cells in vitro. *J Exp Med* 1985; **161**: 526-46.

375. Campbell DJ, Butcher EC. Rapid acquisition of tissue-specific homing phenotypes by $CD4^+$ T cells activated in cutaneous or mucosal lymphoid tissues. *J Exp Med* 2002; **195**: 135-41.

376. Mora JR, Bono MR, Manjunath N *et al.* Selective imprinting of gut-homing T cells by Peyer's patch dendritic cells. *Nature* 2003; **424**: 88-93.

377. Dudda JC, Simon JC, Martin S. Dendritic cell immunization route determines $CD8^+$ T cell trafficking to inflamed skin: role for tissue microenvironment and dendritic cells in establishment of T cell-homing subsets. *J Immunol* 2004; **172**: 857-63.

378. Kunkel EJ, Butcher EC. Chemokines and the tissue-specific migration of lymphocytes. *Immunity* 2002; **16**: 1-4.

379. Picker LJ, Terstappen LW, Rott LS *et al.* Differential expression of homing-associated adhesion molecules by T cell subsets in man. *J Immunol* 1990; **145**: 3247-55.

380. Picker LJ, Michie SA, Rott LS *et al.* A unique phenotype of skin-associated lymphocytes in humans. Preferential expression of the HECA-452 epitope by benign and malignant T cells at cutaneous sites. *Am J Pathol* 1990; **136**: 1053-68.

381. Santamaria Babi LF, Picker LJ, Perez Soler MT *et al.* Circulating allergen-reactive T cells from patients with atopic dermatitis and allergic contact dermatitis express the skin-selective homing receptor, the cutaneous lymphocyte-associated antigen. *J Exp Med* 1995; **181**: 1935-40.

382. Davis RE, Smoller BR. T lymphocytes expressing HECA-452 epitope are present in cutaneous acute graft-versus-host disease and erythema multiforme, but not in acute graft-versus-host disease in gut organs. *Am J Pathol* 1992; **141**: 691-8.

383. Koelle DM, Liu Z, McClurkan CM *et al.* Expression of cutaneous lymphocyte-associated antigen by $CD8^+$ T cells specific for a skin-tropic virus. *J Clin Invest* 2002; **110**: 537-48.

384. Hunger RE, Yawalkar N, Braathen LR *et al.* The HECA-452 epitope is highly expressed on lymph cells derived from human skin. *Br J Dermatol* 1999; **141**: 565-9.

385. Picker LJ, Kishimoto TK, Smith CW *et al.* ELAM-1 is an adhesion molecule for skin-homing T cells. *Nature* 1991; **349**: 796-9.

386. Berg EL, Yoshino T, Rott LS *et al.* The cutaneous lymphocyte antigen is a skin lymphocyte homing receptor for the vascular lectin endothelial cell-leukocyte adhesion molecule 1. *J Exp Med* 1991; **174**: 1461-6.

387. Rossiter H, van Reijsen F, Mudde GC *et al.* Skin disease-related T cells bind to endothelial selectins: expression of cutaneous lymphocyte antigen (CLA) predicts E-selectin but not P-selectin binding. *Eur J Immunol* 1994; **24**: 205-10.

388. Fuhlbrigge RC, Kieffer JD, Armerding D *et al.* Cutaneous lymphocyte antigen is a specialized form of PSGL-1 expressed on skin-homing T cells. *Nature* 1997; **389**: 978-81.

389. Maly P, Thall A, Petryniak B *et al.* The α(1,3)fucosyltransferase Fuc-TVII controls leukocyte trafficking through an essential role in L-, E-, and P-selectin ligand biosynthesis. *Cell* 1996; **86**: 643-53.

390. Knibbs RN, Craig RA, Natsuka S *et al.* The fucosyltransferase FucT-VII regulates E-selectin ligand synthesis in human T cells. *J Cell Biol* 1996; **133**: 911-20.

391. Takahashi R, Mizukawa Y, Yamazaki Y *et al.* In vitro differentiation from naive to mature E-selectin binding CD4 T cells: acquisition of skin-homing properties occurs independently of cutaneous lymphocyte antigen expression. *J Immunol* 2003; **171**: 5769-77.

392. Mizukawa Y, Shitara K, Yamazaki Y *et al.* Development and characterization of a monoclonal antibody specific for fucosyltransferase VII (Fuc-TVII): discordant expression of CLA and Fuc-TVII in peripheral $CD4^+$ and $CD8^+$ T cells. *J Invest Dermatol* 2001; **117**: 743-7.

393. Akdis M, Klunker S, Schliz M *et al.* Expression of cutaneous lymphocyte-associated antigen on human $CD4^+$ and $CD8^+$ Th2 cells. *Eur J Immunol* 2000; **30**: 3533-41.

394. Armerding D, Kupper TS. Functional cutaneous lymphocyte antigen can be induced in essentially all peripheral blood T lymphocytes. *Int Arch Allergy Immunol* 1999; **119**: 212-22.

395. Leung DY, Gately M, Trumble A *et al.* Bacterial superantigens induce T cell expression of the skin-selective homing receptor, the cutaneous lymphocyte-associated antigen, via stimulation of interleukin 12 production. *J Exp Med* 1995; **181**: 747-53.

396. Hudak S, Hagen M, Liu Y *et al.* Immune surveillance and effector functions of $CCR10^+$ skin homing T cells. *J Immunol* 2002; **169**: 1189-96.

397. Reiss Y, Proudfoot AE, Power CA *et al.* CC chemokine receptor (CCR)4 and the CCR10 ligand cutaneous T cell-attracting chemokine (CTACK) in lymphocyte trafficking to inflamed skin. *J Exp Med* 2001; **194**: 1541-7.

398. Campbell JJ, Hedrick J, Zlotnik A *et al.* Chemokines and the arrest of lymphocytes rolling under flow conditions. *Science* 1998; **279**: 381-4.

399. Rot A, Von Andrian UH. Chemokines in innate and adaptive host defense: basic chemokinese grammar for immune cells. *Annu Rev Immunol* 2004; **22**: 891-928.

400. Vulcano M, Albanesi C, Stoppacciaro A *et al.* Dendritic cells as a major source of macrophage-derived chemokine/CCL22 in vitro and in vivo. *Eur J Immunol* 2001; **31**: 812-22.

401. Vestergaard C, Bang K, Gesser B *et al.* A Th2 chemokine, TARC, produced by keratinocytes may recruit CLA^+CCR4^+ lymphocytes into lesional atopic dermatitis skin. *J Invest Dermatol* 2000; **115**: 640-6.

402. Morales J, Homey B, Vicari AP *et al.* CTACK, a skin-associated chemokine that preferentially attracts skin-homing memory T cells. *Proc Natl Acad Sci U.S.A* 1999; **96**: 14470-5.

403. Kunkel EJ, Boisvert J, Murphy K *et al.* Expression of the chemokine receptors CCR4, CCR5, and CXCR3 by human tissue-infiltrating lymphocytes. *Am J Pathol* 2002; **160**: 347-55.

404. Klunker S, Trautmann A, Akdis M *et al.* A second step of chemotaxis after transendothelial migration: keratinocytes undergoing apoptosis release IFN-γ-inducible protein 10, monokine induced by IFN-γ, and IFN-γ-inducible α-chemoattractant for T cell chemotaxis toward epidermis in atopic dermatitis. *J Immunol* 2003; **171**: 1078-84.

405. Fitzhugh DJ, Naik S, Caughman SW *et al.* Cutting edge: C-C chemokine receptor 6 is essential for arrest of a subset of memory T cells on activated dermal microvascular endothelial cells under physiologic flow conditions in vitro. *J Immunol* 2000; **165**: 6677-81.

406. Choi J, Enis DR, Koh KP *et al.* T lymphocyte-endothelial cell interactions. *Annu Rev Immunol* 2004; **22**: 683-709.

407. Grabbe S, Schwarz T. Immunoregulatory mechanisms involved in elicitation of allergic contact hypersensitivity. *Immunol Today* 1998; **19**: 37-44.

408. Willis CM, Young E, Brandon DR *et al.* Immunopathological and ultrastructural findings in human allergic and irritant contact dermatitis. *Br J Dermatol* 1986; **115**: 305-16.

409. Grabbe S, Steinbrink K, Steinert M *et al.* Removal of the majority of epidermal Langerhans cells by topical or systemic steroid application enhances the effector phase of murine contact hypersensitivity. *J Immunol* 1995; **155**: 4207-17.

410. Grabbe S, Varga G, Beissert S *et al.* β2 integrins are required for skin homing of primed T cells but not for priming naive T cells. *J Clin Invest* 2002; **109**: 183-92.

411. Scheper RJ, Dinther-Janssen AC, Polak L. Specific accumulation of hapten-reactive T cells in contact sensitivity reaction sites. *J Immunol* 1985; **134**: 1333-6.

412. Rustemeyer T, de Groot J, von Blomberg BM *et al.* Assessment of contact allergen cross-reactivity by retesting. *Exp Dermatol* 2002; **11**: 257-65.

413. Mizukawa Y, Yamazaki Y, Teraki Y *et al.* Direct evidence for interferon-γ production by effector-memory-type intraepidermal T cells residing at an effector site of immunopathology in fixed drug eruption. *Am J Pathol* 2002; **161**: 1337-47.

414. Hwang JM, Yamanouchi J, Santamaria P *et al.* A critical temporal window for selectin-dependent $CD4^+$ lymphocyte homing and initiation of late-phase inflammation in contact sensitivity. *J Exp Med* 2004; **199**: 1223-34.

415. Jones CM, Cose SC, McNally JM *et al.* Diminished secondary CTL response in draining lymph nodes on cutaneous challenge with herpes simplex virus. *J Gen Virol* 2000; **81**: 407-14.

416. Mallon E, Powell S, Mortimer P *et al.* Evidence for altered cell-mediated immunity in postmastectomy lymphoedema. *Br J Dermatol* 1997; **137**: 928-33.

417. Turk JL. In: *Delayed hypersensitivity*, 3rd Edition edn. Amsterdam: Elsevier, 1980.

418. Young DB, Stewart GR. Tuberculosis vaccines. *Br Med Bull* 2002; **62**: 73-86.

419. Poulter LW, Seymour GJ, Duke O *et al.* Immunohistological analysis of delayed-type hypersensitivity in man. *Cell Immunol* 1982; **74**: 358-69.

420. Platt JL, Grant BW, Eddy AA *et al.* Immune cell populations in cutaneous delayed-type hypersensitivity. *J Exp Med* 1983; **158**: 1227-42.

421. Gibbs JH, Ferguson J, Brown RA *et al.* Histometric study of the localisation of lymphocyte subsets and accessory cells in human Mantoux reactions. *J Clin Pathol* 1984; **37**: 1227-34.

422. Kalish RS, Johnson KL. Enrichment and function of urushiol (poison ivy)-specific T lymphocytes in lesions of allergic contact dermatitis to urushiol. *J Immunol* 1990; **145**: 3706-13.

423. McCluskey RT, Benacerraf B, McCluskey JW. Studies on the specificity of the cellular infiltarte in delayed hypersensitivity reactions. *J Immunol* 1963; **90**: 466-77.

424. Diffey BL, Oliver RJ, Farr PM. A portable instrument for quantifying erythema induced by ultraviolet radiation. *Br J Dermatol* 1984; **111**: 663-72.

425. Maini MK, Wedderburn LR, Hall FC *et al.* A comparison of two techniques for the molecular tracking of specific T-cell responses; $CD4^+$ human T-cell clones persist in a stable hierarchy but at a lower frequency than clones in the $CD8^+$ population. *Immunology* 1998; **94**: 529-35.

426. Cook JE, Beverley PC. Analysis of lymphocyte diversity in the elderly: heteroduplex analysis and alternative techniques. *Exp Gerontol* 2001; **36**: 583-9.

427. Wack A, Montagna D, Dellabona P *et al.* An improved PCR-heteroduplex method permits high-sensitivity detection of clonal expansions in complex T cell populations. *J Immunol Methods* 1996; **196**: 181-92.

428. Foster GR, Germain C, Jones M *et al.* Human T cells elicit IFN-α secretion from dendritic cells following cell to cell interactions. *Eur J Immunol* 2000; **30**: 3228-35.

429. Eady RA, Leigh IM, Pope FM. Anatomy and Organization of Human Skin. In: *Textbook of Dermatology* (Champion,RH, Burton,JL, Burns,DA et al, eds), Sixth edn., Vol. 1. Blackwell Science Ltd, 1998: 37-111.

430. Van Damme N, Baeten D, De Vos M *et al.* Chemical agents and enzymes used for the extraction of gut lymphocytes influence flow cytometric detection of T cell surface markers. *J Immunol Methods* 2000; **236**: 27-35.

431. Abuzakouk M, Feighery C, O'Farrelly C. Collagenase and Dispase enzymes disrupt lymphocyte surface molecules. *J Immunol Methods* 1996; **194**: 211-6.

432. Mulder WM, Koenen H, van de Muysenberg AJ *et al.* Reduced expression of distinct T-cell CD molecules by collagenase/DNase treatment. *Cancer Immunol Immunother* 1994; **38**: 253-8.

433. Szabo SK, Hammerberg C, Yoshida Y *et al.* Identification and quantitation of interferon-γ producing T cells in psoriatic lesions: localization to both $CD4^+$ and $CD8^+$ subsets. *J.Invest Dermatol* 1998; **111**: 1072-8.

434. Novelli M, Savoia P, Cambieri I *et al.* Collagenase digestion and mechanical disaggregation as a method to extract and immunophenotype tumour lymphocytes in cutaneous T-cell lymphomas. *Clin Exp Dermatol* 2000; **25**: 423-31.

435. Curry MP, Norris S, Golden-Mason L *et al.* Isolation of lymphocytes from normal adult human liver suitable for phenotypic and functional characterization. *J Immunol Methods* 2000; **242**: 21-31.

436. Curry JL, Qin JZ, Robinson J *et al.* Reactivity of resident immunocytes in normal and prepsoriatic skin using an ex vivo skin-explant model system. *Arch Pathol Lab Med* 2003; **127**: 289-96.

437. Pope M, Betjes MG, Hirmand H *et al.* Both dendritic cells and memory T lymphocytes emigrate from organ cultures of human skin and form distinctive dendritic-T-cell conjugates. *J Invest Dermatol* 1995; **104**: 11-7.

438. Kiistala U, Mustakallio KK, Rorsman H. Suction blisters in the study of cellular dynamics of inflammation. *Acta Derm Venereol* 1967; **47**: 150-3.

439. Kuhns DB, DeCarlo E, Hawk DM *et al.* Dynamics of the cellular and humoral components of the inflammatory response elicited in skin blisters in humans. *J Clin Invest* 1992; **89**: 1734-40.

440. Holden CA, Parish WE. Atopic Dermatitis. In: *Textbook of Dermatology* (Champion,RH, Burton,JL, Burns,DA et al, eds), Sixth Edition edn. Blackwell Science Ltd., 1998: 681-708.

441. Black AK, Greaves MW, Hensby CN *et al.* A new method for recovery of exudates from normal and inflamed human skin. *Clin Exp Dermatol* 1977; **2**: 209-16.

442. Sellati TJ, Waldrop SL, Salazar JC *et al.* The cutaneous response in humans to Treponema pallidum lipoprotein analogues involves cellular elements of both innate and adaptive immunity. *J Immunol* 2001; **166**: 4131-40.

443. Ebert LM, McColl SR. Up-regulation of CCR5 and CCR6 on distinct subpopulations of antigen-activated $CD4^+$ T lymphocytes. *J Immunol* 2002; **168**: 65-72.

444. Geginat J, Sallusto F, Lanzavecchia A. Cytokine-driven proliferation and differentiation of human naive, central memory, and effector memory $CD4^+$ T cells. *J Exp Med* 2001; **194**: 1711-9.

445. Penninger JM, Irie-Sasaki J, Sasaki T *et al.* CD45: new jobs for an old acquaintance. *Nat Immunol* 2001; **2**: 389-96.

446. Peachey RD. Skin temperature and blood flow in relation to the speed of suction blister formation. *Br J Dermatol* 1971; **84**: 447-52.

447. Kiistala U. Dermal-epidermal separation. II. External factors in suction blister formation with special reference to the effect of temperature. *Ann Clin Res* 1972; **4**: 236-46.

448. Barr RM, Walker SL, Tsang W *et al.* Suppressed alloantigen presentation, increased TNF-α, IL-1, IL-1Ra, IL-10, and modulation of TNF-R in UV-irradiated human skin. *J Invest Dermatol* 1999; **112**: 692-8.

449. Skouge JW, Morison WL, Diwan RV *et al.* Autografting and PUVA. A combination therapy for vitiligo. *J Dermatol Surg Oncol* 1992; **18**: 357-60.

450. Kolgen W, Both H, van Weelden H *et al.* Epidermal langerhans cell depletion after artificial ultraviolet B irradiation of human skin in vivo: apoptosis versus migration. *J Invest Dermatol* 2002; **118**: 812-7.

451. Gupta S, Shroff S, Gupta S. Modified technique of suction blistering for epidermal grafting in vitiligo. *Int J Dermatol* 1999; **38**: 306-9.

452. Peachey RD. Some factors affecting the speed of suction blister formation in normal subjects. *Br J Dermatol* 1971; **84**: 435-46.

453. Kiistala U. Suction blister device for separation of viable epidermis from dermis. *J Invest Dermatol* 1968; **50**: 129-37.

454. Kiistala U. Dermal-epidermal separation. I. The influence of age, sex and body region on suction blister formation in human skin. *Ann Clin Res* 1972; **4**: 10-22.

455. Lowe LB, Jr., van der Leun JC. Suction blisters and dermal-epidermal adherence. *J Invest Dermatol* 1968; **50**: 308-14.

456. Gupta S, Kumar B. Suction blister induction time: 15 minutes or 150 minutes? *Dermatol Surg* 2000; **26**: 754-6.

457. Falabella R. Suction blistering as a research and therapeutic tool in dermatology. *Int J Dermatol* 2000; **39**: 670-1.

458. Beck JS, Gibbs JH, Potts RC *et al.* Histometric studies on biopsies of tuberculin skin tests showing evidence of ischaemia and necrosis. *J Pathol* 1989; **159**: 317-22.

459. Turk JL. The histology of delayed hypersensitivity reactions in the skin. In: *Delayed hypersensitivity*, 3rd Edition edn. Amsterdam: Elsevier, 1980: 45-53.

460. Moser B, Loetscher P. Lymphocyte traffic control by chemokines. *Nat Immunol* 2001; **2**: 123-8.

461. Li B, Rossman MD, Imir T *et al.* Disease-specific changes in γδ T cell repertoire and function in patients with pulmonary tuberculosis. *J.Immunol.* 1996; **157**: 4222-9.

462. Carding SR, Egan PJ. γδ T cells: functional plasticity and heterogeneity. *Nat Rev Immunol* 2002; **2**: 336-45.

463. Hoft DF, Brown RM, Roodman ST. Bacille Calmette-Guerin vaccination enhances human γδ T cell responsiveness to mycobacteria suggestive of a memory-like phenotype. *J Immunol* 1998; **161**: 1045-54.

464. Szereday L, Baliko Z, Szekeres-Bartho J. γ/δ T cell subsets in patients with active Mycobacterium tuberculosis infection and tuberculin anergy. *Clin Exp Immunol* 2003; **131**: 287-91.

465. van Reijsen FC, Bruijnzeel-Koomen CA, Kalthoff FS *et al.* Skin-derived aeroallergen-specific T-cell clones of Th2 phenotype in patients with atopic dermatitis. *J Allergy Clin Immunol* 1992; **90**: 184-93.

466. Gerdes J, Lemke H, Baisch H *et al.* Cell cycle analysis of a cell proliferation-associated human nuclear antigen defined by the monoclonal antibody Ki-67. *J Immunol* 1984; **133**: 1710-5.

467. Rentenaar RJ, Gamadia LE, van DerHoek N *et al.* Development of virus-specific $CD4^+$ T cells during primary cytomegalovirus infection. *J Clin Invest* 2000; **105**: 541-8.

468. Reed JR, Vukmanovic-Stejic M, Fletcher JM *et al.* Telomere erosion in memory T cells induced by telomerase inhibition at the site of antigenic challenge in vivo. *J Exp Med* 2004; **199**: 1433-43.

469. Hislop AD, Gudgeon NH, Callan MF *et al.* EBV-specific $CD8^+$ T cell memory: relationships between epitope specificity, cell phenotype, and immediate effector function. *J Immunol* 2001; **167**: 2019-29.

470. Callan MF, Fazou C, Yang H *et al.* $CD8^+$ T-cell selection, function, and death in the primary immune response in vivo. *J Clin Invest* 2000; **106**: 1251-61.

471. Flynn KJ, Riberdy JM, Christensen JP *et al.* In vivo proliferation of naive and memory influenza-specific $CD8^+$ T cells. *Proc Natl Acad Sci U.S.A* 1999; **96**: 8597-602.

472. Kursar M, Bonhagen K, Kohler A *et al.* Organ-specific $CD4^+$ T cell response during Listeria monocytogenes infection. *J Immunol* 2002; **168**: 6382-7.

473. Topham DJ, Castrucci MR, Wingo FS *et al.* The role of antigen in the localization of naive, acutely activated, and memory $CD8^+$ T cells to the lung during influenza pneumonia. *J Immunol* 2001; **167**: 6983-90.

474. Sallusto F, Schaerli P, Loetscher P *et al.* Rapid and coordinated switch in chemokine receptor expression during dendritic cell maturation. *Eur J Immunol* 1998; **28**: 2760-9.

475. Sozzani S, Allavena P, D'Amico G *et al.* Differential regulation of chemokine receptors during dendritic cell maturation: a model for their trafficking properties. *J Immunol* 1998; **161**: 1083-6.

476. Pasare C, Medzhitov R. Toll pathway-dependent blockade of $CD4^+CD25^+$ T cell-mediated suppression by dendritic cells. *Science* 2003; **299**: 1033-6.

477. Sakaguchi S, Takahashi T, Yamazaki S *et al.* Immunologic self tolerance maintained by T-cell-mediated control of self-reactive T cells: implications for autoimmunity and tumor immunity. *Microbes Infect* 2001; **3**: 911-8.

478. Lombardi G, Sidhu S, Batchelor R *et al.* Anergic T cells as suppressor cells in vitro. *Science* 1994; **264**: 1587-9.

479. Lechler R, Chai JG, Marelli-Berg F *et al.* The contributions of T-cell anergy to peripheral T-cell tolerance. *Immunology* 2001; **103**: 262-9.

480. Lombardi G, Dunne PJ, Scheel-Toellner D *et al.* Type 1 IFN maintains the survival of anergic $CD4^+$ T cells. *J Immunol* 2000; **165**: 3782-9.

481. Marshall DR, Turner SJ, Belz GT *et al.* Measuring the diaspora for virus-specific $CD8^+$ T cells. *Proc Natl Acad Sci U.S.A* 2001; **98**: 6313-8.

482. Kaplan D. Autocrine secretion and the physiological concentration of cytokines. *Immunol Today* 1996; **17**: 303-4.

483. Sakaguchi S. Regulatory T cells: key controllers of immunologic self-tolerance. *Cell* 2000; **101**: 455-8.

484. Shevach EM. Certified professionals: $CD4^+CD25^+$ suppressor T cells. *J Exp Med* 2001; **193**: F41-F46.

485. Pawelec G, Adibzadeh M, Rehbein A *et al.* In vitro senescence models for human T lymphocytes. *Vaccine* 2000; **18**: 1666-74.

486. Robertson JD, Gale RE, Wynn RF *et al.* Dynamics of telomere shortening in neutrophils and T lymphocytes during ageing and the relationship to skewed X chromosome inactivation patterns. *Br J Haematol* 2000; **109**: 272-9.

487. Iwama H, Ohyashiki K, Ohyashiki JH *et al.* Telomeric length and telomerase activity vary with age in peripheral blood cells obtained from normal individuals. *Hum Genet* 1998; **102**: 397-402.

488. Bodnar AG, Ouellette M, Frolkis M *et al.* Extension of life-span by introduction of telomerase into normal human cells. *Science* 1998; **279**: 349-52.

489. Borthwick NJ, Lowdell M, Salmon M *et al.* Loss of CD28 expression on $CD8^+$ T cells is induced by IL-2 receptor γ chain signalling cytokines and type I IFN, and increases susceptibility to activation-induced apoptosis. *Int Immunol* 2000; **12**: 1005-13.

490. Akiyama M, Hideshima T, Hayashi T *et al.* Cytokines modulate telomerase activity in a human multiple myeloma cell line. *Cancer Res* 2002; **62**: 3876-82.

491. Orteu, C. H. Regulation of cutaneous T cell apoptosis and its relevance to chronic inflammatory skin disease. MD thesis 1999. Royal Free and University College Medical School, UCL.

492. Sundararaj KP, Wood RE, Ponnusamy S *et al.* Rapid shortening of telomere length in response to ceramide involves the inhibition of telomere binding activity of nuclear glyceraldehyde-3-phosphate dehydrogenase. *J Biol Chem* 2004; **279**: 6152-62.

493. Ogretmen B, Schady D, Usta J *et al.* Role of ceramide in mediating the inhibition of telomerase activity in A549 human lung adenocarcinoma cells. *J Biol Chem* 2001; **276**: 24901-10.

494. Fujisawa H, Kondo S, Wang B *et al.* The expression and modulation of IFN-α and IFN-β in human keratinocytes. *J Interferon Cytokine Res* 1997; **17**: 721-5.

495. Voehringer D, Koschella M, Pircher H. Lack of proliferative capacity of human effector and memory T cells expressing killer cell lectinlike receptor G1 (KLRG1). *Blood* 2002; **100**: 3698-702.

496. Akbar AN, Beverley PC, Salmon M. Will telomere erosion lead to a loss of T-cell memory? *Nat Rev Immunol* 2004; **4**: 737-43.

497. Zhang Y, Cosyns M, Levin MJ *et al.* Cytokine production in varicella zoster virus-stimulated limiting dilution lymphocyte cultures. *Clin Exp Immunol* 1994; **98**: 128-33.

498. Bonifati C, Trento E, Cordiali-Fei P *et al.* Increased interleukin-7 concentrations in lesional skin and in the sera of patients with plaque-type psoriasis. *Clin Immunol Immunopathol* 1997; **83**: 41-4.

499. Yamada N, Wakugawa M, Kuwata S *et al.* Changes in eosinophil and leukocyte infiltration and expression of IL-6 and IL-7 messenger RNA in mite allergen patch test reactions in atopic dermatitis. *J Allergy Clin Immunol* 1996; **98**: S201-S206.

500. Stanley MA. Imiquimod and the imidazoquinolones: mechanism of action and therapeutic potential. *Clin Exp Dermatol* 2002; **27**: 571-7.